Mathematical modelling of telomere dynamics

QI QI

Thesis submitted to The University of Nottingham
for the degree of Doctor of Philosophy

June 2011

Abstract

Telomeres are repetitive elements of DNA which are located at the ends of chromosomes. During cell division, telomeres on daughter chromomeres shorten until the telomere length falls below a critical level. This shortening restricts the number of cell divisions. In this thesis, we use mathematical modelling to study dynamics of telomere length in a cell in order to understand normal ageing (telomere shortening), Werner's syndrome (a disease of accelerated ageing) and the immortality of cells caused by telomerase (telomere constant length maintenance).

In the mathematical models we compared four possible mechanisms for telomere shortening. The simplest model assumes that a fixed amount of telomere is lost on each replication; the second supposes that telomere loss depends on telomere length; for the third case the amount of telomeres loss per division is fixed but the probability of dividing depends on telomere length; the fourth cases has both telomere loss and the probability of division dependent on telomere length. We start by developing Monte Carlo simulations of normal ageing using these four cases. Then we generalize the Monte Carlo simulations to consider Werner's syndrome, where the extra telomeres are lost during replication accelerate the ageing process. In order to investigate how the distribution of telomere length varies with time, we derive, from the discrete model, continuum models for the four different cases. Results from the Monte Carlo simulations and the deterministic models are shown to be in good agreement.

In addition to telomere loss, we also consider increases in telomere length caused by the enzyme telomerase, by appropriately extending the earlier Monte Carlo

simulations and continuum models. Results from the Monte Carlo simulations and the deterministic models are shown to be in good agreement. We also show that the concentration of telomerase in cells can control their proliferative potential.

Acknowledgements

Firstly, I want to express my acknowledge to my supervisors Jonathan Wattis and Helen Byrne, who were always been there when I needed them and also giving guidance, encouragement and support all through my time at Nottingham. I can not imagine doing a PhD without their help.

I am also very grateful to all my friends in Nottingham University who made PhD studies more colorful and fun. I would also like to thank Peter Stewart and Lei Yan, for demonstrating MATLAB to me when I first started my PhD. My thanks also go to Oliver Bain, for helping me a lot in correcting the English in my reports and presentations.

I wish to thank Hilary Londsdale, Helen Culiffe, Dave Parkin and the rest of support staff in the School of Mathematical Sciences, who helped me in numerous ways.

My special thanks go to my boyfriend Chenbo Yi, for staying so late at university when writing up. Big massive thanks to my family, mum and dad, who supported me throughout.

Contents

List of Tables

List of Figures

Introduction

1.1 Introduction

Getting old is one of the most natural things in the world. Understanding why/how we age and what controls the length of a person's life has become an active area of research. Different animals have a wide variety of lifespan. For example, the lifespan of rats is about 3 years, a cat is about 15 years and the life expectancy of human beings is about 75 years to 120 years. The average human lifespan has increased from 45 years old two thousands years ago to today's 75 years old. A number of factors have contributed to these changes. These include improvements in our environment, better medical care, the development of science and technology [3]. In addition to considering external factors, we should also consider what happens inside the human body. It is composed of organs, which are composed of cells. Therefore in order to better understand ageing, we should start by considering what happens to an individual cell and its progeny and how changes associated with ageing are affected by processes occurring at the subcellular level, such as changes in telomere length [4].

During the early 20th century, people believed that normal cells were immortal and that getting old was caused by activity outside the cell. In the 1960s Hayflick and Moorehead [5] performed a series of experiments which overturned the view that normal cell were immortal. Their experiments involved letting normal human fibroblasts cells replicate and they found that the cells

could not divide forever; after a certain number of cell divisions the population of cells reached a finite limit, which is called the Hayflick limit. After that, the cells stopped replicating and became senescent. Cellular senescence is defines as a state in which cell replication is arrested, but the cell may remain alive and functional for many years before it dies [6]. In later work, Hayflick and Moorehead observed that in the mouse lens epithelium, the number of senescent cells increases as the animal ages. They also found that some types of cell became immortal: these include abnormal cells and cancer [7]. Hayflick and Moorehead's pioneering work has excited considerable interest in researchers and interested in understanding ageing.

1.2 Telomeres

We need to consider what happens inside a cell to find out why most cells have a finite replication limit. Normal human cells contain two kinds of genetic material: DNA and RNA. In general, double-stranded DNA is organized into 46 chromosomes (see Figure 1.1). Chromosomes also contain DNA binding proteins and different organisms contain different numbers of chromosomes. Telomeres are repetitive DNA which are located at the ends of chromosomes. The major role of telomeres is to protect the chromosomes against the loss of genetic material and to prevent fragments of chromosomes from rejoining [8]. RNA is a single-stranded long chain molecule of nucleotides, which carries genetic information and is involve in protein synthesis.

The telomeres of different species contains different repeated sequences of telomeric DNA, *e.g.*, Tetrahymena has the telomeric repeats GGGGTT [9], arabidopsis thaliana has the telomeric repeats AGGGTTT [10], humans have the telomeric repeats TTAGGG [11]. Recent research has focused on how telomeres control proliferation in human cells.

When a cell divides, its chromosomes are duplicated in a process called DNA replication. When chromosomes are duplicated, one of the daughter chromo-
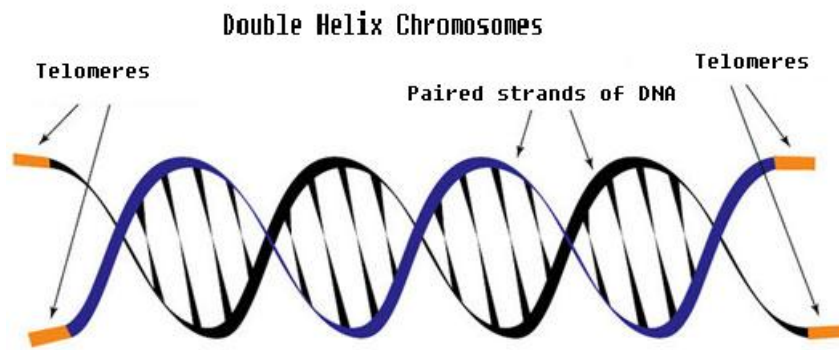
Figure 1.1: *Paired strands of DNA formed the double helix chromosomes.*

somes is shortened at the 5′ end due to the unidirectional synthesis of a new chain. This was first suggested in the early 1970s by Olovnikov [12] who also pointed out that on each replication a certain number of DNA sequences would be lost until the telomere length falls below a critical level. When this happens the cell stops replicating [13]. Olovnikov's hypothesis is consistent with the Hayflick limit. Experiment data shows telomere length in normal human cells is approximately 3k to 15k basepairs with the telomere shorting rate is $50 - 200$ basepairs per replication [14].
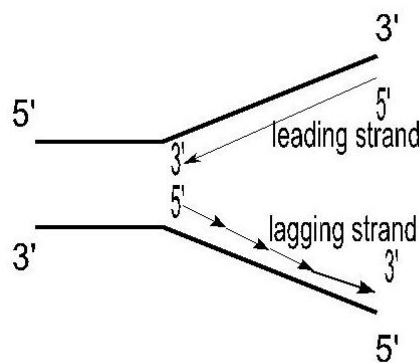
Figure 1.2: *Replication fork. As the fork moves from right to left, opening the parent DNA, new bases are added to the leading and lagging strands. The thick lines indicate the template strands. The thin lines indicate the replicated strands and the arrows show the direction of replication.*

3

Before cell division, the two strands of DNA separate at a certain point and form a "bubble". Replication proceeds from the bubble either as a unidirectional or a bidirectional process. During replication, the double-stranded DNA splits into two single strands at the origin, forming a Y-shaped replication fork. Figure 2.1 illustrates how replication starts at the 5′ end and moves in the 5′ to 3′ direction on both the leading and lagging strands. As replication proceeds from the 5′ to the 3′ direction, the new sub-chain on the leading strand (as illustrated in Figure 2.1) can be continuously synthesized in the same direction of, 5′ to 3′, by using the strand of the DNA double helix in a 3′ to 5′ as a template. However on the lagging strand, replication is more complicated. The sequence on the lagging strand cannot be constructed in the 3′ to 5′ direction on the template strands. Instead, before replication primase (RNA primer) must attach separately at the starting point and short sequences of 5′ to 3′ are formed. These discontinuous segments are called Okazaki fragments, being named after the person who discovered them [15]. Eventually Okazaki fragments are linked by DNA ligase, to produce a continuous, single-stranded DNA. After the lagging strand forms, the binding RNA primer is removed. This leads to shortening of the telomere at the 5′ end. This process is known as the replication problem.

When the telomere length is critically short, telomeres lose their protective function, triggering DNA damage which can lead to end-to-end fusions, chromosome breakage, or rejoining. These changes cause permanent cell replication arrest. While end-replication causes telomeres to shorten, it is not the only mechanism by which telomeres shorten; other factors that contribute to telomere shortening include environmental (life) stress [16], the accumulation of single strand breaks [17] and oxidative stress [18]. Since telomere length always shortens (if we do not consider extension factors, such as telomerase), there is a limit time for at which the cell halts replication due to telomere length restriction. In this thesis, we use telomere length as a key factor in determining a cell's proliferative capacity and we assume that end-replication problem is the only factor which can cause telomere shortening. The amount of telomere loss varies during replication. We consider different mechanisms by which telomere length may be regulated and use discrete/stochastic models (Chapter 2) and

deterministic/continuum models (Chapter 4) to study how telomere length in a single cell changes of time in order to understand normal ageing.

1.3   Senescence and ageing

A cell is said to be senescent if it stops dividing. Senescence was first identified by Hayflick and Moorhead in 1961. They observed that there was a limit to the number of times that a normal cell could to divide [5]. Most human cells go through 30-60 population doubling before they reach senescence. Cell senescence is different from cell apoptosis. Apoptosis is the process of programmed cell death. During apoptosis, a cell begins to shrink and its DNA becomes fragmented, leading to chromatin condensation which causes the nucleus to break up into small pieces. Apoptotic cells continue to shrink and package themselves into cell fragments which can be removed by macrophages and neighboring cells [8]. While a few senescent cells are removed by phagocytosis, most senescent cells will remain alive and functional for many years before they are removed [19].

There is evidence that telomere shortening is directly related to cell senescence. Experiments reported in [20] reveal that the telomeres of human fibroblasts which are senescent are shorter than replication cells and that the proportion of cells which are dividing is directly proportional to the mean telomere length. Allsopp and Harley suggested the existence of a critical telomere length which triggers DNA damage and induces cell senescence. In our discrete/stochastic models (in Chapter 2, 3, 5), we specify critical telomere length such that if the telomere length of the chromosomes is lower than this critical value, then cell replication will halt and the cell will remain in the senescent state.

There is a strong link between cellular senescence and ageing [21]. Observations of newborn baby's cells indicate there are almost no senescent cells. A small number of senescent cells are detected in adults and a large number in older people. These results suggest that the number of senescent cells increases

with donor age. Thus one of the key factors in normal ageing is the accumulation of senescent cells. While the accumulation of senescent cells is not normally harmful, they can express factors, which affect neighboring cells. These factors include degradative enzymes which may disrupt the cell's microenvironment, causing mutations and changes in normal tissue structure and function [22]. These changes also contribute to ageing.

The process of senescence is quite complicated and involves many different mechanisms, apart from telomere shortening. Senescence can be caused in different ways including: oxidative stress [23] [24], mitochondrial dysfunction [18], somatic mutation [25]. In the following sections we will explain briefly how these stresses affect telomere length and cell senescence, but in our model we assume that only telomere length regulates cellular senescence.

1.4 Other factors cause senescent and ageing

Many independent studies show that oxidative stress can cause telomere shortening and DNA damage. The accumulation of oxidative damage has also been identified as a major cause of ageing. Studies show that oxidative stress can accelerate telomere shorting in fibroblasts by causing damage to telomeric fragments of DNA, especially on the 5' site of 5'-GGG-3' in the telomere sequence [26]. Experiments using sheep embryos and human fibroblasts [27] were exposed to different oxygen concentration revealed that under 5% oxygen (hypoxia) the cells have significantly longer proliferation times than under 20% oxygen (normoxia) level, because normoxia levels lead to increase in DNA damage. An increase in oxidative stress, can accelerate telomere loss, leading to the early onset of cell senescence. Thus oxidative stress responsible for cellular senescence. However, under conditions of oxidative stress, telomere length can be maintained [17].

Mitochondria are tiny organelles that generate energy for cells. They are the major source of reactive oxygen species. Longer-lived mammals generally have

fewer mitochondria, which suggests that the density of mitochondria may influence ageing [28]. There is experimental evidence to support this. For example an increase in the number of mitochondrial in human diploid fibroblasts will rapidly induce senescence [29].

Somatic mutations alter gene structures. Therefore, in principle, the accumulation of mutations in somatic cells should cause normal cell functions to be lost or cell death to be triggered, thus speeding up the ageing process. Further, the frequency of somatic mutations increases dramatically with age, which suggests that the mutation rate increases exponentially rather than remaining unchanged or increasing linearly in time [30]. Somatic theory, which is based on experimental observations, suggest that DNA damage, genetic mutations and abnormal chromosomes cause cell senescence and death [31].

1.5 Capping of Chromosome ends

In 2000 Blackburn [32] suggested that telomeres have two states: capped and uncapped, and that they switch stochastically between the two states. Capping protects a telomere end from breaking or rejoining and also allows the cell to replicate. During cell division, temporary uncapping occurs. While a telomere is uncapped, telomerase can act on it. Once telomerase has finished elongating the telomere, it switches back to the capped state. Blackburn also suggested that when the length of a telomere is too short or there is insufficient active telomerase, telomeres will become uncapped. Under certain circumstances, telomeres can switch between the uncapped and capped states [33]. If a cell remains in the uncapped state for too long, it will experience DNA damage, which prevents its from switching back. The uncapped state will then trigger replication arrest.

Since telomeres switch stochastically between the capped and uncapped states, a population of cells will not start/finish division at the same time. Therefore, when we model cell division we need to consider the probability of cell divi-

sion. In our Chapters 2 and 4, we model cell replication in normal ageing by allowing the probability of cell division and different amount of telomere loss to vary with telomere length.

1.6 Werner's syndrome

Werner's syndrome is an inherited disease in which the most characteristic feature is the rapid appearance of ageing (see Figure 1.3). This normally appears in the second or third decade when patients develop grey hair, wrinkled skin, alopecia, diabetes mellitus and juvenile cataracts, etc [34]. The average lifespan for Werner's syndrome patients is about 46 and their deaths are usually linked to malignant tumors.
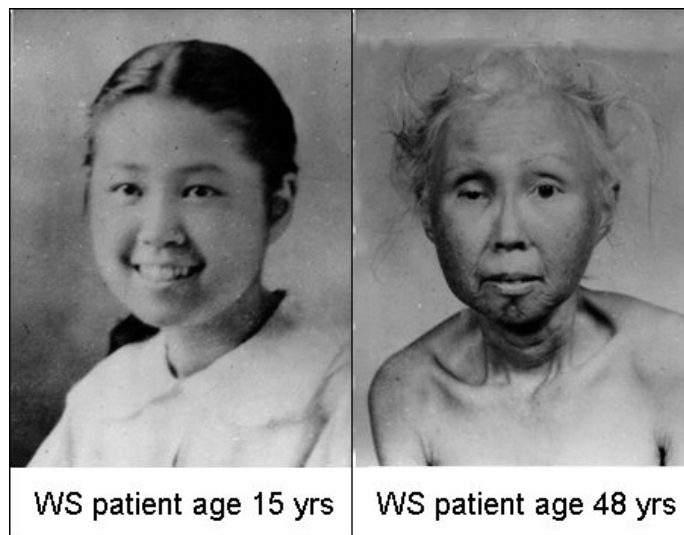
Figure 1.3: *Pictures of Werner's syndrome patients.*

To gain a better understanding of Werner's syndrome, we start at the cellular level. Fibroblasts from Werner's syndrome patients can only achieve roughly 20 population doublings, which is 40 population doublings less than normal human fibroblasts. The limited lifespan of Werner's syndrome patients is caused by a genomic instability, such as chromosomal aberration [35], large spontaneous deletions of the DNA sequence, which cause accelerated telomere loss, attenuated apoptosis and mutations in telomerase. Report on patient with

Werner's syndrome from 1939-1995, show that most have cancer [36]. Because Werner's syndrome cells exhibit genomic instability, telomere dysfunction (loss of end-capping structure or loss of telomeric repeat sequence), promotes the early onset cancer [37].

The molecular pathway of Werner's syndrome is unknown, though several hypotheses have been proposed, such as mutator phenotype, in this the Werner's syndrome patient developed chromosomal aberration, deletions [38], and a higher somatic mutation rate [39]. There is strong evidence that Werner's syndrome accelerates a cell's journey to senescence. Experiments in [40] have shown dramatic shortening of telomeres in Werner's syndrome fibroblasts and B-lymphoblastoid cells happen faster than in normal fibroblasts and B-lymphoblastoid cells. This suggests that dramatic telomere shortening can trigger cell senescence earlier in Werner's syndrome. Other observations include that when a population of Werner's syndrome cells becomes senescent, it has a wide range of telomere lengths 3.5 k to 18.5 k basepairs. This is a much wider range than from a population of normal cells typically 5.5 k to 9 k basepairs. A possible explanation for this is that Werner's syndrome cells contain some critically short telomeres whereas most cells contain chromosomes with longer telomeres. Telomere dysfunctions occur due to critically short telomeres; in the absence of recombination, this would trigger senescent [41].

Another hypothesis proposed in [42] is that a mutation in the Werner Syndrome gene (WRN) plays an important role in Werner syndrome. WRN lies on chromosome 8 in humans and is a member of the RecQ helicase family. RecQ helicase play an important role in DNA repair, maintenance of genomic instability and homologous recombination [42]. This is the one of the most important physiological roles of the WRN protein.

Thus Werner's syndrome can be used as a model for accelerated ageing. In Chapter 3 we combine the abrupt telomere shortening caused by Werner's syndrome and with normal ageing. Since the molecular pathway for Werner's syndrome is unknown, we assume that telomere shortening can happens at either

end of chromosomes.

Until now we have focussed on the telomere shortening or abrupt shortening and how this may shortening our lifespan. Now we focus on in germline and immortal cells in which telomere length can be maintained or extended in a number of different ways, such as telomerase and alternative lengthening of telomeres (ALT). We introduce these ideas in the following section.

1.7 Telomerase

Telomerase is an enzyme which has two major components: the telomerase reverse transcriptase TERT and the template RNA component (hTR or hTERC). These can be encoded to provide a template to add telomeric repeat sequences to chromosomes which lengthen the telomere [8]. Telomerase action was initially discovered in 1985 by Greider and Blackburen. When they extracted it from Tetrahymena cells and added it into the oligomer (the telomere primer), then they observed that telomeric GGGGTT repeats were added to the 3′ ends.

The amount of telomerase in a normal human cell is limited, except during early fetal development [43]. For immortal cells (with long or indefinite life spans) such as germline cells and most tumor cells, telomerase activity is high and easy to detect [44] [45]. The direct evidence for telomerase increasing telomere length in human cells was gained by co-culturing telomerase negative cells with telomerase expressing cells. The lifespan of co-culturing telomerase negative cells was extended by at least 20 population doubling [46]. This suggests that telomerase can extend human life. The principle by which human telomerase is believed to act is by adding specific DNA sequence repeats TTAGGG onto the 3′ ends of chromosomes.

The pathway describing telomerase activity has yet to be identified. Some experiments suggest that telomerase does not act on all telomeres at each cell cycle and that telomere elongation depends on telomere length, with shorter

telomeres elongating more frequently than longer ones [47] [48]. The action of telomerase on shorter telomeres is large and can rapidly lengthen them [49]. Some experiments suggested that, in human tumor cells, telomerase acts on most leading and lagging daughter chromosomes in a manner that is independent of telomere length [50]. These results indicate that telomere length is not the only factor involved in activating telomerase. In the stochastic and deterministic telomerase models of Chapter 5, we focus on how telomerase extends cell proliferation in normal ageing. We not only assume that the telomere gain caused by telomerase is fixed, but also consider cases for which the amount of telomere gain also depends on telomere length.

Thus, the telomere exists in an equilibrium between a telomerase-extendible state, which allows telomere extension, and a non-extendible state. This balance is called telomere length homeostasis [48] [51]. The longer the length of a telomere the higher the probability that it is in the non-extendible state. The shorter the telomere the higher the probability that it is in the extendible state. The mechanism regulating telomere length homeostasis is that, longer telomere normally switches to a non-extendible state which cannot be lengthened via telomerase. In that state, telomere length keeps decreasing due to the end replication problem. When the telomere length reaches a lower limit, the telomere switches to the extendible state, in which telomerase can lengthen the telomere. As the telomere length gets longer, the cycle will repeat.

1.8 Alternative lengthening of telomeres (ALT)

Telomerase plays an important role in maintaining the telomere length, but it is not the only mechanism. There is some evidence that, in the absence of telomerase activity, some immortal cells and tumor cells maintain their telomere length by a mechanism called alternative lengthening of telomere (ALT) [52] [53].

Telomere recombination can be observed experimentally by inserting two or

three DNA tags into the telomere of ALT cells, at population doubling 23. After population doubling 63, the number of tagged telomeres in the cell increases to 10 [54]. These results indicate that telomeric recombination has occurred. The ALT events involve recombination, but details of the mechanism by which this occurs remain unclear. Two alternative hypotheses have been proposed.

Some people have proposed that recombination can be achieved without copying telomeric sequences, by using unequal sister chromatid exchange instead. This can also extend proliferation [55]. Equal sister chromatid exchange can not affect the cell's proliferation. Unequal sister chromatid exchange increases the total number of cells which leads to longer proliferation. For another people have proposed that telomere elongation can be achieved by using existing telomeric sequence from other chromosomes as a template [56], this causes a net gain in telomeric sequences.

1.9 Mathematical modelling of cells proliferation

Levy *et al.* [1] modelled telomere shortening due to the "end-replication" problem by developing a single chromosome model. When the chromosome is duplicated, the new chain in the daughter chromosome is shortened by a constant amount on the 5' end due to the unidirectional synthesis of a new chain. Their model predicts that the average telomere length decreases linearly with generation number and is consistent with experimental data. They also determined the fraction of dividing chromosomes. In our model of normal ageing (Chapter 2), we also assumed that the "end-replication" problem causes the telomere shortening. Our chromosome model (Case I) is similar to Levy's model; we fix the amount of telomere shortening during each replication and we obtain the mean telomere length and the fraction of replicating chromosomes. We also determine a cell-level model in which each cell contains 46 chromosomes.

Arino *et al.* [57] extended Levy's work, by assuming that the lifespan of individual cells were independent (which is more realistic) and termed a cell senescent

if the length of the shortest telomere in the cell fell below a critical value. In our stochastic cells models (Chapters 2 and 3) we also use the shortest telomere in the cells to determine cell senescence. In Arino's model they assumed constant telomere loss and viewed cell proliferation as a branching process. They fitted their model to two sources of the data, obtaining good agreement in both cases. Oloffson and Kimmel [58] extended Arino's model, to allow for cell death. Since the cells die without replication, they obtained that the cells no longer growth exponential. The models developed in this thesis do not consider cell death, all cells are assumed to exist in one of two states: replicating and senescent. Once a chromosome becomes senescent it will remains in that state in the absence of telomerase activation.

The three models described above are based on the assumption that all chromosomes lose the same amount of telomere on each division. The stochastic and deterministic model of normal ageing that we developed are also based on this assumption (see Case I in Chapters 2 and 4 respectively). Motivated by Levy and Arino's work, Rubelj [59] developed a stochastic model in which there was gradual telomere shortening and also abrupt telomere shortening. Abrupt telomere shortening occurs in the telomeric border region and is more common among short chromosomes. When abrupt telomere shortening occurs, the cell will only replicate a certain number of times. In order to prevent all cells having the same proliferative potential, Rubelj assumed that there was a non zero probability that a replicative cell did not divide and that this probability was proportional to the cell's age. Results predicted that in the later generations (before all the cells had become senescent) the distribution of telomeres is bimodal. This prediction is qualitatively different from that obtained the gradual telomere shortening model. Guided by Rubelj's work, when we simulated Werner's syndrome (Chapter 3), we assume that there is the constant loss of telomeres (caused by normal ageing) and the probability of extra loss (caused by Werner's syndrome). The resulting stochastic cell model also exhibits a distribution of telomere length that is bimodal at later generations.

In addition to the "end-replication problem", oxidative stress, somatic muta-

tions in nuclear and mitochondrial DNA are all causes of telomere shortening. Sozou and Kirkwood [60] used oxidative stress to measure the rate of telomere shortening and introduced somatic mutations as a secondary cause of senescence. In their simulations the level of oxidative stress is assumed to depend on the numbers of mutant mitochondrial with in a cell. They used the numbers of normal and damaged mitochondria in the cell and the probability of a mitochondrion suffering a mutation during cell replication, to estimate the proportion of mitochondria that are damaged. They assumed that the telomere shortening rate is linearly proportional to the damage rate. They modelled somatic mutations by assuming a small nuclear mutation rate per cell cycle. This means that if a cell suffers a somatic mutation, then it will only replicate certain number of times. The simulation results obtained from their stochastic models fit the experimental data well. Sozou and Kirkwood also stochastically modelled a variety of oxidative stress, somatic mutation and mitochondrial DNA separately, to see how each change affects the cell senescence.

Kirkwood and Proctor modelled telomere shortening due to oxidative stress [61]. The main mechanisms for telomere loss is still assumed to be the "end-replication problem". However, there is additional loss associated with processing the single-strand breaks. Single-strand breaks happen during replication and can occur anywhere on the parent telomere, affecting telomere length. They also assumed that the frequency of single-strand breaks depends on the level of oxidative stress. Their model agrees well with experimental data, predicting that under oxidative stress, single strand breaks play an important role in telomere shortening. In later work Kirkwood and Proctor [62] extended this model [61] by distinguishing between capped and uncapped states, assuming that uncapped telomeres will not replicate. The probability of being uncapped is modelled via a Hill function which depends on telomere length. Their improved stochastic model exhibits results which are similar to original one, but give further insight into how the capped state affects ageing.

Richter *et al.* [63] incorporated DNA repair as a positive feedback mechanism into their model of telomere shortening. They model the telomere shortening

rate, y, as follows

$$y = y_0 + y_1 \, \text{ROS} - y_2 \text{DNA repairs} \, ,$$

y_0 as a constant caused by the end replication problem, y_1ROS is a loss of telomere due to reactive oxygen species (ROS), y_2 is the DNA repair rate which varies depending on the level of DNA damage, more damage leading to more repair. Since there is maximum rate at which DNA repairs can occur, a sigmoid function is used. The model accounts for uncapping in a similar way to that used by Proctor and Kirkwood [62]. The resulting simulation also fits the experimental data well.

While many mechanisms are known to cause telomere shortening, the exact rate of shortening is still unclear. Most mathematical models assume a constant rate of telomere loss; recently Buijs *et al*. [64] modelled telomere shortening as dependent on telomere length itself. They assumed a telomere loss rate which was linearly dependent on telomere length, so that

$$\text{telomere loss} = \text{constant} + \text{telomere length} \times \text{factor} \, .$$

where the constant loss is caused by the end-replication problem and the second term is attributed to a shortening factor which can be estimated by comparison with experimental data. These results confirm that telomere shortening is dependent on telomere length.

Portugal *et al*. took a different approach, developed a stochastic model in which telomere shortening occurs at a constant rate and the probability of cell division depends on the telomere length [65]. The probability of division is assumed to be proportional to the difference between telomere length and a critical length. The resulting stochastic model yields approximately Gompertzian growth in which cells have a replication rate that decreases linearly with telomere length.

Motivated by Levy *et al*. [1], Buijs *et al*. [64] and Portugal *et al*. [65], in this thesis we consider four different rules or models for describing cell division and telomere shorting in the stochastic and deterministic models presented in

Chapter 2 and 4. First, a constant telomere loss model with a constant cell division rate; second, a length-dependent telomere loss model with a constant cell division rate; third, a constant telomere loss model with length-dependent division rate; fourth, a length-dependent telomere loss and length-dependent dividing rate which is new.

Blagoev developed a mathematical model to study the effect of telomerase activity on cell proliferation [66]. At each cell division, the rate of telomere loss was assumed to be of the form

$$\text{telomere loss} = \text{constant loss} - \text{telomere gain} \times \text{extension probability}.$$

The extension probability was determined on the basis of three independent probabilities, namely, the probability that the telomere was in an extendible state (in an open state telomerase can associate with the telomere), the probability of telomerase associating with the telomere and the probability of telomerase being in the neighborhood of the telomere. They performed simulations for telomeres which were shorter and longer than the equilibrium length. They found that after several replications, both systems approach the same steady state length. In Chapter 5 we developed a model that incorporates telomerase and which differs from that of Blagoev, by using a different telomere loss and gain terms. In our model we assume that telomerase acts on the telomere all the time. We start by considering the simplest case for which the net amount of telomere loss per replication is equal to the constant telomere loss (due to ageing) minus a constant telomere gain (due to telomerase). We then extend the model by assuming that both telomere shortening (due to ageing) and telomere extension (due to telomerase) are telomere length dependent. The new model converges to an equilibrium length which is consistent with the Blagoev model.

1.10   Outline of Thesis

Since telomere length is a key factor in determining a cell's proliferative potential, our aim in this thesis is to investigate the mechanisms that regulate telomere length and to understand how telomere shortening affects the ageing pro-

cess. We use a combination of discrete/stochastic and deterministic/continuum models to study the dynamics of telomere length in a single cell in order to understand normal ageing, Werner's syndrome and immortal cells. The thesis is divided into five further chapters as follows.

In Chapter 2, we consider stochastic models of normal ageing. Our Monte Carlo simulations are applied to four cases by not only consider the telomere shortening but also the probability of cell divisions in both chromosomes level and cell level.

In Chapter 3, we consider a stochastic model of Werner's syndrome. We not only consider the case where Werner's syndromes occurs every generation, but also the case where Werner's syndrome occurs stochastically combined with normal ageing.

In Chapter 4, we developed continuum models of normal ageing, using the four different cases as in Chapter 2. We determined the models in both chromosomes level and cell level.

In Chapter 5, we consider the telomere lengthening caused by telomerase. We introduce Monte Carlo simulations and continuum models for two different cases. Case I, there is a constant telomere loss (normal ageing) with a constant telomere gain (due to telomerase). Case II, there is length-dependent telomere loss (normal ageing) with length-dependent telomere gain (due to telomerase).

In Chapter 6, we review the thesis, summarize our results we and suggest the directions for future work.

Stochastic simulations of normal ageing

2.1 Introduction

In order to understand why people age, we start from the basic unit of the human body: the cell. Each human cell contains 46 chromosomes. Chromosomes carry genetic material, namely DNA, and protein. The region of repetitive DNA at the end of the chromosomes, called telomeres [8], protect against the loss of genetic material and regulate chromosome fragments rejoining each other. When the telomere length is critically short, chromosomes become uncapped, which leads to end-to-end fusions, chromosome breakage, or rejoining. Therefore chromosomal instability depends on the telomere state and length.

Before cell division, the two strands of the DNA are separated at a certain origin under the influence of proteins, forming a "bubble". Replication proceeds either as an unidirectional or a bidirectional process from the bubble. During replication, the double-stranded DNA splits into two single strands at the origin, forming a Y-shaped replication fork (see Figure 2.1).

Figure 2.1 illustrates how replication starts at the 5′ end and moves in the 5′ to 3′ direction on both the leading and lagging strands. As the replication process only occurs in the 5′ to 3′ direction of synthesis, on the leading strand, the new
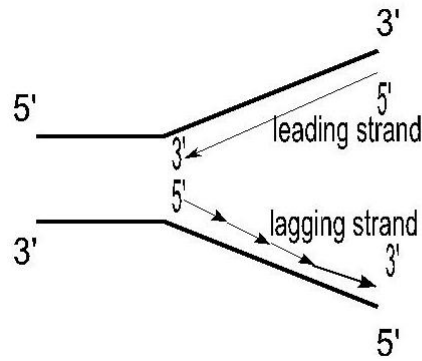
Figure 2.1: *Replication fork. As the fork moves left, opening the parent DNA, new bases are added to leading and lagging strands. The thick lines indicate the template strands. The thin lines indicate the replicated strands and the arrows show the direction of replication.*

sub-chain can be continuously synthesized since this in the same direction ($5'$ to $3'$), but on the lagging strand replication is more complicated. The sequence on the lagging strand cannot be constructed in the $3'$ to $5'$ direction. Instead, before replication a primase (RNA primer) must attach separately at the starting point and short sequences of $5'$ to $3'$ are formed, these discontinuous segments are called Okazaki fragments, being named after the person who discovered them. Eventually Okazaki fragments are linked by DNA ligase, which results a continuous stranded of DNA. After the lagging strand forms, the binding RNA primer is removed [15]. This results in a shortening of the telomere at the $5'$ end. This is called the end replication problem.

A number of basepairs are lost from one end of the chromosome due to incomplete replication of the DNA strand. During chromosome replication, normal chromosome replication produces one chromosome which is identical to its parent and one chromosome which is slightly shorter. To simplify the chromosome replication process illustrated in Figure 2.1, so that it can be modelled mathematically, we assume that m, h are the number of basepairs of the telomere at each end of the chromosome and we assume that y is the average number of basepairs lost per replication. The replication and division processes as shown in Figure 2.2.
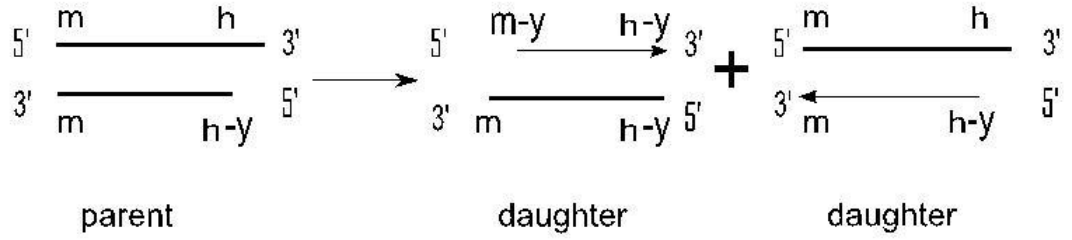
Figure 2.2: *Illustration of the effects of chromosome replication on telomere length. The thick lines indicate the template (parent) strands. Thin lines denote the replicated strands of the template in the daughter chromosomes and arrows indicate the direction of replication.*

In the parent chromosomes, as shown in Figure 2.2, the shorter strand of DNA is manufactured from the longer strand, which results in an inherited deletion of y basepairs at the $5'$ end. In each daughter chromosome one strand of DNA is from the parent, indicated by thick lines with telomere lengths of (m, h) at the left and right hand ends of the upper strand respectively and $(m, h - y)$ on the lower strand. The other strand is synthesized in a replication process, giving strand telomere lengths $(m, h - y)$ and $(m - y, h - y)$ respectively. The change in telomere lengths of both strands can be written more compactly as

$$\begin{pmatrix} m & h \\ m & h - y \end{pmatrix} \rightarrow \begin{pmatrix} m & h \\ m & h - y \end{pmatrix} + \begin{pmatrix} m - y & h - y \\ m & h - y \end{pmatrix}. \tag{2.1.1}$$

Cells have a limit growth, was first discovered by Hayflick and Moorehead [5] in the 1960s. When one of the telomeres of the chromosome falls below a threshold value, the chromosome stops replicating [12]. This lower level of the telomere length is called the critical value. If the telomere length of the chromosome is lower than the critical value, the cell remains in the senescent state. A chromosome can not divide forever, after several divisions it will stop replicating and become senescent due to telomere length restriction. Thus telomere length

is a key factor in determining a cell's potential for proliferation.

We consider the dynamics of telomere loss in a cell in order to understand the normal ageing process. In this chapter we perform Monte Carlo simulations of the the chromosome model and cell model (46 chromosomes). The amount of telomere lost per chromosome replication and the probability that a chromosome divides may varies. For example chromosomes with longer telomeres may lose more telomeres and have a greater probability of dividing than those with shorter telomeres see [64] and [65]. Therefore we consider four different cases of the model. In Case I a fixed amount telomere loss every generation. In Case II, telomere loss dependent on the telomere length; in Case III, a fixed amount of telomere is lost, but cell-division occurs with a probability dependent on telomere length. Case IV is a combination of Case II and Case III, where telomere loss and the probability of cell division are dependent on telomere length. In each case we are interested in the average telomere length of the chromosomes and the fraction of the dividing chromosomes (or cells).

All the models presented in this section are based on the following assumptions: first, there is no telomere elongation during the chromosome replication, such as that caused by telomerase activity and there are no recombination events between telomeres, etc. Second, a cell can only exist in one of two states: a dividing state or a senescent state. When a cell becomes senescent, it will remain in that state: it can not start dividing again. We do not consider cell death in the system.

Iteration number can be defined as follow: if there are 200 cells in the initial state, in the first iteration we check every cell to see whether it can divide. If a cell can divide, it produces two daughter cells, both of which will be present in the next iteration. If a cell cannot divide, it remains in the next iteration. Then one iteration has occurred. In many experiments the population doubling time is the time-scale of interest [67]. The population doubling is the time required for the cell number to double. For example, if there are 200 cells initially and the population increases to 400 cells, then one population doubling has occurred.

In the simulations presented in this thesis, we used generation number = iteration number, as the time-scale of interest due to its mathematical simplicity. We note, however, that in the literature, generation number is sometimes taken to mean population doublings. The duration of "a generation" we use is fixed, whereas the population doubling time varies as cells age due to cells becoming senescent. Generation time and population doubling are identical initially if all cells are able to divide, otherwise one population doubling time is longer than one generation time.

2.2 The chromosome model

2.2.1 Tracking one chromosome in each generation

To simulate telomere shortening in a single chromosome, we use the chromosome replication rule (2.1.1) and fix zero as the critical value of the telomere length at which cells become senescent. We consider a chromosome with initial telomere lengths of $m = h = 6000$ basepairs and a loss rate of $y = 200$ basepairs per replication. Putting these values of m, h, y in (2.1.1), the average telomere length of the parent chromosome is 5950 basepairs ($[6000 + 6000 + 6000 + (6000 - 200)] \div 4 = 5950$). Before chromosomes reach senescence, we expect exponential growth in their number, however, due to the restrictions of computer memory, we randomly pick one of the two daughter chromosomes. Let randomly picked chromosome replicate and then randomly pick one of two chromosomes. Repeated this process many times until the length of the telomere becomes too short for replication to occur (when the telomere length falls below the critical value). The chromosome then stops replicating and becomes senescent. During each generation we record the telomere length of the chromosomes.

In order to see how telomere length varies with generation number, we perform 8000 simulations. Figure 2.3 shows that as the generation number increases, the average telomere length of the population decreases from 5950 basepairs to 150 basepairs. Thereafter the average telomere length remains the same, indicat-
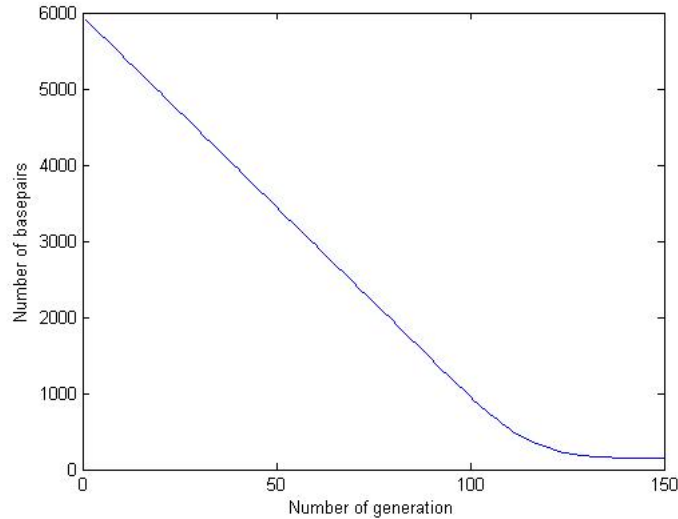
Figure 2.3: *The average telomere length of 8000 simulations plotted against generation number for the single chromosome model. Parameter values: $m = h = 6000$ basepairs and $y = 200$ basepairs per replication.*

ing that replication has halted and that the population has become senescent. Between generations 1 and 100, telomere length decreases linearly with generation number, indicating that the average rate of telomere loss during this stage is constant. After generation 100, the curve plateaus to a constant value of about 150 basepairs where telomere loss halts. The results presented in Figure 2.3 were obtained by setting $y = 200$ basepairs per replication, which corresponds to an average loss of $y/4 = 50$ basepairs per telomere per generation. A naive calculation suggests it would take about 119 generations for a telomere of length 5950 basepairs to shorten to length zero and become senescent. In practice random selection of the daughter chromosomes causes a small delay in the time takes to reach senescence.

The case present here is the simplest one, where telomere loss and the probability of chromosome divides are both constant. We introduce four cases, to investigate the effect of making telomere loss and the probability of division.

23

2.2.2 Unified view of Cases I-IV

If we denote by K_n^g the number of chromosomes with telomere length n at generation g and by y the number of basepairs that are lost when a cell divides, then by applying the replication rule (2.1.1), we deduce that the discrete chromosome replication process can be written as

$$K_n^g \rightarrow K_n^{g+1} + K_{n-y}^{g+1}, \quad \text{with probability } P_{div}. \tag{2.2.1}$$

In practice the amount of telomere lost (y) per chromosome replication may vary. For example, chromosomes with longer telomeres may lose more telomere than those with shorter telomeres (see [64] and [65]). We denote by $Y(n)$ the amount of telomere lost from a telomere of length n. We postulate that $Y(n)$ is linearly dependent on the telomere length at generation $(g-1)$, so that,

$$Y(n) = y_0 + y_1 n, \tag{2.2.2}$$

where y_0 and y_1 are constants.

In practice the probability that a chromosome divides may not always be constant and chromosomes with longer telomeres may have a greater probability of dividing than ones with shorter telomeres. Therefore, we assume the probability of a chromosome dividing, $P_{div}(n)$, is dependent on the chromosome's telomere length n where $0 \leq P_{div}(n) \leq 1$. We postulate the form

$$P_{div}(n) = (a + bn)^\alpha, \tag{2.2.3}$$

where a and b are constants, α is a parameter which controls P_{div}, with $0 \leq \alpha \leq 1$.

In order to see clearly how changes in average telomere lengths depend on telomere loss $Y(n)$ and the probability that a chromosome divides $P_{div}(n)$, we consider 4 different cases, as outlined in Table 2.1.

Case I is the simplest, with a constant telomere loss (y_0) basepairs per division and fixed probability of cell division ($P_{div} = 1$). Case II is slightly more complicated than Case I, telomere loss now depending on telomere length ($y(g) =$

Case	$P_{div}(n)$	$Y(n)$
Case I	$P_{div}(n) = 1$	$Y(n) = y_0$
Case II	$P_{div}(n) = 1$	$Y(n) = y_0 + y_1 n$
Case III	$P_{div}(n) = (a + bn)^\alpha$	$Y(n) = y_0$
Case IV	$P_{div}(n) = (a + bn)^\alpha$	$Y(n) = y_0 + y_1 n$

Table 2.1: 4 cases where parameters a, b, α, y_0, y_1 are constant.

$y_0 + y_1 n$) although the probability of cell division remains fixed. For Case III, we assumed that telomere loss occurs at a constant rate as for Case I. However the probability of cell division depends on telomere length $P_{div} = (a + bn)^\alpha$. For Case IV both the rate of telomere loss and the probability of chromosomes replication depend on telomere length. If the parameters y_0, y_1, α, a, b are chosen appropriately, Cases I, II and III can be considered as special cases of Case IV: Case I is recovered from Case IV when $y_1 = 0$ and $\alpha = 0$. Case II is obtained by fixing $\alpha = 0$ and Case III when $y_1 = 0$. Simulation results for these 4 cases are presented below.

2.2.3   Pseudocode for the simulations

Definitions of variable and parameter: N = "the number of chromosomes in the cell", $NGen$ = "the number of generations to be simulated", Data(i).NumCell = "the number of cells at generation i", Data(i).Chrom stores the telomere lengths of the four ends of the chromosome in generation i. The pseudocode used in this chapter are listed below:

```
Data(1).NumCell=1;  %Initial number of cells
Data(1).Chrom=Initial telomere length of each chromosomes in a cell;
y0, y1 determine amount of telomere loss;
a, b,  alpha determine probability of cell replication;
for i=2:NGen %First main loop;
    nc=0; % counter for the number of cells.
    %Consider replication of each cell;
    for j=1:Data(i-1).NumCell %Second main loop;
```

```
n=mean(Data(i-1).Chrom(:,:,j)); %average telomere length.
y=y0+y1*n; %telomere loss function y.
P=(a+b*n)^{alpha}; %probability of cells dividing
If telomere length exceeds critical value and
    random number < P (probability of cell division);
    Then cell divides;
    for each chromosomes generate two daughter chromosomes
    and allocate daughter chromosomes randomly to
    daughter cells;
else
    cell remains same in next generation if cell does
    not divide;
end
end % end of second loop-replicating cells;
If number of cells over 200, we need passage: randomly select 200.
end % end of first main loop - generation number.
```

This is one simulation, we can repeat this to obtain average telomere length and the average fraction of senescent cells. For the chromosome model we pick $N = 1$ and for the cell model we pick $N = 46$ instead. To simulate for each case, we need to choose specific parameter values for y_0, y_1 and a, b and α separately. More infirmations about the MATLAB code is listed in Appendix A.1.

2.2.4 Case I: Constant loss of telomeres

Our simulations start with a single chromosome and we track its progeny over each generation until the total number of chromosomes exceeds 200. We then passage by randomly selecting 200 of these chromosomes. In the next generation, all chromosomes divide (if their telomeres are sufficiently long to allow replication), and when the population exceeds 200, we passage so that once again 200 chromosomes are selected from the population. This process is repeated until all telomere lengths are too short to allow further replication. At this stage the entire population is senescent. We use the same simulation method as in Section 2.2.3, with parameters $y_1 = 0$ and $\alpha = 1$.
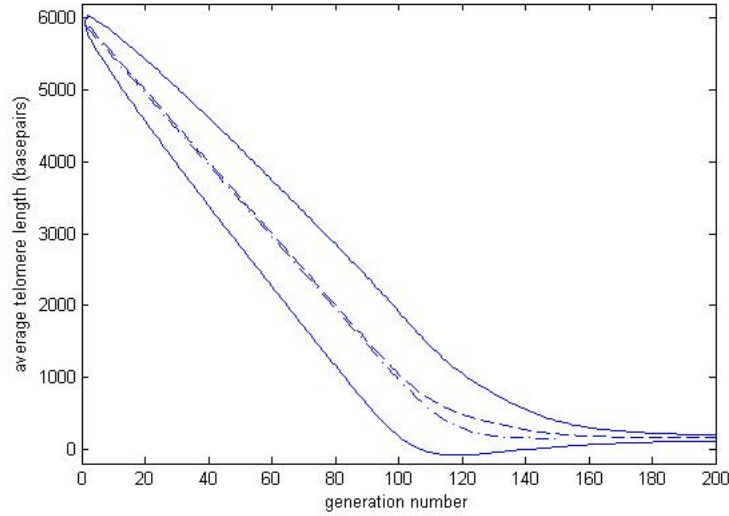
Figure 2.4: *Averaged results of 1000 simulations; the dashed line is the average telomere length plotted against generation number of passaging model, the solid lines indicated two standard deviations above and below the mean. The dash-dotted line shows how the average telomere length varies with generation number for the earlier single chromosome model. Both models use the same parameters, m = h = 6000 and y = 200.*

At each generation we record not only the average telomere length but also the number of chromosomes that have just replicated. We denote by $N(g)$ the number of chromosomes at generation g, $\phi_{div}(g)$ represents the fraction of dividing chromosomes at generation $(g-1)$ and $\phi_{sen}(g)$ the fraction of senescent chromosomes at generation $(g-1)$, so that

$$\phi_{div}(g) = \frac{N(g) - N(g-1)}{N(g-1)}, \quad \phi_{sen}(g) = 1 - \phi_{div}(g). \tag{2.2.4}$$

For comparison with the ageing model presented in Section 2.2.1, we performed simulations, fixing $m = n = 6000$ basepairs for the initial chromosomes and assuming $y = 200$ basepairs are deleted during each replication.

Figure 2.4 shows that as the generation number increases, the average telomere length decreases, reaching a value of 150 basepairs after about 150 generations. Thereafter, the average telomere length remains constant, which indicates that

replication has stopped and that senescence has occurred. Comparison of the dashed line and the dash-dotted line shows good agreement between the cell passaging model and the earlier model of telomere shortening in a single chromosome. Figure 2.4 also shows how the standard deviation increases as the generation number increases, reaching a maximum value of 450 at generation 90 before decreasing almost to zero at generation 180.

(a)   (b)
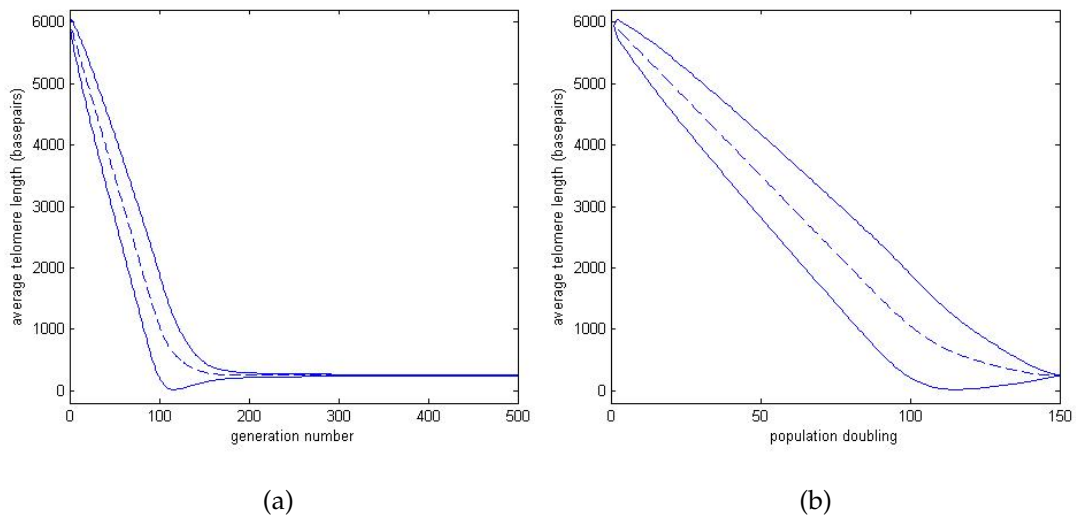
Figure 2.5: *In Figure 2.5(a), the dashed line shows how the average (over 1000 simulations) of telomere length per chromosome varies with generation number, the solid line above (below) the dashed line is the average telomere length plus (minus) twice the standard deviation. Figure 2.5(b) use the same simulation data from Figure 2.5(a). In Figure 2.5(b), the dashed line shows how the average of telomere length per chromosome varies with population doublings, the solid line above (below) the dashed line is the average telomere length plus (minus) twice the standard deviation.*

In Figure 2.5 we represent the results from Figure 2.4 in order to show how the average telomere length changes with generation numbers (2.5(a)) and population doublings (2.5(b)). In Figure 2.5(b), for the first 100 population doublings, the average telomere length decreases linearly as the number of population doublings increases; thereafter the average telomere length slowly asymptotes to 200. We note also that the number of population doublings approaches 150 when the generation number approaches 500. This is because when some of the chromosomes are senescent, it takes more than one generation to achieve

population doubling.

(a)   (b)
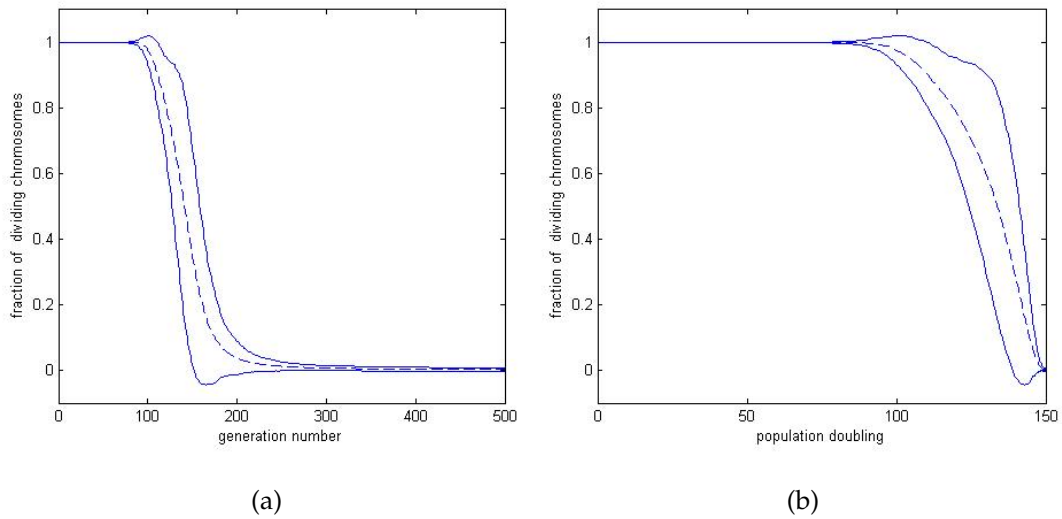
Figure 2.6: *Average results of 1000 simulations. In Figure 2.6(a), the dashed line is the fraction of dividing chromosomes plotted against generation number, the solid lines indicate two standard deviations above and below the fraction of dividing chromosomes. Figure 2.6(b) uses the simulation data from Figure 2.6(a). In Figure 2.6(b), the dashed line is the fraction of dividing chromosomes plotted against population doubling, the solid lines indicate two standard deviations above and below the fraction of dividing chromosomes.*

In Figure 2.6 we show how, for the simulation results presented in Figure 2.5, the fraction of dividing chromosomes changes with both generation number and population doubling. Figure 2.6(a) shows that from generation 1 to 90, all chromosomes are replicating. Comparing Figures 2.5(a) and 2.6(a) we note that during this period the rate of loss of telomere is constant. After generation 90 some chromosomes stop replicating and the fraction of senescent chromosomes rapidly increases from zero. After generation 180 the dashed line tends to zero slowly, as the fraction of senescent chromosomes approaches unity. This explains why the standard deviation plotted in Figure 2.5(a) changes with generation number in the manner observed. Between generations 9 and 90, all 200 of the randomly selected chromosomes replicate to produce 400 chromosomes from which we select 200 for the next generation. At generation 90 the telomere length of some chromosomes has reached its minimum and they stop repli-

cating. Chromosomes with longer telomeres continue to divide, reducing the average telomere length and causing the distribution of lengths to approach a limiting vale and the standard deviation to fall. After generation 180 nearly all chromosomes are senescent. In this case any chromosomes that are 'randomly selected' maintain their minimum telomere length on each subsequent generation and therefore variation is close to zero. Figures2.6(b) shows how the fraction of dividing cells changes with population doubling rather than generation number. Before 90 population doubling, all the chromosomes replicate due to all chromosomes having significant longer telomeres during that period as shown in Figure 2.5(b). Thereafter some of the chromosomes become senescent, leading to a reduction in the proportion of dividing chromosomes until the entire population is senescent at approximately 150 population doublings.

2.2.5 Case II: Telomere loss depend on telomere length

In this section the simulations are similar to those presented in Section 2.2.4. We consider a single chromosome, with telomere length 5950 basepairs and passage it to senescence. The difference between these simulations and those of Section 2.2.4 is that the rate of telomere loss is non-constant (compare (2.1.1) and (2.2.2)). For comparison with the simpler case of a constant loss of telomeres at each generation, and in order to make the average telomere loss 200 basepairs per generation, we fix $y_0 = 100$ in (2.2.2). We choose y_1 so that the remaining 100 basepairs are lost by a telomere of length 2975 (the median telomere length), *i.e.*, $100 = 2975y_1$ hence $y_1 = 1/30$, so that (2.2.2) becomes $Y(n) = 100 + y_1/30$.

In Figure 2.7, we show how the average rate of telomere loss decreases with generation number when shortening is length-dependent. At earlier generations the average telomere length decreases more rapidly than for the constant loss model. However once the average telomere length falls below 3000 basepairs, the average telomere length decreases more slowly. After generation 180, the average telomere length for both models is similar as all chromosomes are senescent.
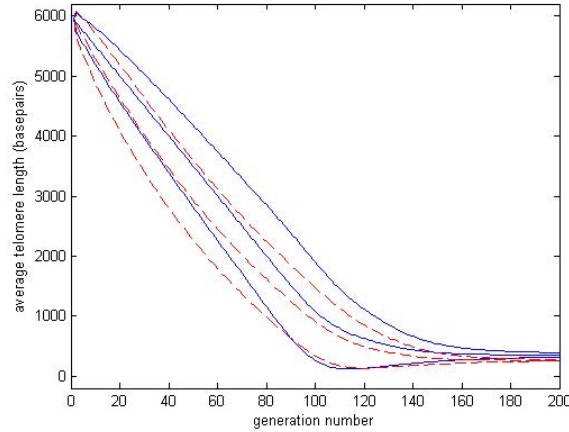
Figure 2.7: *Averaged results of 1000 simulations. The dashed lines indicate results of the passaging model with telomere length dependent shorting ($Y(n) = 100 + y_1/30$). The middle dashed line shows how the average telomere length varies with generation number , the dashed lines above and below indicated two standard deviations above and below the mean. The solid lines show how telomere shortening proceeds when telomere shortening is independent of length ($Y(n) = 200$). The middle solid line shows how the average telomere length varies with generation number and the solid lines above and below are the two standard deviations above and belove the mean.*

Figure 2.8 shows how the fraction of dividing chromosomes for the length dependent and constant loss models changes with generation numbers when telomere loss is length-dependent. Between generations 1 and 80 all chromosomes in both models divide because their telomeres are sufficiently long. After generation 80, the fraction of dividing chromosomes initially decreases more rapidly while telomere loss occurs at a constant, although the fractions are the same again by generation 160. For later generations, the fraction of dividing chromosomes in the length-dependent model decreases more rapidly than for the model with constant loss and their fractions of both models eventually approach zero. The model with constant telomere loss reaches senescence more rapidly for the following reason. The senescence starts around generation 80, at which time the length-dependent model loses $Y(n) = 100 + 1600/30 = 153$ basepairs per generation and then the telomere loss decreases from 153 to 100. Consequently telomere loss is much smaller than for the model with a con-

31
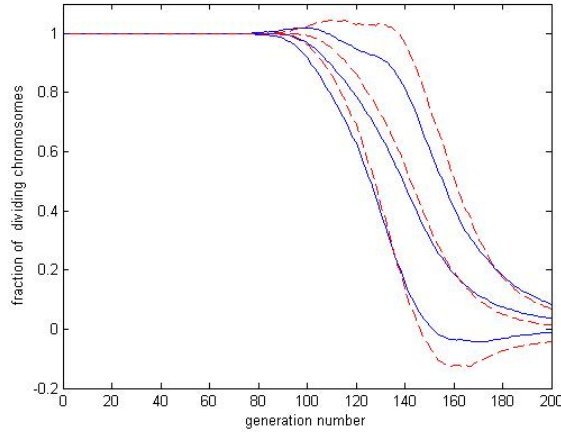
Figure 2.8: *Averaged results of 1000 simulations. The dashed lines indicate results of the passaging model with telomere length dependent shorting ($Y(n) = 100 + y_1/30$). The middle dashed line is the average fraction of dividing chromosomes plotted against generation number, the dashed lines above and below indicated two standard deviations above and below the average. The solid lines indicate the results of a passaging model with constant telomere loss per replication ($Y(n) = 200$). The middle solid line is the average fraction of dividing chromosomes plotted against generation number, the solid lines above and below indicated two standard deviations above and below the average.*

stant telomere loss of 200 basepairs event for the constant loss model has longer telomere length (400 basepairs) at generation 80.

In figures 2.9(a) and 2.9(b) we show how the average telomere length and the fraction of dividing chromosomes changes as the number of population doublings increases. Before 90 population doublings, all chromosomes replicate with an approximately linear reduction in average telomere length as the number of population doublings increases. After that, the fraction of dividing chromosomes decreases and approaches zero after approximately 160 population doubling by which time the average telomere length is approximately 250 basepairs.

(a)   (b)
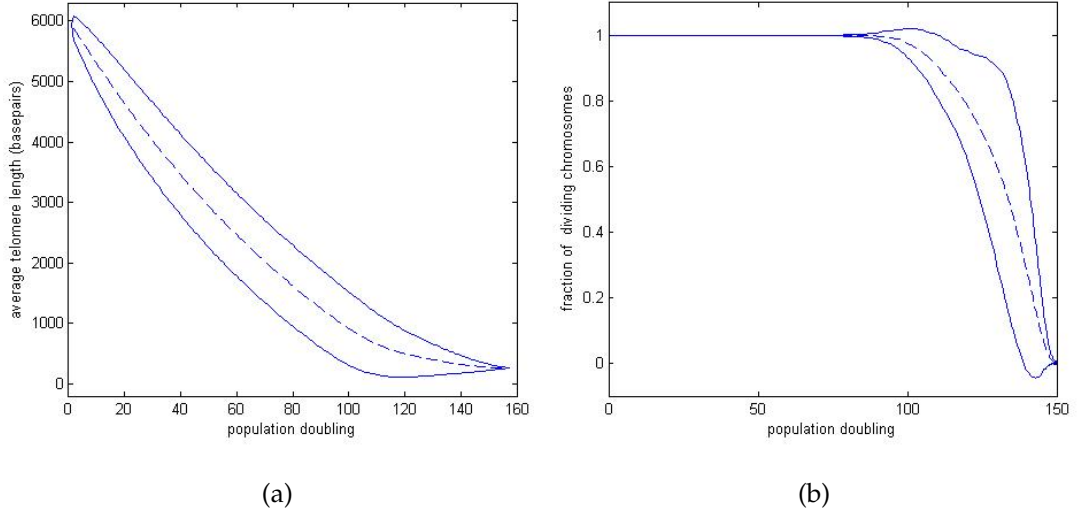
Figure 2.9: *In Figure 2.9(a), the dashed line shows how telomere length changes with population doublings when shortening is length-dependent (Case II of the average of 1000 simulations), the solid lines delineate two standard deviations above and below the average. Figure 2.9(b) uses the same simulation data from Figure 2.9(a). In Figure 2.9(b), the dashed line shows how the fraction of dividing chromosomes changes with population doubling, the solid lines indicated two standard deviations above and below the fraction of dividing chromosomes.*

2.2.6   Case III: Chromosome division dependent on telomere length

For cases I and II, we distinguish two types of chromosomes: those which can divide and those which are senescent. By contrast, for Case III since the probability of cell duration is no longer constant, we distinguish three types of chromosomes: those which have just divided, those which could have divided but did not divide and those which are senescent. We denote by $N(g)$ the number of chromosomes at generation g and by $\phi_{div_a}(g)$ the fraction of chromosomes that divided at generation $(g-1)$, so that

$$\phi_{div_a}(g) = \frac{N(g) - N(g-1)}{N(g-1)} . \tag{2.2.5}$$

At each generation, we monitor the telomere length of all $N(g)$ chromosomes and we use this information to determine how many cells are senescent (*i.e.* how many cells cannot divide because their chromosome are too short). We denote by $N_s(g)$ the number of chromosomes which are senescent at generation g. Then $(N(g) - N_s(g))$ represents the number of chromosomes which could

33

divide on the next generation. We denote by $\phi_{sen}(g)$ the fraction of senescent chromosomes at generation g and by $\phi_{div}(g)$ the fraction of chromosomes which could divide on generation $(g+1)$, so that

$$\phi_{sen}(g) = \frac{N_s(g)}{N(g)}, \tag{2.2.6}$$

$$\phi_{div}(g) = \frac{N(g) - N_s(g)}{N(g)}. \tag{2.2.7}$$

We denote by $\phi_{div_p}(g)$ the proportion of chromosomes which have the potential to divide, but do not do so at generation $g+1$, so that

$$\phi_{div_p}(g) = \phi_{div}(g) - \phi_{div_a}(g). \tag{2.2.8}$$

The simulations presented in this section are similar to those presented in Section 2.2.4. We start with a single chromosome with telomere length of 5950 basepairs, and passage its progeny to senescence. We denote by L_i the initial average telomere length of a chromosome and by L_c the critical telomere length of the chromosome. The new feature of these simulations is that the probability of chromosome division now depends on telomere length, as in (2.2.3) where we fix $L_i = 5950$ basepairs and $L_c = 200$ basepairs. For the simplest case, we fix $\alpha = 1$ so that P_{div} is linearly dependent on telomere length. We ensure that $0 \leq P_{div} \leq 1$ by choosing $a = -L_{critical}/(L_{initial} - L_{critical})$ and $b = n/(L_{initial} - L_{critical})$. With these choice, we have $P_{div} = (n - 200)/5750$. We estimate y, the assumed constant amount of telomeres lost per replication by requiring, for consistency with Case I, that an average telomere 200 basepairs are lost per replication. We assume further that this average loss rate is achieved when the telomeres are of length $L_{initial}/2 = 2975$. With P_{div} defined above, we estimate y by requiring $P_{div}(L = 2975)y = 200$, so that $y = 414$ basepairs. To summarize, for Case III we have $y = 414$ and $P_{div} = (n - 200)/5750$.

In Figure 2.10, the average telomere length for Case III is plotted against generation number and shown to decrease faster than Case I until about generation 90. This is because for Case III $Y(n) = 414$ which is more than twice the value used for Case I. The probability of replication P_{div}, decreases linearly with telomere length and before generation 90, $P_{div} > 1/2$, combining these
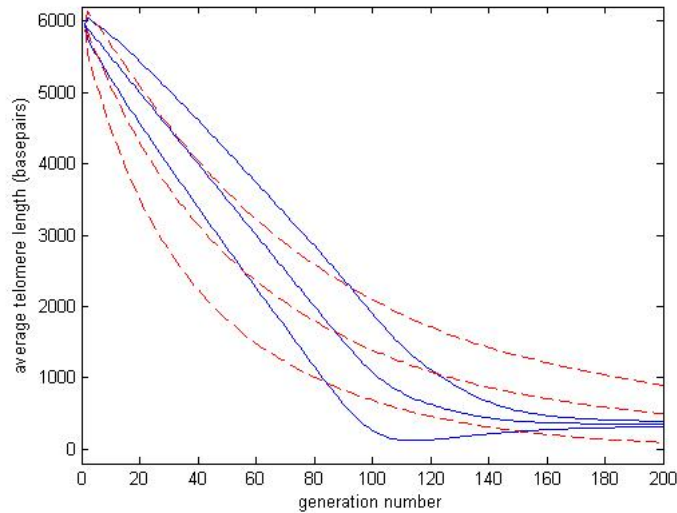
Figure 2.10: *Average results of 1000 simulations. The dashed lines indicate the results for Case III with $P_{div}(n) = (n - 200)/5750$ and a constant loss of $Y(n) = 414$ basepairs per replication. The middle dashed line is the average telomere length plotted against generation, the dashed lines above and below indicated two standard deviations above and below the mean. The solid lines indicate the results for Case I with a constant telomere loss of $Y(n) = 200$ basepairs. The middle solid line is the average telomere length plotted against generation number and the solid lines above and below are the two standard deviations above and belove the mean.*

results it is clear that the average telomere loss for Case III is greater than for Case I (200 basepairs) at least initially. When the telomere length decreases below 2975 basepairs, the average amount of telomere lost per generation for Case III is less than 200 basepairs. The average telomere length for both models reaches 1700 basepairs by generation 90. After generation 90 the average telomere length decreases faster for Case I than Case III, and by generation 180, the average telomere lengths of both models are similar and remain fixed thereafter because all cells are senescence.

Figure 2.11 shows how for cases I and III the fraction of dividing chromosomes $\phi_{div}(g)$ changes with generation number. For Case I, all chromosomes divide between generations 1 and 90. After that, some chromosomes become senescent and the fraction of dividing chromosomes decreases from 1, and slowly

35
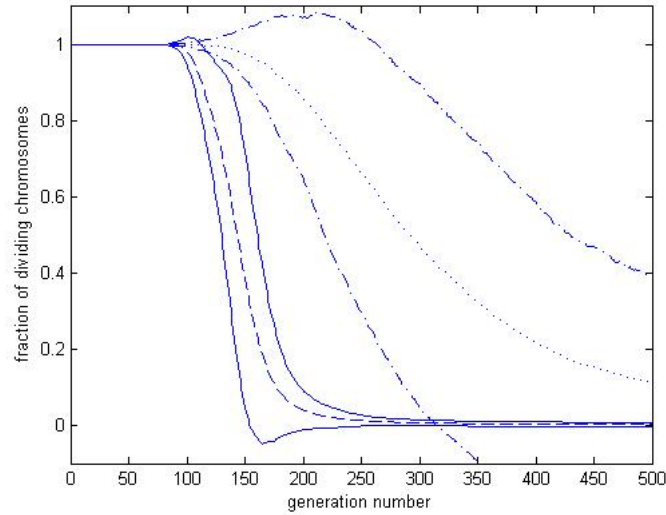
Figure 2.11: *Average results of 1000 simulations. The dotted lines indicate the mean fraction of dividing chromosomes $\phi_{div}(n)$ plotted against generation number for Case III with $P_{div}(n) = (n - 200)/5750$ and a constant loss of $Y(n) = 414$ basepairs. The dash-dotted lines above and below indicated two standard deviations above and below the mean. The dashed line indicates the mean fraction of dividing chromosomes plotted against generation number for Case I with a constant telomere loss of $Y(n) = 200$. The solid lines above and below indicate two standard deviations above and below the mean.*

approaches zero . For Case III, the cells do not become senescent until about generation 120 and 30 generations later than for Case I (see Figure 2.11). The reason for that is at generation 90, both models predict the same average telomere length 1700 basepairs (see Figure 2.10), but for Case III, after generation 90, $P_{div}(n) < 1/4$ ($P_{div}(n) < (1700 - 200)/5750$) which results cells in becoming senescent later than Case I. After generation 120, for Case III, some chromosomes become senescent and the fraction of dividing chromosomes decreases more slowly for Case III than Case I. The large increase in standard deviation with generation number arises because events with small probabilities occur over many generations.

In figures 2.12 we show how the proportion of each type of chromosome changes with generation numbers (a) and population doubling (b). At each generation

<center>(a)   (b)</center>
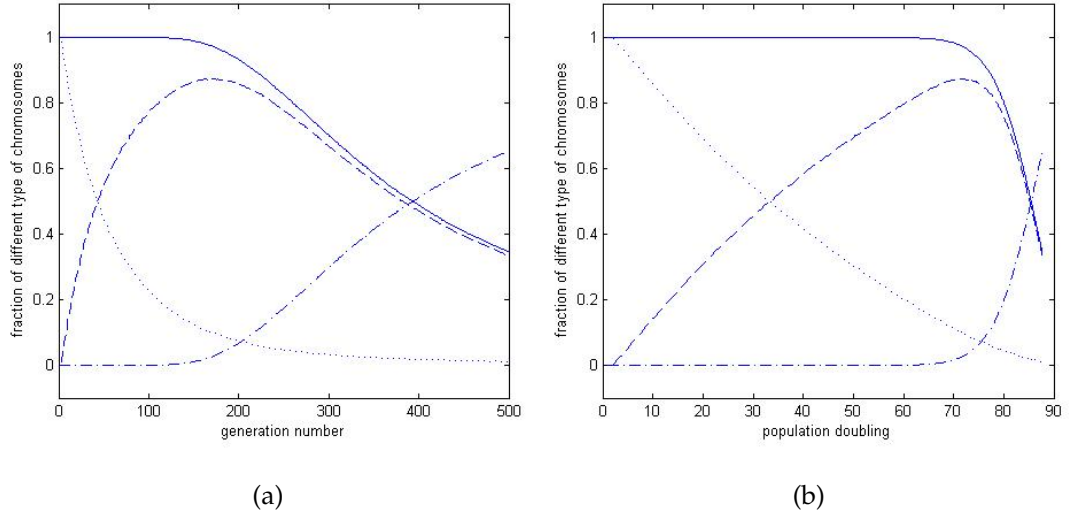
Figure 2.12: *Average results of 1000 simulations of Case III with $L_i = 5950$ basepairs, $P_{div}(n) = (n - 200)/5750$ and a constant loss of $Y(n) = 414$ basepairs. In Figure 2.12(a), the dash-dotted line indicates the fraction of senescent chromosomes ϕ_{sen} plotted against generation number. The dotted line indicates the fraction of chromosomes which actually divided ϕ_{div_a} in the previous generation. The dashed line indicates the fraction of chromosomes which still have the potential to divide but did not divide in the previous generation ϕ_{div_p} due to the probability of dividing. The solid line indicates the fraction of non-senescent chromosome ϕ_{div}. Figure 2.12(b) use the same simulation data from Figure 2.12(a). In Figure 2.12(b), the dash-dotted line indicates the fraction of senescent chromosomes ϕ_{sen} plotted against population doublings. The dotted line indicates the fraction of chromosomes which actually divided ϕ_{div_a} in the previous population doublings. Same notation as in (a).*

number, ϕ_{div} the fraction of dividing chromosomes which can replicate consists of chromosomes which divided (ϕ_{div_a}) and chromosomes which could have divided but failed to do so (ϕ_{div_p}). We note that the fraction of cells which actually divide ϕ_{div_a} decreases and that the proportion of senescent chromosomes ϕ_{sen} increases over time. The fraction of chromosomes which have the potential to divide, but do not do so ϕ_{div_p}, increases with generation numbers, attaining a max value at about generation 150 before declining to zero. This quantity decreases monotonically with generation number. As a check on our numerics we calculate the sum $\phi_{div_a} + \phi_{div_p} + \phi_{sen}$, noting that this quality should and is be equal to unity.

<center>37</center>

2.2.7 Case IV: Telomere loss and chromosome division depend on telomere length

From the literature review we know telomere length plays an important role in both telomere loss and chromosome division, so we develop a model with both telomere loss dependent on telomere length and chromosomes division depend on telomere length, which is a combination of Sections 2.2.5 and 2.2.6. The telomere loss rule follows (2.2.2) and the probability of chromosome divides follows (2.2.3).

For Cases I and II, we distinguish two types of chromosomes: those which can divide and those which are senescent. For Case III, we distinguish three types of chromosomes: those which have just divided, those which could divide but do not and those which are senescent. For Case IV, since the probability for chromosomes divides varies with telomere length, we again distinguish three types of chromosomes, as for Case III and we use (2.2.5)-(2.2.8) to calculate ϕ_{div_a}, ϕ_{sen}, ϕ_{div} and ϕ_{div_p} respectively.

The simulations performed in this section are similar to those in Section 2.2.4. We start with a single chromosome with telomere length 5950 basepairs and passage its progeny to senescence. We use telomere loss and chromosome division are both depends on telomere length, as in equation (2.2.2), (2.2.3) respectively. We fix $L_c = 200$ basepairs, $L_i = 5950$ basepairs and $\alpha = 1$, therefore $P_{div}(n) = (n - 200)/5750$. For a fair comparison, we must ensure that the average telomere loss is 200 basepairs per replication, we fix $y_0 = 207$ basepairs half the value used in Case III, the remaining 207 basepairs are lost by the form $y_1 n$, so to balance the median telomere length 2975 basepairs having a probability of $P = 1/2$, $207 = 2975 y_1$, yielding $y_1 \approx 1/14$. So $Y(n) = 207 + n/14$. For ease of comparison we summaries in Table 2.2. The expressions that we use for P_{div} and $Y(n)$ for cases I-IV.

In Figure 2.13, we compare cases I and IV. Initially the average telomere length for Case IV decreases faster than for Case I (*i.e.* until generation 92). This is

Case	$P_{div}(n)$	$Y(n)$
Case I	1	200
Case II	1	$100 + \frac{n}{30}$
Case III	$\frac{n-200}{5750}$	414
Case IV	$\frac{n-200}{5750}$	$207 + \frac{n}{14}$

Table 2.2: The summary of expressions for $P_{div}(n)$ and $Y(n)$ for cases I-IV.
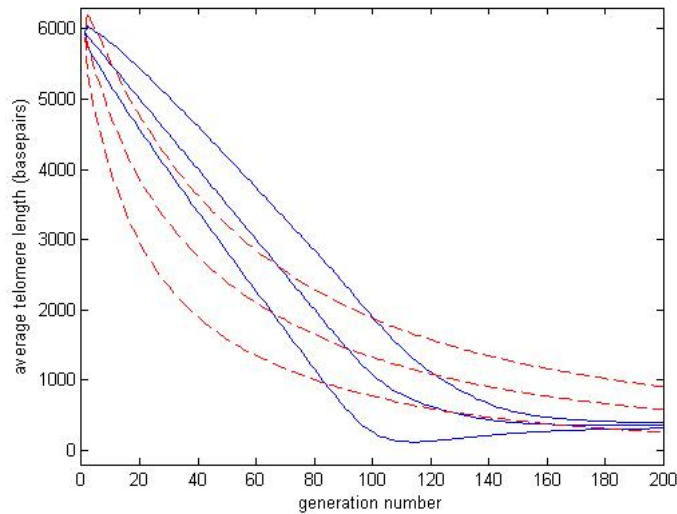
Figure 2.13: *Average results of 1000 simulations. The dashed lines indicate the results for Case IV with $P_{div}(n) = (n - 200)/5750$ and $y(g) = 207 + n/14$ basepairs. The middle dashed line is the average telomere length plotted against generation, the dashed lines above and below indicated two standard deviations above and below the mean. The solid lines indicate the results for Case I with a constant telomere loss of $Y(n) = 200$ basepairs. The middle solid line is the average telomere length plotted against generation number and the solid lines above and below are two standard deviations above and below the mean.*

because for Case IV $Y(n) = 207 + n/14$ and $P_{div}(n) = (n - 200)/5750$. When $L = 3075$ basepairs, $P_{div} = 0.5$ and $Y(n) = 426$ so that the average telomere loss is $P_{div}(n)Y(n) = 213$ basepairs. Consequently telomeres whose lengths n exceed 3075 basepairs have $P_{div}(n) > 0.5$ and $Y(n) > 426$, and as a result, the average telomere loss ($P_{div} \times Y(n)$) exceeds 200 basepairs, the average loss for Case I. For both cases the average telomere length reaches 1500 basepairs

at generation 92. For Case IV, when the telomere length reaches 1500 base-pairs, $P_{div}(n) = 0.278$ and $Y(n) = 314$ basepairs, so the average telomere loss $(P_{div} \times Y(n))$ is 87 basepairs, which is less than the average loss for Case I. After generation 180, the average telomere length for Case I approaches a constant, indicating that the population is senescent. However for Case IV, as the telomere length decreases, P_{div} decreases, so that telomere length decreases slowly and the population reaches senescence slowly as well.
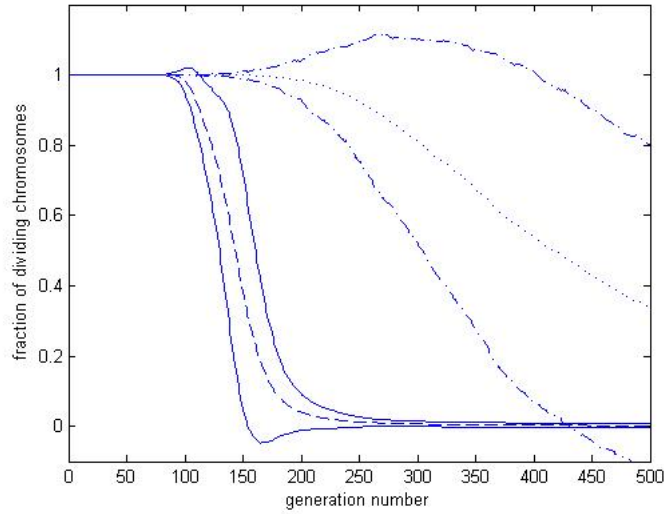
Figure 2.14: *Average results of 1000 simulations. The dotted lines indicate the mean fraction of dividing chromosomes $\phi_{div}(n)$ for Case IV plotted against generation number of passaging model with $P_{div}(n) = (n - 200)/5750$ and $Y(n) = 207 + n/4$ basepairs. The dash-dotted lines above and below indicated two standard deviations above and below the mean. The dashed lines indicate the fraction of dividing chromosomes plotted against generation number for Case I. The solid lines above and below indicate two standard deviations above and below the fraction of dividing chromosomes (Case I).*

In Figure 2.14 we compare ϕ_{div} the fraction of dividing chromosomes for cases I and IV. For Case I, all chromosomes can divide between generations 1 to 80. After that, some of the chromosome become senescent and the fraction of dividing chromosomes decreases monotonically from unity to zero. In Case IV, the fraction of dividing chromosomes ϕ_{div} remains it unity until generation 170,

90 generation later than for Case I. This is because, the average telomere length for Case IV reaches the critical telomere length of 200 basepairs later than for Case I. After 170 generations, ϕ_{div} for Case IV decreases slowly to zero. Since $P_{div}(n) = (n - 200)/5750$, the probability of division and the average telomere length decrease, as the generation number increases, causing a slower approach to senescence.

(a)   (b)
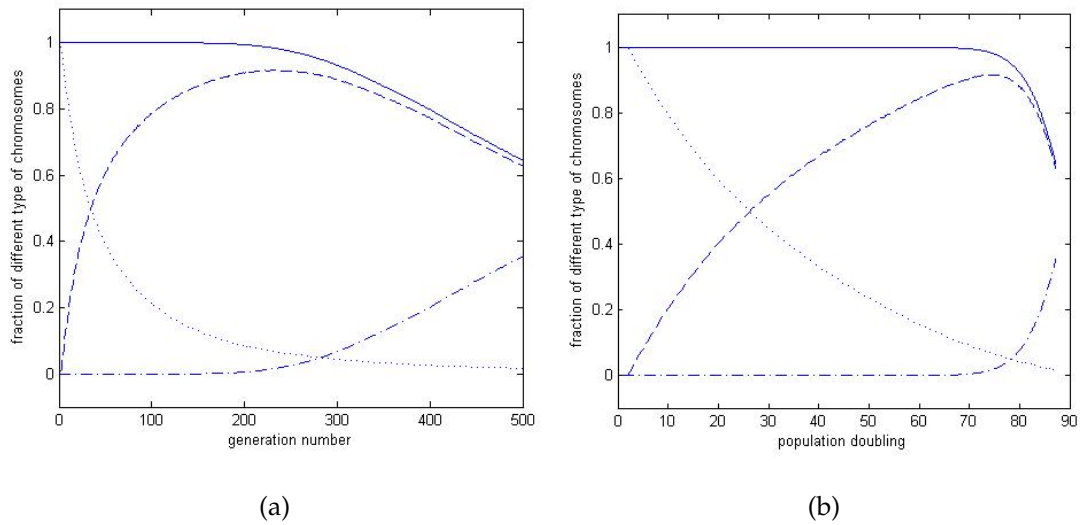
Figure 2.15: *Average results of 1000 simulations of Case IV with $L_i = 5950$, $P_{div}(n)$ $= (n - 200)/5750$ and $Y(n) = 207 + n/4$. In Figure 2.15(a), the dash-dotted line indicates the fraction of senescent chromosomes ϕ_{sen} plotted against generation number. The dotted line indicates the fraction of chromosomes which actually divided ϕ_{div_a} in the previous generation. The dashed line indicates the fraction of chromosomes which still have the potential to divide but did not divide in the previous generation ϕ_{div_p} due to the probability of dividing. The solid line indicates the fraction of non-senescent chromosome ϕ_{div}. Figure 2.15(b) the same data as Figure 2.15(a) plotted against population doublings.*

In Figure 2.15 we show how the proportion of each type of chromosome changes with generation number (*a*) and population doubling (*b*). We note that the fraction of cells which actually divide ϕ_{div_a} decreases and that the proportion of senescent chromosomes ϕ_{sen} increases over time. The fraction of chromosome

which have the potential to divide, but do not do so ϕ_{div_p}, increases with generation numbers, attaining a max value at about generation 150 before declining to zero. As a check on our numerics we calculate the sum $\phi_{div_a} + \phi_{div_p} + \phi_{sen}$, noting that this quality should be equal to unity.

2.3 The cell model

2.3.1 Preliminaries

The chromosome model presented in Section 2.2 can be seen as a simple case of the cell model for which there is only one chromosome in each cell. We use N to denote the number of chromosomes in the cell. This number differs between organisms. For example small deer contain only 6 chromosomes while carp contain over 100 chromosomes [68]. Since there are 46 chromosomes in a normal human cell, in this section we fix $N = 46$. Before the cell replicates, we check that none of the telomeres within the cell have fallen below the critical value. If one of the chromosomes has reached the critical value, then the cell will not replicate. If a cell replicates, it produces two daughter cells. We assume that daughter chromosomes are allocated randomly to each of the daughter cells.

Each chromosome obeys the replication rule (2.2.1), $K_n^g \rightarrow K_n^{g+1} + K_{n-L}^{g+1}$. For stochastic simulations we keep track of the length of each chromosomes in cell. However, for theoretical analysis of telomere length dynamics (Chapter 4), we only keep track of total telomere length in the cell. We use C_m^g to denote a cell with total telomere length m at generation g. We still use $Y(n)$ to denote the amount of telomere lost during each chromosomes replication; g represents the generation number, P_{cdiv} denote the probability of cell division. If a cell replicates, the daughter chromosomes are randomly allocated to the daughter cells. There are 2^N ways in which the $2N$ daughter chromosomes can be randomly allocated to the two daughter cells. The discrete cell replication rule can be

written as

$$C_m^g \rightarrow C_{m-jL}^{g+1} \quad + \quad C_{m-(N-j)L}^{g+1} \quad j = 0, 1, .., N$$

$$\text{with probability } 2^{-N} \binom{N}{j} \text{ and } P_{cdiv}. \qquad (2.3.1)$$

In this section we continue to use length dependent telomere loss, so that

$$Y(n) = y_0 + y_1 n, \qquad (2.3.2)$$

where y_0 and y_1 are constants. The cell division rate also depends on telomere length via

$$P_{cdiv}(n) = (a + bn)^\alpha, \qquad (2.3.3)$$

where a b and α are constants.

In the following section we reconsider the four cases of telomere shortening that were introduced in Section 2.2. The cell-level expressions for P_{div} and $Y(n)$ are summarized in Table 2.3. In Case I telomere loss and probability of cell division are both constant; in Case II telomere loss is length-dependent; in Case III replication is probabilistic with constant loss; in Case IV replication is probabilistic with length-dependent loss.

Case	Probability of cell dividing P_{cdiv}	telomere loss $Y(n)$
Case I	$P_{cdiv} = 1$	$Y(n) = y_0$
Case II	$P_{cdiv} = 1$	$Y(n) = y_0 + y_1 n$
Case III	$P_{cdiv} = (a + bn)^\alpha$	$Y(n) = y_0$
Case IV	$P_{cdiv} = (a + bn)^\alpha$	$Y(n) = y_0 + y_1 n$

Table 2.3: 4 cell-level cases where parameter a, b, α, y_0, y_1 are constants.

2.3.2 Case I: Constant telomere loss and constant probability of cell division

We start with a single cell, fixing $m = n = 6000$ basepairs for each of its 46 chromosomes. We assume that $Y(n) = 200$ basepairs are deleted from each

daughter chromosome during each replication event. We use the passaging method outlined in Sections 2.2.4 and 2.2.3 with parameter $N = 46$, so that at each generation we record not only the average telomere length of the cell but also the average shortest telomere length of the 46 chromosomes in each cell.

(a)   (b)
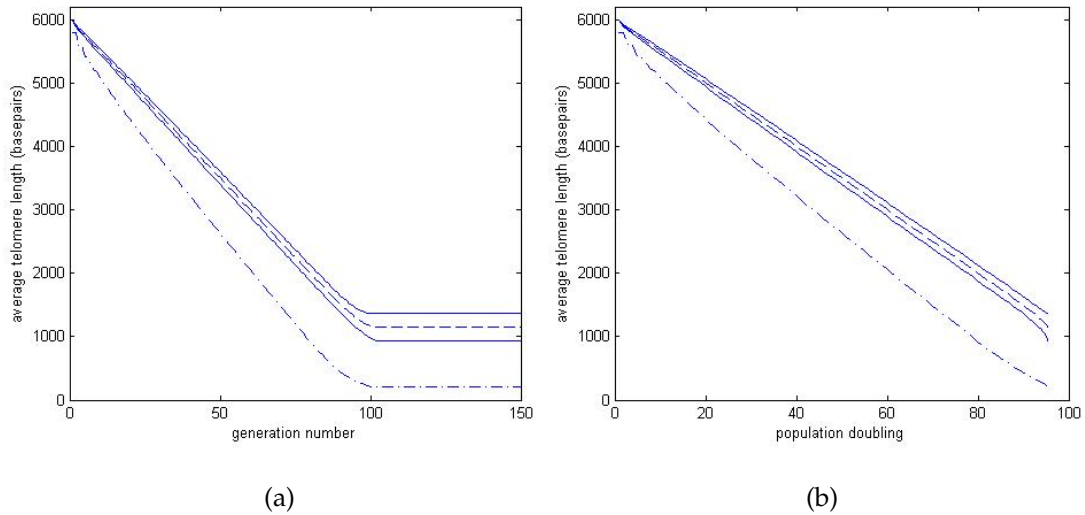
Figure 2.16: *In Figure 2.16(a), the dashed line is the average of 1000 simulations of telomere length of the chromosome against generation numbers, the solid line above (below) is the average telomere length plus (minus) twice the standard deviation. The dash-dot line shows the average length of the shortest telomere in a cell. Figure 2.16(b) use the same simulation data from Figure 2.16(a) plotted against h population doubling.*

In Figure 2.16 we present the average results of 1000 simulations in order to show how the average telomere length changes with generation number (2.16(a)) and population doublings (2.16(b)). Figure 2.16(a) shows that as the generation number increases from 1 to 90, the average telomere length of the cells decreases linearly. After generation 90, the solid curve plateaus at a constant value of about 1100 basepairs. After generation 100, telomere loss halts because all the cells are senescent (Figure 2.17(a)). Figure 2.16(a) also shows how the average length of the shortest telomere in a cell decreases linearly as the generation number increases until generation 100, but it decreases faster than the average telomere length . The shortest telomere length reaches 200 basepairs (the critical length) at about generation 100. This explains why cells became senescent with

long average telomere length (1100 basepairs), because for the cell replication rule, when the shortest telomere length of the chromosomes in the cell reaches critical value, the whole cell stops replicating, even through all the rest of the chromosomes still have longer telomeres. So when the average of the shortest telomere length reaches 200 basepairs (at about 100 generations), the whole population becomes senescent. Figure 2.16(b) shows the same phenomenon as figures 2.16(a), in the population doubling time scale. With constant probability of cell division, when all telomere length of the cell over the critical length, there is little difference between generation number and population doublings.

(a)   (b)
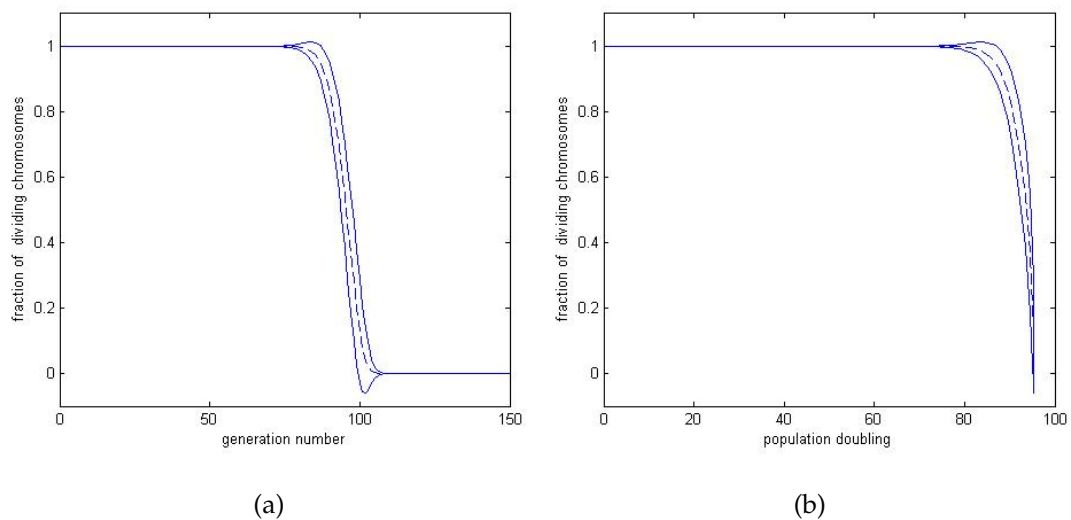
Figure 2.17: *Averaged results of 1000 simulations from the same simulations as Figure 2.16. In Figure 2.17(a), the dashed line is the fraction of dividing cells plotted against generation number, the solid lines indicated two standard deviations above and below the fraction of dividing cell. Figure 2.17(b) the same data as Figure 2.17(a) plotted against population doubling.*

In Figure 2.17 we show how, for the simulation results presented in Figure 2.16, the fraction of dividing cells changes with both generation number (*a*) and population doubling timescales (*b*). From these figures we see that before generation 90, population doubling and generation numbers are identical since all the chromosomes replicate. Thereafter the generation number increases to 110 while the population doubling slowly approaches to 95 which means that some of the cells are senescent. When the population stops rising, all cells are

senescent. Figure 2.16(b) shows that initially the average telomere length decreases linearly and stops decreasing at 95 population doublings where the mean telomere length is 1100 basepairs. Figure 2.17(b) reveals that cells start to become senescent after about 80 population doublings and that all cells are senescent after about 95 population doublings.
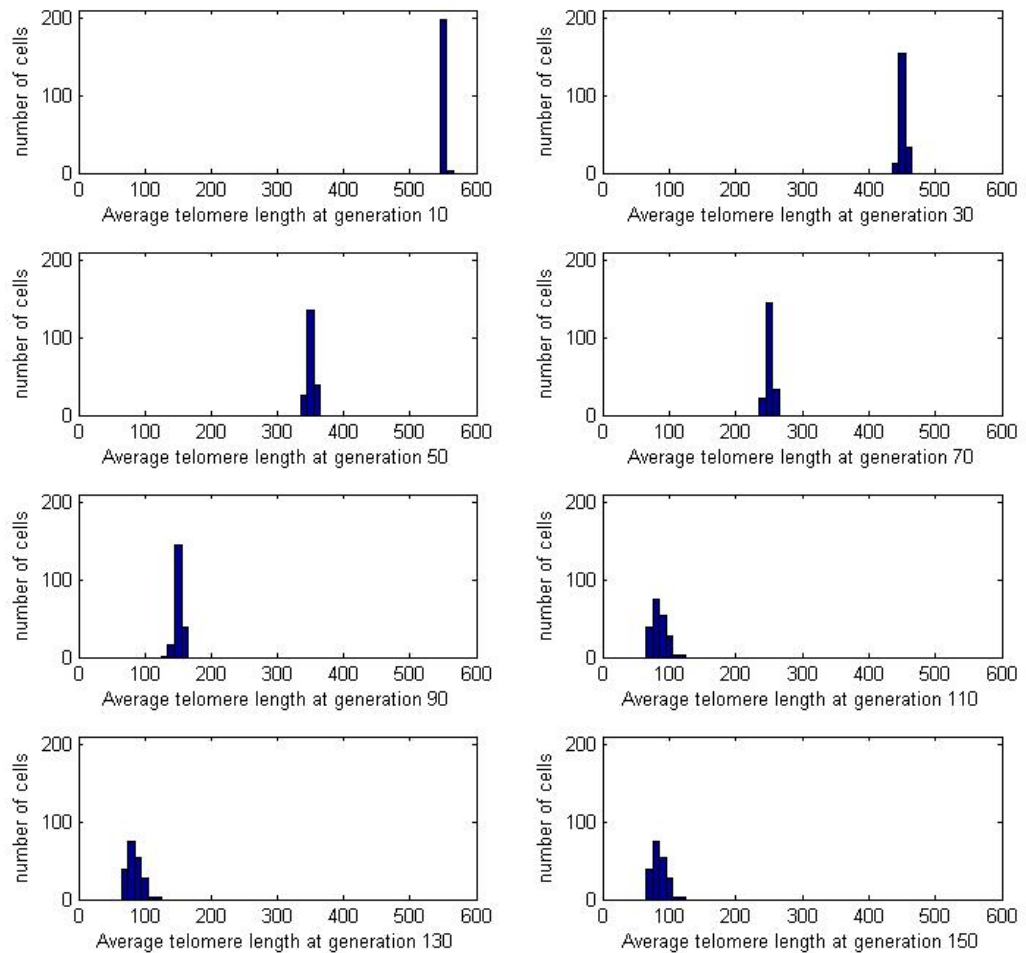
Figure 2.18: *Series of plots showing the distribution of average telomere lengths within a population of 200 cells at generations 10, 30, 50, 70, 90, 110, 130, 150, when chromosomes shortening and replication are described by Case I. In order to see clearly how the distributions change we reduced the horizontal scale (average telomere length) by a factor of 10.*
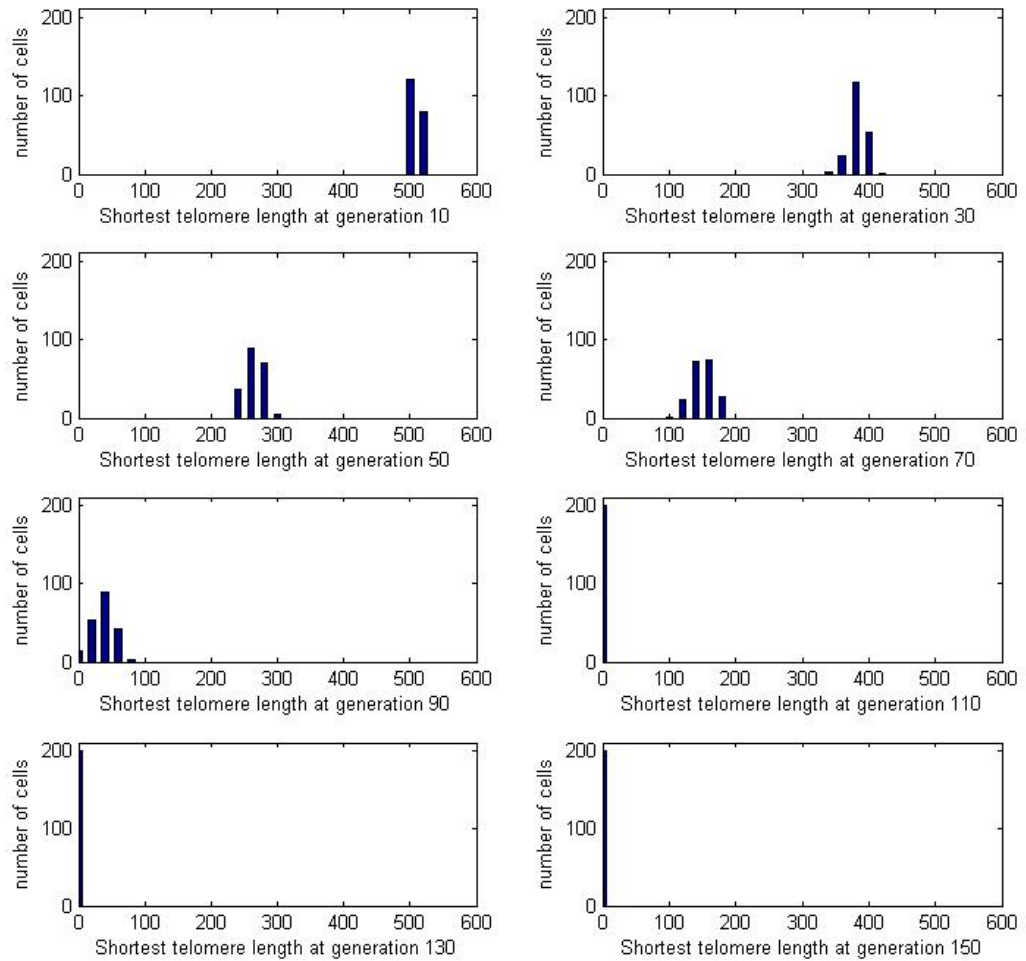
Figure 2.19: *Series of plots showing the distribution of average shortest telomere lengths from a population of 200 cells at generations 10, 30, 50, 70, 90, 110, 130, 150, when chromosomes shortening and replication are described by Case I. In order to see clearly how the distributions change we reduced the horizontal scale (average telomere length) by a factor of 10.*

In order to determine the distribution of telomere lengths we illustrate the average and shortest telomere length of 200 cells in one simulation at generations 10, 30, 50, 70, 90, 110, 130, 150 respectively. The resulting data is presented in Figures 2.18 and 2.19. As the generation number increases the distribution spreads out and moves towards the region of lower telomere lengths. The graphs in Figure 2.18 show that the corresponding results for generations 110, 130, 150 are identical, indicating that the cells are not replicating. This is confirmed by the

results presented in Figure 2.19 which show that at generation 110 the shortest telomeres have reached the critical length.

2.3.3   Unified view of Cases I-IV

In this section the simulations are similar to those for normal cell ageing presented in Section 2.3.2. We start with a cell which has a 46 chromosomes and average telomere length of 46 chromosomes is 5950 basepairs, and follow its progeny to senescence. We use $Y(n)$(see (2.3.2)) to denote the telomere loss and P_{cdiv} (2.3.3) for the probability of cell division.

In previous chromosome simulations, we chose chromosome division P_{div} as a constant ($\alpha = 0$, cases I and II) or linearly dependent on telomere length ($\alpha = 1$ cases III and IV). In this section, we not only consider cell division which depends linearly on telomere length ($\alpha = 1$), but also cases for which $0 \leq \alpha \leq 1$. For cases I and III, the three parameters α, y_0 and y_1 are chosen to ensure that the average telomere loss per chromosomes replication is 200 basepairs. We fix $\alpha = 0, 0.25, 0.5, 0.75, 1$ separately with a constant telomere loss of $Y(n)$, and for cases II and IV length-dependent telomere loss $Y(n)$ is given by (2.3.3). The parameter values listed in Table 2.4, correspond to 10 different cases each of which gives a mean telomere loss of 200 basepairs per chromosome replication.

Case I is the simplest, where the cell always divides if the telomere length of all its chromosomes exceed the critical length. Further, during replication the loss of telomere is constant (200 basepairs). Case I is identical to the model we present in Section 2.3.2. Case II has the same cell dividing probability as Case I, but the telomere loss $Y(n)$ in each replication is dependent on telomere length. In order to make the average telomere loss 200 basepairs, we pick $y_0 = 100$ (half of value of $Y(n)$ in Case I), and balance the median telomere length of 2975 basepairs via $200 = 100 + 2975y_1$, to obtain $y_1 = 1/30$, hence in Case II, $Y(n) = 100 + n/30$. In Case III-I, the probability of cell replication is dependent on telomere length. In order to obtain an average telomere loss of 200 basepairs we pick the medium point of the telomere length $L = 2975$ basepairs and let

Case	α	y_0	y_1
Case I	0	200	0
Case II	0	100	$\frac{1}{30}$
Case III-I	0.25	240	0
Case III-II	0.5	288	0
Case III-III	0.75	345	0
Case III-IV	1	414	0
Case IV-I	0.25	120	$\frac{1}{25}$
Case IV-II	0.5	144	$\frac{1}{21}$
Case IV-III	0.75	172.5	$\frac{1}{17}$
Case IV-IV	1	207	$\frac{1}{14}$

Table 2.4: The parameters values in Table 2.2 generate 10 different cases, each of which has an average telomere loss of 200 basepairs per chromosome replication.

$P_{cdiv}(n)Y(n) = 200$ which implies $Y(n) = 240$ when $\alpha = 0.25$. Following the same rule we obtain the values of $Y(n)$ for cases III-II, III-III, III-IV specified in Table 2.4. In Case IV-I, the way we calculate $Y(n)$ is similar to that for Case II. We fix $y_0 = 120$, which is half the value of y_0 in Case III-I and to balance the other half we choose $y_1 = 1/25$. Similarly the expressions for $Y(n)$ for cases IV-II, IV-III, IV-IV follow.

We split the 10 cases in Table 2.4 into two groups, according to whether telomere shortening depends on telomere length (group 2, which contains cases II, IV-I, IV-II, IV-III, IV-IV) or not (group 1, which contains cases I, III-I, III-II, III-III, III-IV).

Figure 2.20 shows how the average telomere length of the cells in Cases I and III changes with generation number and population doubling for different values of P_{cdiv}. Before generation 80, Case III-IV loses telomeres at the fastest rate followed by Case III-III, III-II, III-I, I which is similar to the single chromosome constant loss model. When the cells reach senescence, Case III-IV remains with

(a)   (b)
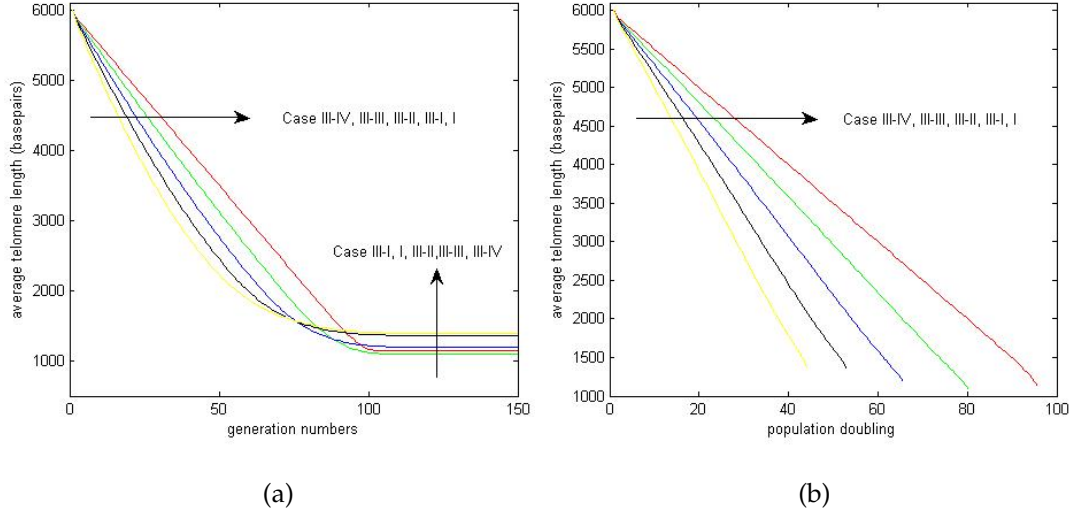
Figure 2.20: *Average results of 1000 simulations. In Figure 2.20(a), average cell telomere length plotted against generation number for Cases I, III-I, III-II, III-III, III-IV (with parameters shown in Table 2.4). Figure 2.20(b) the same data as Figure 2.20(a) plotted against population doublings.*

the longest telomeres length of the cell followed by cases III-III, III-II, I,III-I; this is because Case III-IV has the largest constant loss y_0. From Figure 2.20(b) it is clear that, as the population doubling increases, the average telomere length decreases linearly and Case III-IV loses telomeres at the fastest rate followed by cases III-III, III-II, III-I, I.

For cases I and II, we distinguish two types of cells: those which can divide and those which are senescent. By contrast, for cases III and IV since the probability of cell duration is no longer constant, we distinguish three types of cells: those which have just divided, those which could have divided but did not, and those which are senescent. We denote by $NC(g)$ the number of cells at generation g, so that

$$\phi_{cdiv_a}(g) = \frac{NC(g) - NC(g-1)}{NC(g-1)} .$$ (2.3.4)

On each generation, we monitor the telomere length of all $NC(g)$ cells and we use this information to determine how many cells are senescent (*i.e* how many cells cannot divide because their chromosome are too short). We denote by $NC_s(g)$ the number of cells which are senescent at generation g. Then

50

$(NC(g) - NC_s(g))$ represents the number of cells which could divide on the next generation. We denote by $\phi_{csen}(g)$ the fraction of senescent cells at generation g and by $\phi_{cdiv}(g)$ the fraction of chromosomes which could divide on generation $(g + 1)$, so that

$$\phi_{csen}(g) \quad = \quad \frac{NC_s(g)}{NC(g)}, \tag{2.3.5}$$

$$\phi_{cdiv}(g) \quad = \quad \frac{NC(g) - NC_s(g)}{NC(g)}. \tag{2.3.6}$$

We denote by $\phi_{cdiv_a}(g)$ the fraction of cells that actually divide at generation g and $\phi_{cdiv_p}(g)$ the fraction of cells that have the potential to divide, but not do so at generation g, so that

$$\phi_{cdiv_p}(g) = \phi_{cdiv}(g) - \phi_{cdiv_a}(g). \tag{2.3.7}$$

For comparison of cases III and IV with cases I and II, we use the fraction of dividing chromosomes $\phi_{cdiv}(g)$ for cases III and IV where $\phi_{cdiv}(g) = \phi_{cdiv_a}(g) + \phi_{cdiv_p}(g)$.

(a)   (b)
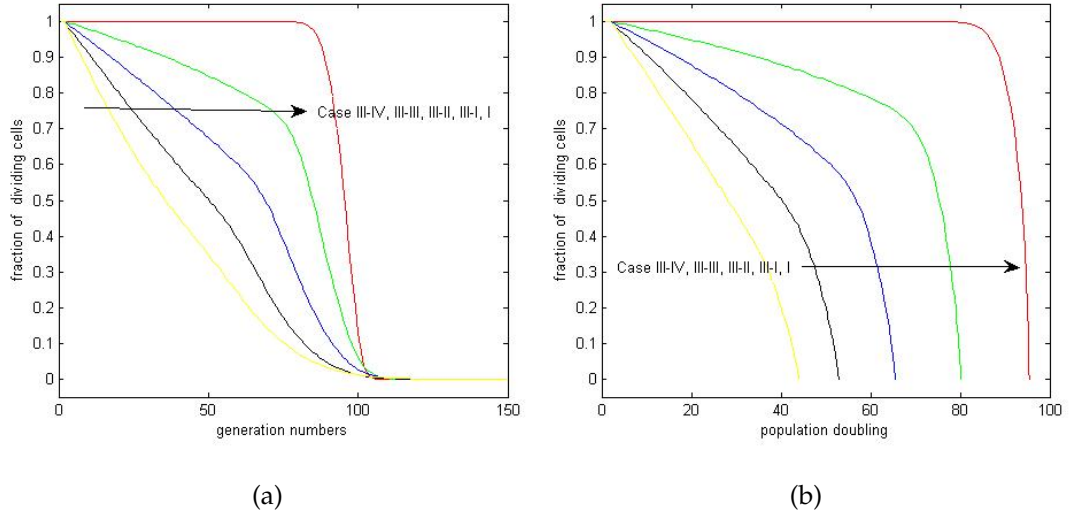
Figure 2.21: *In Figure 2.21(a), fraction of dividing cells $\phi_{cdiv}(g)$ plotted against generation number for cases I, III-I, III-II, III-III, III-IV (with the parameters shown in Table 2.4). Figure 2.21(b) the same data as Figure 2.21(a) plotted against against population doublings. Average results of 1000 simulations.*

In Figure 2.21 we show how the fraction of dividing cells $\phi_{cdiv}(g)$ for cases I

and III varies with generation numbers (a) and population doublings (b). Figure 2.21(a) shows that the bigger α is, the smaller P_{cdiv}, which results in the fraction of dividing cells for Case III-IV decreasing most rapidly, followed by cases III-III, III-II, III-I, I. Whatever the value of P_{cdiv}, cases I and III reach senescence at about the same time (generations 110 to 120). Comparing the results of the cell model with the chromosome model for cases I and III-IV, the main difference is that the cell model reaches senescence earlier with a longer average telomere length than the chromosome model. This is due to senescence being triggered by the shortest telomere of 46 hitting a lower threshold.

| (a) | (b) |
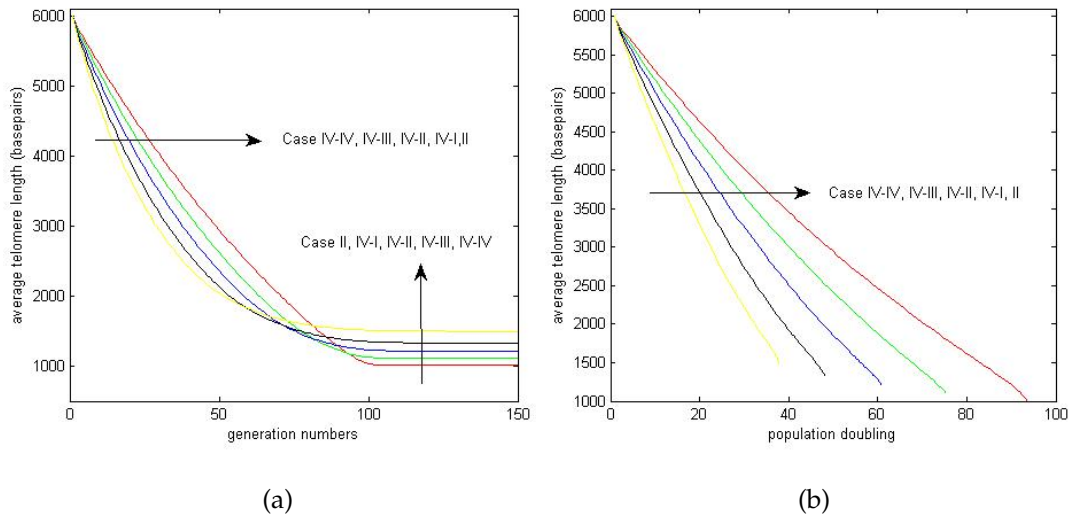
Figure 2.22: *In Figure 2.22(a), average telomere length plotted against generation number for cases II, IV-I, IV-II, IV-III, IV-IV. (with the parameters shown in Table 2.4). Figure 2.22(b) the same data as Figure 2.22(a) plotted against population doublings..Average results of 1000 simulations.*

In Figures 2.22(a) and 2.23(a) the average telomere length of the cell and the fraction of dividing cells are plotted against generation number for cases II, IV-I, IV-II, IV-III, IV-IV respectively. Figures 2.22(a) and 2.23(b) shows the same simulation data as in Figures 2.22(a) and 2.23(b) respectively, plot against population doubling instead. The behavior of the five cases in these four figures is almost identical to that depicted in Figures 2.20 and 2.21.

(a)   (b)
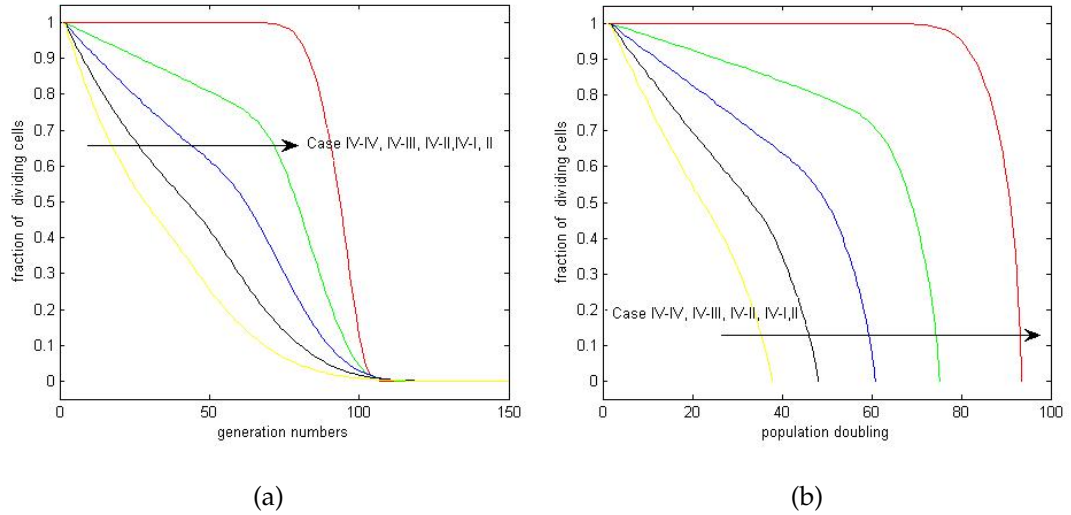
Figure 2.23: *In Figure 2.23(a), fraction of dividing cells $\phi_{cdiv}(g)$ plotted against generation number for Cases I, III-I, III-II, III-III, III-IV (with the parameters shown in Table 2.4). Figure 2.23(b) the same data as Figure 2.23(a) plotted against population doublings. Average results of 1000 simulations.*

Hence, although the single chromosome model is a gross simplification of the more realistic $N = 46$ chromosome cell model, it retains all the essential mechanisms of ageing and senescence.

2.4 Conclusions

In this chapter we have developed a chromosome-level model and a cell-level model of telomere loss during replication and compared four different choices for chromosome replication and telomere shortening rules. Case I represents the constant telomere loss model in which a fixed amount of telomere is lost during chromsome/cell replication. In 1992 Levy *et al*. [1] modelled telomere shortening with a constant telomere loss caused by the "end-replication" problem. Their model predicted average telomere length decreases linearly with generation numbers. In our first model we see that the average telomere length of the chromosomes in the cell decreases linearly when the population doubling or generation numbers increases before the cells became senescent which is consistent with Levy's work (see Figure 2.24 (A)). Figure 2.24 (A) shows that

our simulation results are identical to Levy's work (the two lines lie over each other) and we also compared with the data he used.
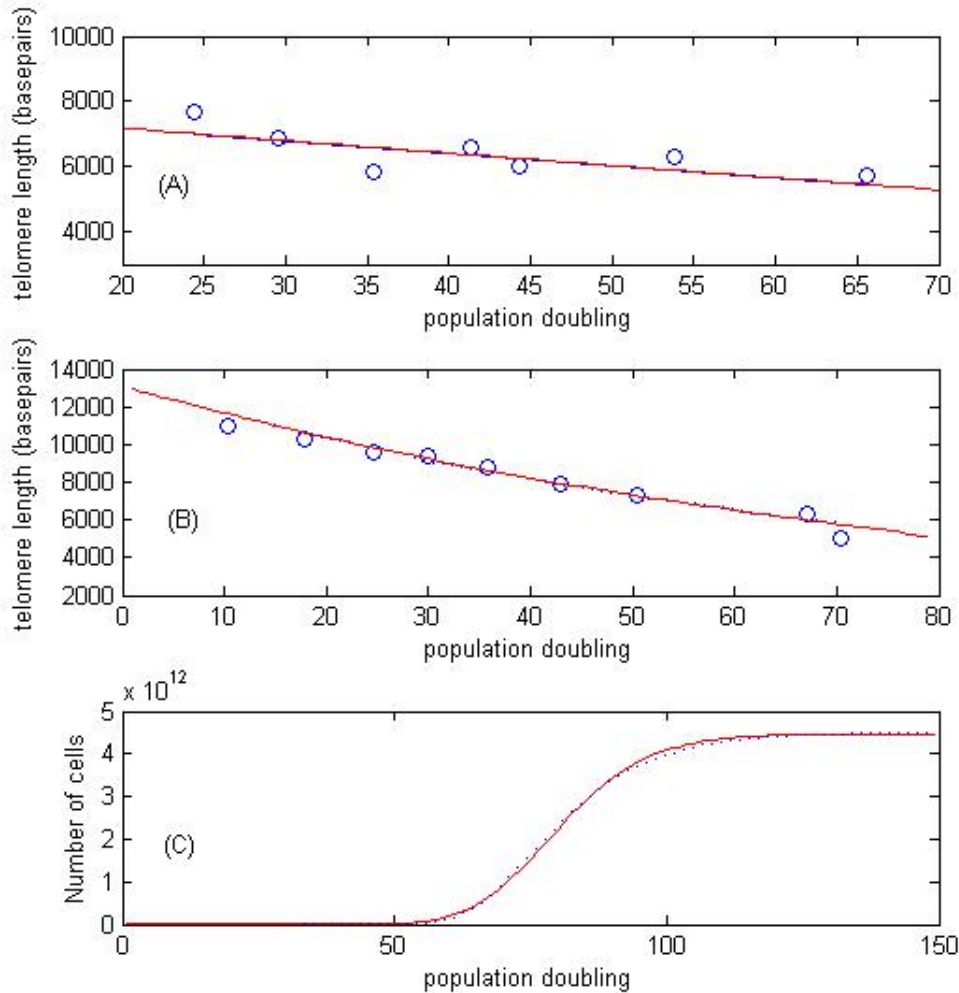
Figure 2.24: (*A*) *The circles are the experimental data from [1]. The solid line is our simulation result of average telomere length plotted against population doubling and the dotted line is Levy's results.* (*B*) *The circles are experimental data from [2]. The solid line is our simulation result and the dotted line is Buijs' results. Note that the solid and dotted lines coincide.* (*C*) *The solid line indicates the number of cells plotted against population doublings for Case III and the dotted line is Gompertzian growth. All three plots demonstrate the close agreement between our simulation results, those of previous models, and experimental data.*

Case II corresponds to the situation in which telomere loss during chromo-

some/cell replication is dependent on the length of the telomere. In 2004 Buijs [64] simulated how telomere shortening is dependent on telomere length. Figure 2.24 (*B*) shows that our simulation results for Case II are consistent with Buijs' results and with the experimental data used by Buijs. In Case III, the probability of cell division is a random process dependent on telomere length whereas telomere loss occurs at a constant rate. In 2008 Portugal [65] developed a similar stochastic model in which telomere shortening occurs at a constant rate but cell division depends on telomere length. Their focus was on the growth rate of the cell more than average telomere length and they predicted a Gompertzian growth in the cell population. Figure 2.24 (*C*) shows that the cell population in our simulations can be fitted by Gompertzian growth. However, in our second and third models we focus on how average telomere length changes with generation numbers and the fraction of the dividing cells and the comparisons of these data with Case I.

While the first three models have been used by previous researchers, the work relating to Case IV is new. In Case IV, we combined telomere length dependent loss with a probabilistic cell division model with probability dependent on telomere length. If the parameters are chosen appropriately, Case I, II and III can be considered as special cases of Case IV. By verifying the parameter to see how the cell's lifespan changes when both telomere shortening and the division probability dependent on telomere length. Our Monte Carlo simulations suggest that the average telomere length of the chromosomes in each cell decreases when the population doubling or generation number increases until the cells become senescent. After that the average telomere length of the chromosomes in the cell slowly approaches a limiting value, at which stage all the cells are senescent. We also consider how the fraction of dividing cells changes as the generation number increases. We notice that cells with one chromosome become senescent when their telomeres are at about 150 to 250 basepairs. However, the cell model with 46 chromosomes reaches senescence at about 1150 to 1500 basepairs, because if the length of one chromosome is lower than the critical value and all the other of chromosomes contain longer telomeres, the cell must still stop dividing. Thus, as the number of chromosomes in the cell

increases, the average telomere length at which they become senescent also increases.

(a)   (b)
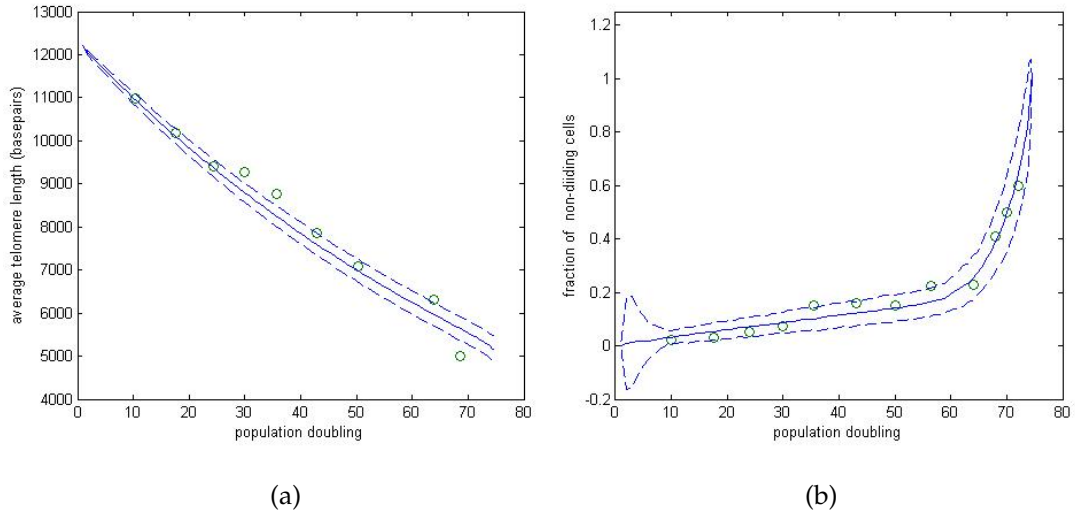
Figure 2.25: *Average results of 200 simulations for Case IV. The circles are the experimental data from [2]. In Figure 2.25(a), the solid line is the average telomere length plotted against population doubling, the dashed lines indicated two standard deviations above and below the mean. In Figure 2.25(b), the solid line is the fraction of non-dividing cells plotted against population doubling, the dashed lines indicate two standard deviations above and below the fraction of dividing cells.*

Figure 2.25 demonstrates that our stochastic simulation results for Case IV can be made to fit well with experimental data [2] in both average telomere length and the fraction of non-dividing cells. So we can use our model to compare with experimental data to estimate the amount of telomere loss and the probability of a cell dividing, for example to fitted data [2], we use initial telomere length 12200 k basepairs and amount of telomere loss is $Y(n) = 10 + 0.043n$ and the probability of cell dividing is $P_{div}(n) = (n/12200 - 0.03)^{0.25}$.

In this Chapter we only developed a stochastic model, in Chapter 4 we introduce and analyze mathematical models of these cases separately, in order to see how the telomere length and fraction of senescent cells vary with time (population doubling/generation number) as well as the shape of the distribution.

Stochastic simulations of Werner's syndrome

3.1 Introduction

Werner's syndrome is an inherited disease in which the most characteristic feature is the rapid appearance of ageing, which appears in the second or third decade when patients develop grey hair, alopecia and atrophic skin [34]. Most Werner's syndrome patients die in their forties, their deaths usually being linked to cancer [69].

To gain a better understanding of Werner's syndrome, we start at the cellular level. Experiments have shown that dramatic shortening of telomeres in Werner's syndrome fibroblasts happens faster than in normal cells [70]. Cells from Werner's syndrome patients show large deletions in DNA [38], so Werner's syndrome accelerates a cell's journey to senescence. When a population of Werner's syndrome cells become senescent, it has a wider range of telomere lengths than a population of normal cells. The molecular pathway of Werner's syndrome is unknown. A possible explanation is that Werner's syndrome cells contain some very short telomeres with most of chromosomes retaining longer telomeres [41]. These short telomeres cause premature senescence.

In order to model Werner's syndrome, we assume that there is an extra loss in

telomere length [71] when a cell divides. Thus we treat Werner's syndrome as an accelerated model of normal ageing. In this chapter, we generalize the chromosome replication rule to include extra deletions caused by Werner syndrome and we use a similar method to that presented in Chapter 2 to model Werner's syndrome. We develop a deterministic chromosome model (assuming that Werner's syndrome deletions occur at every replication) and a more general refined stochastic model (which combines with normal ageing and Werner's syndrome). Then we scale up these models from the chromosome level to the cell level.
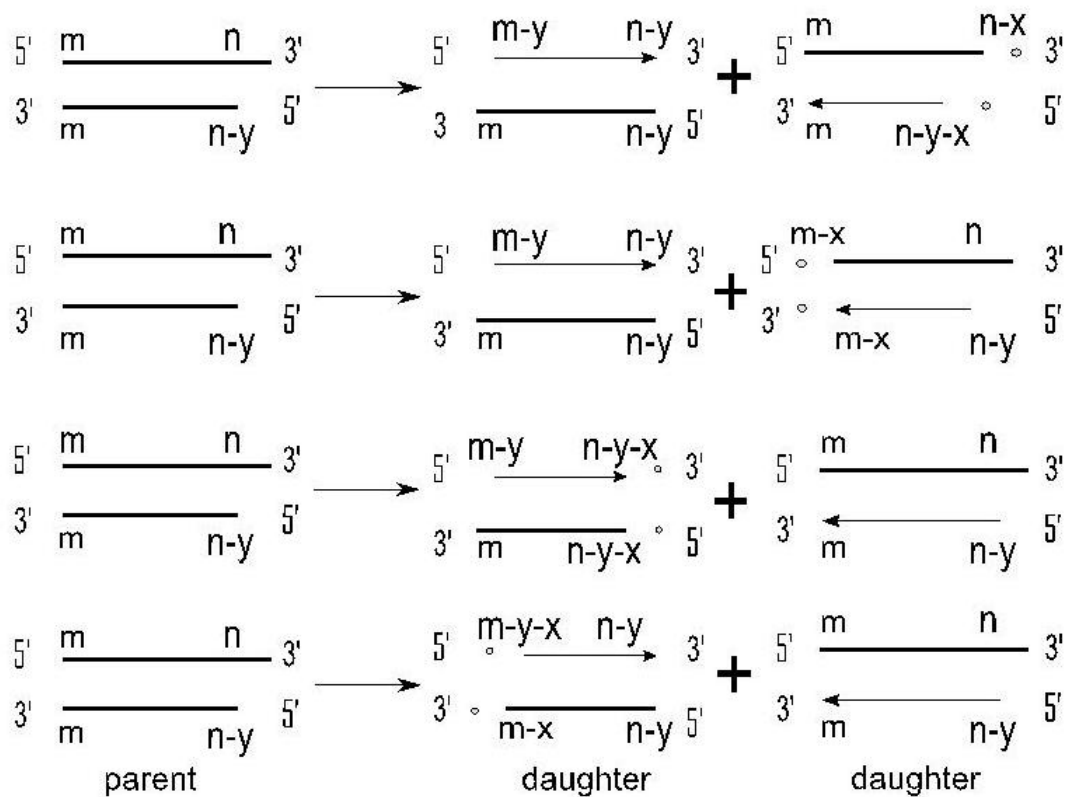
Figure 3.1: *Illustration of the effects of chromosome replication with Werner's syndrome. The thick lines indicate the template (parent) strands. The thin lines indicate the replicated strands of the template in the daughter chromosomes. The arrows show the directions of replication and m, n, n − y, m − x, etc indicate the telomere lengths.*

In Werner's syndrome the replication process is more complicated than for normal ageing. We assume that m, n are the number of basepairs of the telomere at each end of the chromosome. During replication, not only are y basepairs

lost from one of the daughter chromosome as in normal ageing, but there is an additional loss of x basepairs at one or other end of one of the daughter chromosomes. As a result, depending on where the additional loss occurs, there are 4 different ways in which replication can occur, we illustrate the replication and dividing process in Figure 3.1.

In Figure 3.1, in each daughter chromosome, one strand of DNA is from the parent (indicated by a thick line), one daughter cell has the same telomere length as its parent and the other has x fewer of basepairs. The additional loss of telomere can occur from any of the four sides of strands which gives four possible outcomes of the replication process. The other strand, indicated by the thin line is manufactured in a replication process of the template in the daughter chromosome which loses y basepairs during replication. In daughter chromosomes if we remove longer telomere strand to the top and shorter stand to the bottom, so replication in Figure 3.1, can be written more compactly as

$$
\begin{pmatrix} m & n \\ m & n-y \end{pmatrix} \rightarrow \begin{pmatrix} n-y & m \\ n-y & m-y \end{pmatrix} + \begin{pmatrix} m & n-x \\ m & n-y-x \end{pmatrix}, \tag{3.1.1a}
$$

$$
\begin{pmatrix} m & n \\ m & n-y \end{pmatrix} \rightarrow \begin{pmatrix} n-y & m \\ n-y & m-y \end{pmatrix} + \begin{pmatrix} m-x & n \\ m-x & n-y \end{pmatrix}, \tag{3.1.1b}
$$

$$
\begin{pmatrix} m & n \\ m & n-y \end{pmatrix} \rightarrow \begin{pmatrix} n-y-x & m \\ n-y-x & m-y \end{pmatrix} + \begin{pmatrix} m & n \\ m & n-y \end{pmatrix}, \tag{3.1.1c}
$$

$$
\begin{pmatrix} m & n \\ m & n-y \end{pmatrix} \rightarrow \begin{pmatrix} n-y & m-x \\ n-y & m-y-x \end{pmatrix} + \begin{pmatrix} m & n \\ m & n-y \end{pmatrix}. \tag{3.1.1d}
$$

Chromosome replication is restricted by telomere length: if this exceeds some critical length, then (3.1.1a)-(3.1.1d) happen with equal probability 1/4. In normal ageing, chromosomes stop replicating when the telomere length reaches a critical value which we have assumed to be zero. In Werner's syndrome there is a range of telomere lengths for which the chromosome may attempt to replicate and fail part way through, leaving just the parent chromosome. Generally,

there are four possible outcomes

$$
\begin{pmatrix} m & y \\ m & 0 \end{pmatrix} \rightarrow \begin{pmatrix} 0 & m \\ 0 & m-y \end{pmatrix} + \begin{pmatrix} m & y-x \\ m & -x \end{pmatrix}, \tag{3.1.2a}
$$

$$
\begin{pmatrix} m & y \\ m & 0 \end{pmatrix} \rightarrow \begin{pmatrix} 0 & m \\ 0 & m-y \end{pmatrix} + \begin{pmatrix} m-x & y \\ m-x & 0 \end{pmatrix}, \tag{3.1.2b}
$$

$$
\begin{pmatrix} m & y \\ m & 0 \end{pmatrix} \rightarrow \begin{pmatrix} -x & m \\ -x & m-y \end{pmatrix} + \begin{pmatrix} m & y \\ m & 0 \end{pmatrix}, \tag{3.1.2c}
$$

$$
\begin{pmatrix} m & y \\ m & 0 \end{pmatrix} \rightarrow \begin{pmatrix} 0 & m-x \\ 0 & m-y-x \end{pmatrix} + \begin{pmatrix} m & y \\ m & 0 \end{pmatrix}. \tag{3.1.2d}
$$

Both the daughter chromosomes in (3.1.2b) and (3.1.2d) are viable (with non-negative-telomere length), but outcomes (3.1.2a) and (3.1.2c) produce one viable (non-negative-telomere length) daughter and one non-viable (negative-telomere length) daughter chromosome. In practise, chromosomes cannot have negative telomere length so (3.1.2a) and (3.1.2c) cannot happen. Instead, the mother chromosomes will remain the same in this generation. When one end of a Werner's syndrome chromosome reaches the critical telomere length, the three possible outcomes following replication are

$$
\begin{pmatrix} m & y \\ m & 0 \end{pmatrix} \rightarrow \begin{pmatrix} 0 & m \\ 0 & m-y \end{pmatrix} + \begin{pmatrix} m-x & y \\ m-x & 0 \end{pmatrix}, \tag{3.1.3a}
$$

$$
\begin{pmatrix} m & y \\ m & 0 \end{pmatrix} \rightarrow \begin{pmatrix} 0 & m-x \\ 0 & m-x-y \end{pmatrix} + \begin{pmatrix} m & y \\ m & 0 \end{pmatrix}, \tag{3.1.3b}
$$

$$
\begin{pmatrix} m & y \\ m & 0 \end{pmatrix} \rightarrow \begin{pmatrix} m & y \\ m & 0 \end{pmatrix}. \tag{3.1.3c}
$$

Since we assume (3.1.2a)-(3.1.2d) happen with equal probability 1/4, so we assume (3.1.3a) and (3.1.3b) happen with equal probability 1/4 and (3.1.3c) happens with probability 1/2. We use MATLAB to run the stochastic simulations and the pseudocode for there simulations is similar to that in Chapter 2 Section 2.2.3. The difference is that when a cell replicates, it follows the Werner's syndrome replication rule above or a combination of the Werner's syndrome

replication rule with the normal ageing replication rule together.

All the models presented in this section are based on the following assumptions: first, there is no telomere elongation during chromosome replication as there is no telomerase activity and no recombination events between telomeres. Second, in a Werner's syndrome intermediate senescent state, some mechanisms of replication are available, but others are prohibited. If the stochastic term indicates a prohibited type of replication (such as in (3.1.2b) and (3.1.2d)), we assume that the cell does not divide and instead remains the same (as in 3.1.3c), but if an acceptable form of replication is chosen (such as (3.1.2a) and (3.1.2c)), then it occurs as in (3.1.3a) and (3.1.3b). Third, we do not consider cell death, that is there is no cell removal from the system.

3.2 Chromosome level model of Werner's syndrome

3.2.1 Pure Werner's syndrome model

We use the same passaging method as in Chapter 2. Our simulations start with a single chromosome and we track its progeny over subsequent generations until the total number of chromosomes exceeds 200. We then passage by randomly selecting 200 of these chromosomes. In the next generation, all chromosomes divide (if their telomeres are sufficiently long to allow replication), and we passage so that once again 200 chromosomes are selected from the population. This process is repeated until all telomeres are too short to allow further replication. At this stage the entire population is senescent. During division, the rule for chromosome replication is as follows: if a telomere has not reached the critical length then the four outcomes in (3.1.1a)-(3.1.1d) occur with equal probabilities 1/4. When the length of one of the telomeres reaches the critical value, then the chromosome stops replicating with probability 1/2 (case (3.1.3c)) and the other two possible outcomes cases ((3.1.3a) and (3.1.3b)) occur with equal probabilities 1/4.

For comparison with our earlier results for normal telomere shortening, we start our simulations with a single chromosome for which $m = n = 6000$ basepairs. We fix $y = 200$ and $x = 200$ basepairs and choose the critical telomere length to be 200 basepairs. We allow the new chromosome to replicate. On each generation chromosomes are selected for replication and one of (3.1.1a)-(3.1.1d) is chosen at random provided that the telomere length exceeds the critical length, otherwise one of (3.1.3a)-(3.1.3c) is chosen at random replication when one of telomere length is equal to the critical length, and replication is attempted. This process is repeated until all telomere lengths are too short to allow further replication. At this stage the entire population is senescent.

At each generation we record not only the average telomere length but also the number of chromosomes that have just replicated. We denote by $N(g)$ the number of chromosomes at generation g, $\phi_{div}(g)$ represents the fraction of dividing chromosomes at generation $(g-1)$ and $\phi_{sen}(g)$ the fraction of senescent chromosomes at generation $(g-1)$, so that

$$\phi_{div}(g) = \frac{N(g) - N(g-1)}{N(g-1)}, \quad \phi_{sen}(g) = 1 - \phi_{div}(g). \quad (3.2.1)$$

In Figure 3.2 we show how the average telomere length for Werner's syndrome and normal ageing vary with generation number (Figure 3.2(a)) and population doubling (Figure 3.2(b)). In Figure 3.2(a), as the generation number increases, the average telomere length of Werner's syndrome simulation decreases, reaching a value of 250 basepairs after about 100 generation. Thereafter, the average telomere length remains constant, which indicates that replication has stopped and that senescence has occurred. Hence in Werner's syndrome, telomere shortening is much faster than in normal ageing (in normal ageing it takes about 150 generations for senescence to occur). Figure 3.2(b) shows that the same phenomenon, vary with population doublings instead of generation number.

Figure 3.3 we show how the fraction of dividing chromosomes for Werner's syndrome and normal ageing vary with generation numbers (Figure 3.3(a)) and population doubling (Figure 3.3(b)). Figure 3.3(b) shows how before 90

(a) (b)
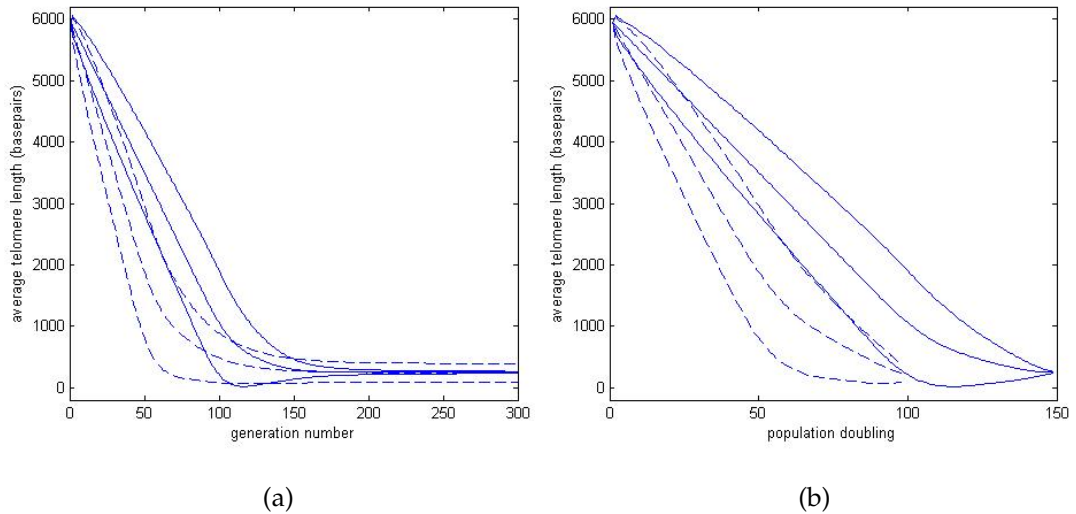
Figure 3.2: *Average of 2000 simulations. The middle dashed line indicates the average length of telomere plotted against generation number (Figure 3.2(a)) and population doubling (Figure 3.2(b)) with the Werner's syndrome active x = y = 200 basepairs per replication, the dashed lines above and below are the means plus or minus twice the standard deviation. The middle solid line is the average length of telomere plotted against generation number (Figure 3.2(a)) and population doubling (Figure 3.2(b)) with normal ageing y = 200 basepairs, the solid lines above and below are the means plus or minus twice the standard deviation. Figure 3.2(b) use the same simulation data from Figure 3.2(a).*

population doubling, all the chromosomes are replicating, after generation 180 nearly all chromosomes are senescent. Figure 3.3(a) shows that simulation of Werner's syndrome from generation 1 to 40, all chromosomes are replicating. Comparing Figures 3.3(a) and 3.2(a) we note that during this period the rate of loss of telomere is constant. At generation 40 the telomere length of some of the chromosomes reaches their minimum and stop replicating. Chromosomes with longer telomeres continue to divide, reducing the average telomere length and cause an increase in the spread or standard deviation of the distribution of lengths. After generation 40 some chromosomes stop replicating and the fraction of senescent chromosomes rapidly increases from zero. After generation 110 nearly all chromosomes are senescent.

63

(a)   (b)
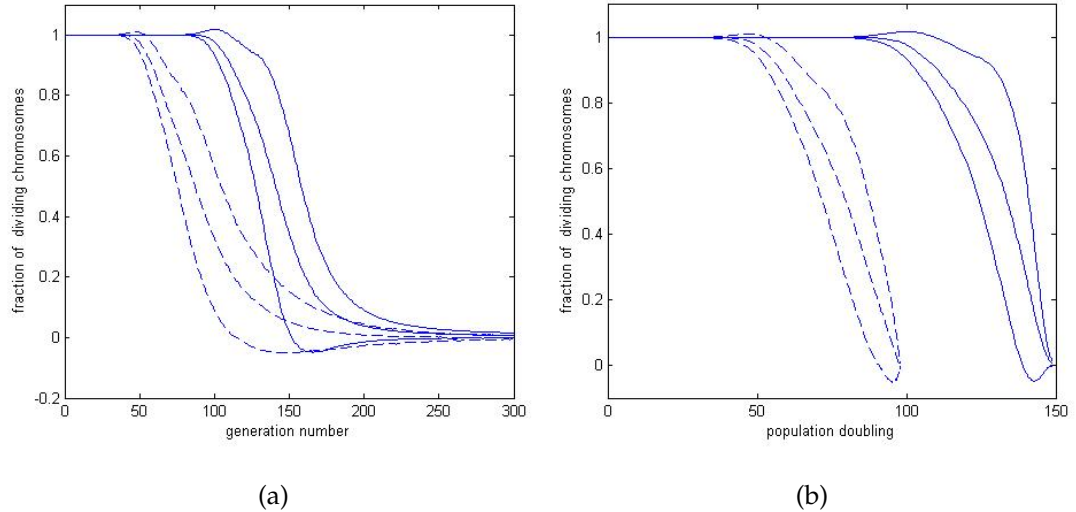
Figure 3.3: *Average of 2000 simulations. The middle dashed line is the fraction of dividing chromosomes plotted against generation number (Figure 3.3(a)), and against population doubling (Figure 3.3(b)) with the Werner's syndrome active $x = y = 200$ basepairs, the dashed line above or below is the mean plus or minus twice the standard deviation. The middle solid line is the fraction of dividing chromosomes plotted against generation number (Figure 3.3(a)), and against population doubling (Figure 3.3(b)) with the normal ageing $y = 200$ basepairs, the solid line above or below is the mean plus or minus twice the standard deviation. Figure 3.3 use the same simulation data from Figure 3.2.*

3.2.2 Combination model with normal ageing and Werner's syndrome

Additional deletions associated with Werner's syndrome do not necessarily happen after each replication event. In this section, we assume that when a replication occurs shortening is governed by Werner's syndrome (one of (3.1.1a)-(3.1.1d) or (3.1.3a)-(3.1.3c)) with probability p and otherwise with probability $1 - p$, division is regulated by (2.1.1) (normal ageing, $K_n^g \to K_n^{g+1} + K_{n-y}^{g+1}$).

When a Werner's syndrome deletion occurs, replication follows one of equations (3.1.1a)-(3.1.1d), each with equal probability $1/4$, provided that the telomere length exceeds the critical telomere length. Chromosome replication follows one of equations (3.1.3a)-(3.1.3b) with equal probability $1/4$ and (3.1.3c) with probability $1/2$ if the telomere length is less than or equal to the critical telomere length. Using the same notation as before, y is the amount of telomere

64

lost in normal ageing and x is the amount of extra telomere lost due to Werner's syndrome.

We not only focus on the average telomere length and the fraction of dividing chromosomes through time (evolution of generation number or population doubling), but also on how telomere length and the fraction of dividing chromosomes changes as p, the probability of Werner's syndrome deletion, varies. We assume that the product of $xp = $ constant, in order to make the average amount of telomere lost per replication the same. We consider a range of values of x, p where $xp = 200$, see Table 3.1. For comparison we also present results for the case $p = x = 0$ which corresponds to normal ageing. The case $p = 1$ corresponds to previous case in Section 3.2.1.

p	0	0.2	0.4	0.6	0.8	1
x	0	1000	500	333	250	200

Table 3.1: Values of p and x.

We use the passaging method described in Section 2.2.4, starting with a single chromosome with initial telomere length $m = n = 6000$ basepairs and $y = 200$ basepairs. The average telomere loss per replication in Werner's syndrome is such that $xp = 200$ basepairs. Still use 200 basepairs as the critical telomere length. We simulate 6 different choices of p and x (see Table 3.1).

Figure 3.4 shows the average telomere length against population doubling, for five different probabilities of Werner's syndrome happening and the case of normal ageing. As the population doubling increase, the average telomere length of all the Werner's syndrome cases decrease and approaches 100 population doubling, 50 population doubling less than normal ageing ($p = 0, x = 0$). When the probability of Werner's deletions lies between 0.4 and 1, there is little difference in average telomere loss between the population doubling. At larger p, the curves in Figure 3.4 drop linearly and then have a sharp transition to horizontal. We summarize the data from Figure 3.4 in Table 3.2 where the average
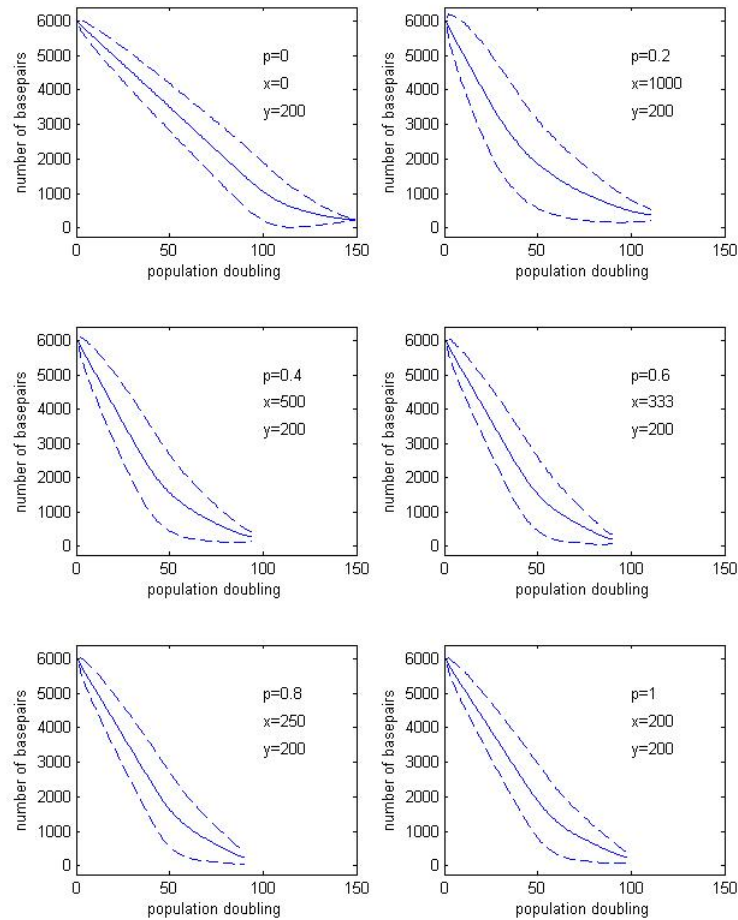
Figure 3.4: *Series of plots showing how, for Werner's syndrome, the average telomere length varies with population doublings. For each value of p, average results from 2000 simulation are presented. Parameter Values: $y = 200$, $(p, x) = (0, 0)$; $(0.2, 1000)$; $(0.4, 500)$; $(0.6, 333)$; $(0.8, 250)$; $(1, 200)$. Key: the solid line is the average telomere length, the dashed lines are the average average telomere length plus (minus) 2 standard deviations.*

telomere length approaches a constant (chromosome became senescent). Table 3.2 shows that the average telomere length in Werner's syndrome reaches a constant faster than normal ageing ($p = 0$). Apart from $p = 0.2$, under Werner's syndrome, all population becomes senescent after 93 population doubling. If we were only to consider the average effects of Werner's deletions, all cases (except $p = 0$) should yield the same results, because the average rate of telom-

66

ere loss on each replication is the same (200 basepairs). When the chromosomes become senescent, the six cases approach different constant values.

p	x	Population doubling	Average telomere length
0	0	150	250
0.2	1000	110	387
0.4	500	93	300
0.6	333	89	216
0.8	250	89	247
1	200	97	244

Table 3.2: Data from Figure 3.4.

p	senescent first appear	population becomes senescent
0	85	150
0.2	11	110
0.4	20	93
0.6	27	89
0.8	31	89
1	35	97

Table 3.3: Summary of data from Figure 3.5.

Figure 3.5 shows how, for Werner's syndrome the fraction of non-senescent chromosomes varies with population doubling and p. Apart from the normal ageing all the graphs are similar. We summarize the data in Table 3.3 which shows that under Werner's syndrome ($p > 0$), the lower the value of p, the sooner the chromosomes become senescence and all become senescent after approximately the same number of population doubling.

Figure 3.6(a) shows how the standard deviation of average telomere length
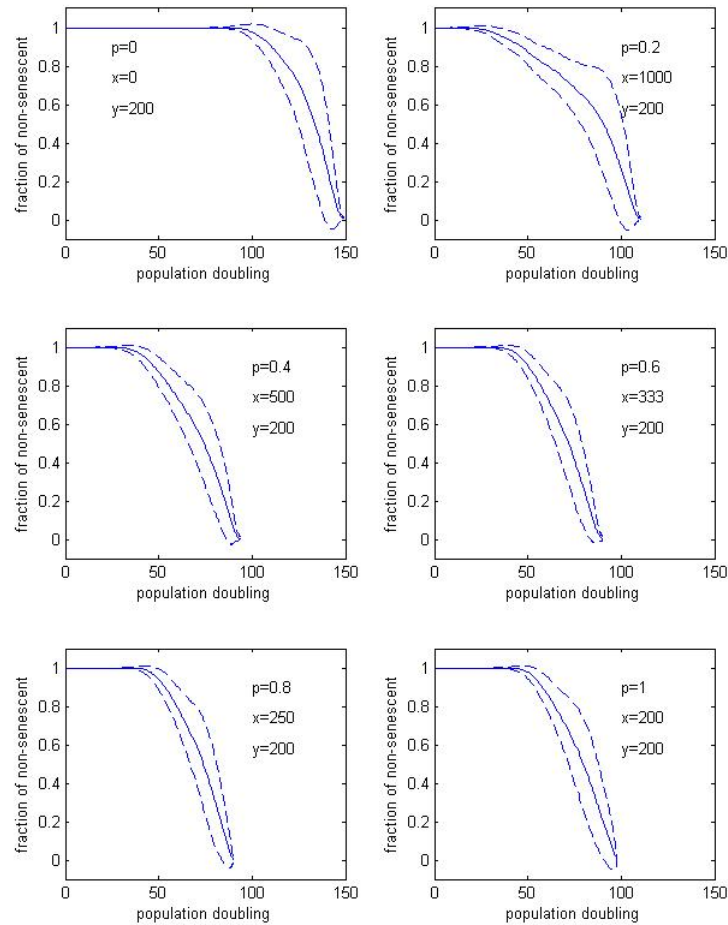
Figure 3.5: *Series of plots showing how, for Werner's syndrome, the proportion of non-senescent chromosomes varies with population doublings. For each value of p, average results from 2000 simulation are presented. Parameter Values: $y = 200$, $(p, x) = (0, 0); (0.2, 1000); (0.4, 500); (0.6, 333); (0.8, 250); (1, 200)$. Key: the solid line is the average fraction of non senescent chromosomes, the dashed lines are the average mean plus (minus) 2 standard deviations.*

varies with population doublings (*a*). As *p* increases, the peak of the standard deviation of average telomere length shrinks and moves to later times (generation number or population doubling). Comparing these figures with Table 3.3 we see the peak happens after the chromosomes start to senescence. The standard deviation approaches a constant indicating that the entire population reaches senescent, when there are no more changes in chromosome length. Fig-

(a)　　　　　　　　　　　　　　　　(b)
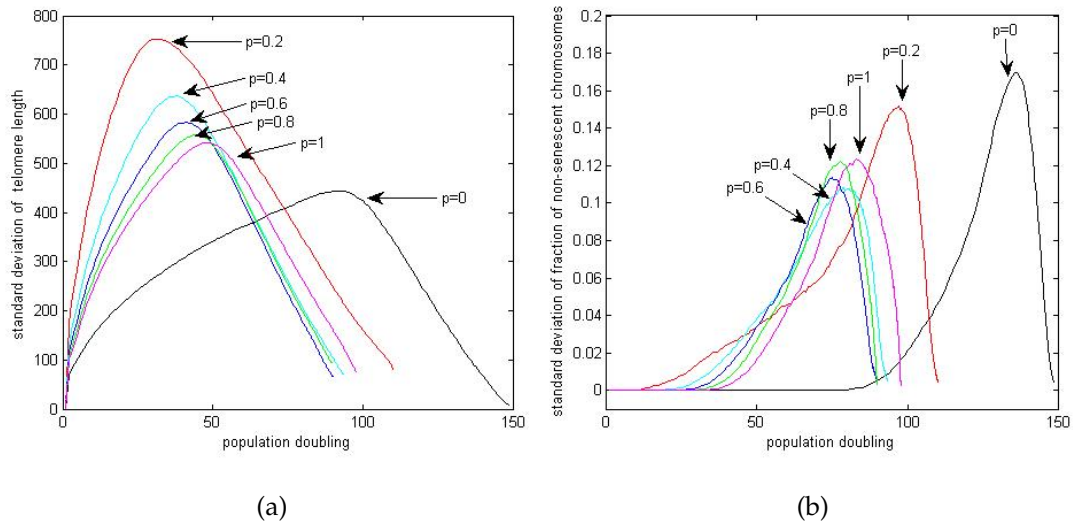
Figure 3.6: *Figure 3.6(a) showing how, for Werner's syndrome, the standard deviation of the average telomere length varies with population doubling, showed in simulations in (Figure 3.4). Figure 3.6(b) showing how the standard deviation of the fraction of non-senescent chromosomes varies with population doublings showed in simulations of (Figure 3.5) for p = 0, 0.2, 0.4, 0.6, 0.8, 1.*

ure 3.6(b) shows how the standard deviation of the fraction of non senescent chromosomes varies with population doublings. At early times the standard deviation is zero since all chromosomes are dividing. Once senescent chromosomes appear (see Table 3.3), the standard deviation increases, reaching a maximum point and then decreasing to a constant value at which time the entire population has become senescent. The figures reveal that for $0.4 \leq p \leq 1$ the shape of curves are similar.

3.3 Cell level model Werner's syndrome

3.3.1 Introduction

The chromosome level model of Werner's syndrome presented in Section 3.2 can be viewed as the simplest cell model, with only one chromosome per cell. We now extend our model to account for the fact that there are 46 chromosomes in a normal human cell. Before the cell replicates, it checks all 46 chromosomes, to make sure none of them will fall below the critical value at which senes-

cence occurs. If one of the chromosomes has reached this critical value, then the cell will not replicate. During cell division, the rules of chromosome replication are: if the the telomere has not reached or fall below the critical length, then the four possible outcomes (3.1.1a)-(3.1.1d) occur with equal probability ($p = 0.25$). By contrast, when one of the telomeres reaches the critical value, then the chromosome stops replicating with probability 0.5 (cases (3.1.3c) or it divides according to either (3.1.3a) or (3.1.3b), with equal probabilities 0.25. After replication daughter chromosomes are allocated randomly to each of the two daughter cells.

3.3.2 Pure Werner's syndrome cell model

We start with a single cell, fixing $m = n = 6000$ basepairs for each of its 46 chromosomes and assume that $y = 200$ basepairs are deleted due to normal ageing whereas $x = 200$ basepairs are deleted due to Werner's syndrome. As before we use 200 basepairs as the critical telomere length and passage the cells as outline in Section 3.2.1. The rules for replication under Werner's syndrome follows those presented in the introduction (3.3.1). We denote by $NC(g)$ the number of cells at generation g, $\phi_{cdiv}(g)$ is the fraction of dividing cells at generation $g - 1$ and $\phi_{csen}(g)$ is the fraction of senescent cells at generation $(g - 1)$. Then we have

$$\phi_{cdiv}(g) = \frac{NC(g) - NC(g-1)}{NC(g-1)}, \quad \phi_{csen}(g) = 1 - \phi_{cdiv}(g). \qquad (3.3.1)$$

In Figure 3.7 we plot the evolution of the average telomere length against generation number, comparing cells affected with Werner's syndrome with those undergoing normal ageing and plot how they varies with generation number (Figure 3.7(a)) and population doubling (Figure 3.7(b)). In Figure 3.7(a) as the generation number increases, the average length of telomere with Werner's syndrome decreases, reaching a value of 1750 basepairs after about 50 generation. Thereafter, the average telomere length remains constant, which indicates that senescence has occurred. If the shortest telomere in the cell falls below the critical value, the whole cell stops replicating, even if all the rest of the

(a)   (b)
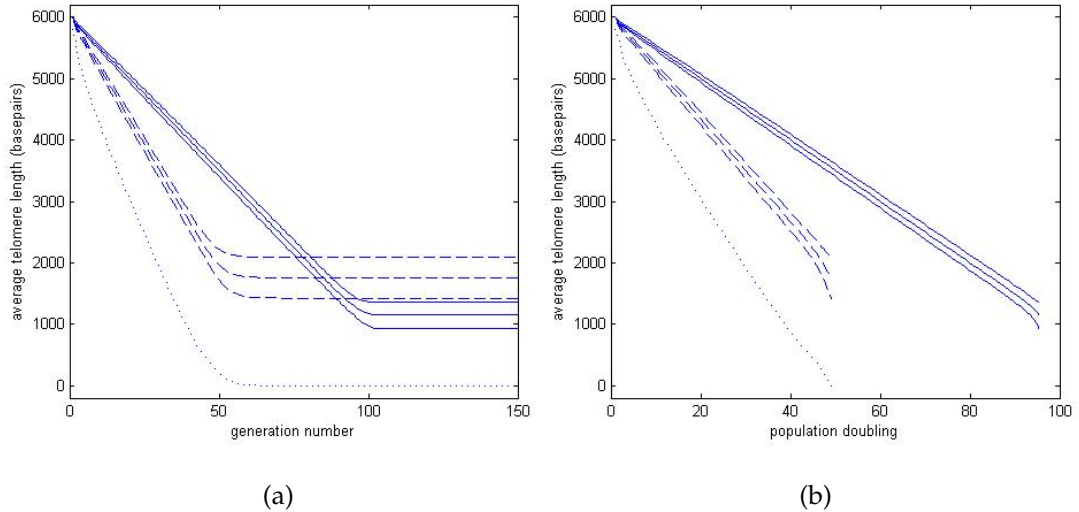
Figure 3.7: *The middle dashed line indicates the average length of telomere of the cells plotted against generation number (Figure 3.7(a)) and population doubling (Figure 3.7(b)) with the Werner's syndrome active $x = y = 200$ basepairs per replication, the dashed lines above and below are the means plus or minus twice the standard deviation. The dotted line indicates the average shortest telomere length of the cells plotted against generation number (Figure 3.7(a)) and population doubling (Figure 3.7(b)). The middle solid line is the average length of telomere of the cells plotted against generation number (Figure 3.7(a)) and population doubling (Figure 3.7(b)) with normal ageing $y = 200$ basepairs, the solid lines above and below are the means plus or minus twice the standard deviation. Figure 3.7(b) use the same simulation data from Figure 3.7(a). Average of 2500 simulations.*

chromosomes still have longer telomeres. When the average shortest telomere length in the cell reaches zero after about 50 generations, the cell stops replicating. This explains why senescent cells have telomeres whose average length is longer than their normal counterparts (1750 basepairs) rather than 1150 basepairs. Comparing these results with those for normal ageing, shows that in Werner's syndrome the rate of telomere shortening is approximately twice as faster as in normal ageing. In normal ageing it takes 100 generations for the telomere length of a cell to decrease from 5950 basepairs to 1150 basepairs, whereas with Werner's syndrome and $x = 200$ basepairs it takes 50 generations for senescence to occur. Figure 3.7(b) shows the same phenomena as Figure 3.7(a).

(a)   (b)
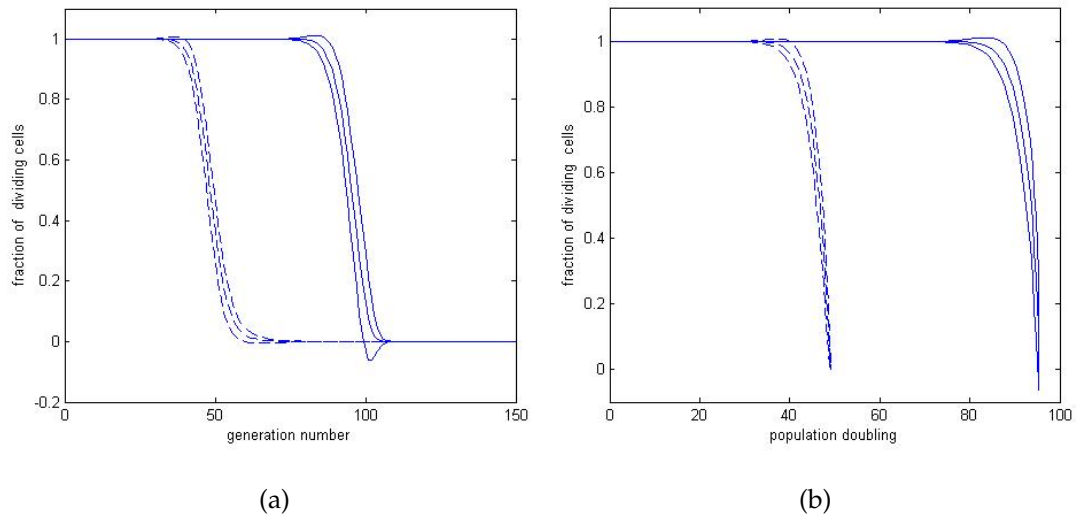
Figure 3.8: *The middle dashed line is the fraction of dividing cells plotted against generation number (Figure 3.8(a)), and against population doubling (Figure 3.8(b)) with the Werner's syndrome active $x = y = 200$ basepairs, the dashed line above or below is the mean plus or minus twice the standard deviation. The middle solid line is the fraction of dividing cells plotted against generation number (Figure 3.8(a)), and against population doubling (Figure 3.8(b)) with the normal ageing $y = 200$ basepairs, the solid line above or below is the mean plus or minus twice the standard deviation. Figure 3.8 use the same simulation data from Figure 3.7. Average of 2500 simulations.*

Figure 3.8 shows how the fraction of dividing cells in Werner's syndrome and normal ageing varies with generation number (Figure 3.8(a)) and population doubling (Figure 3.8(b)). For Werner's syndrome, from generations 1 to 30, all cells are replicating in Werner's simulation. After generation 35 some cells stop replicating and the fraction of senescent chromosomes rapidly increases from zero. After generation 60 the dashed line tends to zero slowly, as the fraction of senescent cell approaches unity. In normal ageing simulations, cells start to become senescent at generation 75 and the entire population is senescent by generation 110, which is approximately twice as many generations as it takes for the Werner's syndrome simulations. These results also indicate that Werner's syndrome accelerates the ageing process.

72

3.3.3 Combination cell model with normal ageing and Werner's syndrome

In this section, we use a similar simulation method to that outlined in in Section 3.2.2. We assume that for each chromosome replication extra Werner's syndrome deletions occur with probability p, while normal ageing deletions occur with probability $1 - p$. When the additional Werner's syndrome deletions occur, the chromosome replication is via one of equations (3.1.1a)-(3.1.1d), each occurring probability, 1/4, provided that the telomere length exceeds the critical value. Otherwise replication is via one of equations (3.1.3a)-(3.1.3b) which occur with equal probability 1/4 or via equation (3.1.3c) which occurring with probability 1/2. When the telomere length of the chromosome falls below than the critical value, then the cell becomes senescent.

We investigate how evolution of the average telomere length and the fraction of dividing cells changes with generation number and population doubling. We also consider how these quantities depend on p, the probability that extra deletions occurs. We start with a single cell with 46 chromosomes, each having initial telomere length $m = n = 6000$ basepairs. We fixed $y = 200$ basepairs as the telomere loss cause by normal ageing. To facilitate comparison between the different cases, we fix the average amount of telomere loss per replication so that $xp =$ constant (200 basepairs) and vary p as stated in Table 3.1.

Figure 3.9 shows how the average telomere length per cell varies with population doublings, for five cases of Werner's syndrome and one for normal ageing. The larger p, the sharper the transition from linear decay to plateau for as senescence. As the population doubling increases, the average telomere length of all the Werner's syndrome cases decreases and approaches 45 population doubling which is about half the number for normal ageing ($p = 0, x = 0$), since the telomere loss per replication in Werner's syndrome is twice that of normal ageing. For the Werner's syndromes simulations, the cells reach senescence at approximately the same population doubling, regardless of the value of p.
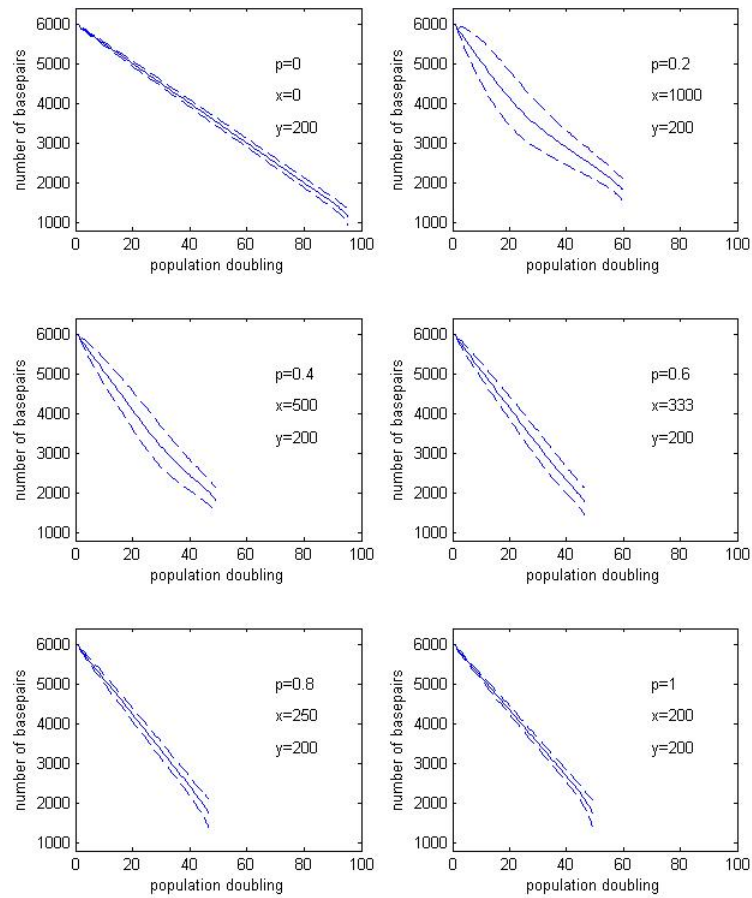
Figure 3.9: *Series of plots showing how, for Werner's syndrome, the average telomere length of the cell with 46 chromosomes varies with population doublings. The different plots correspond to different probabilities with which the extra deletions associated with Werner's syndromes occur. For each value of p, average results from 2000 simulation are presented. Parameter Values: $y = 200$, $(p, x) = (0,0)$; (0.2,1000); (0.4,500); (0.6,333); (0.8,250); (1,200). Key: the solid line is the average telomere length, the dashed lines are the average average telomere length plus (minus) 2 standard deviations.*

In Table 3.4 we summarize some of the data from the simulations presented in Figure 3.9. These data relate to the average telomere length and when the population approaches senescence. The table shows that the average telomere length of the cells approaches a constant more rapidly when Werner's syndrome occurs. Apart from $p = 0.2$, when Werner's syndrome occurs, the cells become

p	x	Population doubling	Average telomere length
0	0	90	1150
0.2	1000	60	1840
0.4	500	50	1830
0.6	333	46	1790
0.8	250	46	1750
1	200	50	1760

Table 3.4: Data from Figure 3.9.

senescent after about 48 population doubling. From Table 3.4, we also note that when Werner's syndrome occurs, the average telomere length of the cell at senescence is significantly longer than for normal ageing.

p	senescent first appear	population becomes senescent
0	74	90
0.2	9	60
0.4	17	50
0.6	23	46
0.8	28	46
1	31	50

Table 3.5: Summary of data from Figure 3.10.

Figure 3.10 shows how, for Werner's syndrome, the fraction of non senescent cells varies with population doubling and with probability p. Apart from the normal ageing case ($p = 0$) and when $p = 0.2$, all the graphs are similar. We summarize some of these data in Table 3.5, which shows that the lower the value of p (apart $p = 0$) the earlier the cells start to senescence and the later the whole population becomes senescent.

Figure 3.11(a) shows how the standard deviation of the cells's telomere length varies with population doublings. In Werner's syndrome as p increases, the
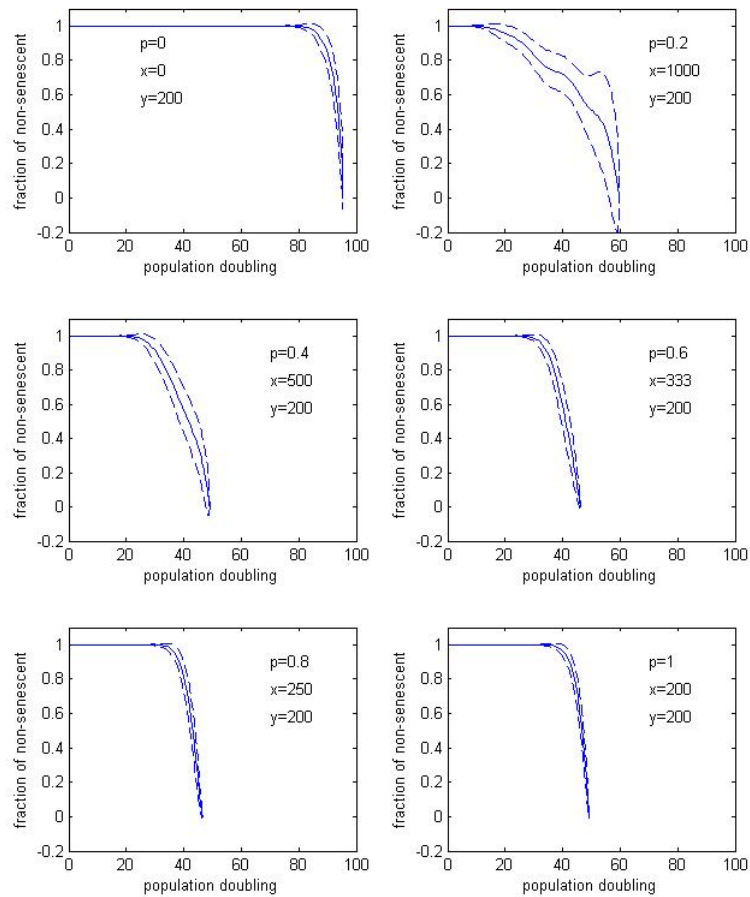
Figure 3.10: *Series of plots showing how for Werner's syndrome, the proportion of non-senescent cells varies with population doublings. The different plots correspond to different probabilities with which the extra deletions associated with Werner's syndromes occur. For each value of p, average results from 2000 simulation are presented. Parameter Values: $y = 200$, $(p, x) = (0,0)$; (0.2,1000); (0.4,500); (0.6,333); (0.8,250); (1,200). Key: the solid line is the average fraction of non senescent chromosomes, the dashed lines are the average mean plus (minus) 2 standard deviations.*

peak of standard deviation of average telomere length of the cell reduces in height and moves to later times (population doubling). Comparing these figures with Table 3.5, we see that the peak happens after the cells first became senescent. The standard deviation of telomere length approaches a constant (dependent on p), indicating that the entire population has become senescent. Figure 3.11(b) shows how the standard deviation of the fraction of non-senescent

76

(a)   (b)
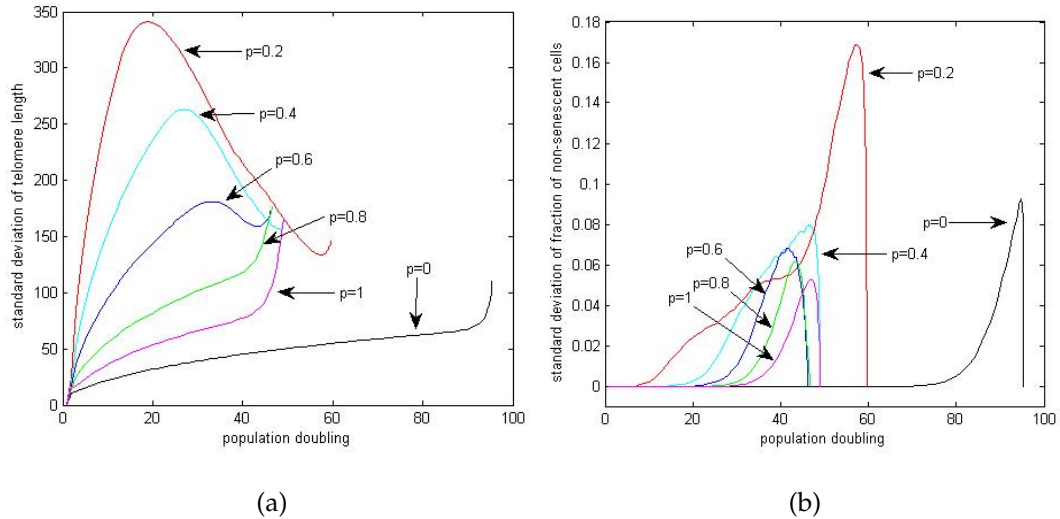
Figure 3.11: *Figure 3.11(a) showing how, for Werner's syndrome, the standard deviation of the average telomere length varies with population doubling, showed in simulations in (Figure 3.9). Figure 3.11(b) showing how the standard deviation of the fraction of non-senescent chromosomes varies with population doublings showed in simulations of (Figure 3.10) for p = 0, 0.2, 0.4, 0.6, 0.8, 1.*

cells varies with generation and population doubling. The maximum peak of each standard deviation happens after all the population has become senescent.

In order to illustrate the distribution of telomere lengths in Werner's syndrome, we have calculated the average and shortest telomere length of 200 cells in one simulation, at generations 10, 15, 20, 25, 30, 35, 40, 45 respectively. The resulting data is presented in Figures 3.12 and 3.13. In Figure 3.12 as the generation number increases the mean telomere length reduces. The distribution slowly spreads out and moves towards the lower telomere length. In Figure 3.13, at generations 10, 15 and 20, we observe that the distribution of the shortest telomere length is bimodal, the generation number increases, the distribution becomes to unimodal and approaches zero telomere length. At generation 45, nearly all the cells have zero telomere length and are senescent. The average telomere length, however is still quite long (see Figure 3.12).
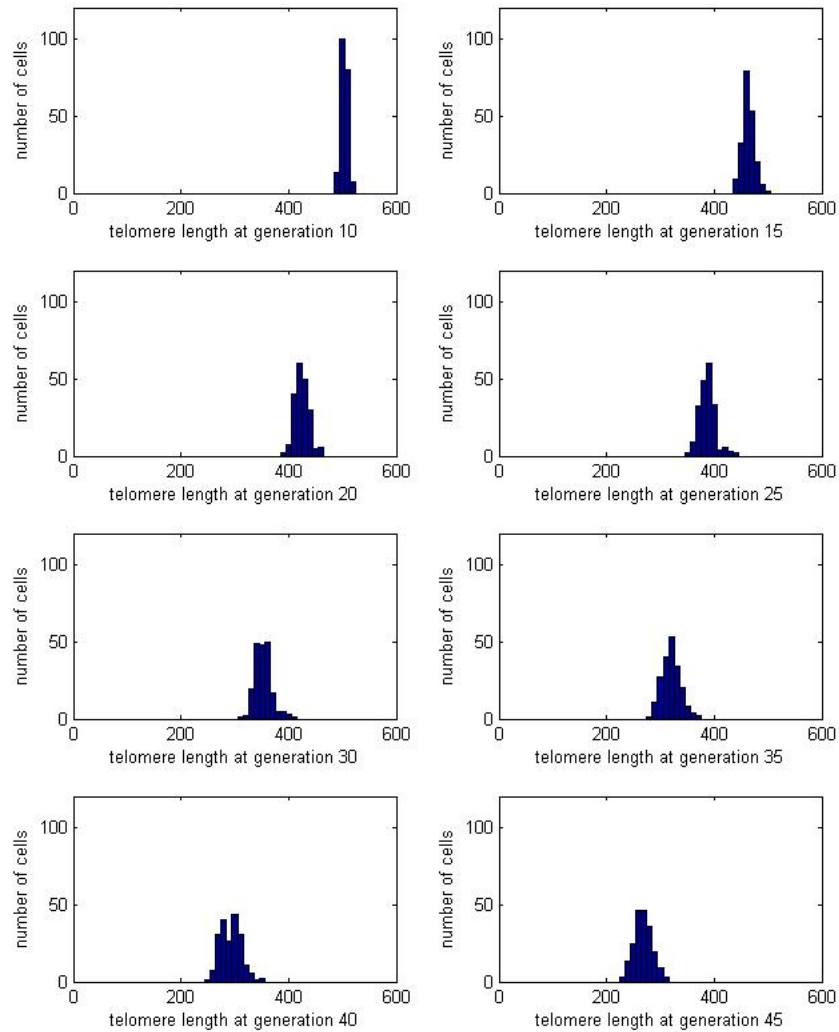
Figure 3.12: *Histogram of average telomere length of the cell for range of generation number in one simulation of Werner's syndrome with $p = 0.2$. The horizontal scale in graph is reduced by a factor of 10.*

3.4 Conclusion

In this chapter we have showed the effects on chromosome replication and telomere length of Werner's syndrome. During replication, not only are y basepairs lost from one of the daughter chromosomes, as in normal ageing, but there is an additional loss of x basepairs at one or other end of one of the daughter
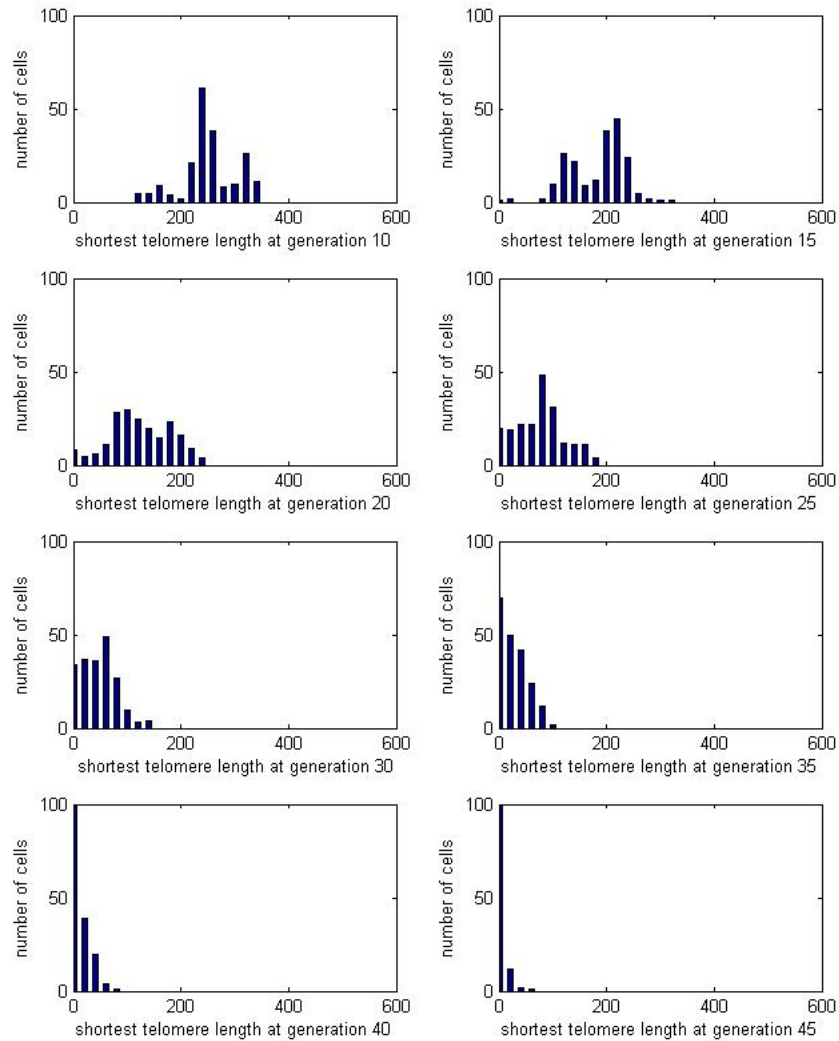
Figure 3.13: *Histogram of shortest telomere length of the cell for range of generation number in one simulation of Werner's syndrome with $p = 0.2$. The horizontal scale in graph is reduced by a factor of 10.*

chromosomes. Based on the replication rule, we developed a chromosome-level model and a cell-level model for Werner's syndrome. In each model we developed a deterministic system where Werner's syndrome occurs all the time ($p = 1$) and stochastic model where Werner's syndrome occurs with probability p and normal ageing occurs with probability $1 - p$. Comparing the results of Werner's syndrome and normal ageing, shows that Werner's syn-

drome cells (chromosomes) reach senescence earlier than normal ageing which indicates that Werner's syndrome can accelerate the ageing process matching the Werner's syndrome's characteristic clinical feature, the rapid appearance of ageing [34].

Another significant observation from the cell model is that when cells with Werner's syndrome become senescent, they contain longer telomeres than normal ageing cells. Figure 3.7 indicates that the shortest telomere length of the chromosomes in the cells reach the critical value, even the average telomere length is still quite long. These results are consistent with an explanation of Werner's syndrome cells [41], which predicts that population of Werner's syndrome cells will contain some very short telomeres but the majority will retain longer telomeres. Thus we observe that Werner's syndrome not only can an accelerate telomere shortening, but also that short telomeres in cells can cause premature senescence. Both of these properties contribute to accelerated ageing that characterizes Werner's syndromes.

Continuum models of telomere shortening in normal ageing

4.1 Introduction

Normal chromosome replication produces one chromosome which is identical to its parent and one which is slightly shorter. In this chapter, we use the chromosome replication rules introduced in Chapter 2. We denote by m, h are the numbers of basepairs in the telomere at each end of the chromosome and by y, the average number of basepairs lost per replication. We represent the replication process in the following manner:
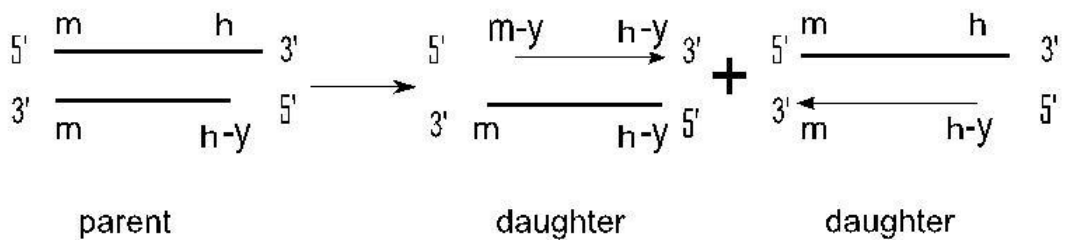
Figure 4.1: *Chromosome replication rule.*

In this chapter, we denote by n the average telomere length of a pair chro-

mosomes (four ends), by K_n^g the number of chromosomes with total telomere length n at generation g and by Y the number of basepairs that are lost when a cell divides. Then the discrete chromosome replication process depicted in Figure (4.1) can be written as

$$K_n^g \rightarrow K_n^{g+1} + K_{n-Y}^{g+1},\qquad(4.1.1)$$

and we assume that this event occurs with probability P_{div}. In general, the telomere loss Y during chromosome replication may vary and the probability that a chromosome divides may not always be constant. For example, chromosomes with longer telomeres have the potential to lose more basepairs than those with shorter telomeres and may have a greater probability of dividing than ones with shorter telomeres [64] [65]. Consequently in this chapter we continue to assume $Y(n) = y_0 + y_1 n$ and $P_{div}(n) = (a + bn)^\alpha$ where y_0, y_1, a, b and α are constants and n is the average telomere length of chromosomes (four ends). As in Chapter 2, we will develop chromosome and cell-based models and consider 4 different cases. For comparison with Chapter 2 , the cases we consider are as outlined in Table 4.1.

Case	P_{div}	Y
Case I	$P_{div} = 1$	$Y(n) = L$
Case II	$P_{div} = 1$	$Y(n) = y_0 + y_1 n$
Case III	$P_{div} = (a + bn)^\alpha$	$Y(n) = L$
Case IV	$P_{div} = (a + bn)^\alpha$	$Y(n) = y_0 + y_1 n$

Table 4.1: Summary of the rules for cell division and telomere shortening that we consider.

Case I has constant telomere loss $Y(n) = y_0$ basepairs and dividing probability $P_{div} = 1$. Case II has length-dependent loss $Y(n) = y_0 + y_1 n$ basepairs where y_0, y_1 are constant and n is average telomere length of chromosomes and dividing probability $P_{div} = 1$. Case III has constant loss $Y(n) = L$ basepairs and the probability of dividing is dependent on telomere length $P_{div} = (a + bn)^\alpha$ where a, b, α are constants. Case IV has length-dependent loss $Y(n) = y_0 + y_1 n$

basepairs and the probability of dividing is dependent on telomere length as well $P_{div} = (a + bn)^\alpha$. In Chapter 2 we have already simulated the stochastic models for chromosome model (Section 2.2) and cell model(Section 2.3) respectively with four different cases. In this chapter we focus on the continues model instead of discrete model, we formulate Monte Carlo descriptions and continuum analogues (PDE) of these models.

In 1992 Levy *et al*. modelled the telomere shortening using a constant telomere loss, Case I [1]. Their model predict average telomere length decreases linearly with generation numbers and consistent with experimental data. Stochastic simulation for Case II and Case III were developed by Buijs [64] *et al*. and Portugal [65] *et al*. respectively. For Case III, Portugal [65] only consider the cell replication rate is linearly depends on the telomere length, apart from that, we also consider the nonlinear cases in cell-level model. The work relating to Case IV is new. Our main aim in this chapter is to build models that combine a variable rate of telomere shortening with a variable probability of cell division, to see how the cell's lifespan changes when both telomere shortening and division depend on telomere length (Case IV).

4.2 Mathematical chromosome model of normal ageing

In the following sections, we start with the chromosomes model where we assumed each cell contained only one chromosome. If one of the chromosomes has reached this critical value, the cell will not replicate. If a cell replicates, it produces two daughter cells. Here we are going to consider four different cases, summarized in Table 4.1. In each cases we focus on the continuum model instead discrete model, we formulate Monte Carlo descriptions and continuum analogues (PDE) of these models.

4.3 Case I: Constant loss of telomeres

4.3.1 *Discrete model*

In Case I both the telomere loss per replication and the probability of cell division are constant. We denote by K_n^g the number of chromosomes with telomere length n at generation g and by L the number of basepairs that are lost when a chromosome divides, and assume that the chromosomes evolve according to the discrete chromosome replication:

$$K_n^g \rightarrow K_n^{g+1} + K_{n-L}^{g+1}, \quad \text{with probability } P_{div} = 1, \tag{4.3.1}$$

where g, n, $L \in \mathbb{N}$. We assume that initially there is one chromosome with telomere length $n_{initial} = Q$ basepairs. We replace (4.3.1) by the following kinetic equation:

$$K_n^{g+1} = K_n^g + K_{n+L}^g. \tag{4.3.2}$$

We assume that (4.3.2) admits separable solutions of the form $K_n^g = e^{\gamma g + \chi n}$ where the growth rate γ depends on χ the decays rate of the distribution in n. Substituting the trial solution into (4.3.2) leads to the dispersion relation for

$$e^{\gamma(g+1)+\chi n} = e^{\gamma g + \chi n} + e^{\gamma g + \chi(n+L)},$$

$$\text{or} \quad e^{\gamma} = 1 + e^{\chi L}. \tag{4.3.3}$$

This describes how quickly the distribution which decays with rate χ in n, grows in time, g. Rapidly decaying distributions $(-\chi \gg 1)$ grow more slowly (have a smaller χ) than distributions which decay slowly in n, that is $(-\chi \ll 1)$.

4.3.2 *Continuum model*

We wish to construct a continuum description of the process (4.3.3). If we assume that χ is small then this expression reduces to

$$\gamma \approx \ln 2 + \frac{\chi L}{2} + \frac{1}{8}\chi^2 L^2. \tag{4.3.4}$$

Our aim here is to develop a PDE with the same relation as (4.3.4). In general, the number of chromosomes K becomes very large over a few generations and

can therefore be treated as a continuous variable. We also replace the discrete generation number g by a continuous time variable, t. Since the telomere length in the normal human cells is approximately 3k to 15k basepairs and the average telomere loss during chromosome replication is $50 - 200$ basepairs [14] , which is much less than the initial telomere length, we can treat telomere length, n, as a continuous variable. To construct a continuous model in which telomere length q and generation number g are continuous, we replace K_n^g by $K(n, t)$ where $t = g$, so $t, n, K \in \mathbb{R}$. The continuous analogue of (4.3.2) is assumed to be the simplest partial differential equation which has the same dispersion relation as (4.3.4), so that

$$\frac{\partial K}{\partial t} = K \ln 2 + \frac{1}{2} L \frac{\partial K}{\partial n} + \frac{1}{8} L^2 \frac{\partial^2 K}{\partial n^2} . \tag{4.3.5}$$

We assume that at $t = 0$ we have a single chromosome, with mean telomere length $n_{initial} = Q$. So that $K(n, 0) = \delta(n - Q)$. We solve (4.3.5) by prescribing the following initial and boundary conditions:

$$K(n, 0) = \delta(n - Q) \quad \text{and} \quad K(n, t) \to 0 \quad \text{as} \quad n \to \pm\infty . \tag{4.3.6}$$

This is an approximation to the more restrictive conditions of $\partial K / \partial n = 0$ at $n = 0$ and $n = Q + h$ for some $h > 0$, since telomere of length greater than Q and less than zero cannot be constructed. However we note that (4.3.2) implies $\partial K / \partial n \to 0$ as $n \to \infty$ and when interpreting the results later, we only consider $n \geq 0$. Here $K(n, t) / (\int K(j, t) dj)$ is the probability density function.

4.3.3 *Fourier analysis*

The derivation of (4.3.5) can be explained more rigorously by considering the evolution of the system in Fourier space. Firstly we note that (4.3.1) implies exponential growth of the form $K_n^g = 2^g f(n, g)$ where $f(n, g)$ is the probability density function and $\int f(n, g) dn = 1$. Hence (4.3.2) can be written as

$$f(n, g + 1) = \tfrac{1}{2}[f(n, g) + f(n + L, g)] . \tag{4.3.7}$$

Now we use Fourier transform, where $\hat{f}(k, g) = \mathcal{F}(f(n, g)) = \int_{-\infty}^{\infty} e^{ikn} f(n, g) dn$. Then (4.3.7) can be transform to

$$\hat{f}(k, g + 1) = \tfrac{1}{2}(1 + e^{-ikL}) \hat{f}(k, g) . \tag{4.3.8}$$

We expand $\hat{f}$ about $\hat{f}(k, g + \frac{1}{2})$ using Taylor series to obtain

$$\hat{f}(k, g + \tfrac{1}{2}) + \frac{1}{2}\frac{\partial \hat{f}(k, g + \frac{1}{2})}{\partial g} = \frac{1}{2}(1 + e^{-ikL})\left[\hat{f}(k, g + \tfrac{1}{2}) - \frac{1}{2}\frac{\partial \hat{f}(k, g + \frac{1}{2})}{\partial g}\right].$$

(4.3.9)

Smooth distributions which vary slowly in n correspond to small values of k. Assuming the solution $f(n, g)$ is slowly varying in n, (4.3.9) can be written as

$$\hat{f}(k, g + \tfrac{1}{2}) + \frac{1}{2}\frac{\partial \hat{f}(k, g + \frac{1}{2})}{\partial g}$$

$$= \quad \frac{1}{2}\left(2 - ikL + \frac{i^2 k^2}{2}\right)\left[\hat{f}(k, g + \tfrac{1}{2}) - \frac{1}{2}\frac{\partial \hat{f}(k, g + \frac{1}{2})}{\partial g}\right], \quad (4.3.10)$$

and further rearrange and expanding leads to

$$\frac{\partial \hat{f}(k, g + \frac{1}{2})}{\partial g} = \hat{f}(k, g + \tfrac{1}{2})\left(-\frac{1}{2}ikl + \frac{1}{8}i^2 k^2 L^2\right).$$

(4.3.11)

Now we invert the Fourier transform, to gain

$$\frac{\partial f(n, t)}{\partial t} = \frac{1}{2}L\frac{\partial f(n, t)}{\partial n} + \frac{1}{8}L^2\frac{\partial^2 f(n, t)}{\partial n^2}.$$

(4.3.12)

Since $K_n^g = 2^g f(n, g)$, we can write $2^t K(n, t) = f(n, t)$ where $f(n, t)$ is also a probability density function, $t = g$ and $\int f(n, t)dn = 1$. Hence (4.3.12) can be written as (4.3.5).

4.3.4 *General solution for PDE*

Consider the following linear partial differential equation

$$\frac{\partial K}{\partial t} = \alpha K + \beta\frac{\partial K}{\partial n} + D\frac{\partial^2 K}{\partial n^2},$$

(4.3.13)

with initial condition $K(n, 0) = \delta(n - Q_{initial})$ and boundaries conditions $K \to 0$ as $n \to \pm\infty$ where α, β, D and $Q_{initial}$ are constants. We use Fourier transform to solve (4.3.13). In terms of the Fourier transforms $\hat{K}(k, t)$

$$\hat{K}(k, t) \quad = \quad \mathcal{F}(K) = \int_{-\infty}^{\infty} e^{ikn} K(n, t)dn, \qquad (4.3.14)$$

$$\mathcal{F}\left(\frac{\partial K}{\partial n}\right) \quad = \quad \int_{-\infty}^{\infty} \frac{\partial K(n, t)}{\partial n}e^{ikn}dn = \int_{-\infty}^{\infty} \frac{\partial}{\partial n}(e^{ikn}K) - ike^{ikn}Kdn$$

$$= \quad [e^{ikn}K]_{-\infty}^{\infty} - ik\hat{K}(k, t), \qquad (4.3.15)$$

The requirement that $K(n, t) \to 0$ as $n \to \pm\infty$ implies that $[e^{ikn}K]_{-\infty}^{\infty} = 0$ and
hence that

$$\mathcal{F}\left(\frac{\partial K}{\partial n}\right) = -ik\hat{K}(k, t). \qquad (4.3.16)$$

Consequently further derivatives can be easily calculated and

$$\mathcal{F}\left(\frac{\partial^2 K}{\partial n^2}\right) = -ik\mathcal{F}\left(\frac{\partial K}{\partial n}\right) = -k^2\hat{K}(k, t). \qquad (4.3.17)$$

Substituting with (4.3.14), (4.3.16), (4.3.17) in (4.3.13) supplies the following
ODE for $\hat{K}$

$$\frac{\partial \hat{K}}{\partial t} = \alpha\hat{K} - \beta ik\hat{K} - Dk^2\hat{K} = \left(\alpha - \beta ik - Dk^2\right)\hat{K}, \qquad (4.3.18)$$

with solution

$$\hat{K} = A(k)\exp\left[\left(\alpha - \beta ik - Dk^2\right)t\right], \qquad (4.3.19)$$

where $A(k)$ is an arbitrary function. The initial conditions $K(n, 0) = \delta(n - Q_{initial})$ transform to give

$$\hat{K}(k, 0) = \int_{-\infty}^{\infty} e^{ikn}\delta(n - Q_{initial})dn = e^{ikQ_{initial}}. \qquad (4.3.20)$$

We substitute (4.3.20) into (4.3.19) to find $A = e^{ikQ_{initial}}$, hence

$$\hat{K} = \exp\left[\left(\alpha - \beta ik - Dk^2\right)t + ikQ_{initial}\right]. \qquad (4.3.21)$$

Inverting the Fourier transform we obtain the general solution

$$\begin{aligned}
K(n, t) &= \mathcal{F}^{-1}(\hat{K}) = \frac{1}{2\pi}\int_{-\infty}^{\infty} e^{-ikn}\hat{K}(k, t)dk \\
&= \frac{1}{2\sqrt{\pi Dt}}\exp\left[\alpha t - \frac{(n + \beta t - Q_{initial})^2}{4Dt}\right]. \qquad (4.3.22)
\end{aligned}$$

Let $\mu = Q_{initial} - \beta t, \sigma = \sqrt{2Dt}$, so (4.3.22) can be written as

$$K(n, t) = \frac{e^{\alpha t}}{\sqrt{2\pi\sigma^2}}\exp\left[-\frac{(n - \mu)^2}{2\sigma^2}\right]. \qquad (4.3.23)$$

This is a Gaussian distribution, with mean μ and variance σ^2 and growth rate
$e^{\alpha t}$.

4.3.5 *General solution for our model*

Using the method outlined above, with $\alpha = \ln 2$, $\beta = \frac{1}{2}L$, $D = \frac{1}{8}L^2$ and $Q_{initial} = Q$, we deduce that the solution for (4.3.5) is that

$$K(n,t) = \frac{2^{t+1}}{L\sqrt{2\pi t}} \exp\left[-\frac{2(n + \frac{1}{2}Lt - Q)^2}{L^2 t} \right].$$ (4.3.24)

This is a Gaussian distribution, with mean $Q - Lt/2$ and variance $L^2 t/4$. For
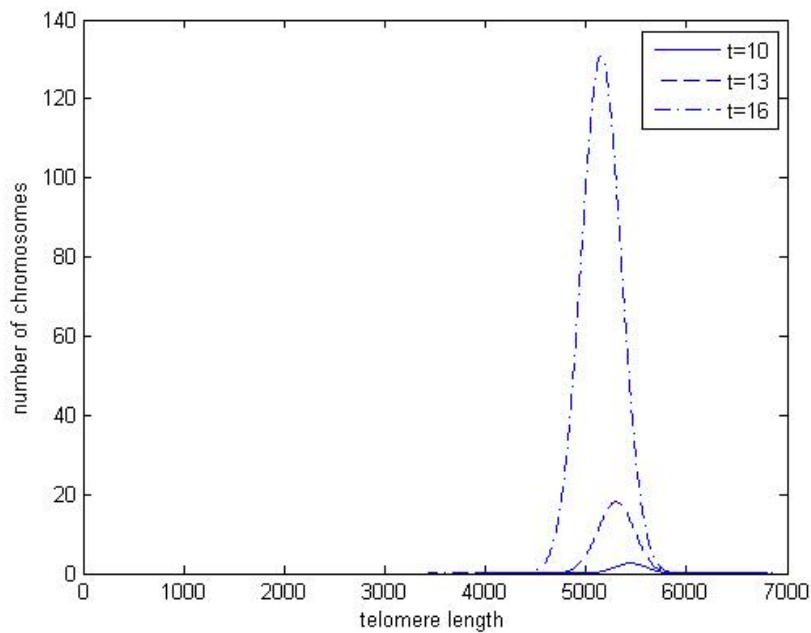
Figure 4.2: *Distribution of telomere length with $t = 10, 13, 16$.*

comparison with the stochastic simulations, we pick $Q = 6000$ basepairs and $L = 100$ basepairs. Figure 4.2 shows that, the chromosome number increases exponentially with time and the distribution of telomere length moves towards the left it becomes more diffuse.

Figure 4.3 indicates that the average telomere length decreases linearly before the chromosome becomes senescent, are suit which is in good agreement with stochastic simulation presented in Chapter 2 Section 2.2.4.
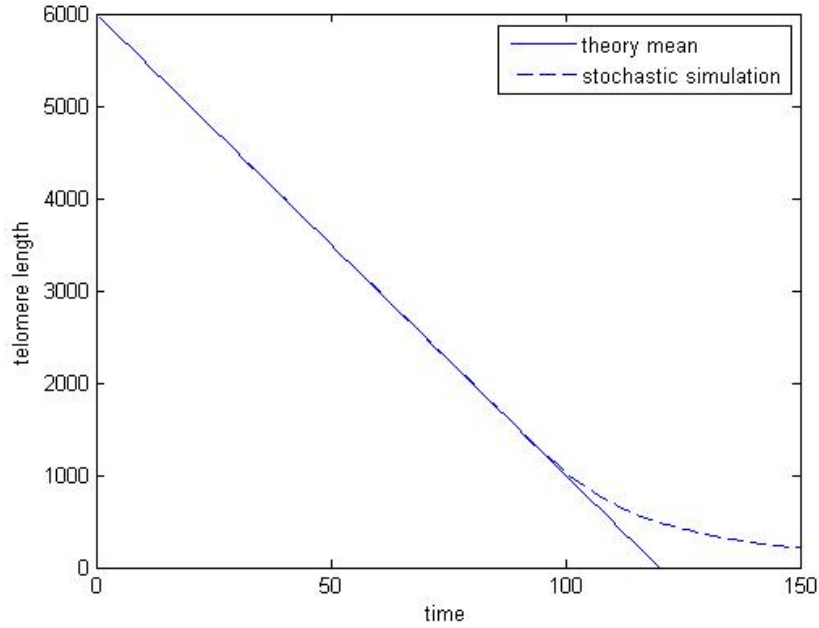
Figure 4.3: *Average telomere loss against time. Solid line is the theory mean $Q -
Lt/2$ and dashed line is the stochastic simulation which did on the first year.*

4.4 Case II: telomere loss depends on telomere length

As before, we denote by K_n^g the number of chromosomes with mean telomere
length n at generation g. The amount of telomere lost during replication now
depends on telomere length so that $Y(n) = y_0 + y_1 n$ where y_0, y_1 are positive
constants and $0 \leq 1 \leq 1$. We remark that Case I is a special case of Case II, with
$y_1 = 0$. The chromosome replication process can be written as

$$K_n^g \rightarrow K_n^{g+1} + K_{n-y_0-y_1 n}^{g+1}, \tag{4.4.1}$$

Using (4.4.1), we know that K_n^{g+1} can come from K_n^g or K_j^g where $j - y_0 - y_1 j =
n$, which implies $j = (n + y_0)/(1 - y_1)$. Hence the process is modelled mathe-
matically via the following kinetic equation

$$K_n^{g+1} = K_n^g + K_{\frac{n+y_0}{1-y_1}}^g. \tag{4.4.2}$$

We seek trial solutions to (4.4.2) of the form $K_n^g = e^{\gamma g}(\alpha + \beta n)^p$ where the
growth rate γ depends on n, α, β and p as follows

$$e^\gamma = 1 + \left[\frac{1}{1 - y_1} + \frac{y_0 \beta - y_1 \alpha}{(1 - y_1)(\alpha + \beta n)} \right]^p. \tag{4.4.3}$$

We require that the growth rate γ be independent of telomere length n and hence fix $\alpha = y_0\beta/y_1$ so that (4.4.3) simplifies to give

$$e^\gamma = 1 + (1 - y_1)^{-p}.$$

The limit $p \to 0$ corresponds to the limit $\chi \to 0$ used for Case I. In order to convert the system (4.4.2) into one more similar to Case I, we transform from n to x via $e^x = y_0 + y_1 n$, or equivalently

$$x = \ln(y_0 + y_1 n). \qquad (4.4.4)$$

With $\tilde{K}_x^g = K_n^g$, we have

$$K_{\frac{n+y_0}{1-y_1}}^g = \tilde{K}_{\ln\left(y_0 + y_1\left(\frac{n+y_0}{1-y_1}\right)\right)}^g = \tilde{K}_{\ln(y_0+y_1 n)-\ln(1-y_1)}^g = \tilde{K}_{x-\ln(1-y_1)}^g,$$

which implies (4.4.2) can be written as

$$\tilde{K}_x^{g+1} = \tilde{K}_x^g + \tilde{K}_{x+\tilde{L}}^g, \qquad (4.4.5)$$

where $\tilde{L} = -\ln(1 - y_1)$. We assume that (4.4.5) admits separable solutions of the form $\tilde{K}_x^g = e^{\gamma g + \chi x}$ where the growth rate $\gamma = \gamma(\chi)$ is such that $e^\gamma = 1 + e^{\chi L}$ or equivalently

$$e^\gamma = 1 + e^{-\chi \ln(1-y_1)}. \qquad (4.4.6)$$

If we assume $\chi \ll 1$ then (4.4.6) reduces to give

$$\gamma \approx \ln 2 - \frac{1}{2}\chi \ln(1 - y_1) + \frac{1}{8}\chi^2 \ln^2(1 - y_1). \qquad (4.4.7)$$

Compare equations (4.3.4) and (4.4.7), we conclude that the dispersion relation for Case II is identical to that for Case I with $L = -\ln(1 - y_1)$.

For the continuous model we replace the generation number by a continuous time variable t and K_n^g and $\tilde{K}_x^g$ by $K(n, t)$ and $\tilde{K}(x, t)$ respectively. Equation (4.4.5) is replaced by the simplest partial differential equation that possesses the dispersion relation (4.4.7), so that

$$\frac{\partial \tilde{K}(x, t)}{\partial t} = \ln(2)\tilde{K}(x, t) - \frac{1}{2}\ln(1 - y_1)\frac{\partial \tilde{K}(x, t)}{\partial x} + \frac{1}{8}\ln^2(1 - y_1)\frac{\partial^2 \tilde{K}(x, t)}{\partial x^2}.$$
$$(4.4.8)$$

Since $x = \ln(y_0 + y_1 n)$, we have

$$\frac{d}{dx} = \frac{y_0 + y_1 n}{y_1} \frac{d}{dn}, \qquad (4.4.9)$$

$$\frac{d^2}{d^2 x} = \frac{(y_0 + y_1 n)^2}{y_1^2} \frac{d^2}{d^2 n} + \frac{y_0 + y_1 n}{y_1} \frac{d}{dn}, \qquad (4.4.10)$$

and we deduce that the partial differential equation for $K(n,t)$ is

$$\frac{\partial K(n,t)}{\partial t} = \ln(2) K(n,t) + \frac{(y_0 + y_1 n)[\ln^2(1 - y_1) - 4\ln(1 - y_1)]}{8 y_1} \frac{\partial K(n,t)}{\partial n} +$$

$$\frac{(y_0 + y_1 n)^2 \ln^2(1 - y_1)}{8 y_1^2} \frac{\partial^2 K(n,t)}{\partial n^2}. \qquad (4.4.11)$$

We assume that when $t = 0$, $K(n,t)$ is $K(n,0) = \delta(n - Q)$ and $\frac{y_1}{y_0 + y_1 n} \int_{-\infty}^{\infty} \delta(x - \ln(y_0 + y_1 Q)) dx = 1$. Equivalently, since $x = \ln(y_0 + y_1 n)$ we have $\tilde{K}(x,0) = \frac{y_1}{y_0 + y_1 Q} \delta(x - \ln(y_0 + y_1 Q))$.

Using the approach outlined in Section (S4.3.4), with $\alpha = \ln 2$, $\beta = -\frac{1}{2} \ln(1 - y_1)$, $D = \frac{1}{8} \ln^2(1 - y_1)$, $Q_{initial} = \ln(y_0 + y_1 Q)$ and

$$\tilde{K}(x,0) = \frac{y_1}{y_0 + y_1 Q} \delta(x - \ln(y_0 + y_1 Q)). \qquad (4.4.12)$$

We deduce that the general solution of (4.4.8) is

$$\tilde{K}(x,t) = -\frac{\sqrt{2} 2^t y_1}{(y_0 + y_1 Q)\sqrt{t\pi} \ln(1 - y_1)} \times$$

$$\exp\left\{ -\frac{2[x - \frac{t}{2}\ln(1 - y_1) - \ln(y_0 + y_1 Q)]^2}{t \ln^2(1 - y_1)} \right\}. \qquad (4.4.13)$$

Further the solution for K_n^g is

$$K_n^g = -\frac{\sqrt{2} 2^t y_1}{(y_0 + y_1 Q)\sqrt{t\pi} \ln(1 - y_1)} \times$$

$$\exp\left\{ -\frac{2[\ln(y_0 + y_1 n) - \frac{t}{2}\ln(1 - y_1) - \ln(y_0 + y_1 Q)]^2}{t \ln^2(1 - y_1)} \right\}. \qquad (4.4.14)$$

In the above expressions we view n as a real number. In practice, it is restricted to integers in the range $0 \le n \le N_{max}$. We introduce $\mu_n(t)$ to represent the

average telomere length of a chromosome at time t so that

$$\mu_n(t) = \frac{\int_0^{N_{max}} nK(n,t)dn}{\int_0^{N_{max}} K(n,t)dn}, \tag{4.4.15}$$

where $N_{max} = Q$ is the maximum telomere length at time t (this cannot exceed the initial telomere length). Since $x = \ln(y_0 + y_1 n)$, we can rewrite (4.4.15) in terms of $\tilde{K}(x,t)$ as

$$\mu_n(t) = \frac{\int_{\ln y_0}^{\ln(y_0+y_1 Q)} \left(\frac{e^x - y_0}{y_1}\right) \tilde{K}(x,t)e^x dx}{\int_{\ln y_0}^{\ln(y_0+y_1 Q)} \tilde{K}(x,t)e^x dx}. \tag{4.4.16}$$

Using $\sigma_n(t)$ to denote the variance of the telomere length at time t, we find

$$\begin{aligned} \sigma_n^2(t) &= \frac{\int_0^{N_{max}} [n - \mu_n(t)]^2 K(n,t)dn}{\int_0^{N_{max}} K(n,t)dn} \\ &= \frac{\int_{\ln y_0}^{\ln(y_0+y_1 Q)} \left[\frac{e^x - y_0}{y_1} - \mu_n(t)\right]^2 \tilde{K}(x,t)e^x}{\int_{\ln y_0}^{\ln(y_0+y_1 Q)} \tilde{K}(x,t)e^x dx}. \end{aligned} \tag{4.4.17}$$

For comparison with our earlier stochastic simulations (see Chapter 2), we choose $Q = 5950$ basepairs, $y_0 = 50$ and $y_1 = 1/60$ in which case the amount of telomere loss at each replication is identical to that for the stochastic simulations. A comparison of our results is presented in Figure 4.4. The mean telomere length of the stochastic simulation lies within two standard deviations of the $\mu_n(t)$ theoretical mean. Before $t = 120$ the mean telomere length, $\mu_n(t)$, for the theoretical model lies within two standard deviations of the mean of the stochastic simulation. At long times the theoretical estimate of $\mu_n(t)$ is more than two standard deviations less than the stochastic mean, since at these times nearly all the chromosomes have become senescent.

When chromosomes divide they produce two daughter chromosomes with non-negative telomere length. From (4.4.2), we require that the telomere length be
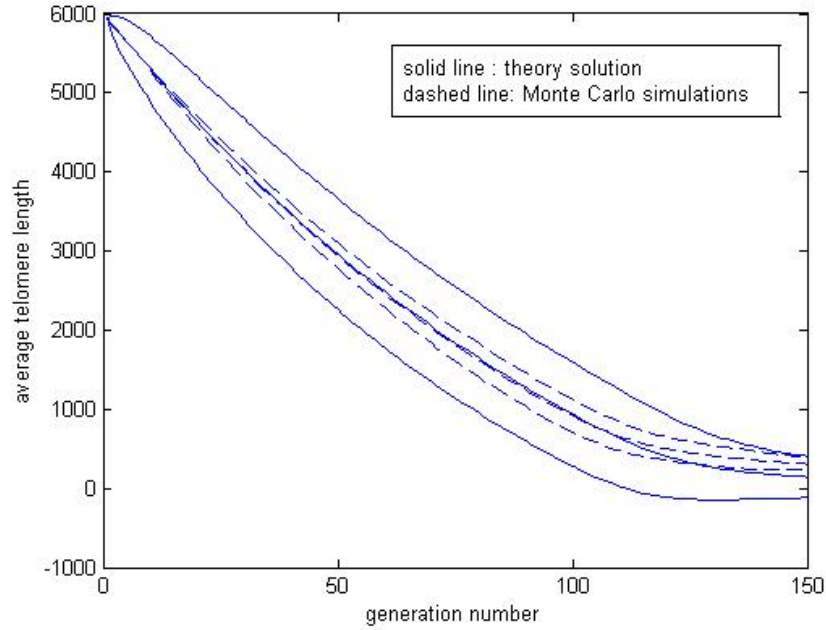
Figure 4.4: *The middle solid line is the average telomere length $\mu_n(t)$ (4.4.15) and
the solid lines above and below is the average telomere length $\mu_n(t)$ plus or minus two
standard deviations, $\sigma_n(t)$ (4.4.17). The middle dashed line is the average telomere
length against generation number in stochastic simulation which we obtained early
and the dashed lines above and below is the average telomere length of stochastic sim-
ulations plus or minus two standard deviations.*

greater than $y_0/(1 - y_1)$ for cell division to occur. A telomere length less than
$y_0/(1 - y_1)$ leads to cell senescence. Hence the fraction of dividing chromo-
somes $\phi_{div}(t)$, can be described by

$$
\phi_{div}(t) = \frac{\displaystyle\int_{\frac{y_0}{1-y_1}}^{N_{max}} K(n,t)dn}{\displaystyle\int_{0}^{N_{max}} K(n,t)dn} = \frac{\displaystyle\int_{\ln\left[y_0+y_1\left(\frac{y_0}{1-y_1}\right)\right]}^{\ln(y_0+y_1Q)} K(x,t)e^x dx}{\displaystyle\int_{\ln y_0}^{\ln(y_0+y_1Q)} K(x,t)e^x dx} . \tag{4.4.18}
$$

In Figure 4.5 we show how the fraction of dividing chromosomes changes over
time for the stochastic and continuum models. The theoretical fraction $\phi_{div}(t)$
and the stochastic fraction are identically the same until $t = 110$ and then di-
verge slightly but still remain within two standard deviations of each other.
Thus continuum model still a good approximation to discrete one.

93
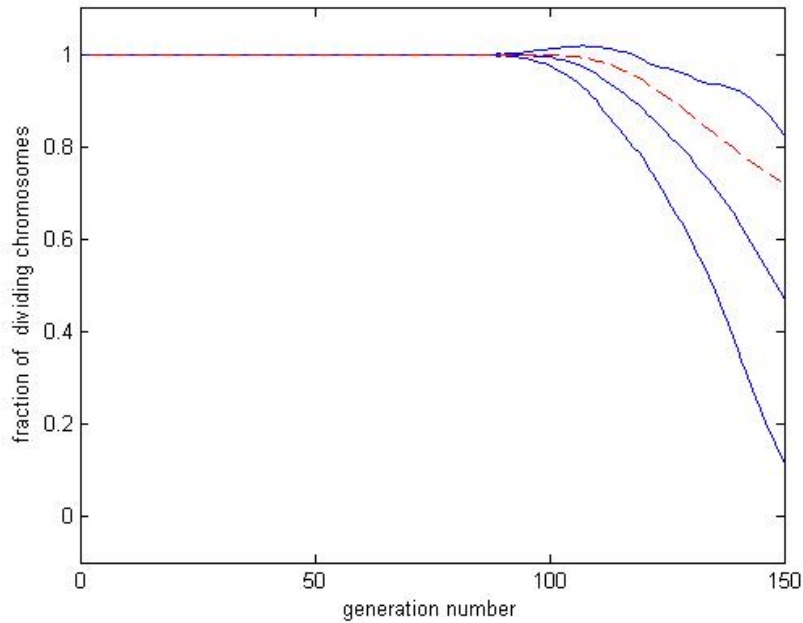
Figure 4.5: *The dashed line shows the proportion of dividing cells $\phi_{diving}(t)$ (4.4.18). The solid line in the middle is the fraction of dividing chromosomes from our stochastic simulations. The solid lines above and below are two standard deviations away from the fraction of dividing chromosomes stochastic simulations.*

4.5   Case III: length-dependent chromosome division

The probability of a chromosome replicating is $P_{div} = an + b$ where a, b are constants chosen such that $0 \leq P_{div} \leq 1$. Since we start with one chromosome with initial telomere length Q and the discrete reaction equation can be written as

$$K_n^{g+1} = K_n^g + (an + b)K_{n+L}^g, \quad \text{with probability} \quad an + b. \qquad (4.5.1)$$

We approximate (4.5.1) by the continuous system

$$K_n^g = K(x, t) \quad \text{with} \quad K(x, 0) = \delta(x - Q). \qquad (4.5.2)$$

where $t = gh$ ($h \ll 1$), $x = n/Q$ and $\psi = L/Q$. We substitute from (4.5.2) into (4.5.1) to obtain

$$K(x, t + h) = K(x, t) + (aQx + b) K(x + \psi, t). \qquad (4.5.3)$$

94

Since L, the telomere loss is much smaller than the Q, the initial telomere length, so $\psi \ll 1$. Thus we assume that

$$a \ll 1 \ll Q \quad \text{and} \quad aQ \sim O(1) \quad \text{and} \quad \psi \ll 1. \tag{4.5.4}$$

Under these assumptions, we can perform a Taylor series expansion of (4.5.3) to obtain

$$K + hK_t = K + (aQx + b)\left(K + \psi K_x + \frac{1}{2}\psi^2 K_{xx}\right), \tag{4.5.5}$$

$$K_t = \frac{(aQx + b)}{h}\left(K + \psi K_x + \frac{1}{2}\psi^2 K_{xx}\right), \tag{4.5.6}$$

we assume $b \sim O(h)$ and introduce

$$\hat{x} = \frac{(aQx + b)}{h}, \quad \text{so} \quad \frac{\partial}{\partial \hat{x}} = \frac{aQ}{h}\frac{\partial}{\partial x}, \tag{4.5.7}$$

and we $K(x,0) = \delta(x - Q)$ transforms to give $K(\hat{x},0) = \delta(\hat{x} - \hat{Q})$ where $\hat{Q} = (aQ + b)/h$. If we introduce $l = aQ\psi/h = aL/h$ then (4.5.6) can be written as

$$K_t = \hat{x}\left(K + lK_{\hat{x}} + \frac{1}{2}l^2 K_{\hat{x}\hat{x}}\right). \tag{4.5.8}$$

We assume that (4.5.8) admits solutions of the form

$$K(\hat{x},t) = g(t)f(\hat{x},t), \tag{4.5.9}$$

where $g(t) = \int_0^\infty K(\hat{x},t)d\hat{x}$ is the total number of chromosomes in the system at time t. Consequently, $f(\hat{x},t)$ represents their probability distribution, so that

$$\int_{\hat{x}=0}^\infty f(\hat{x},t)d\hat{x} = 1, \tag{4.5.10}$$

with $f \to 0$ as $\hat{x} \to 0$ and $f_{\hat{x}} \to 0$ as $\hat{x} \to \infty$. We also define the average telomere length

$$\hat{\mu}(t) = \int_{\hat{x}=0}^\infty \hat{x}f(\hat{x},t)d\hat{x}, \tag{4.5.11}$$

and $\mu = (h\hat{\mu} - b)/(aQ)$.

If we substitute with (4.5.9) in (4.5.8) and integrate with respect to $\hat{x}$, then we have:

$$\int_0^\infty \frac{\partial}{\partial t}[g(t)f(\hat{x},t)]d\hat{x} = \int_0^\infty \hat{x}\left[g(t)f(\hat{x},t) + lg(t)f_{\hat{x}}(\hat{x},t) + \frac{1}{2}l^2 g(t)f_{\hat{x}\hat{x}}(\hat{x},t)\right]d\hat{x},$$

implies

$$g_t(t) = g(t)\left\{\hat{\mu}(t) + l[\hat{x}f(\hat{x},t)]_0^\infty - l + \frac{1}{2}l^2[\hat{x}f_{\hat{x}}(\hat{x},t)]_0^\infty - \frac{1}{2}l^2[f(\hat{x},t)]_0^\infty\right\},$$
$$g_t(t) = g(t)(\hat{\mu}(t) - l). \tag{4.5.12}$$

Equation (4.5.12) is an evolution equation for the total number of chromosomes in the system and $\hat{f}(\hat{x},t)$ control the shape distribution of the telomere length. We determine how $\hat{f}(\hat{x},t)$ evolves by substituting (4.5.9) into (4.5.8) to obtain

$$g_t(t)f(\hat{x},t) + g(t)f_t(\hat{x},t) = \hat{x}g(t)\left[f(\hat{x},t) + lf_{\hat{x}}(\hat{x},t) + \frac{1}{2}l^2f_{\hat{x}\hat{x}}(\hat{x},t)\right]. \tag{4.5.13}$$

Inserting (4.5.12) into (4.5.13) yields

$$f_t(\hat{x},t) = [\hat{x} - \hat{\mu}(t) + l]f(\hat{x},t) + l\hat{x}f_{\hat{x}}(\hat{x},t) + \frac{1}{2}l^2\hat{x}f_{\hat{x}\hat{x}}(\hat{x},t). \tag{4.5.14}$$

We multiply (4.5.14) by $\hat{x}$ and integrate once with respect to $\hat{x}$ to obtain

$$\int_0^\infty \hat{x}f_t(\hat{x},t)d\hat{x} = \int_0^\infty (\hat{x}^2 - \hat{\mu}\hat{x} + l\hat{x})f(\hat{x},t)d\hat{x} + \int_0^\infty l\hat{x}^2 f_{\hat{x}}(\hat{x},t)d\hat{x} +$$
$$\int_0^\infty \frac{1}{2}l^2\hat{x}^2 f_{\hat{x}\hat{x}}(\hat{x},t)d\hat{x}, \tag{4.5.15}$$
$$\hat{\mu}_t(t) = \int_0^\infty \hat{x}^2 f(\hat{x},t)d\hat{x} - \hat{\mu}^2(t) - l\hat{\mu}(t) + l^2, \tag{4.5.16}$$

where

$$\int_0^\infty \hat{x}^2 f_x(\hat{x},t)d\hat{x} = [f(\hat{x},t)\hat{x}^2]_0^\infty - 2\int_0^\infty f(\hat{x},t)\hat{x}d\hat{x} = -2\hat{\mu}(t), \tag{4.5.17}$$
$$\int_0^\infty \hat{x}^2 f_{xx}(\hat{x},t)d\hat{x} = -2[f(\hat{x},t)\hat{x}]_0^\infty + 2\int_0^\infty f(\hat{x},t)d\hat{x} = 2. \tag{4.5.18}$$

If we introduce the variance of f, so $Var[f] = \int_0^\infty \hat{x}^2 fd\hat{x} - \hat{\mu}^2$, then $\hat{\mu}_t(t) = Var[f] - l\hat{\mu}(t) + l^2$ and $Var[f]$ evolves according to

$$\frac{d}{dt}Var[f] = \frac{d}{dt}\left(\int_0^\infty \hat{x}^2 fd\hat{x} - \hat{\mu}^2\right) = \int_0^\infty \hat{x}^2 f_t d\hat{x} - 2\hat{\mu}\hat{\mu}_t$$
$$= \int_0^\infty \hat{x}^2\left\{[\hat{x} - \hat{\mu}(t) + l]f + l\hat{x}f_{\hat{x}} + \frac{1}{2}l^2\hat{x}f_{\hat{x}\hat{x}}\right\}d\hat{x} - 2\hat{\mu}\hat{\mu}_t$$
$$= \int_0^\infty \hat{x}^3 fd\hat{x} + (l - \hat{\mu} - 3l)(Var[f] + \hat{\mu}^2) + 3l^2\hat{\mu}$$
$$\quad -2\hat{\mu}[Var[f] - l\hat{\mu}(t) + l^2]$$
$$= \int_0^\infty \hat{x}^3 fd\hat{x} - \hat{\mu}^3 - 3\hat{\mu}Var[f] - 2Var[f]l + l^2\hat{\mu}, \tag{4.5.19}$$

where

$$\int_0^\infty \hat{x}^3 f_{\hat{x}} d\hat{x} = -3 \int_0^\infty \hat{x}^2 f d\hat{x} = -3(Var[f] + \hat{\mu}^2), \qquad (4.5.20)$$

$$\int_0^\infty \hat{x}^3 f_{\hat{x}\hat{x}} d\hat{x} = 6 \int_0^\infty \hat{x} f d\hat{x} = 6\hat{\mu}. \qquad (4.5.21)$$

Equations (4.5.16) and (4.5.19) reveal how the moments of f depend on higher order moments. Since (4.5.14) does not, in general, admit explicit analytical solutions, we investigate the dynamics of (4.5.14) by considering the asymptotic limit for which $l \ll 1$ and the governing PDE simplifies.

4.5.1 *First order PDE*

Neglecting terms which are quadratic in the small parameter $l \ll 1$, (4.5.14) simplifies to give:

$$f_t(\hat{x}, t) = [\hat{x} - \hat{\mu}(t) + l] f(\hat{x}, t) + l\hat{x} f_{\hat{x}}(\hat{x}, t). \qquad (4.5.22)$$

We use the method of characteristics to solve this first order PDE. We introduce the characteristic variables where $ds = dt = -d\hat{x}/(l\hat{x}) = df/[(\hat{x} - \mu + l)f]$ and parameterized the initial conditions on $s = 0$ by α so that when $s = 0$, $t = 0$, $x = \alpha$, $f = \delta(\alpha - \hat{Q})$.

$$\frac{dt}{ds} = 1 \Rightarrow t = s,$$

since $t = 0$ when $s = 0$.

$$\frac{d\hat{x}}{ds} = -l\hat{x} \Rightarrow \hat{x} = \alpha e^{-ls},$$

since $\hat{x} = \alpha$ when $s = 0$. Finally

$$\frac{df}{ds} = [\hat{x} - \hat{\mu}(t) + l] f \Rightarrow \ln f = -\frac{\alpha}{l} e^{-ls} - \int_0^s \hat{\mu}(t) ds + ls + A_3,$$

$$\Rightarrow f = \delta(\alpha - \hat{Q}) \exp\left[\frac{\alpha}{l} + ls - \frac{\alpha}{l} e^{-ls} - \int_0^s \hat{\mu}(t) ds\right], \qquad (4.5.23)$$

since $f = \delta(\alpha - \hat{Q})$ when $s = 0$.

Since $\hat{x} = \alpha e^{-ls}$ we have

$$\alpha = \hat{x} e^{ls} = \hat{x} e^{lt}. \qquad (4.5.24)$$

We substitute $t = s$ and $\alpha = \hat{x}e^{lt}$ in (4.5.23) to obtain

$$f(\hat{x}, t) = \delta(\hat{x}e^{lt} - \hat{Q}) \exp\left[\frac{\hat{x}e^{lt}}{l} + lt - \frac{\hat{x}}{l} - \int_0^t \hat{\mu}(s)ds\right]. \qquad (4.5.25)$$

We know that $\int_{\hat{x}=0}^{\infty} f(\hat{x}, t)d\hat{x} = 1$, so we let $u = \hat{x}e^{lt} \Rightarrow \hat{x} = ue^{-lt}$ and $du = e^{lt}d\hat{x}$, then

$$1 = \int_{\hat{x}=0}^{\infty} f(\hat{x}, t)d\hat{x} = e^{-lt} \int_{\hat{x}=0}^{\infty} \delta(u - \hat{Q}) \exp\left[\frac{u}{l} + lt - \frac{ue^{-lt}}{l} - \int_0^t \hat{\mu}(s)ds\right] du,$$

$$\exp\left[\int_0^t \hat{\mu}(s)ds\right] = \int_{\hat{x}=0}^{\infty} \delta(u - \hat{Q}) \exp\left(\frac{u}{l} - \frac{ue^{-lt}}{l}\right) du = \exp\left[\frac{\hat{Q}}{l}(1 - e^{-lt})\right],$$

$$\int_0^t \hat{\mu}(s)ds = \frac{\hat{Q}}{l}(1 - e^{-lt}),$$

and hence
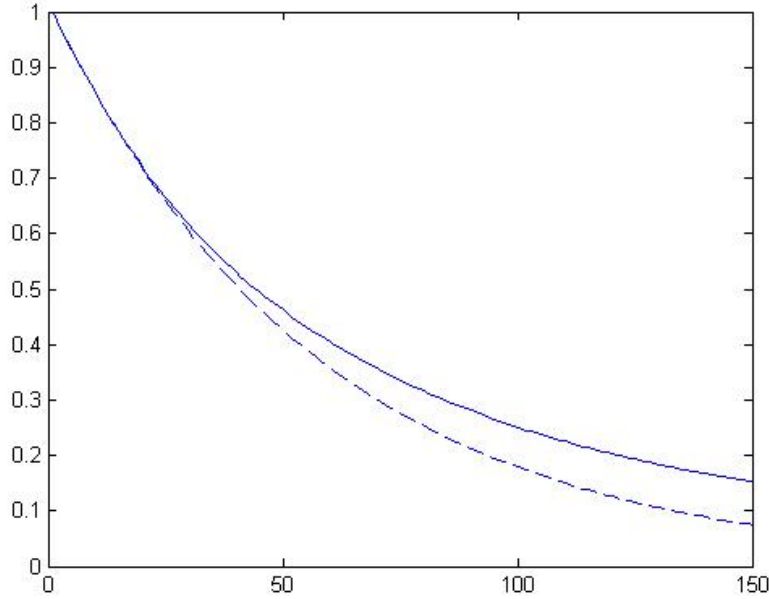
Figure 4.6: *The solid line is the computer simulation in Chapter 2 Case III (Section 2.2.6), mean telomere length with initial telomere length 5950, plotted against generation number. The dashed line is theoretical mean $\mu(t)$ (4.5.26), plotted against generation number, with parameters $a = 1/6000$, $h = 1$, $L = 100$, $l = aL/h$ and $\hat{Q} = 1$.*

$$\hat{\mu}(t) = \hat{Q}e^{-lt}. \qquad (4.5.26)$$

In Figure 4.6 we use (4.5.26) to plot $\hat{\mu}(t)$ against time (dashed line). For comparison present we simulation results for Case III from Chapter 2 (Section 2.2.6) (solid line), which shows how the length of the telomere (normalized by its initial length) varies with generation number. At early times (before generation 25) the two lines are identical; at later times the theoretical mean decreases faster than the stochastic simulation and as time increase the difference between the two curves increases. This result indicates that the expression for $\hat{\mu}(t)$ obtained from the first order PDE is not accurate at longer times, probably due to the spread (variance of the distribution somehow slowing down the loss of telomere).

Now we solve for $g(t)$, total number of chromomeres in the system noting first that, from (4.5.25) and (4.5.26)

$$
\begin{aligned}
f(\hat{x}, t) &= \delta(\hat{x}e^{lt} - \hat{Q}) \exp\left[\frac{\hat{x}e^{lt}}{l} + lt - \frac{\hat{x}}{l} - \frac{\hat{Q}}{l}(1 - e^{-lt})\right] \\
&= \delta(\hat{x}e^{lt} - \hat{Q}) \exp\left[\frac{\hat{x}(e^{lt} - 1) - \hat{Q}(1 - e^{-lt})}{l} + lt\right]. \quad (4.5.27)
\end{aligned}
$$

We put (4.5.26) back into (4.5.12) to obtain that:

$$
g_t(t) = g(t)(\hat{Q}e^{-lt} - l), \quad (4.5.28)
$$

hence

$$
g(t) = B \exp\left(-\frac{\hat{Q}}{l}e^{-lt} - lt\right). \quad (4.5.29)
$$

where B is a constant. Our initial condition for $g(t)$ is $g(0) = 1$, so $B = e^{\hat{Q}/l}$ (4.5.29) can be rewritten as

$$
g(t) = \exp\left[\frac{\hat{Q}}{l}(1 - e^{-lt}) - lt\right]. \quad (4.5.30)
$$

The expression for the number of chromosomes used in Figure 4.7 is (4.5.30). Since $l \ll 1$ so (4.5.30) can be rewritten as $g(t) \approx \exp[(\hat{Q} - l)t]$. This indicate that the growth rate approximately has exponential growth. But Figure 4.7 shows the chromosome has exponential growth rate until $t = 40$, then it starts
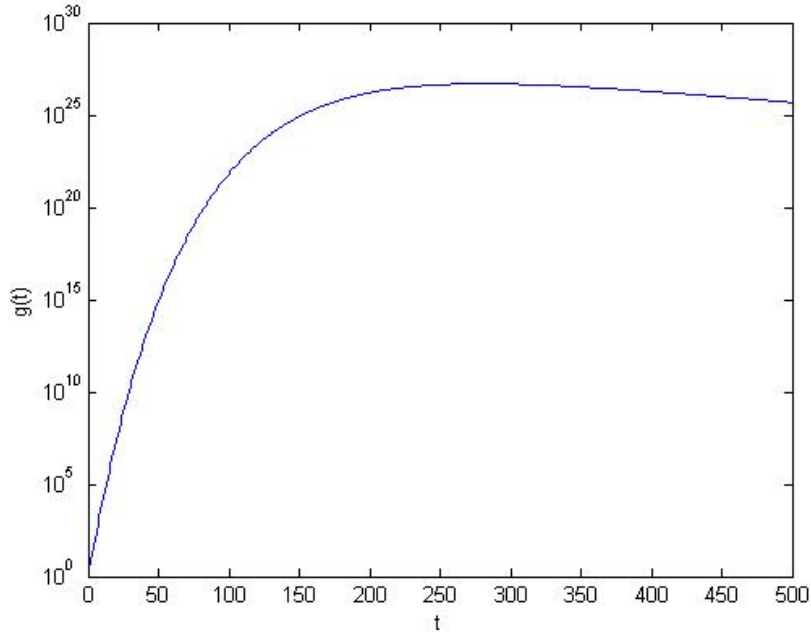
Figure 4.7: *Plot $g(t)$ (4.5.30), the total number of chromosomes in the system , varies on a logarithmic scale with time t, with parameters given by $a = 1/6000$, $b = -1/30$, $h = 1$, $L = 400$, $l = aL/h$ and $\hat{Q} = (1 + b)/h$.*

decrease, then approach a constant where indicate the chromosomes become senescent. For our model we only need to consider the $g(t)$ increase part.

Our analysis of the first order PDE (4.5.22) supplies expressions for $\hat{\mu}(t)$, $g(t)$ and $f(\hat{x}, t)$. However these expressions are only valid for short times. For greater accuracy, we must consider the second order PDE (4.5.14). Before we go to the second order PDE, first we solve second order PDE numerically.

4.5.2 *Numerical results*

We use MATLAB to solve second order PDE numerically. MATLAB has a standard solver for ordinary differential equations (ODEs) ode45 which uses a Runge-Kutta method with a variable time step to solve

$$f_t(\hat{x}, t) = [\hat{x} - \hat{\mu}(t) + l] f(\hat{x}, t) + l\hat{x} f_{\hat{x}}(\hat{x}, t) + \frac{1}{2} l^2 \hat{x} f_{\hat{x}\hat{x}}(\hat{x}, t), \qquad (4.5.31)$$

subject to the initial condition $f(\hat{x}, 0) = \delta(\hat{x} - \hat{Q})$ and boundary conditions; $f(\hat{x} = 1, t) = 0$ and $\frac{df}{dt}|_{\hat{x}=0} = 0$.

100

In order to use the ODE solver we first reduce (4.5.31) to a system of ODEs
by performing finite difference approximations on the spatial derivatives. In
particular, we use central differences to approximate $\partial \hat{f}_k / \partial \hat{x}$ and $\partial^2 \hat{f}_k / \partial \hat{x}^2$, so
that

$$\frac{\partial \hat{f}_k}{\partial \hat{x}} \approx \frac{\hat{f}_{k+1} - \hat{f}_{k-1}}{2 \triangle x}, \tag{4.5.32}$$

$$\frac{\partial^2 \hat{f}_k}{\partial \hat{x}^2} \approx \frac{\hat{f}_{k+1} - 2\hat{f}_k + \hat{f}_{k-1}}{(\triangle x)^2}, \tag{4.5.33}$$

where $\hat{f}_k = \hat{f}(k \triangle x, t)$ and $\triangle x$ is the mesh spacing for the spacial discretisa-
tion. Let $\hat{x}_k = k \triangle x$, $k = 1, 2, 3, .., k_{end}$. Since $f(\hat{x}, 0) = \delta(\hat{x} - \hat{Q})$, we transform
the initial conditions to $f(k_{end} - 1, 0) = 0.1/\triangle x$, $f(k_{end} - 2, 0) = 0.8/\triangle x$ and
$f(k_{end} - 3, 0) = 0.1/\triangle x$. So (4.5.31) can be reduced to the ODEs system

$$f_t(1, t) = [\hat{x} - \hat{\mu}(t) + l]f(\hat{x}_1, t) + \frac{1}{2(\triangle x)^2}l^2 \hat{x}_1 (f(\hat{x}_2, t) - 2f(\hat{x}_1, t)), \tag{4.5.34}$$

and for $i = 2..i_{end} - 1$,

$$\begin{aligned} f_t(k, t) &= [\hat{x} - \hat{\mu}(t) + l]f(\hat{x}_k, t) + \frac{1}{2 \triangle x}l\hat{x}_k[f(\hat{x}_{k+1}, t) - f(\hat{x}_{k-1}, t)] \\ &\quad + \frac{1}{2(\triangle x)^2}l^2 \hat{x}_1[f(\hat{x}_{i+1}, t) - 2f(\hat{x}_i, t) + f(\hat{x}_{i-1}, t)], \tag{4.5.35} \\ f_t(k_{end}, t) &= 0. \tag{4.5.36} \end{aligned}$$

Now we use MATLAB to solve this system of ODEs.

In Figure 4.8, we present the numerical solutions for $f(\hat{x}, t)$ for (4.5.31), differ-
ent times t. When $t = 2$, the distribution of $f(\hat{x}, t)$ looks like a Dirac δ function
which agrees with our initial conditions. As time t increases, the distribution
$f(\hat{x}, t)$ becomes more dispersed and moves toward the left hand side like trav-
eling wave. When $t = 25$, the distribution peaks near $\hat{x} = 0.72$, when $t = 50$,
the distribution peaks near $\hat{x} = 0.58$, which means it takes $\triangle t = 25$ for the dis-
tribution move 0.24 to the left hand side, suggestion the speed of propagation
is 0.01. When $t = 100$, the distribution peaks near $\hat{x} = 0.5$, which means that
the profile moves more slowly as time increases. The distributions at $t = 200$
and $t = 300$ are almost identical, suggesting that the system has evolved to a
steady state.
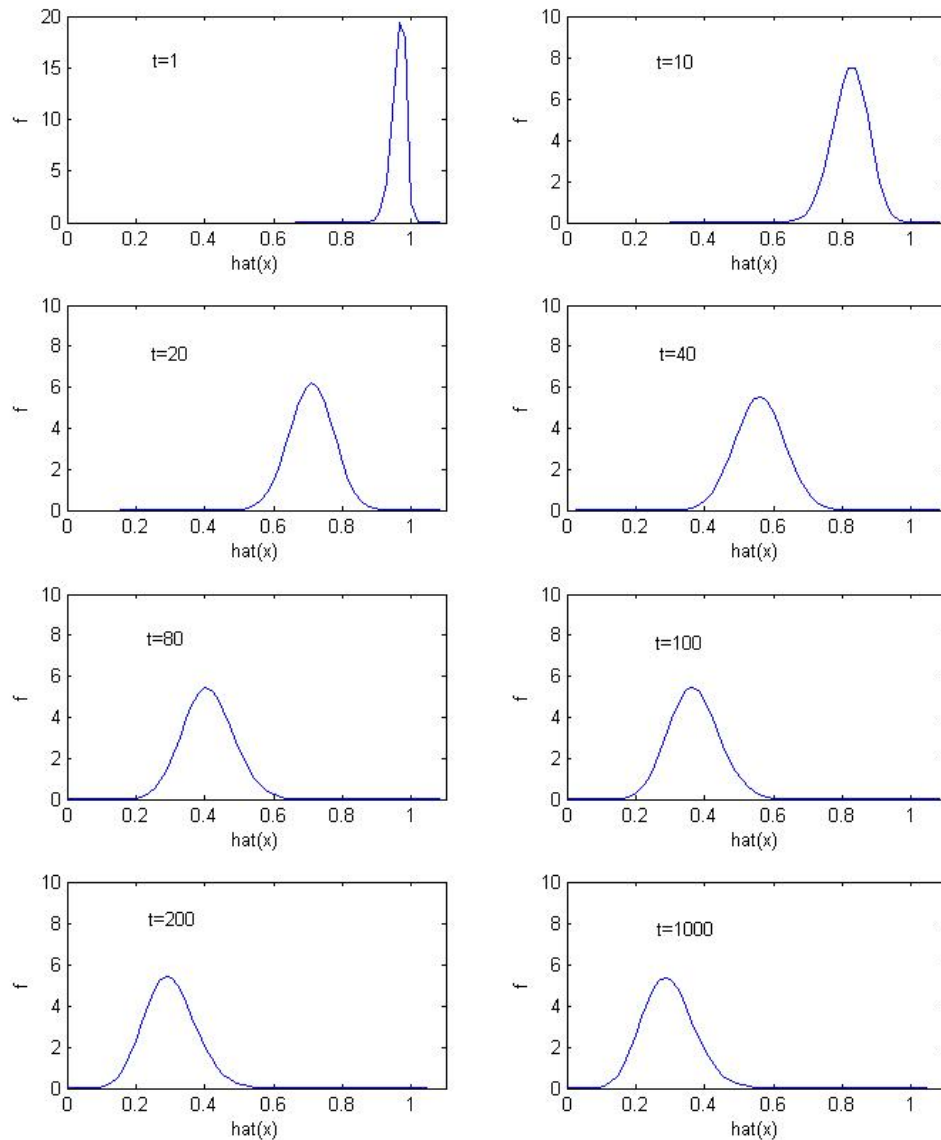
Figure 4.8: *Numerical solution of $f(\hat{x}, t)$ plotted against $\hat{x}$ with $t = 2, 25, 50, 100,$
200, 300. With parameters $a = 0.95/6000$, $b = 0.05$, $h = 1$, $L = 100$, $l = 0.0158$
and $\hat{Q} = 1$.*

The profile for $f(\hat{x}, t)$ looks symmetric at both early and long times, see Figure
4.8 . However plots of $log(f)$ against time, Figure 4.9, indicate that at large
times, f is no longer symmetric.
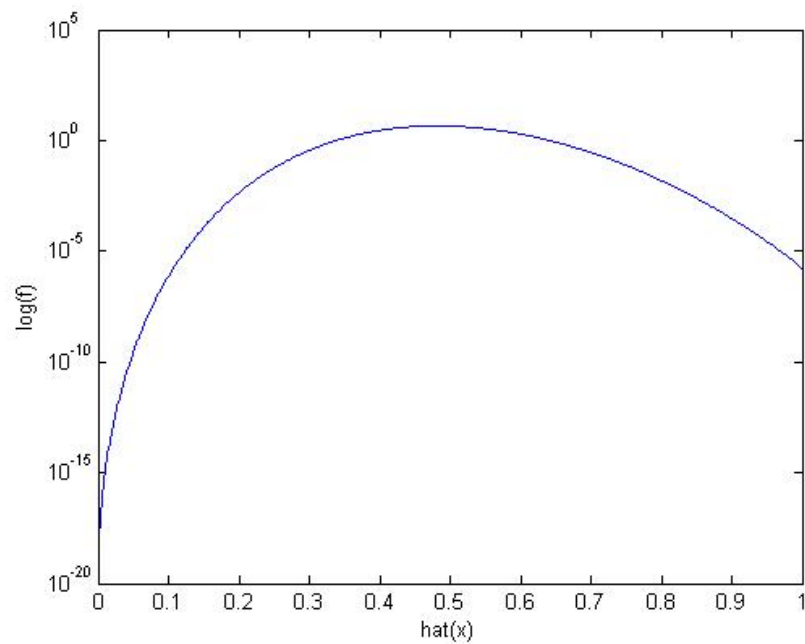
Figure 4.9: *Top graph shows $log(f)$ plotted against $\hat{x}$ at $t = 200$.*
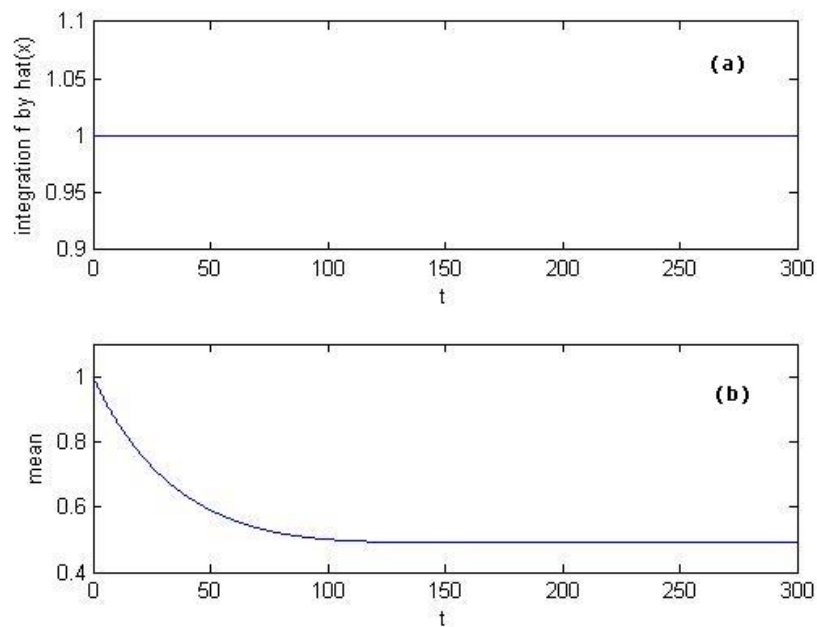
Figure 4.10: (a) *As a check on our numerical methods, we verify that $\int f(\hat{x}, t)d\hat{x} \approx 1$.* ($b$) *plots of the numerically computed mean, $\hat{\mu(t)}$. With parameters $a = 0.95/6000$, $b = 0.05$, $h = 1$, $L = 100$, $l = 0.0158$ and $\hat{Q} = 1$.*

103

As a check on the accuracy of our numerical solution, we calculate $\int f(\hat{x}, t)d\hat{x}$. Figure 4.10(a) shows that $\int f(\hat{x}, t)d\hat{x} \approx 1$, which agrees with our requirement for the function of f. Figure 4.10(b) shows that the numerically calculated mean, $\hat{\mu}$, decreases slowly until $t = 100$ and remains constant thereafter.

In order to investigate how telomere length is distributed near $\hat{\mu}$, we need to look at the moment of function $f(\hat{x}, t)$ of a real variable about mean $\hat{\mu}$. Let $U_n = \int_{-\infty}^{\infty}(\hat{x} - \hat{\mu})^n f(\hat{x}, t)d\hat{x}$, where n is positive integer. Normally the first moment about the mean, U_1 is zero and the second central moment U_2 about the mean is the variance. The third central moment, U_3 is a measure of the lopsidedness of the distribution, also called the skewness, if the third central moment is zero the distribution is symmetric.

Figure 4.11 shows that the first moment about mean is $U_1 = 0$ as we expected and the varices, U_2 increases with time until $t = 150$ and after that approach to a constant. The third moment, U_3 is a positive value, indicating that the distribution of telomere length is skewed to the right, which means the tail is heavier on the right and the distribution is concentrated more closely to the left side of the mean. Due to U_3 being small, the distribution still looks symmetric. The fourth moment, U_4 roughly increases linearly with time t for $t < 100$. We notice that the shape of U_2 and U_4 are quite similar, thus we obtain the relation that $U_4 \approx 3U_3^2$ (see Figure 4.12).

From the numerical results, we generally understand the how the distribution of telomere length, mean and moment, varies with time. Now we analyze the second order PDE with asymptotically over various time scales.

4.5.3 *Asymptotic analysis of second order PDE*

In order to determine how the distribution of the solution of (4.5.14) spreads, we retain higher-order terms in our analysis. Accordingly we now consider the second order PDE

$$f_t(\hat{x}, t) = [\hat{x} - \hat{\mu}(t) + l]f(\hat{x}, t) + l\hat{x}f_{\hat{x}}(\hat{x}, t) + \frac{1}{2}l^2\hat{x}f_{\hat{x}\hat{x}}(\hat{x}, t). \qquad (4.5.37)$$
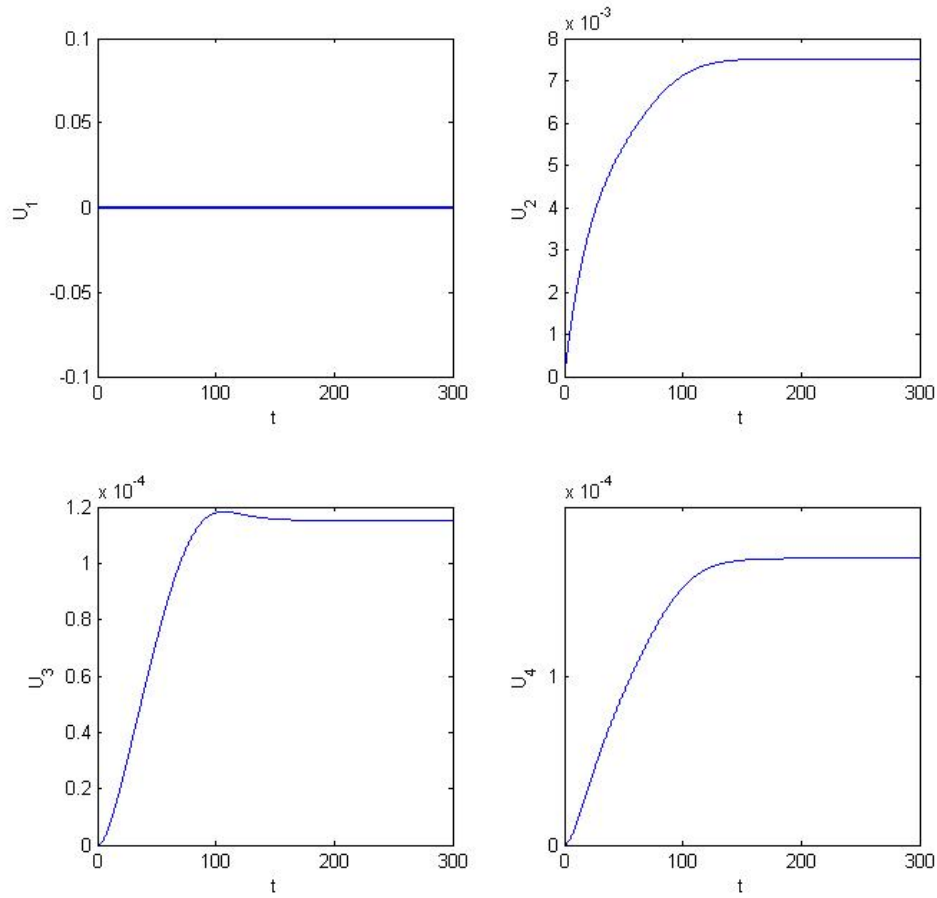
Figure 4.11: *Figure shows the U_1, U_2, U_3, U_4 plotted against t from the numerical
solution.*

We let

$$\hat{x} = s(t) + z, \tag{4.5.38}$$

where $s(t) = Qe^{-lt}$, be our leading order estimate of the mean of the distri-
bution, however, since our higher order analysis below will introduce variance
and skewness to the distribution, we use I_n to indicate

$$I_n = \int_{-\infty}^{\infty} z^n \hat{f}(z,t)dz, \tag{4.5.39}$$

where n is an integer. Since $\int f(\hat{x},t)d\hat{x} = 1$ we have $\int f(z,t)dz = 1$ so that the
mean of the distribution is given by

$$\hat{\mu}(t) = \int \hat{x}f(\hat{x},t)dx = \int (s+z)f(z,t)dz = s + I_1, \tag{4.5.40}$$
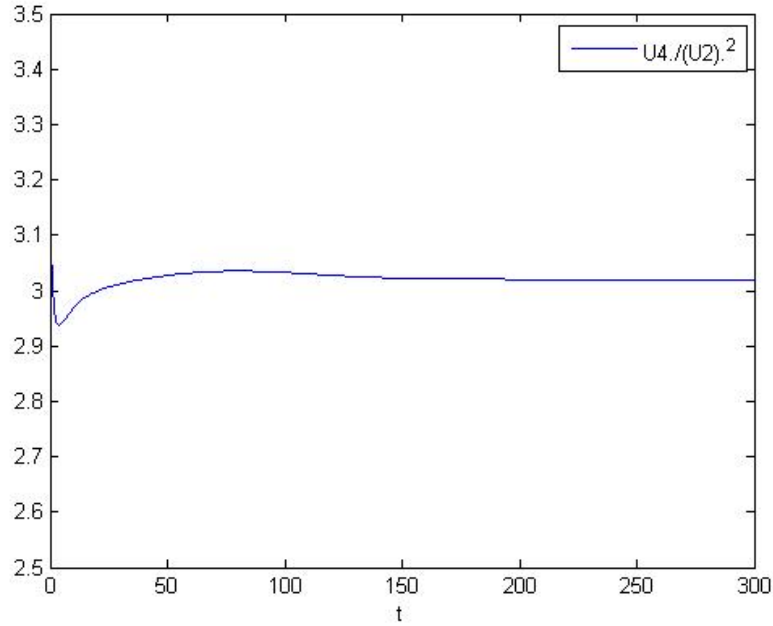
Figure 4.12: *U_4/U_2^2 plotted against t from the numerical solution.*

We use $z = \hat{x} - s(t)$ to transform the independent variables from $(\hat{x}, t)$ to (z, t), and $f(\hat{x}, t)$ to $\hat{f}(z, t)$, noting that

$$\frac{\partial}{\partial \hat{x}} = \frac{\partial}{\partial z}, \tag{4.5.41}$$

$$\frac{\partial}{\partial t} = \frac{\partial}{\partial t} - s_t \frac{\partial}{\partial z}. \tag{4.5.42}$$

Under this transformation (4.5.37) can be rewritten as

$$\hat{f}_t - s_t \hat{f}_z = (s + z - \hat{\mu} + l)\hat{f} + l(s + z)\hat{f}_z + \frac{1}{2}l^2(s + z)\hat{f}_{zz}, \tag{4.5.43}$$

or

$$\hat{f}_t = (z + l - I_1)\hat{f} + lz\hat{f}_z + \frac{1}{2}l^2(s + z)\hat{f}_{zz}. \tag{4.5.44}$$

If we multiply both sides of (4.5.44) by z and integrate, we deduce

$$\int_{-\infty}^{\infty} z\hat{f}_t dz = \int_{-\infty}^{\infty} z(z + l - I_1)\hat{f}dz + \int_{-\infty}^{\infty} lz^2 \hat{f}_z dz + \int_{-\infty}^{\infty} \frac{1}{2}l^2 z(s + z)\hat{f}_{zz} dz,$$

$$\frac{dI_1}{dt} = I_2 + (l - I_1)I_1 - 2lI_1 + l^2 = I_2 - (l + I_1)I_1 + l^2, \tag{4.5.45}$$

where we have used

$$\int_{-\infty}^{\infty} z^2 \hat{f}_z dz = [z^2 \hat{f}]_{-\infty}^{\infty} - 2 \int_{-\infty}^{\infty} z \hat{f} dz = -2I_1,$$

$$\int_{-\infty}^{\infty} z \hat{f}_{zz} dz = [z \hat{f}_z]_{-\infty}^{\infty} - \int_{-\infty}^{\infty} \hat{f}_z dz = 0,$$

$$\int_{-\infty}^{\infty} z^2 \hat{f}_{zz} dz = [z^2 \hat{f}_z]_{-\infty}^{\infty} - 2 \int_{-\infty}^{\infty} z \hat{f}_z dz = -[2z\hat{f}]_{-\infty}^{\infty} + 2 \int_{-\infty}^{\infty} \hat{f} dz = 2.$$

Multiplying both sides of (4.5.44) by z^2 and integrating, we obtain

$$\int_{-\infty}^{\infty} z^2 \hat{f}_t dz = \int_{-\infty}^{\infty} z^2 (z + l - I_1) \hat{f} dz + \int_{-\infty}^{\infty} l z^3 \hat{f}_z dz + \int_{-\infty}^{\infty} \frac{1}{2} l^2 z^2 (s + z) \hat{f}_{zz} dz,$$

$$\frac{dI_2}{dt} = I_3 + (l - I_1)I_2 - 3l I_2 + l^2 s + 3l^2 I_1$$

$$= I_3 - (2l + I_1)I_2 + l^2 s + 3l^2 I_1, \tag{4.5.46}$$

where we have used

$$\int_{-\infty}^{\infty} z^3 \hat{f}_z dz = [z^3 \hat{f}]_{-\infty}^{\infty} - 3 \int_{-\infty}^{\infty} z^2 \hat{f} dz = -3I_2,$$

$$\int_{-\infty}^{\infty} z^3 \hat{f}_{zz} dz = [z^3 \hat{f}_z]_{-\infty}^{\infty} - 3 \int_{-\infty}^{\infty} z^2 \hat{f}_z dz = -[3z^2 \hat{f}]_{-\infty}^{\infty} + 6 \int_{-\infty}^{\infty} z \hat{f} dz = 6I_1.$$

Multiplying both sides of (4.5.44) by z^3 and integrating, we obtain

$$\int_{-\infty}^{\infty} z^3 \hat{f}_t dz = \int_{-\infty}^{\infty} z^3 (z + l - I_1) \hat{f} dz + \int_{-\infty}^{\infty} l z^4 \hat{f}_z dz + \int_{-\infty}^{\infty} \frac{1}{2} l^2 z^3 (s + z) \hat{f}_{zz} dz,$$

$$\frac{dI_3}{dt} = I_4 + (l - I_1)I_3 - 4l I_3 + 3l^2 s I_1 + 6l^2 I_2$$

$$= I_4 - (3l + I_1)I_3 + 3l^2 s I_1 + 6l^2 I_2, \tag{4.5.47}$$

where we have used

$$\int_{-\infty}^{\infty} z^4 \hat{f}_z dz = [z^4 \hat{f}]_{-\infty}^{\infty} - 4 \int_{-\infty}^{\infty} z^3 \hat{f} dz = -4I_3,$$

$$\int_{-\infty}^{\infty} z^4 \hat{f}_{zz} dz = [z^4 \hat{f}_z]_{-\infty}^{\infty} - 4 \int_{-\infty}^{\infty} z^3 \hat{f}_z dz = -[4z^3 \hat{f}]_{-\infty}^{\infty} + 12 \int_{-\infty}^{\infty} z^2 \hat{f} dz = 12I_2.$$

Since I_1, I_2, I_3 all depend on higher order moments, we need a closure assumption, in order to solve systems ODEs for I_1, I_2 and I_3. From the numerical solution we obtain $U_4 \approx 3U_2^2$, so we assume $I_4 \approx 3I_2^2$, thus (4.5.47) can be written as

$$\frac{dI_3}{dt} = 3I_2^2 - (3l + I_1)I_3 + 3l^2 s I_1 + 6l^2 I_2. \tag{4.5.48}$$

Since the PDE involves in I_1 (or $\hat{\mu}(t)$) which is more complicated to solve for explicitly, we solve the ODEs (put ODEs from Table 4.2 have displayed as equation arrays) which describe the solutions of the PDE (4.5.48) by considering different time scales.

$$\hat{f}_t = (z + l - I_1)\hat{f} + lz\hat{f}_z + \frac{1}{2}l^2(s + z)\hat{f}_{zz} \quad (4.5.44)$$

$$\frac{dI_1}{dt} = I_2 - (l + I_1)I_1 + l^2 \quad (4.5.45)$$

$$\frac{dI_2}{dt} = I_3 - (2l + I_1)I_2 + l^2 s + 3l^2 I_1 \quad (4.5.46)$$

$$\frac{dI_3}{dt} = 3I_2^2 - (3l + I_1)I_3 + 3l^2 s I_1 + 6l^2 I_2 \quad (4.5.48)$$

Table 4.2: To summarizing the system of equations we need to solve.

4.5.4 *The first, short time scale*

To solve

$$\hat{f}_t = (z + l - I_1)\hat{f} + lz\hat{f}_z + \frac{1}{2}l^2(s + z)\hat{f}_{zz}. \quad (4.5.49)$$

We construct solution to (4.5.49) by considering initially the limit $t = O(1)$ and $z = O(l)$. We rescale z by writing $z = l\hat{z}$ in which case (4.5.49) transforms to

$$\hat{f}_t = (l\hat{z} + l - I_1)\hat{f} + l\hat{z}\hat{f}_{\hat{z}} + \frac{1}{2}(s + l\hat{z})\hat{f}_{\hat{z}\hat{z}}. \quad (4.5.50)$$

Since $l \ll 1$ and $t = O(1)$, we write $s(t) = \hat{Q}e^{-lt} \approx \hat{Q}$ and we anticipate $I_1 = O(l)$ or $I_1 = O(l^2)$. In either case, at leading order (4.5.50) implies

$$\hat{f}_t = \frac{\hat{Q}}{2}\hat{f}_{\hat{z}\hat{z}}. \quad (4.5.51)$$

We distinguish two separate regions here: an outer region in which $[\hat{x} - \hat{\mu}(t)] \gg 1$ and $f = 0$ and an inner region in which $[\hat{x} - \hat{\mu}(t)] \ll 1$. We give details of the inner solution below.

Recall that our initial conditions are $f(\hat{x}, 0) = \delta(\hat{x} - \hat{Q})$, where $\hat{x} = s(t) + z$. This implies that $\hat{f}(z, 0) = \delta(s + z - \hat{Q}) \approx \delta(z)$ since on this time scale $s = \mu = \hat{Q}$. Further $\hat{f}(\hat{z}, 0) = \delta(l\hat{z})$. We can solve (4.5.51) by using the Fourier transform, which yields the solution

$$\hat{f}(\hat{z}, t) = \frac{1}{l\sqrt{2\pi\hat{Q}t}} \exp\left(-\frac{\hat{z}^2}{2\hat{Q}t}\right), \quad (4.5.52)$$

108

since $\hat{z} = (\hat{x} - \hat{Q})/l$. We remark that

$$f(\hat{x}, t) = \frac{1}{l\sqrt{2\pi\hat{Q}t}} \exp\left[-\frac{(\hat{x} - \hat{Q})^2}{2l^2\hat{Q}t}\right]. \qquad (4.5.53)$$
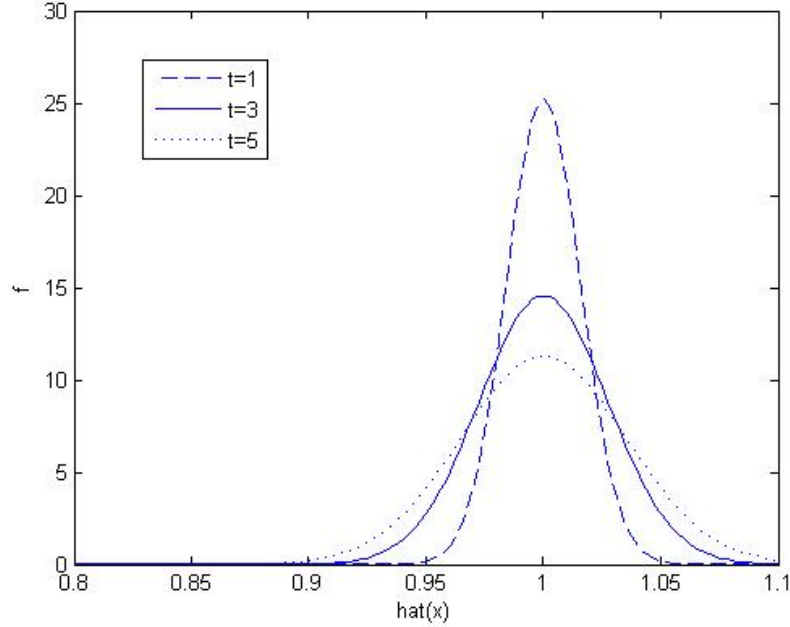
Figure 4.13: $f(\hat{x}, t)$ *varies with* $\hat{x}$ *and with* $t = 1, 3, 5$ *respectively. With parameters* $a = 0.95/6000, b = 0.05, h = 1, L = 100, l = 0.0158$ *and* $\hat{Q} = 1$.

Figure 4.13 shows that, the solution for $f(\hat{x}, t)$ is an Gaussian distribution with means $\hat{\mu} = \hat{Q}$ and variance $= l^2\hat{Q}t$. As time increases, the distribution's variance increases, however, the center of the distribution remains unchanged.

$$
\begin{aligned}
\text{Variance}[f(\hat{x}, t)] &= \int_{-\infty}^{\infty}(\hat{x} - \hat{\mu})^2 f(\hat{x}, t)d\hat{x} = \int_{-\infty}^{\infty}(\hat{Q} + z - \hat{Q})^2 f(\xi, t)ldz \\
&= l^2\hat{Q}t = I_2.
\end{aligned} \qquad (4.5.54)
$$

From (4.5.39), we determine I_1 and I_3:

$$
\begin{aligned}
I_1 &= \int_{-\infty}^{\infty} z\hat{f}(z, t)dz = \int_{-\infty}^{\infty} \frac{z}{l\sqrt{2\pi\hat{Q}t}} \exp\left(-\frac{\hat{z}^2}{2\hat{Q}t}\right)dz = 0, \quad (4.5.55) \\
I_3 &= \int_{-\infty}^{\infty} z^3\hat{f}(z, t)dz = \int_{-\infty}^{\infty} \frac{z^3}{l\sqrt{2\pi\hat{Q}t}} \exp\left(-\frac{\hat{z}^2}{2\hat{Q}t}\right)dz = 0. \quad (4.5.56)
\end{aligned}
$$

From the solution of leading order PDE we obtain that $I_2 = l^2\hat{Q}t$ and $I_1 = I_3 = 0$. In order to see how I_1, I_2 and I_3 change over time. We consider the full system rather than the leading order PDE only and use the equations we obtained

earlier, namely (4.5.45) , (4.5.46), (4.5.48).

Writing $I_2 = l^2 \hat{I}_2$, where $\hat{I}_2 = O(1)$. From (4.5.45), we deduce $I_1/I_2 = O(1)$ so that $I_1 = l^2 \hat{I}_1$, where $\hat{I}_1 = O(1)$. We remark that $I_1 = O(l^2)$ is consistent with our earlier assumption that $I_1 = O(l)$ or smaller. Since $I_4 = 3I_2^2$, we deduce further that $I_4 = l^4 \hat{I}_4$, where $\hat{I}_4 = O(1)$. From (4.5.48), we deduce I_3 has the same order of I_4, which implies $I_3 = l^4 \hat{I}_3$, where $\hat{I}_3 = O(1)$. Putting these back into equations (4.5.45), (4.5.46), (4.5.48), we obtain

$$\frac{d\hat{I}_1}{dt} = \hat{I}_2 - (l + l^2 \hat{I}_1)\hat{I}_1 + 1 \,, \tag{4.5.57}$$

$$\frac{d\hat{I}_2}{dt} = l^2 \hat{I}_3 - (2l + l^2 \hat{I}_1)\hat{I}_2 + \hat{Q} + 3l^2 \hat{I}_1 \,, \tag{4.5.58}$$

$$\frac{d\hat{I}_3}{dt} = 3\hat{I}_2^2 - l^2 \hat{I}_1 \hat{I}_3 - 3l\hat{I}_3 + 3\hat{Q}\hat{I}_1 + 6\hat{I}_2 \,, \tag{4.5.59}$$

and since $l \ll 1$, we deduce that at leading order

$$\frac{d\hat{I}_1}{dt} = \hat{I}_2 + 1 \,, \tag{4.5.60}$$

$$\frac{d\hat{I}_2}{dt} = \hat{Q} \,, \tag{4.5.61}$$

$$\frac{d\hat{I}_3}{dt} = 3\hat{I}_2^2 + 3\hat{Q}\hat{I}_1 + 6\hat{I}_2 \,, \tag{4.5.62}$$

Solving (4.5.61) subject to $\hat{I}_2(0) = 0$, we obtain

$$\hat{I}_2(t) = \hat{Q}t \,. \tag{4.5.63}$$

Substitution from (4.5.63) in (4.5.60) and integrating subject to $\hat{I}_1(0) = 0$, supplies

$$\hat{I}_1(t) = \frac{1}{2}\hat{Q}t^2 + t \,. \tag{4.5.64}$$

Put (4.5.63), (4.5.64) back to (4.5.62) using $\hat{I}_3(0) = 0$ we obtain,

$$\hat{I}_3(t) = \frac{3}{2}\hat{Q}^2 t^3 + \frac{9}{2}\hat{Q}t^2 \,, \tag{4.5.65}$$

To summarize, the leading order solutions for I_1, I_2, I_3 are given by:

$$I_1(t) = \frac{1}{2}tl^2(\hat{Q}t + 1) \,, \quad I_2(t) = l^2 \hat{Q}t \,, \quad I_3(t) = \frac{3}{2}\hat{Q}t^2 l^4(\hat{Q}t + 3) \,. \tag{4.5.66}$$

This analysis is based on $t = O(1)$ which is the short time scale and in order to investigate the dynamics of the full system, we now consider on the next time scale, where t is larger but still less than $O(l^{-1})$.

4.5.5 *Second time scale*

To solve

$$\hat{f}_t = (z + l - I_1)\hat{f} + lz\hat{f}_z + \frac{1}{2}l^2(s + z)\hat{f}_{zz}, \qquad (4.5.67)$$

we let $t = l^{-\sigma}t_2$ where $1 > \sigma > 0$ and $z = l^\theta\hat{z}$ where t_2, z are $O(1)$. By matching to equations (4.5.66), we deduce $I_1 \sim l^2 t^2 = l^{2-2\sigma}\hat{I}_1$, $I_2 \sim l^2 t = l^{2-\sigma}\hat{I}_2$ and $I_3 \sim l^4 t^3 = l^{4-3\sigma}\hat{I}_3$ where $\hat{I}_1, \hat{I}_2, \hat{I}_3$ are $O(1)$. Using these scalings we deduce that (4.5.67) can be written as

$$l^\sigma \hat{f}_{t_2} = (l^\theta\hat{z} + l - l^{2-2\sigma}\hat{I}_1)\hat{f} + l\hat{z}\hat{f}_{\hat{z}} + \frac{1}{2}l^{2-2\theta}(s + l^\theta\hat{z})\hat{f}_{\hat{z}\hat{z}}. \qquad (4.5.68)$$

In the first time scale, the PDE contains the term $\hat{f}_{t_1}$ and $\hat{f}_{\hat{z}\hat{z}}$ only, in the second time scale, we still need the time derivative $\hat{f}_{t_2}$ and the diffusion term $\hat{f}_{\hat{z}\hat{z}}$ and one of the $\hat{f}$ or $\hat{f}_{\hat{z}}$ terms. If we fix $\sigma = 2 - 2\theta = 1$, which gives the leading order equation $0 = \hat{I}_1\hat{f}$ which is not what we expect. So we fix $\sigma = \theta = 2 - 2\theta$, which implies $\sigma = \theta = 2/3$. Since $l \ll 1$, $s = \hat{Q}e^{-l^{1/3}t_2} \approx \hat{Q}$ and (4.5.68) implies

$$\hat{f}_{t_2} = (\hat{z} - \hat{I}_1)\hat{f} + \frac{\hat{Q}}{2}\hat{f}_{\hat{z}\hat{z}}, \qquad (4.5.69)$$

where $t_2 = l^{2/3}t$, $\hat{z} = l^{-2/3}z$ are both $O(1)$, hence $t \sim O(l^{-2/3})$ and $z \sim O(l^{2/3})$. We assume $\hat{f}$ admits a solution of the form $\hat{f} = e^{-\int \hat{I}_1 dt_2}\phi(t_2, \hat{z})$. Then (4.5.69) implies

$$-\hat{I}_1 e^{-\int \hat{I}_1 dt_2}\phi + e^{-\int \hat{I}_1 dt_2}\phi_{t_2} = (\hat{z} - \hat{I}_1)e^{-\int \hat{I}_1 dt_2}\phi + \frac{\hat{Q}}{2}e^{-\int \hat{I}_1 dt_2}\phi_{\hat{z}\hat{z}}, \qquad (4.5.70)$$

which simplifies to

$$\phi_{t_2} = \hat{z}\phi + \frac{\hat{Q}}{2}\phi_{\hat{z}\hat{z}}. \qquad (4.5.71)$$

Since $I_1 = l^{2/3}\hat{I}_1$, $I_2 = l^{4/3}\hat{I}_2$ and $I_3 = l^2\hat{I}_3$, (4.5.45), (4.5.46), (4.5.48) can be written as

$$\frac{d\hat{I}_1}{dt_2} = \hat{I}_2 - (l^{1/3} + l\hat{I}_1)\hat{I}_1 + l^{2/3}, \qquad (4.5.72)$$

$$\frac{d\hat{I}_2}{dt_2} = \hat{I}_3 - (2l^{1/3} + l\hat{I}_1)\hat{I}_2 + s + 3l^{2/3}\hat{I}_1, \qquad (4.5.73)$$

$$\frac{d\hat{I}_3}{dt_2} = 3\hat{I}_2^2 - \hat{I}_1\hat{I}_3 - 3l^{1/3}\hat{I}_3 + 3s\hat{I}_1 + 6l^{2/3}\hat{I}_2, \qquad (4.5.74)$$

since $l \ll 1$, which at the leading order reduces to

$$\frac{d\hat{I}_1}{dt_2} = \hat{I}_2 - \hat{I}_1^2, \quad \frac{d\hat{I}_2}{dt_2} = \hat{I}_3 - \hat{I}_1\hat{I}_2 + \hat{Q}, \quad \frac{d\hat{I}_3}{dt_2} = 3\hat{I}_2^2 - \hat{I}_1\hat{I}_3 + 3\hat{Q}\hat{I}_1. \quad (4.5.75)$$

Equations (4.5.75) implies

$$\frac{d\hat{I}_1}{d\hat{I}_2} = \frac{\hat{I}_2 - \hat{I}_1^2}{\hat{I}_3 - \hat{I}_1\hat{I}_2 + \hat{Q}}, \quad \frac{d\hat{I}_3}{d\hat{I}_2} = \frac{3\hat{I}_2^2 - \hat{I}_1\hat{I}_3 + 3\hat{Q}\hat{I}_1}{\hat{I}_3 - \hat{I}_1\hat{I}_2 + \hat{Q}}. \quad (4.5.76)$$

Since we expect $\hat{I}_2 \to +\infty$, from (4.5.76), this suggests $\hat{I}_1 \sim \hat{I}_2^{1/2}$, $\hat{I}_3 \sim 3\hat{Q} + 3\hat{I}_2^2/\hat{I}_1 \sim 3\hat{Q} + 3\hat{I}_2^{3/2}$, this pseudo-steady state is stable if the denominator is positive, which implies

$$\hat{Q} + \hat{I}_3 - \hat{I}_1\hat{I}_2 \approx 4\hat{Q} + 2\hat{I}_2^{3/2}, \quad (4.5.77)$$

hence clearly the denominator is positive since $\hat{Q} > 0$. Now we consider the equation for $\hat{I}_2(t_2)$, which reduces to

$$\frac{d\hat{I}_2}{dt_2} = 4\hat{Q} + 2\hat{I}_2^{3/2}, \quad (4.5.78)$$

hence as I_2 increases, $\hat{I}_2 \to \infty$ also and $\hat{I}_2 \sim (t_{2c} - t_2)^{-2}$ where t_{2c} is the time when the t_2 time-scale finishes, hence $\hat{I}_1 \sim (t_{2c} - t_2)^{-1}$, $\hat{I}_3 \sim 3(t_{2c} - t_2)^{-3}$. Since the second time-scale t_2 is a slow time scale, but $\hat{I}_1$, $\hat{I}_2$ and $\hat{I}_3$ blow up as t_2 approaches t_{2c}, we need to consider the third time scale t_3, defined by $t_2 = t_{2c} - l^q t_3 = l^{2/3}t$ for some $q > 0$ and in t_3 the scaling are

$$I_1 = l^{2/3-q}\tilde{I}_1, \quad I_2 = l^{4/3-2q}\tilde{I}_2, \quad I_3 = l^{2-3q}\tilde{I}_3, \quad (4.5.79)$$

with $\tilde{I}_1$, $\tilde{I}_2$, $\tilde{I}_3$ all $O(1)$. Putting these scalings and $\hat{z} \sim l^{2/3-q}$ into (4.5.69), we observe that the second derivative term becomes subdominant, leading to

$$\hat{f}_{t_3} = (\hat{z} - \hat{I}_1)\hat{f}, \quad (4.5.80)$$

together with other terms, which enter the leading order balance in the next timescale. The effect of the terms in (4.5.80) is to introduce a skew to the distribution. After the third time scale there are more time scales, which we are not going to solve in details (since they may contain log terms) and in which I_1, I_2 and I_3 grow larger. Instead we jump to the long time scale.

4.5.6 *Very long time scale*

To solve the equation

$$\hat{f}_t = (z + l - I_1)\hat{f} + lz\hat{f}_z + \frac{1}{2}l^2(s+z)\hat{f}_{zz},$$ (4.5.81)

over the long time scale we let $t = l^{-1}t_3$ and $z = l^\theta \hat{z}$ where $t_3, z = O(1)$. The
quantity s can be written as e^{-t_3}, which is also $O(1)$. We assume $I_1 = l^\alpha \hat{I}_1$ where
$\hat{I}_1 = O(1)$. Under these rescaling (4.5.81) can be written as

$$l\hat{f}_{t_3} = (l^\theta \hat{z} + l - l^\alpha \hat{I}_1)\hat{f} + l\hat{z}\hat{f}_{\hat{z}} + \frac{1}{2}l^{2-2\theta}(e^{-t_3} + l^\theta \hat{z})\hat{f}_{\hat{z}\hat{z}}.$$ (4.5.82)

Simplifying, we obtain

$$\hat{f}_{t_3} = (l^{\theta-1}\hat{z} + 1 - l^{\alpha-1}\hat{I}_1)\hat{f} + \hat{z}\hat{f}_{\hat{z}} + \frac{1}{2}l^{1-2\theta}(e^{-t_3} + l^\theta \hat{z})\hat{f}_{\hat{z}\hat{z}}.$$ (4.5.83)

Over the long time scale the terms involving e^{-t_3} become more important than
the terms $l^\theta \hat{z}$, so we fix $\theta - 1 = 1 - 2\theta$ which implies $\theta = \frac{2}{3}$. For the second time
scale we know $I_1 = O(l^{2/3})$, so we still use this relation in the long time scale,
which implies $\alpha = 2/3$, so

$$\hat{f}_{t_3} = (l^{-1/3}\hat{z} + 1 - l^{-1/3}\hat{I}_1)\hat{f} + \hat{z}\hat{f}_{\hat{z}} + \frac{1}{2}l^{-1/3}(e^{-t_3} + l^{2/3}\hat{z})\hat{f}_{\hat{z}\hat{z}}.$$ (4.5.84)

Since $l \ll 1$, we deduce that at leading order

$$0 = (\hat{z} - \hat{I}_1)\hat{f} + \frac{1}{2}e^{-t_3}\hat{f}_{\hat{z}\hat{z}}.$$ (4.5.85)

This has the form of an Airy equation, the relevant solution being

$$\hat{f}(\hat{z}, t_3) = C_1(t_3)Ai\left(2^{\frac{1}{3}}\exp^{\frac{1}{3}t_3}(\hat{I}_1 - \hat{z})\right),$$ (4.5.86)

where $C_1(t_3)$ ia an arbitrary function of t_3 and

$$Ai(\hat{z}) = \frac{1}{\pi}\int_0^\infty \cos\left(\frac{\Psi^3}{3} + \hat{z}\Psi\right)d\Psi.$$

The $Bi(\hat{z})$ function has exponential grow behaviour which we don't expect in
our solution. In the time available we have not been able to derive asymptotic
approximation for $\hat{I}_1(t_3)$. However, we expect $\hat{I}_1$ to increase in time, so we
assume $\hat{I}_1 \sim t_3$ and if we set $C_1(t_3)$ to be constant, we can plot $\hat{f}(\hat{z}, t_3)$ against $\hat{z}$.
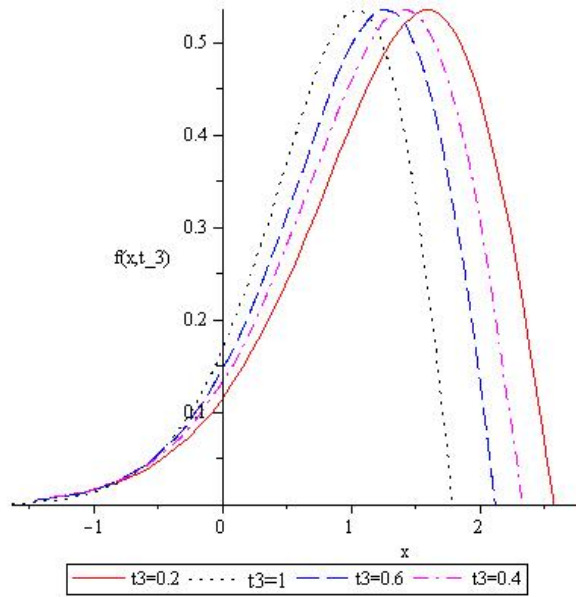
Figure 4.14: *Graph of $f(\hat{x}, t)$ against $\hat{x}$ over the longtime scale with different $lt = t_3 = O(1)$.*

We notice that the distribution moves to the right (to larger values of $\hat{z}$) as time increases. However we know $x = s(t) + z$, so

$$\hat{f}(x, t_3) = C_1(t_3) Ai \left(2^{\frac{1}{3}} \exp^{\frac{1}{3} t_3} l^{-\frac{2}{3}} (I_1 - x + s) \right). \tag{4.5.87}$$

We plot (4.5.87) against x, and observe that it moves to the left (to smaller values of x)(see Figure 4.14). The width of the distribution reduces slightly as it moves, however by judicious choice of $C_1(t_3)$ the area under the curve can be maintained at unity. Also note that the distribution is noticeably skewed.

4.6 Case IV: length-dependent loss and length-dependent division

Case IV combines cases II and III, namely length-dependent loss and a length-dependent probability of division. In Case IV the amount of telomere lost during replication depends on the telomere length via $Y(n) = y_0 + y_1 n$ where y_0, y_1 are constants and $0 < y_1 < 1$ and the probability of a chromosome replicating

is $P_{div} = an + b$ where a, b are constants chosen to ensure that $0 \leq P_{div} \leq 1$. The
discrete reaction equation for a single chromosome can be written as

$$\hat{K}_n^g \rightarrow \hat{K}_n^{g+1} + \hat{K}_{n-y_0-y_1n}^{g+1}, \quad \text{with probability} \quad an + b. \tag{4.6.1}$$

Writing K_n^g as the number of chromosomes of type $\hat{K}_n^g$. Since the loss term $n \rightarrow$
$n - y_0 - y_1n$ implies $(n + y_0)/(1 - y_1) \rightarrow n$, we obtain

$$K_n^{g+1} = K_n^g + (an + b)K_{\frac{n+y_0}{1-y_1}}^g, \quad \text{together with} \quad K_n^0 = \delta_{n,Q}, \tag{4.6.2}$$

Since $y_1 \ll 1$, (4.6.2) can be approximately written as

$$K_n^{g+1} = K_n^g + (an + b)K_{n+y_0+y_1n}^g, \quad \text{together with} \quad K_n^0 = \delta_{n,Q}. \tag{4.6.3}$$

We assume that K_n^g, the solution to (4.6.3) can be approximated by the continuous variable

$$K_n^g = K(x,t) \quad \text{with} \quad K(x,0) = \delta(x - Q), \tag{4.6.4}$$

where $t = gh$, $x = n/Q$ and h is small. We assume that at $t = 0$, we start with a
single chromosome with telomere length Q basepairs, hence $K_n^0 = \delta_{n,Q}$, which
when we take the continuum limit supplies $K(x,0) = \delta(x - 1)$. We substitute
from (4.6.4) into (4.6.3) and obtain

$$K(x, t + h) = K(x,t) + (aQx + b) K\left(x + y_1x + \frac{y_0}{Q}, t\right). \tag{4.6.5}$$

In order to make analytical progress, we require $y_1x \ll x$ and $y_0/Q \ll 1$. Hence
we assume $y_1 \sim y_0/Q$ and introduce $l \ll 1$, as a typical size for these quantities.
Nondimensionalising (4.6.5) with $a = \alpha/Q$, $b = \beta$, $y_0 = lQ\hat{y}_0$ and $y_1 = l\hat{y}_1$
where $(\alpha, \beta, \hat{y}_0, \hat{y}_1) \sim O(1)$, we obtain

$$K(x, t + h) = K(x,t) + (\alpha x + \beta) K(x + l\hat{y}_1x + l\hat{y}_0, t). \tag{4.6.6}$$

Since $h, l \ll 1$, $l\hat{y}_1x + l\hat{y}_0 \ll 1$ and we may perform a Taylor series expansion
to obtain

$$K_t = \frac{(\alpha x + \beta)}{h} \left[K + l(\hat{y}_1x + \hat{y}_0)K_x + \frac{l^2}{2}(\hat{y}_1x + \hat{y}_0)^2 K_{xx}\right]. \tag{4.6.7}$$

We assume (4.6.7) admits solutions of the form

$$K(x,t) = \xi(t)f(x,t), \tag{4.6.8}$$

where $\xi(t) = \int_0^\infty K(x,t)dx$ is the total number of chromosomes in the system at time t and $f(x,t)$ represents their probability distribution, so that

$$\int_{x=0}^\infty f(x,t)dx = 1, \tag{4.6.9}$$

with $f \to 0$ as $x \to 0$ and $x \to +\infty$. We also define the mean of the distribution as

$$\mu(t) = \int_{x=0}^\infty xf(x,t)dx. \tag{4.6.10}$$

If we substitute (4.6.8) into (4.6.7) and integrate with respect to x, we find

$$\xi_t = \frac{1}{h}\int_0^{+\infty}\left\{(\alpha x+\beta)\xi[f+l(\hat{y}_1x+\hat{y}_0)f_x+\frac{l^2}{2}(\hat{y}_1x+\hat{y}_0)^2f_{xx}]\right\}dx, \tag{4.6.11}$$

and since

$$\int_0^\infty (\alpha x+\beta)fdx = \alpha\mu+\beta, \tag{4.6.12}$$

$$\int_0^\infty (\alpha x+\beta)(\hat{y}_1x+\hat{y}_0)f_xdx = -(\beta\hat{y}_1+\alpha\hat{y}_0)-2\alpha\hat{y}_1\mu, \tag{4.6.13}$$

$$\int_0^\infty (\alpha x+\beta)(\hat{y}_1x+\hat{y}_0)^2f_{xx}dx = 4\alpha\hat{y}_0\hat{y}_1+2\beta\hat{y}_1^2+6\alpha\hat{y}_1^2\mu, \tag{4.6.14}$$

we obtain

$$\frac{h\xi_t}{\xi} = \alpha\mu+\beta-l(\beta\hat{y}_1+\alpha\hat{y}_0+2\alpha\hat{y}_1\mu)+l^2(2\alpha\hat{y}_0\hat{y}_1+\beta\hat{y}_1^2+3\alpha\hat{y}_1^2\mu). \tag{4.6.15}$$

Equation (4.6.15) is an evolution equation for the total number of chromosomes in the system $\xi(t)$, whilst $f(x,t)$ controls the distribution of telomere lengths. We determine how $f(x,t)$ evolves by substituting (4.6.8) into (4.6.7) to obtain

$$\xi_tf+\xi f_t = \frac{(\alpha x+\beta)\xi}{h}\left[f+l(\hat{y}_1x+\hat{y}_0)f_x+\frac{l^2}{2}(\hat{y}_1x+\hat{y}_0)^2f_{xx}\right]. \tag{4.6.16}$$

Inserting (4.6.15) into (4.6.16) yields

$$\begin{aligned}
f_t &= \frac{1}{h}[\alpha x+l(\beta\hat{y}_1+\alpha\hat{y}_0)-l^2(2\alpha\hat{y}_0\hat{y}_1+\beta\hat{y}_1^2)-\mu(\alpha-2l\alpha\hat{y}_1+3l^2\alpha\hat{y}_1^2)]f+\\
&\quad \frac{l}{h}(\alpha x+\beta)(\hat{y}_1x+\hat{y}_0)f_x+\frac{l^2}{2h}(\hat{y}_1x+\hat{y}_0)^2(\alpha x+\beta)f_{xx}. \tag{4.6.17}
\end{aligned}$$

We solve (4.6.17) subject to $f(x,0) = \delta(x-1)$ and the boundary conditions $f \to 0$ as $x \to \infty$ or $x \to 0$.

Equation (4.6.17) is too complex to solve explicitly, so we investigate its dynamics by construction an asymptotic approximation to (4.6.17) in the lime $l \ll 1$ retaining only terms which are linear in l.

4.6.1 *First order PDE - General Case*

In the limit as $l \ll 1$ retaining terms which are linear in l, (4.6.17 supplies

$$f_t = \frac{1}{h}[\alpha x + l(\beta \hat{y}_1 + \alpha \hat{y}_0) - \mu\alpha(1 - 2l\hat{y}_1)]f + \frac{l}{h}(\alpha x + \beta)(\hat{y}_1 x + \hat{y}_0)f_x.$$

(4.6.18)

We use the method of characteristics to solve this first order PDE. We introduce the characteristic variables where

$$ds = dt = \frac{hdx}{-l(\alpha x + \beta)(\hat{y}_1 x + \hat{y}_0)} = \frac{hdf}{[\alpha x + l(\beta \hat{y}_1 + \alpha \hat{y}_0) - \mu\alpha(1 - 2l\hat{y}_1)]f},$$

(4.6.19)

and parameterized the initial conditions on $s = 0$ by τ so that when $s = 0$, $t = 0$, $x = \tau$, $f = \delta(\tau - 1)$.

$$\frac{dt}{ds} = 1 \Rightarrow t = s,$$

(4.6.20)

since $t = 0$ when $s = 0$. Solving

$$\frac{dx}{ds} = -\frac{l}{h}(\alpha x + \beta)(\hat{y}_1 x + \hat{y}_0), \quad \Rightarrow x = \frac{\beta - A_2(\tau)\hat{y}_0 e^{-lBs/h}}{A_2(\tau)\hat{y}_1 e^{-lBs/h} - \alpha},$$

(4.6.21)

where $B = \alpha\hat{y}_0 - \beta\hat{y}_1$ and $A_2(\tau)$ is an arbitrary function. Since $x = \tau$ when $s = 0$, we have $A_2(\tau) = (\beta + \alpha\tau)/(\hat{y}_1\tau + \hat{y}_0)$ and

$$x(s,\tau) = \frac{e^{-slB/h}\hat{y}_0\tau\alpha + e^{-slB/h}\hat{y}_0\beta - \beta\tau\hat{y}_1 - \beta\hat{y}_0}{-e^{-slB/h}\hat{y}_1\tau\alpha - e^{-slB/h}\hat{y}_1\beta + \hat{y}_1\tau\alpha + \alpha\hat{y}_0}.$$

(4.6.22)

Since initial condition, $f(s = 0, \tau) = \delta(\tau - 1)$ and there is no spreading of distribution, then f remains as a delta function further for all $s > 0$ and hence must be located at $\mu(s, \tau)$, so $\mu(t) = x(s, \tau)|_{\tau=1}$, so

$$\mu(s) = x(s,\tau)|_{\tau=1} = \frac{e^{-slB/h}\hat{y}_0\alpha + e^{-slB/h}\hat{y}_0\beta - \beta\hat{y}_1 - \beta\hat{y}_0}{-e^{-slB/h}\hat{y}_1\alpha - e^{-slB/h}\hat{y}_1\beta + \hat{y}_1\alpha + \alpha\hat{y}_0}.$$

(4.6.23)

Following (4.6.20), we know $s = t$, so

$$\mu(t) = \frac{e^{-tlB/h}\hat{y}_0\alpha + e^{-tlB/h}\hat{y}_0\beta - \beta\hat{y}_1 - \beta\hat{y}_0}{-e^{-tlB/h}\hat{y}_1\alpha - e^{-tlB/h}\hat{y}_1\beta + \hat{y}_1\alpha + \alpha\hat{y}_0}. \tag{4.6.24}$$

From (4.6.24) we deduce that when $B = 0$ both the numerator and denominator are zero. The solution for these special cases is presented below, after the general solution. For the general case, $\mu(t)$ from (4.6.24) supplies $\mu(t) \rightarrow -\alpha/\beta \leq 0$ as $t \rightarrow +\infty$ since α, $\beta \geq 0$. For physically realistic solutions $1 \geq \mu(t) \geq 0$ and hence we only need to consider times for which $\mu(t) \geq 0$.
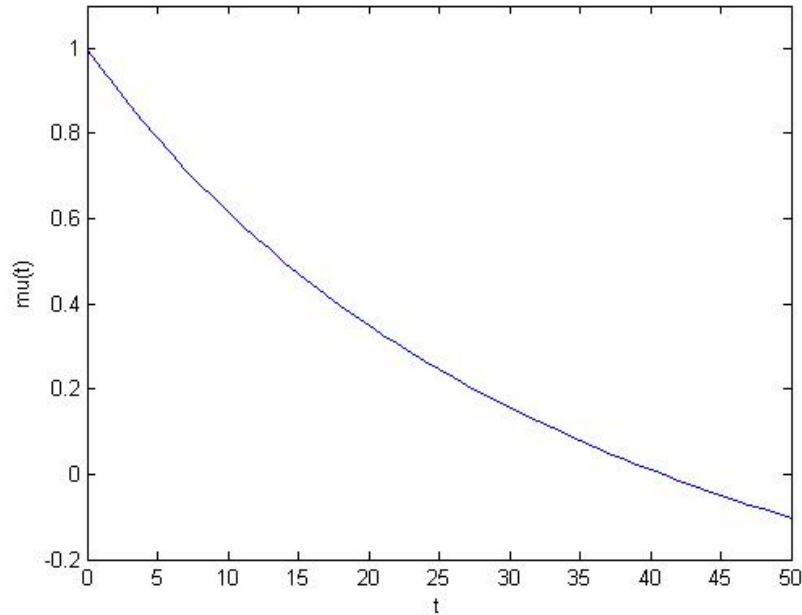
Figure 4.15: *Graph showing $\mu(t)$ (4.6.24) plotted against t with parameters $\alpha = 0.5$, $\beta = 0.5$, $\hat{y}_0 = 0.5$, $\hat{y}_1 = 0.25$, $l = 0.05$.*

In Figure 4.15 we plot $\mu(t)$ against t for a general case and note that the average telomere length decreases from 1 and decreases more slowly as time increases, reaching zero when $t \approx 45$.

To find the time $t = t_c$ at which $\mu(t) = 0$, we solve

$$e^{lBt_c}\beta\hat{y}_1 + e^{lBt_c}\beta\hat{y}_0 - \hat{y}_0\alpha - \hat{y}_0\beta = 0, \tag{4.6.25}$$

which implies

$$t_c = \frac{1}{lB} \ln \left[\frac{\hat{y}_0(\alpha + \beta)}{\beta(\hat{y}_0 + \hat{y}_1)} \right].$$ (4.6.26)

With $B = \alpha\hat{y}_0 - \beta\hat{y}_1$, (4.6.26) supplies

$$t_c = \frac{1}{lB} \ln \left[\frac{B + \beta\hat{y}_1 + \hat{y}_0\beta}{\beta(\hat{y}_0 + \hat{y}_1)} \right] = \frac{1}{lB} \ln \left[1 + \frac{B}{\beta(\hat{y}_0 + \hat{y}_1)} \right],$$ (4.6.27)

where $\alpha, \beta, \hat{y}_0, \hat{y}_1 > 0$. When $B > 0$, $\ln(1 + B/[\beta(\hat{y}_0 + \hat{y}_1)]) > 0$ and $t_c > 0$.
Conversely When $B < 0$, $\ln(1 + B/[\beta(\hat{y}_0 + \hat{y}_1)]) < 0$ and $t_c > 0$. Thus, we
conduce that whenever $B \neq 0$, $t_c > 0$.

In order to compare the results for the mean obtained from the stochastic model
$\mu(g)$ (Section 2.2.7) with the analytical expression from the continuum model
$\mu(t)$, we first rescale the telomere length n by its initial telomere length $x = n/Q$, its divided to obtain $\mu(g)$ in the range $(0,1)$. Secondly, we convert t to g,
where we know the generation number $g = ht$, so $\mu(g)$ can be written as

$$\mu(g) = \frac{e^{-glB}\hat{y}_0\alpha + e^{-glB}\hat{y}_0\beta - \beta\hat{y}_1 - \beta\hat{y}_0}{-e^{-glB}\hat{y}_1\alpha - e^{-glB}\hat{y}_1\beta + \hat{y}_1\alpha + \alpha\hat{y}_0}.$$ (4.6.28)

Figure 4.16 shows that the means from the stochastic simulation (see Section
2.2.7) and the theoretical calculation (4.6.28) are identical before generation 80.
After that, the theoretical mean decreases faster than the stochastic mean, since
in the stochastic simulation, the chromosome can not divide when the telomere
length is lower than the critical telomere length. Whereas in the theoretical cal-
culations, no such restriction on the minimum telomere length is imposed. We
conclude by noting that our theocratical model is valid only when $\mu(t) > 0$.

Having solved for $\mu(t)$, we now return to (4.6.18) to determine the distribu-
tion $f(x, t)$ and hence the evolution of the total number of chromosomes $\xi(t)$.
Now go back to (4.6.19), solving

$$\frac{df}{ds} = \frac{1}{h}[\alpha x + l(\beta\hat{y}_1 + \alpha\hat{y}_0) - \mu\alpha(1 - 2l\hat{y}_1)]f,$$ (4.6.29)

we find

$$\ln f(s, \tau) = \frac{\alpha}{h} \int_0^t x(s, \tau)ds + \frac{lt}{h}(\beta\hat{y}_1 + \alpha\hat{y}_0) - \frac{\alpha}{h}(1 - 2l\hat{y}_1) \int_0^t \hat{\mu}(s)ds + A_3(\tau),$$

119
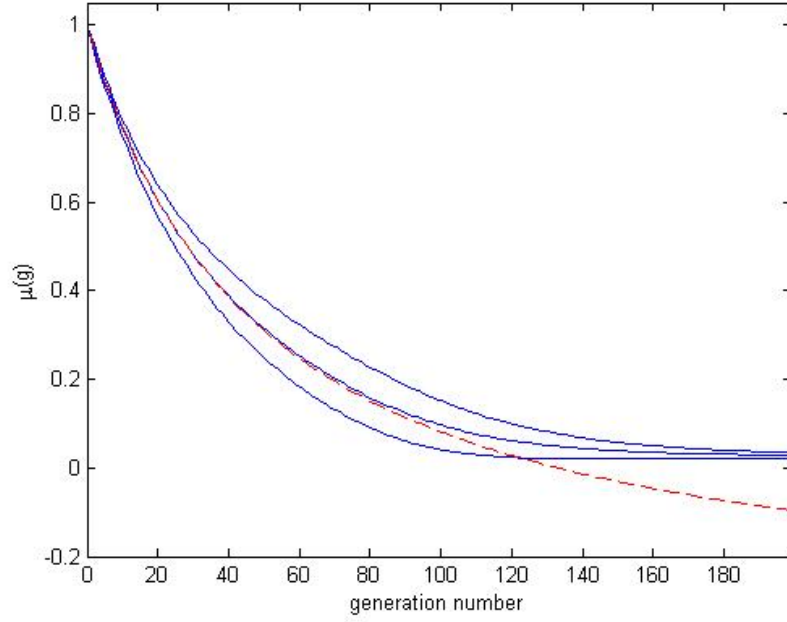
Figure 4.16: *The dashed line shows the $\mu(g)$ from (4.6.28) plotted against generation numbers with parameters $\alpha = 0.8$, $\beta = 0.2$, $\hat{y}_0 = 1$, $\hat{y}_1 = 1.75$, $l = 0.01$. The middle solid line is the average telomere length plotted against generation number from the stochastic simulations with the same parameters, the solid lines above and below indicated two standard deviations above and below the mean.*

where

$$\int_0^t x(s,\tau)ds = -\frac{\beta t}{\alpha} + \frac{h}{l\hat{y}_1\alpha}\left\{\ln[e^{-lBt/h}\hat{y}_1(\alpha\tau+\beta) - \alpha(\hat{y}_1\tau+\hat{y}_0)] - \ln(-B)\right\},$$

hence

$$\begin{aligned}
f(s,\tau) &= A_4(\tau)\exp\left\{-\frac{\beta t}{\alpha} + \frac{lt}{h}(\beta\hat{y}_1 + \alpha\hat{y}_0) - \frac{\alpha}{h}(1-2l\hat{y}_1)\int_{s=0}^{s=t}\hat{\mu}(s)ds+\right. \\
&\left.\frac{h}{l\hat{y}_1\alpha}\left\{\ln[e^{-lBt/h}\hat{y}_1(\alpha\tau+\beta) - \alpha(\hat{y}_1\tau+\hat{y}_0)] - \ln(-B)\right\}\right\},
\end{aligned}$$

(4.6.30)

where $A_4(\tau)$ are arbitrary functions of integration. From (4.6.24), we obtained that

$$\int_0^t \hat{\mu}(s)ds = -\frac{\beta t}{\alpha} + \frac{h}{l\hat{y}_1\alpha}\ln[e^{-lBt/h}\hat{y}_1(\alpha+\beta) - \alpha(\hat{y}_1+\hat{y}_0)] - \frac{h\ln(-B)}{l\hat{y}_1\alpha}.$$

(4.6.31)

Inserting the initial condition $s = 0$, $t = 0$ and $f = \delta(\tau - 1)$ into (4.6.30) implies

$$A_4(\tau) = \delta(\tau - 1). \tag{4.6.32}$$

Equation (4.6.22) yields

$$\tau(s, x) = \frac{\hat{y}_0(\alpha x + \beta) - e^{-lBs/h}\beta(x\hat{y}_1 + \hat{y}_0)}{e^{-lBs/h}\alpha(x\hat{y}_1 + \hat{y}_0) - \hat{y}_1(\alpha x + \beta)}. \tag{4.6.33}$$

and since $s = t$, substitution from (4.6.31) and (4.6.32) into (4.6.30) supplies

$$
\begin{aligned}
f(\tau, t) &= \delta(\tau - 1)(B)^{-2}e^{lBt/h}\left[e^{-lBt/h}\hat{y}_1(\alpha + \beta) - \alpha(\hat{y}_1 + \hat{y}_0)\right]^2 \times \\
&\quad \left[\frac{e^{-lBt/h}\hat{y}_1(\alpha\tau + \beta) - \alpha(\hat{y}_1\tau + \hat{y}_0)}{e^{-lBt/h}\hat{y}_1(\alpha + \beta) - \alpha(\hat{y}_1 + \hat{y}_0)}\right]^{\frac{1}{l\hat{y}_1}}.
\end{aligned}
\tag{4.6.34}
$$

hence

$$
\begin{aligned}
f(x, t) &= \delta\left(\frac{\hat{y}_0(\alpha x + \beta) - e^{-lBt/h}\beta(x\hat{y}_1 + \hat{y}_0)}{e^{-lBt/h}\alpha(x\hat{y}_1 + \hat{y}_0) - \hat{y}_1(\alpha x + \beta)} - 1\right)(B)^{-2+2/l\hat{y}_1} \times \\
&\quad \left[\alpha(\hat{y}_1 + \hat{y}_0) - e^{-lBt/h}\hat{y}_1(\alpha + \beta)\right]^{2 - \frac{1}{l\hat{y}_1}}\exp\left(\frac{lBt}{h} - \frac{Bt}{h\hat{y}_1}\right) \times \\
&\quad \left[e^{-lBt/h}\alpha(x\hat{y}_1 + \hat{y}_0) - \hat{y}_1(\alpha x + \beta)\right]^{-1/l\hat{y}_1},
\end{aligned}
\tag{4.6.35}
$$

or equivalently, $g = t/h$,

$$
\begin{aligned}
f(x, g) &= \delta\left(\frac{\hat{y}_0(\alpha x + \beta) - e^{-lBg}\beta(x\hat{y}_1 + \hat{y}_0)}{e^{-lBg}\alpha(x\hat{y}_1 + \hat{y}_0) - \hat{y}_1(\alpha x + \beta)} - 1\right)(B)^{-2+2/l\hat{y}_1} \times \\
&\quad \left[\alpha(\hat{y}_1 + \hat{y}_0) - e^{-lBg}\hat{y}_1(\alpha + \beta)\right]^{2 - \frac{1}{l\hat{y}_1}}\exp\left(lBg - \frac{Bg}{\hat{y}_1}\right) \times \\
&\quad \left[e^{-lBg}\alpha(x\hat{y}_1 + \hat{y}_0) - \hat{y}_1(\alpha x + \beta)\right]^{-1/l\hat{y}_1}.
\end{aligned}
\tag{4.6.36}
$$

From (4.6.36), it is clear that $f(x, g)$ remains as a delta function, but its amplitude increases over time (or with generation number).

Having found the distribution for $f(x, t)$, we now compute the total number of chromosome $\xi(t)$. We substitute for $\mu(t)$ from (4.6.24) into (4.6.15) to obtain

an expression for $\xi(t)$,

$$
\begin{aligned}
\frac{h\xi_t}{\xi} &= \beta - l(\beta\hat{y}_1 + \alpha\hat{y}_0) + l^2(2\alpha\hat{y}_0\hat{y}_1 + \beta\hat{y}_1^2) + \\
&\quad \frac{\alpha\left(e^{-\frac{tlB}{h}}\hat{y}_0\alpha + e^{-\frac{tlB}{h}}\hat{y}_0\beta - \beta\hat{y}_1 - \beta\hat{y}_0\right)(1 - 2l\hat{y}_1 + 3l^2\hat{y}_1^2)}{-e^{-\frac{tlB}{h}}\hat{y}_1\alpha - e^{-\frac{tlB}{h}}\hat{y}_1\beta + \hat{y}_1\alpha + \alpha\hat{y}_0}, \\
\xi(t) &= (-B)^{-\frac{1-2l\hat{y}_1+3l^2\hat{y}_1^2}{l\hat{y}_1}}\left[e^{-\frac{tlB}{h}}\hat{y}_1(\alpha+\beta) - \alpha(\hat{y}_1+\hat{y}_0)\right]^{\frac{1-2l\hat{y}_1+3l^2\hat{y}_1^2}{l\hat{y}_1}} \times \\
&\quad \exp\left[\frac{tlB}{h}(2l\hat{y}_1 - 1)\right].
\end{aligned}
\tag{4.6.37}
$$

and $\xi(0) = 1$.

We know generation number $g = t/h$, such that

$$
\begin{aligned}
\xi(g) &= (-B)^{-\frac{1-2l\hat{y}_1+3l^2\hat{y}_1^2}{l\hat{y}_1}}\left[e^{-glB}\hat{y}_1(\alpha+\beta) - \alpha(\hat{y}_1+\hat{y}_0)\right]^{\frac{1-2l\hat{y}_1+3l^2\hat{y}_1^2}{l\hat{y}_1}} \times \\
&\quad \exp\left[glB(2l\hat{y}_1 - 1)\right].
\end{aligned}
\tag{4.6.38}
$$

Since $l \ll 1$ and $B = \alpha\hat{y}_0 - \beta\hat{y}_1$, (4.6.38) supplies at leading order

$$
\xi(g) = \left[1 + \frac{\hat{y}_1}{B}(\alpha+\beta)\left(1 - e^{-glB}\right)\right]^{1/l\hat{y}_1} \exp\left(-glB\right).
\tag{4.6.39}
$$

In order to see more clearly how $\xi(g)$ varies with g, we consider two asymptotic limits, one for which $g \sim O(1)$ and a second for which $g \sim O(1/l)$ where $l \ll 1$. When $g \sim O(1)$ and $l \ll 1$, (4.6.39) supplies

$$
\xi(g) \approx \exp[(\alpha+\beta)g].
\tag{4.6.40}
$$

So when $g \sim O(1)$, $\xi(g)$ grows exponentially. When $g \sim O(1/l)$ we write $g = G/l$ where $G \sim O(1)$ and (4.6.39) can be written as

$$
\xi(g) \approx \exp\left[\frac{(\alpha+\beta)}{Bl}\right]\exp\left[\frac{-e^{-GB}(\alpha+\beta)}{Bl}\right].
\tag{4.6.41}
$$

Since $B = \alpha\hat{y}_0 - \beta\hat{y}_1$, can neither be positive, negative or zero. We first consider when $g \sim O(1/l)$ and $B > 0$, $\xi(g) = \bar{a}\exp[\bar{b}\exp(\bar{c}t)]$ which is Gompertzian growth, with upper asymptote constant $\bar{a} = \exp[(\alpha+\beta)/(Bl)]$, growth rate $\bar{c} = B$ and negative contestant $\bar{b} = -(\alpha+\beta)/(Bl)$. Secondly when $B < 0$, let

$C_s = \exp\left[\frac{(\alpha+\beta)}{Bl}\right]$ which is small constant number, $C_{p1} = -(\alpha+\beta)/(Bl)$ which is a positive number and $C_{p2} = -B$ which is also a positive number, so

$$\xi(g) = C_s \exp(C_p e^{C_{p2} G}),\tag{4.6.42}$$

thus $\xi(g)$ also grows exponentially, when $B < 0$. $B = 0$ is a spacial case which we discuss below.
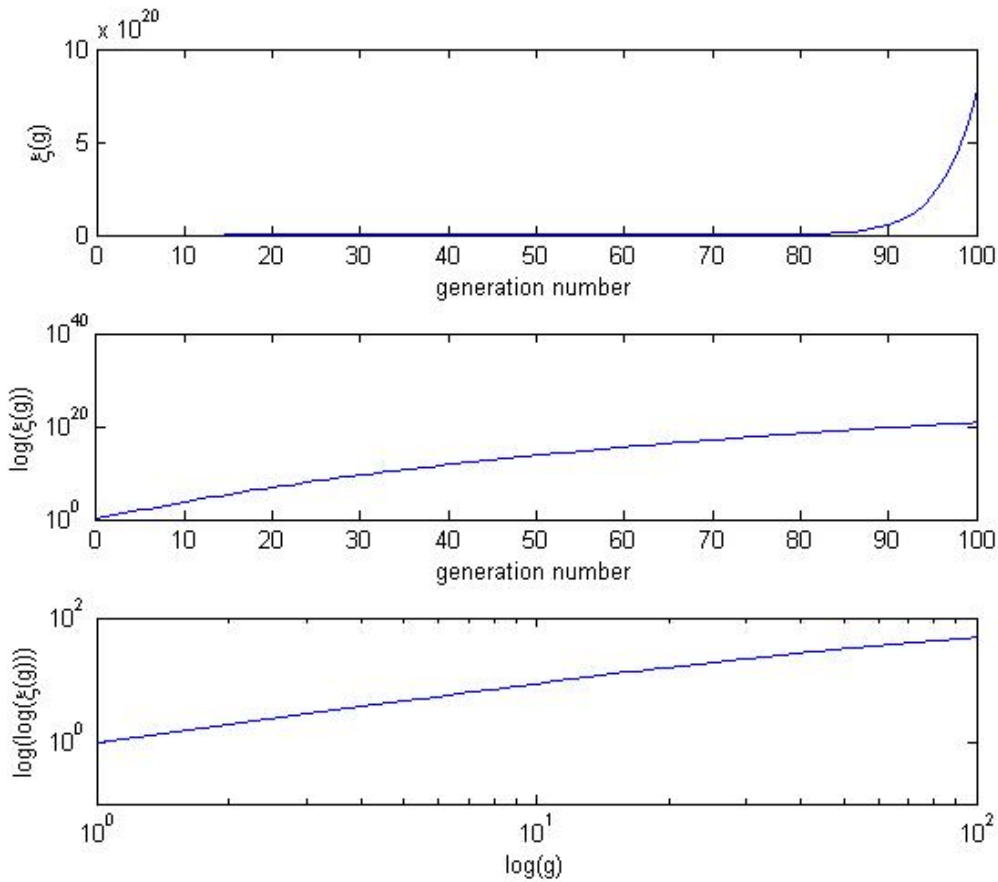
Figure 4.17: *The top graph shows $\xi(g)$ from (4.6.38) plotted against t, the middle graph shows $\log(\xi(g))$ plotted against t and bottom graph shows $\log(\log(\xi(t)))$ against $\log(t)$. With parameters $\alpha = 0.8$, $\beta = 0.2$, $\hat{y}_0 = 1$, $\hat{y}_1 = 1.75$, $l = 0.01$.*

In Figure 4.17 we show how the number of chromosomes grows dramatically with generation number. The middle graph shows $\log(\xi(g))$ plotted against g which is not a straight line which means that $\xi(g)$ does not grow exponentially. The bottom graph in Figure 4.17 shows $\log(\log(\xi(g)))$ increasing linearly with

123

$\log(g)$ which means $\log(\xi(g))$ grows approximately exponentially with $\log(g)$.
We fix the upper limit of g at $g = 100$, because for the parameters used in Figure
4.15 $\mu(g) \geq 0$ when $g < 100$ and therefore we only consider $\xi(g)$ in this range.

4.6.2   *The special case, $B = 0$*

From $\mu(t)$ (4.6.24) we deduce that when $B = 0$ both the numerator and denom-
inator are zero. So we need to reconsider this case when $B = 0$. Due to Case IV
the amount of telomere lost per replication is $Y(n) = y_0 + y_1 n$ and the proba-
bility of a chromosome replicating is $P_{div} = an + b$, $\alpha = aQ$, $b = \beta$, $\hat{y}_0 = y_0$ and
$\hat{y}_1 = y_1 Q$. Since $B = \alpha \hat{y}_0 - \beta \hat{y}_1 = 0$ implies $\alpha \hat{y}_0 = \beta \hat{y}_1$ where there are three
outcomes for solving α. First, when $\hat{y}_0 = \beta = 0$ and $\hat{y}_1 \neq 0$, then $\alpha \in N$. Third,
when $\hat{y}_0 = \hat{y}_1 = 0$ and $\beta \neq 0$, then $\alpha \in N$. Second, when $\hat{y}_0 \neq 0$, $\alpha = \beta \hat{y}_1 / \hat{y}_0$.
Since in practice, during chromosome replication there must be telomere loss,
we deduce that the case $\hat{y}_0 = \hat{y}_1 = 0$ cannot hold and do not consider in further.

Special Case I : $\hat{y}_0 = \beta = 0$

When $\hat{y}_0 = \beta = 0$ and $\hat{y}_1 \neq 0$, implies the amount of telomere lost per replica-
tion is $Y(n) = y_1 n$ and the probability of a chromosome replicating is $P_{div} = an$.
Thus the telomere loss and probability of a chromosome replicating are both
proportional to the telomere length directly. Equation (4.6.18) can be written as

$$f_t = \frac{\alpha}{h}[x - \mu(1 - 2l\hat{y}_1)]f + \frac{l\alpha \hat{y}_1 x^2}{h} f_x. \tag{4.6.43}$$

We introduce the characteristic variables s, where

$$ds = dt = -\frac{hdx}{l\alpha \hat{y}_1 x^2} = \frac{hdf}{\alpha[x - \mu(1 - 2l\hat{y}_1)]f}, \tag{4.6.44}$$

and parameterized the initial conditions on $s = 0$ by τ so that when $s = 0$,
$t = 0$, $x = \tau$, $f = \delta(\tau - 1)$. Solving

$$\frac{dt}{ds} = 1 \Rightarrow t = s, \tag{4.6.45}$$

since $t = 0$ when $s = 0$. Solving

$$\frac{dx}{ds} = -\frac{l\alpha \hat{y}_1 x^2}{h}, \quad \Rightarrow \quad x(s, \tau) = \frac{\tau h}{l\alpha \hat{y}_1 s \tau + h}, \tag{4.6.46}$$

since $x = \tau$ when $s = 0$. Since initial condition, $f(s = 0, \tau) = \delta(\tau - 1)$ and there is no spreading of the distribution, f remains as a delta function for all $s > 0$ and, hence, must be located at $\mu(s) = x(s, \tau) \mid_{\tau=1}$, so

$$\mu(s) = x(s, \tau) \mid_{\tau=1} = \frac{h}{l\alpha \hat{y}_1 s + h}. \tag{4.6.47}$$

From (4.6.45) $s = t$, which implies

$$\mu(t) = \frac{h}{l\alpha \hat{y}_1 t + h}. \tag{4.6.48}$$
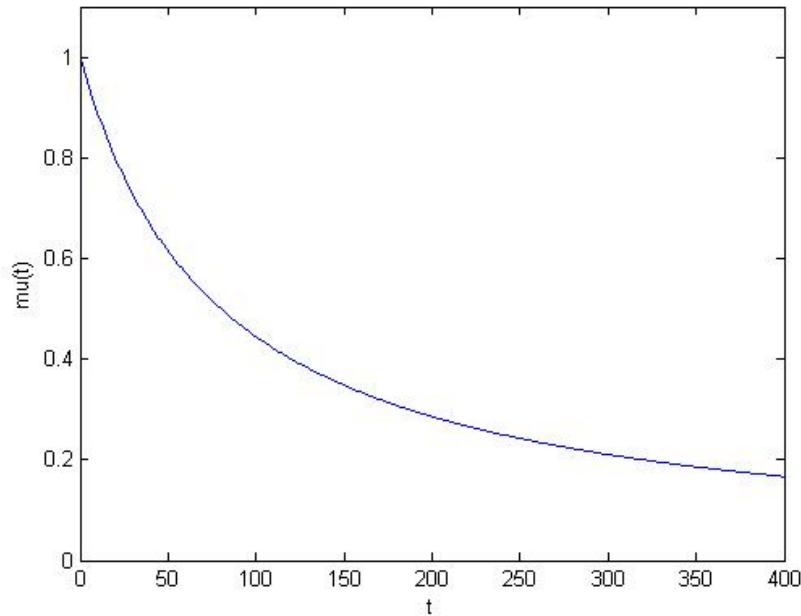
Figure 4.18: *Graph of $\mu(t)$ (4.6.48) plotted against t with parameters $\alpha = 1, \hat{y}_1 = 0.25$, $l = 0.05$, $\hat{y}_0 = \beta = 0$.*

In Figure 4.18 we use (4.6.48) to plot $\mu(t)$ against t for the special Case I, $\hat{y}_0 = \beta = 0$. The average telomere length decreases from unity and decreases slowly as time increases, in this case the $\mu(t)$ can not reach zero, but converges to zero slowly as time increases.

In order to compare the results for the mean obtained from the stochastic model $\mu(g)$ (Section 2.2.7) with the analytical expression from the continuum model $\mu(t)$ (4.6.48), we first rescale the telomere length n by its initial telomere length
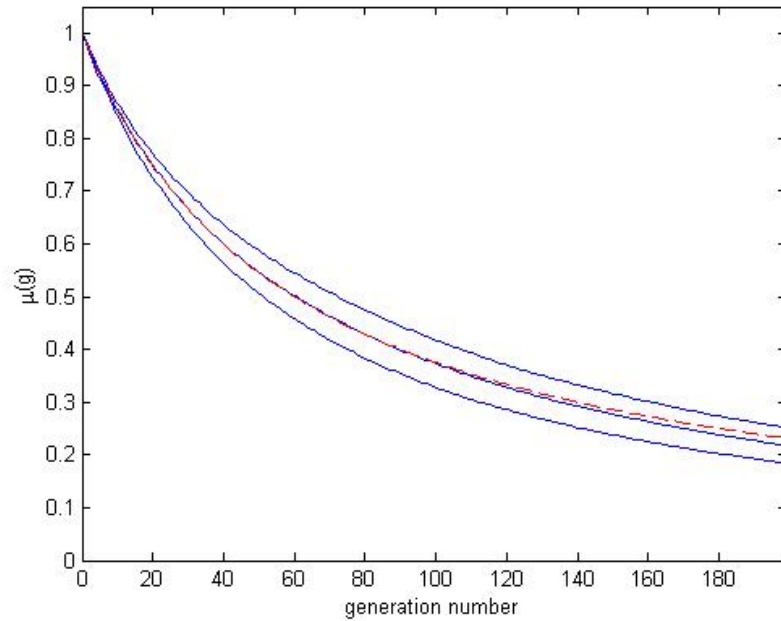
Figure 4.19: *The dashed line shows the $\mu(g)$ from (4.6.49) plotted against generation numbers with parameters $\alpha = 1$, $\beta = 0$, $\hat{y}_0 = 0$, $\hat{y}_1 = 5/3$, $l = 0.01$. The middle solid line is the average telomere length plotted against generation number from the stochastic simulations, the solid lines above and below indicated two standard deviations above and below the mean, for comparison with $\mu(g)/Q$ where $Q = 5950$ basepairs is the initial telomere length.*

$x = n/Q$, its divided to obtain $\mu(g)$ in the range $(0,1)$. Secondly, we convert t to g, where we know the generation number $g = ht$, so $\mu(g)$ can be written as

$$\mu(g) = \frac{1}{l\alpha\hat{y}_1 g + 1} . \tag{4.6.49}$$

In Figure 4.19 we compare plots of $\mu(g)$ generated from the stochastic simulations and the theoretical calculations: they are identical before generation 120. After that, the theoretical mean decreases more slowly than the stochastic mean, but remains within two standard deviations of the stochastic simulations.

Having solved for $\mu(t)$, now we back to method of characteristics, using (4.6.44) to determine the full solution for the distribution $f(x,t)$ and hence the evolu-

tion of the total number of chromosome $\xi(t)$. Solving

$$\frac{df}{ds} = \frac{\alpha}{h}[x - \mu(1 - 2l\hat{y}_1)]f, \qquad (4.6.50)$$

hence

$$f(s, \tau) = A_3(\tau) \exp\left[\frac{\ln(l\alpha\hat{y}_1 t\tau + h) - \ln(h)}{l\hat{y}_1} - \frac{\alpha}{h}(1 - 2l\hat{y}_1)\int_0^t \hat{\mu}(s)ds\right], \qquad (4.6.51)$$

where $A_3(\tau)$ is an arbitrary function of integration. From (4.6.47), we obtain

$$\int_0^t \hat{\mu}(s)ds = \left[\frac{h\ln(l\alpha\hat{y}_1 s + h)}{l\alpha\hat{y}_1}\right]_{s=0}^{s=t} = \frac{h\ln(l\alpha\hat{y}_1 t + h)}{l\alpha\hat{y}_1} - \frac{h\ln(h)}{l\alpha\hat{y}_1}, \qquad (4.6.52)$$

so

$$f = A_3(\tau)(l\alpha\hat{y}_1 t + h)^2\left(\frac{l\alpha\hat{y}_1 t\tau + h}{l\alpha\hat{y}_1 t + h}\right)^{\frac{1}{l\hat{y}_1}} h^{-2}. \qquad (4.6.53)$$

Since $f = \delta(\tau - 1)$ when $s = 0$ and $t = s$, (4.6.53) implies

$$A_3(\tau) = \delta(\tau - 1). \qquad (4.6.54)$$

From (4.6.46), we obtain

$$\tau(s, x) = \frac{xh}{h - l\alpha\hat{y}_1 sx}, \qquad (4.6.55)$$

and we know $s = t$, so substituting (4.6.54), (4.6.55) into (4.6.53) yields

$$f(x, t) = \delta\left(\frac{hx}{h - l\alpha\hat{y}_1 tx} - 1\right)\left[\frac{1}{(h - l\alpha\hat{y}_1 tx)(l\alpha\hat{y}_1 t + h)}\right]^{\frac{1}{l\hat{y}_1}} \times$$
$$h^{\frac{2}{l\hat{y}_1} - 2}(l\alpha\hat{y}_1 t + h)^2. \qquad (4.6.56)$$

Since $g = t/h$, so

$$f(x, g) = \delta\left(\frac{x}{1 - l\alpha\hat{y}_1 xg} - 1\right)\left[\frac{1}{(1 - l\alpha\hat{y}_1 xg)(l\alpha\hat{y}_1 g + 1)}\right]^{\frac{1}{l\hat{y}_1}} \times$$
$$h^{\frac{2}{l\hat{y}_1}}(l\alpha\hat{y}_1 g + 1)^2. \qquad (4.6.57)$$

As we can see from (4.6.57), the function of $f(x, g)$ is now a Delta function with growing amplitude.

Having found distribution of $f(x,t)$, we now analyze the total number of chromosome $\xi(t)$. From the first order PDE, we have found the expression for $\mu(t)$, so we now put (4.6.48) and $\hat{y}_0 = \beta = 0$ back to (4.6.15) to obtain an expression for $\xi(t)$,

$$\frac{\xi_t}{\xi} = \frac{\alpha(1 - 2l\hat{y}_1 + 3l^2\hat{y}_1^2)}{l\alpha\hat{y}_1 t + h}, \tag{4.6.58}$$

hence

$$\xi(t) = \left(\frac{l\alpha\hat{y}_1 t}{h} + 1\right)^{\frac{1 - 2l\hat{y}_1 + 3l^2\hat{y}_1^2}{l\hat{y}_1}}, \tag{4.6.59}$$

since $\xi(0) = 1$. Since $t = gh$, such that

$$\xi(g) = (l\alpha\hat{y}_1 g + 1)^{\frac{1 - 2l\hat{y}_1 + 3l^2\hat{y}_1^2}{l\hat{y}_1}}. \tag{4.6.60}$$

Since $l \ll 1$, $\xi(g) \sim \exp(\alpha g)$.

The top graph in Figure 4.20 show how the number of chromosomes grows dramatically as the generation number increases. The middle graph shows $log(\xi(g))$ plotted against g which is not straight line which mean $\xi(g)$ not grows exponentially. The bottom graph in Figure 4.20 shows $\log(\log(\xi(g)))$ increasing linearly with $\log(g)$ which means $\log(\xi(g))$ grow exponentially with $\log(g)$. In this case as g increases $\xi(t)$ increases, since $\mu(t)$ (obtain from (4.6.48)), tends to zero slowly as $t \to +\infty$ (see Figure 4.18). Cells can't have unlimited growth, so $g \to +\infty$ the situation in this case does not meet the actual situation.

$$\textbf{\textit{Special Case II}: } \alpha = \frac{\beta\hat{y}_1}{\hat{y}_0} \textbf{\textit{ when }} \hat{y}_0 \neq 0$$

In Case IV the amount of telomere lost per replication is $Y(n) = y_0 + y_1 n$ and the probability of a chromosome replicating is $P_{div} = an + b$, $\alpha = aQ$, $b = \beta$, $\hat{y}_0 = y_0$ and $\hat{y}_1 = y_1 Q$. When $\alpha = \beta\hat{y}_1/\hat{y}_0$ and $\hat{y}_0 \neq 0$, implies the amount of telomere lost per replication is $Y(n) = y_0 + y_1 n$ and the probability of a chromosome replicating is $P_{div} = \beta(y_0 + y_1 n)/y_0 = \beta Y(n)/y_0$, which means the probability of a chromosome replicating is proportion to the amount of telomere loss.
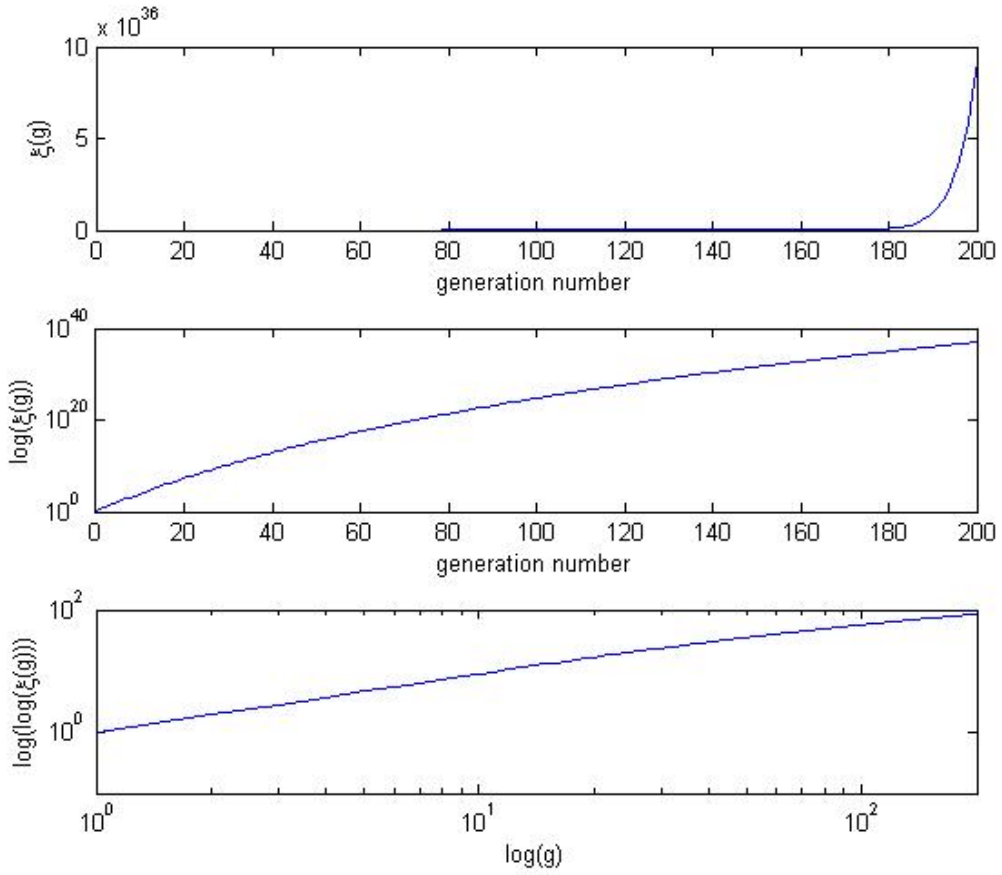
Figure 4.20: *The top graph shows $\xi(g)$ from (4.6.60) plotted against t, the middle graph shows $\log(\xi(g))$ plotted against t and bottom graph shows $\log(\log(\xi(t)))$ against $\log(t)$. With parameters $\alpha = 1, \beta = 0, \hat{y}_0 = 0, \hat{y}_1 = 5/3, l = 0.01$.*

We put $\alpha = \beta \hat{y}_1 / \hat{y}_0$ back to (4.6.18) and hence obtain

$$f_t = \frac{\beta \hat{y}_1}{\hat{y}_0 h}[x + 2l\hat{y}_0 - \mu(1 - 2l\hat{y}_1)]f + \frac{\beta l}{\hat{y}_0 h}(\hat{y}_1 x + \hat{y}_0)^2 f_x. \tag{4.6.61}$$

We introduce the characteristic variables s, where

$$ds = dt = \frac{\hat{y}_0 h dx}{-l\beta(\hat{y}_1 x + \hat{y}_0)^2} = \frac{\hat{y}_0 h df}{\beta \hat{y}_1[x + 2l\hat{y}_0 - \mu(1 - 2l\hat{y}_1)]f}, \tag{4.6.62}$$

and parameterized the initial conditions on $s = 0$ by τ so that when $s = 0$, $t = 0, x = \tau, f = \delta(\tau - 1)$. Solving

$$\frac{dt}{ds} = 1 \Rightarrow t = s, \tag{4.6.63}$$

since $t = 0$ when $s = 0$. Solving

$$\frac{dx}{ds} = -\frac{\beta l}{\hat{y}_0 h}(\hat{y}_1 x + \hat{y}_0)^2 \qquad (4.6.64)$$

implies

$$x(s, \tau) = \frac{\hat{y}_0(\tau h - sl\beta\hat{y}_1\tau - sl\beta\hat{y}_0)}{\tau l\beta\hat{y}_1^2 s + l\beta\hat{y}_1\hat{y}_0 s + \hat{y}_0 h}, \qquad (4.6.65)$$

since $x = \tau$ when $s = 0$, equivalently

$$\tau(s, x) = \frac{\hat{y}_0(xh + sl\beta\hat{y}_0 + slx\beta\hat{y}_1)}{\hat{y}_0 h - xl\beta\hat{y}_1^2 s - l\beta\hat{y}_1\hat{y}_0 s}. \qquad (4.6.66)$$

Since $f(s = 0, \tau) = \delta(\tau - 1)$ and there is no spreading of distribution, f remains
as a delta function further for all $s > 0$ and hence must be located at $\mu(s, \tau)$ and
hence

$$\mu(t) = x(s, \tau) \,|_{\tau=1}^{s=t} = \frac{\hat{y}_0 h - \hat{y}_0 tl\beta(\hat{y}_1 + \hat{y}_0)}{l\beta\hat{y}_1 t(\hat{y}_1 + \hat{y}_0) + \hat{y}_0 h}. \qquad (4.6.67)$$
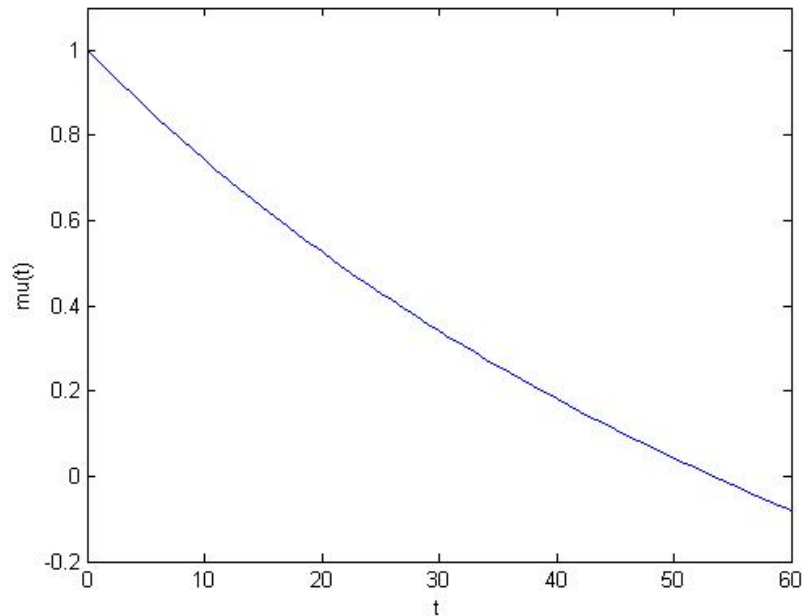
Figure 4.21: *Graph shows $\mu(t)$ plotted against t with parameter $\beta = 0.5$, $\hat{y}_0 = 0.5$,
$\hat{y}_1 = 0.25$, $l = 0.05$.*

In Figure 4.21 we show how the average telomere length $\mu(t)$ decreases from

1 linearly as time increases and reaches zero around $t = 55$. For $t > 55$, $\mu(t)$ continues to decrease, becoming n negative. For physically realistic solutions we only need to consider the times for which $0 \leq \mu(t) \leq 1$. Since $t = gh$, $\mu(t)$ can be written as

$$\mu(g) = \frac{\hat{y}_0 - gl\beta(\hat{y}_1 + \hat{y}_0)}{l\beta\hat{y}_1 g(\hat{y}_1 + \hat{y}_0) + \hat{y}_0} \,. \tag{4.6.68}$$
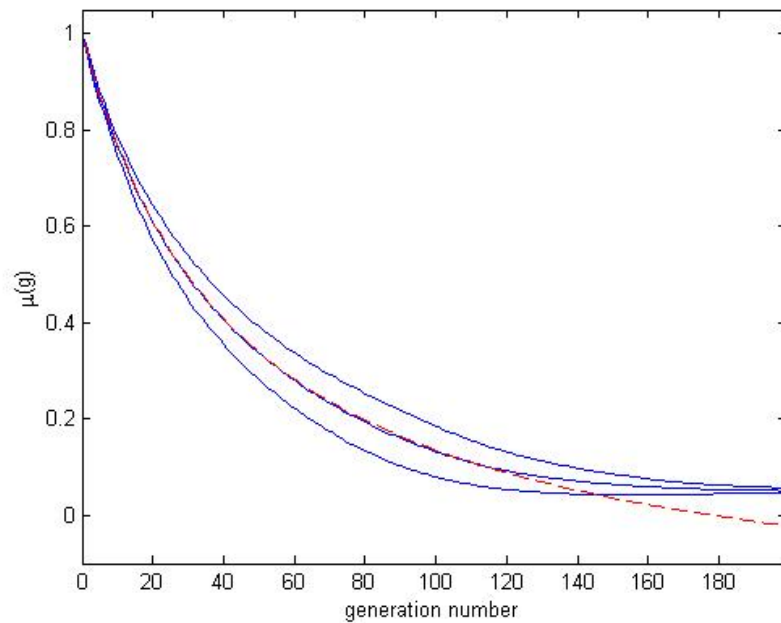
Figure 4.22: *The dashed line shows the $\mu(g)$ from (4.6.68) plotted against generation numbers with parameters $\alpha = 0.8$, $\beta = 0.2$, $\hat{y}_0 = 9$, $\hat{y}_1 = 2.25$, $l = 0.01$. The middle solid line is the average telomere length plotted against generation number from the stochastic simulations with the same parameters, the solid lines above and below indicated two standard deviations above and below the mean, for comparison with $\mu(g)/Q$ (the initial telomere length being Q=5950 basepairs).*

Figure 4.22 shows that from the stochastic and the theoretical calculation of $\mu(t)$ are identical before generation 120. After that the theoretical value of μ (4.6.68) decreases faster than the stochastic one, due to the chromosome can not divide when the telomere length is lower than the critical length, in stochastic simulation. In the theoretical calculations, there is no restriction on the telomere length and the chromosome can always divide, even when the telomere length

is lower than the critical telomere length. Here we only need to consider times
for which $\mu(t) > 0$.

Having solved for $\mu(t)$, we now return to (4.6.61) to find the full solution for
the distribution $f(x, t)$ and hence the evolution of the total number of chromo-
some $\xi(t)$. Solving

$$\frac{df}{ds} = \frac{\beta \hat{y}_1 [x + 2l\hat{y}_0 - \mu(1 - 2l\hat{y}_1)]f}{\hat{y}_0 h}, \tag{4.6.69}$$

where from (4.6.65), we obtain

$$
\begin{aligned}
\int_0^t x(s)ds &= \left[\frac{\hat{y}_0(h \ln(\tau l\beta \hat{y}_1^2 s + l\beta \hat{y}_1 \hat{y}_0 s + \hat{y}_0 h) - sl\beta \hat{y}_1)}{l\beta \hat{y}_1^2} \right]_{s=0}^{s=t} \\
&= \frac{\hat{y}_0}{l\beta \hat{y}_1^2} \left[h \ln(\tau l\beta \hat{y}_1^2 t + l\beta \hat{y}_1 \hat{y}_0 t + \hat{y}_0 h) - tl\beta \hat{y}_1 - h \ln(\hat{y}_0 h) \right].
\end{aligned}
\tag{4.6.70}
$$

and from (4.6.67), we obtain

$$
\begin{aligned}
\int_0^t \hat{\mu}(s)ds &= \left[\frac{\hat{y}_0(h \ln(l\beta \hat{y}_1^2 s + l\beta \hat{y}_1 \hat{y}_0 s + \hat{y}_0 h) - sl\beta \hat{y}_1)}{l\beta \hat{y}_1^2} \right]_{s=0}^{s=t} \\
&= \frac{\hat{y}_0}{l\beta \hat{y}_1^2} [h \ln(l\beta \hat{y}_1^2 t + l\beta \hat{y}_1 \hat{y}_0 t + \hat{y}_0 h) - tl\beta \hat{y}_1 - h \ln(\hat{y}_0 h)].
\end{aligned}
\tag{4.6.71}
$$

hence

$$
\begin{aligned}
f(\tau, t) &= \delta(\tau - 1)(\hat{y}_0 h)^{-2}(l\beta \hat{y}_1^2 t + l\beta \hat{y}_1 \hat{y}_0 t + \hat{y}_0 h)^2 \times \\
&\quad \left(\frac{\tau l\beta \hat{y}_1^2 t + l\beta \hat{y}_1 \hat{y}_0 t + \hat{y}_0 h}{l\beta \hat{y}_1^2 t + l\beta \hat{y}_1 \hat{y}_0 t + \hat{y}_0 h} \right)^{1/l\hat{y}_1},
\end{aligned}
\tag{4.6.72}
$$

since $s = 0$ and $f = \delta(\tau - 1)$. Hence substitution $s = t$ and (4.6.66) into (4.6.72),
we obtain

$$
\begin{aligned}
f(x, t) &= \delta \left(\frac{\hat{y}_0(xh + tl\beta \hat{y}_0 + tlx\beta \hat{y}_1)}{\hat{y}_0 h - xl\beta \hat{y}_1^2 t - l\beta \hat{y}_1 \hat{y}_0 t} - 1 \right) \left(l\beta \hat{y}_1^2 t + l\beta \hat{y}_1 \hat{y}_0 t + \hat{y}_0 h \right)^{2-1/l\hat{y}_1} \times \\
&\quad (\hat{y}_0 h - xl\beta \hat{y}_1^2 t - l\beta \hat{y}_1 \hat{y}_0 t)^{-1/l\hat{y}_1}(\hat{y}_0 h)^{-2+2/l\hat{y}_1}.
\end{aligned}
\tag{4.6.73}
$$

Since $g = t/h$, so

$$
\begin{aligned}
f(x,g) &= \delta\left(\frac{\hat{y}_0(x + gl\beta\hat{y}_0 + glx\beta\hat{y}_1)}{\hat{y}_0 - xl\beta\hat{y}_1^2 g - l\beta\hat{y}_1\hat{y}_0 g} - 1\right)\left(l\beta\hat{y}_1^2 g + l\beta\hat{y}_1\hat{y}_0 g + \hat{y}_0\right)^{2-1/l\hat{y}_1} \times \\
&\quad (\hat{y}_0 - xl\beta\hat{y}_1^2 g - l\beta\hat{y}_1\hat{y}_0 g)^{-1/l\hat{y}_1}(\hat{y}_0)^{-2+2/l\hat{y}_1}.
\end{aligned} \tag{4.6.74}
$$

As we can see from (4.6.74), the function of $f(x,g)$ still stage as a delta function, but with amplitude grows.

From the first order PDE, we found an expression for $\mu(t)$, so we now put (4.6.67) and $\alpha = \beta\hat{y}_1/\hat{y}_0$ back into (4.6.15) to obtain an expression for $\xi(t)$, namely

$$
\frac{h\xi_t}{\xi} = \beta(1 - 2l\hat{y}_1 + 3l^2\hat{y}_1^2)\left[1 + \frac{\hat{y}_1(h - tl\beta\hat{y}_1 - tl\beta\hat{y}_0)}{l\beta\hat{y}_1^2 t + l\beta\hat{y}_1\hat{y}_0 t + \hat{y}_0 h}\right],
$$

hence

$$
\xi(t) = (\hat{y}_0)^{-(1-2l\hat{y}_1+3l^2\hat{y}_1^2)/l\hat{y}_1}\left[\frac{l\beta\hat{y}_1^2 t + l\beta\hat{y}_1\hat{y}_0 t + \hat{y}_0 h}{h}\right]^{(1-2l\hat{y}_1+3l^2\hat{y}_1^2)/l\hat{y}_1}, \tag{4.6.75}
$$

since $\xi(0) = 1$ when $t = 0$. Since $t = gh$

$$
\xi(g) = (\hat{y}_0)^{-(1-2l\hat{y}_1+3l^2\hat{y}_1^2)/l\hat{y}_1}(l\beta\hat{y}_1^2 g + l\beta\hat{y}_1\hat{y}_0 g + \hat{y}_0)^{(1-2l\hat{y}_1+3l^2\hat{y}_1^2)/l\hat{y}_1}. \tag{4.6.76}
$$

The top graph in Figure 4.23 shows the number of chromosomes grows dramatically. The middle graph shows $log(\xi(g))$ plotted against g which is not a straight line which means $\xi(g)$ does not grow exponentially. The bottom graph in Figure 4.23 shows $\log(\log(\xi(g)))$ increasing linearly with $\log(g)$ which means $\log(\xi(g))$ grow exponentially with $\log(g)$.

From the first order PDE, we obtain the solution for average telomere length $\mu(t)$ and the growth rate $\xi(t)$ for both general cases and epical cases. The theoretical $\mu(t)$ and the stochastic simulations are quite identical before the time $\mu(t) > 0$, but the shape of the distribution still remains in the delta function.
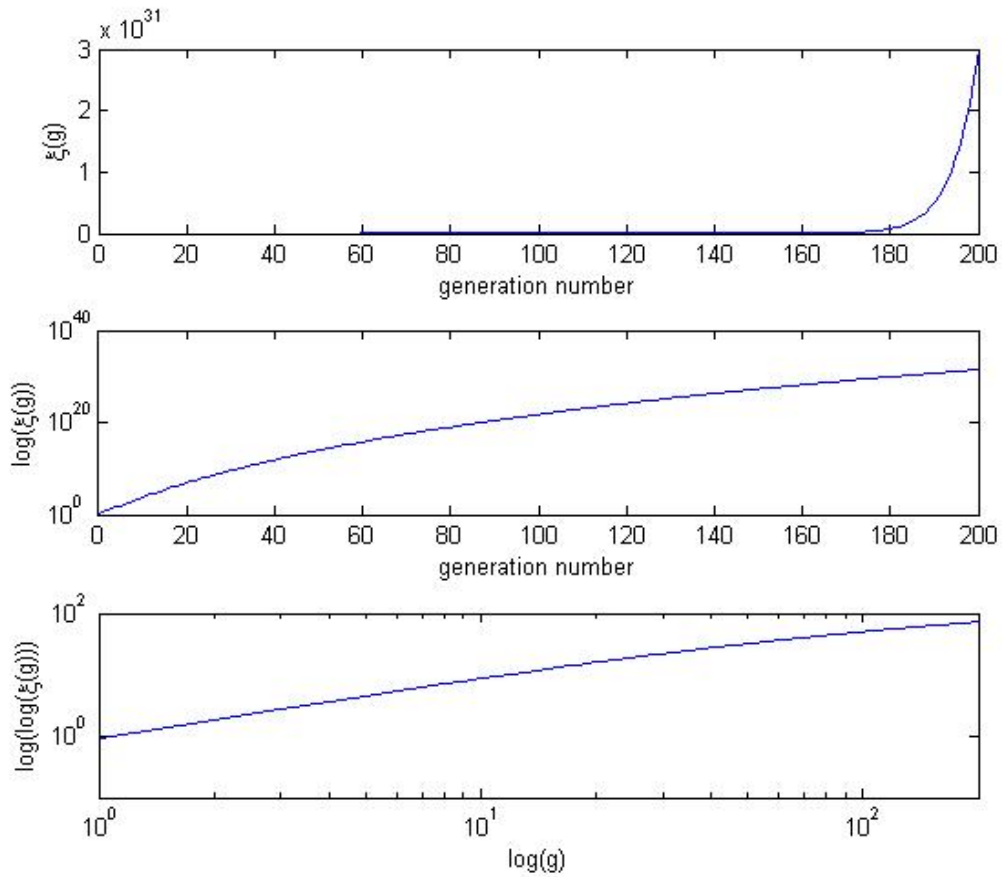
Figure 4.23: *The top graph shows $\xi(g)$ from (4.6.76) plotted against t, the middle graph shows $log(\xi(g))$ plotted against t and bottom graph shows $log(log(\xi(t)))$ against $log(t)$. With parameters $\alpha = 0.8$, $\beta = 0.2$, $\hat{y}_0 = 9$, $\hat{y}_1 = 2.25$, $l = 0.01$.*

In order to understand the how the distribution varies, we need to consider the second order PDE instead of first order PDE. Here we do not do the further analysis on the distributions.

4.7 Mathematical cell model of normal ageing

In the previous section, we assumed each cell contained only one chromosome, whereas in fact, the normal human cell contains 46 chromosomes. In this section we upgrade the single chromosome cell model to an *N* chromosome cell model. The cell model is more complex than the chromosome model. Before the

cell replicates, we need to checks all 46 chromosomes, to make sure none of the
telomeres have fallen below the critical value which causes senescence. If one
of the chromosomes has reached this critical value, the cell will not replicate.
If a cell replicates, it produces two daughter cells. The daughter chromosomes
are allocated randomly to each of the daughter cells. The rule for replication of
chromosomes in the cell is the same as in Figure 4.1. We use m, to denote the
total telomere length in the cell, $Y(m)$, to denote the total amount of telomere
lost during each replication and P_{cdiv} to denote the probability of cell division.
We still consider four different cases as similar as the chromosome model as in
Section 4.2, summarized in Table 4.3.

Case	P_{cdiv}	$Y(m)$
Case I	$P_{cdiv} = 1$	$Y(m) = L$
Case II	$P_{cdiv} = 1$	$Y(m) = y_0 + y_1 m$
Case III	$P_{cdiv} = (a + bm)^{\alpha}$	$Y(m) = L$
Case IV	$P_{cdiv} = (a + bm)^{\alpha}$	$Y(m) = y_0 + y_1 m$

Table 4.3: Summary of the rules for cell division and telomere shortening that
we consider.

4.8 Case I: constant loss

Let N be the number of chromosomes in a cell. Each chromosome obeys the
replication rule (4.1), namely $K_n^g \rightarrow K_n^{g+1} + K_{n-L}^{g+1}$. If the telomere length of each
chromosome in a cell is longer than the critical value then the cell replicates;
otherwise it remains senescent. For the discrete model, we use C_m^g to denote the
number of cells with total telomere length m at generation g. We use $Y(m) = L$
to denote the total amount of telomere lost during each replication; and g to
represent the generation number. If the cell replicates, the daughter chromo-
somes are randomly allocated to the daughter cells in one of the 2^N possible
combinations for the $2N$ chromosomes that are randomly allocated to the two

daughter cells. The discrete cell replication reaction can be written as

$$C_m^g \rightarrow C_{m-jL}^{g+1} + C_{m-(N-j)L}^{g+1} \quad j = 0, 1, .., N \quad \text{with probability } 2^{-N}\binom{N}{j}.$$
$$(4.8.1)$$

Hence, averaging over all the possible arrangements of telomere lengths

$$C_m^g \rightarrow \sum_{j=0}^{N} 2^{-N}\binom{N}{j}\left(C_{m-jL}^{g+1} + C_{m-(N-j)L}^{g+1}\right),$$
$$(4.8.2)$$

which implies

$$C_m^{g+1} = 2^{-N}\sum_{j=0}^{N}\binom{N}{j}\left[C_{m+jL}^g + C_{m+(N-j)L}^g\right].$$
$$(4.8.3)$$

We assume that the solution has the form $C_m^g = e^{\gamma g + \chi m}$ where the growth rate γ depends on the rate of change of the distribution with m, namely χ. For small χ, (4.8.3) supplies

$$e^\gamma = 2^{-N}\sum_{j=0}^{N}\binom{N}{j}\left[e^{j\chi L} + e^{(N-j)\chi L}\right] \approx 2 + NL\chi + \frac{NL^2\chi^2(N+1)}{4},$$

so that

$$\gamma = \ln 2 + \frac{NL\chi}{2} + \frac{NL^2\chi^2}{8}.$$
$$(4.8.4)$$

To develop a continuum model with the same dispersion relation as the discrete one. In general, the number of cells, C, become very large over a few generations and can therefore be treated as a continuous variable. We also replace the discrete generation number g by a continuous time variable, t. Since the amount of telomere loss in the normal human cells, L, is much less than the initial telomere length, we can treat telomere length, m, as a continuous variable. Thus we replace the discrete model for C_m^g by a continuum model for $C(m, t)$. The continuum analogue of (4.8.3) is the simplest partial differential equation which has the same dispersion relation as (4.8.4), namely

$$\frac{\partial C}{\partial t} = C\ln 2 + \frac{1}{2}NL\frac{\partial C}{\partial m} + \frac{1}{8}NL^2\frac{\partial^2 C}{\partial m^2}.$$
$$(4.8.5)$$

Compare this PDE with the single chromosome model, (4.3.5), which is

$$\frac{\partial K}{\partial t} = K\ln 2 + \frac{1}{2}L\frac{\partial K}{\partial n} + \frac{1}{8}L^2\frac{\partial^2 K}{\partial n^2},$$
$$(4.8.6)$$

we notice that these two PDEs are similar, both containing coefficient of $\ln(2)$ in front of C or K, which means the number of cells increases with the same growth rate as the chromosome model. If the total telomere length in the cell is $m = N \times n$, then $\frac{\partial C}{\partial m} = \frac{1}{N}\frac{\partial C}{\partial n}$ and $\frac{\partial^2 C}{\partial m^2} = \frac{1}{N^2}\frac{\partial^2 C}{\partial n^2}$, indicating that the speed of the distribution of $C(m,t)$ moves toward lower telomere lengths is same as the chromosomes model, but the diffusion terms is significantly smaller (by a factor of N).

We are interested in comparing the results of our models with experimental data from experiments on cells taken from human adults. We assume that at same time ($t = 0$) cells have telomere length m_0 and the cells variance $\sigma = \sigma_0$. We assume the sample of cells taken from experiment at $t = t_1$ has average telomere length M_1 and variance $\sigma = \sigma_1$. In order to find σ, we apply similar methods to those of in Section 5.4 to deduce

$$\frac{d}{dt}m(t) = -\frac{1}{2}NL \implies m(t) = m_0 - \frac{1}{2}NLt, \tag{4.8.7}$$

$$\frac{d}{dt}\sigma(t) = \frac{NL^2}{8\sigma(t)} \implies \sigma(t) = \frac{1}{2}\sqrt{NL^2t + 4\sigma_0^2}. \tag{4.8.8}$$

From (4.8.7) and (4.8.8) we obtain $t_1 = 2(m_0 - M_1)/NL$ and $\sigma_1 = \frac{1}{2}\sqrt{NL^2t_0 + 4\sigma_0^2}$. We solve (4.8.5) by prescribing the following initial condition $C(m,0) = \delta(m - M_1)$, where M_1 is the initial telomere length in the starting cell and $\sigma_0 = 0$, use the same method as in Section 4.3 to solve the PDE, we obtain

$$C(m,t) = \frac{2^t\sqrt{2}}{\sqrt{(NL^2t + 4\sigma_1)\pi}} \exp\left[-\frac{2(m + \frac{1}{2}LNt - M_1)^2}{NL^2t + 4\sigma_1}\right]. \tag{4.8.9}$$

We use $\mu_m(t)$ to denote the average telomere length of the cell at time t which can be written

$$\mu_m(t) = \frac{\int_0^{M_{max}} mC(m,t)dm}{\int_0^{M_{max}} C(m,t)dm}. \tag{4.8.10}$$

Using $\sigma_m^2(t)$ to denote the variance of the cell's telomere length at time t, we find

$$\sigma_m^2(t) = \frac{\int_0^{M_{max}} [m - \mu_m(t)]^2 C(m,t) dm}{\int_0^{M_{max}} C(m,t) dm},$$
(4.8.11)

where M_{max}, is the maximum possible telomere length in a cell at time t so that $M_{max} = M_1$ is the initial telomere length.
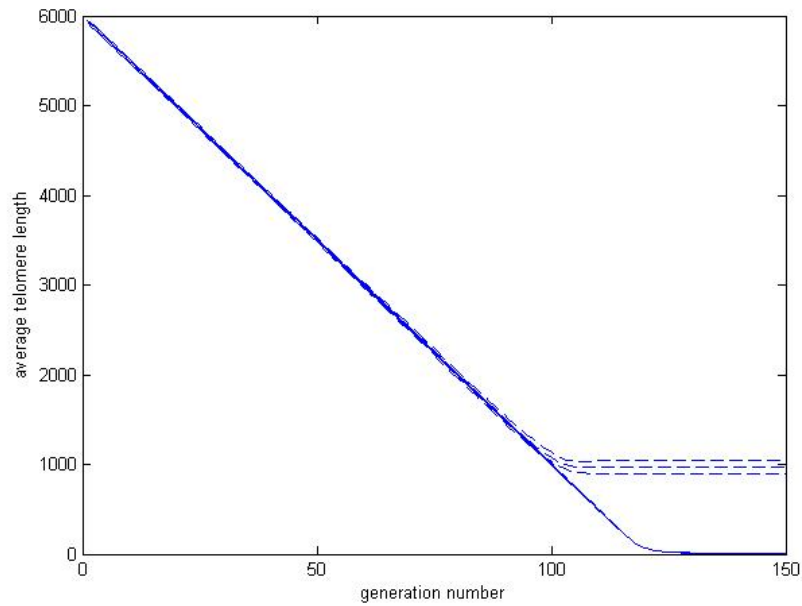
Figure 4.24: *The middle solid line is the average telomere length $\mu_m(t)/N$ and the solid lines above and below are the average telomere lengths $\mu_m(t)/N$ plus or minus two standard deviations. The middle dashed line is the average telomere length against generation number in stochastic simulations (average of 1000 simulations) which we obtained earlier and the dashed lines above and below are the average telomere lengths from computer simulations plus or minus two standard deviations.*

For comparison with the earlier stochastic simulations, we choose, $L = 100$, $N = 46$ and $M_1 = 5950 \times 46$, so that the amount of telomere loss at each replication is identical to the stochastic simulation. A comparison of results is shown in Figure 4.24. We assume that the average telomere length of a chromosome in a cell $\mu_{chro}(t) = \mu_m(t)/N$. Before $t = 90$, the mean chromosome telomere length $\mu_{chro}(t)$ for the theoretical model and the mean telomere length for the

stochastic simulation are identical. Thereafter these curves diverge, the mean telomere length of the stochastic simulation remain 1000 and the average telomere length of the chromosome in the cell $\mu_{chro}(t)$ continues to decrease until it reaches zero. This occurs because in the stochastic simulations we require that if the telomere length of one of the chromosome is zero, then the cell stops replicating and the cell becomes senescent. By contrast, in the theoretical model, the only restriction is that if the cell's average telomere length is zero, then the cell stops replicating.

Inside a cell if the telomere length of a cell's one of the chromosomes reaches the critical length, the cell stops dividing, so we need to consider when a cell reaches senescence. In order to do this we need to look not only at the total telomere length of the cell, but also at the length of each chromosome. We use L_i^g where $i = 1, .., N$ to denote the telomere length of the ith chromosome of a cell at generation g and μ_g denote the average telomere length of the cell. While s_g denotes the standard deviation of telomere length of the cell. Thus

$$\mu_g = \frac{1}{N} \sum_{i=1}^{N} L_i^g, \tag{4.8.12}$$

$$s_g^2 = \sum_{i=1}^{N} \frac{1}{N} (L_i^g - \mu_g)^2, \tag{4.8.13}$$

To analyze the standard deviation of telomere lengths, we define

$$s_{g+1}^2 = \frac{1}{N} \sum_{i=1}^{N} (L_i^{g+1} - \mu_{g+1})^2, \tag{4.8.14}$$

where L_i^g denotes he telomere length at generation g of chromosome i. We assume $L_i^{g+1} = L_i^g$ with probability $P = 1/2$ and $L_i^{g+1} = L_i^g + L$ with probability $1 - P = 1/2$. Then (4.8.14) implies

$$
\begin{aligned}
s_{g+1}^2 &= \frac{1}{N} \sum_{i=1}^{N} \left[P(L_i^g - \mu_{g+1})^2 + (1-P)(L_i^g + L - \mu_{g+1})^2 \right] \\
&= \frac{1}{N} \sum_{i=1}^{N} \left[P \left(L_i^g - \mu_g + \frac{1}{2}L \right)^2 + (1-P) \left(L_i^g + \frac{3}{2}L - \mu_g \right)^2 \right] \\
&= \frac{1}{N} \sum_{i=1}^{N} (\mu_g - L_i^g)^2 + \frac{2PL}{N} \sum_{i=1}^{N} (\mu_g - L_i^g - L) + \frac{3L}{N} \sum_{i=1}^{N} \left(L_i^g - \mu_g + \frac{3}{4}L \right) \\
s_{g+1}^2 &= s_g^2 - 2PL^2 + \frac{9}{4}L^2 = s_g^2 + \frac{5}{4}L^2. \tag{4.8.15}
\end{aligned}
$$

Thus we obtain the recurrence relations $\mu_{g+1} = \mu_g - \frac{1}{2}L$ and $s_{g+1} = \sqrt{s_g^2 + \frac{5}{4}L^2}$. So the mean decreases linearly with rate $L/2$ and the variance of telomere lengths increases linearly with rate $5L^2/4$.

4.8.1 *First order statistic*

Now we know the mean μ and standard deviation s at each time. We assume that the distribution of telomere lengths of the chromosome is $N(\mu, \sigma)$. Senescence of the cell depends on the shortest telomere length of the cell: if the shortest telomere of the cell falls below the critical length, the cell stops replicating and becomes senescent. If we randomly pick a sample of 46 from $N(\mu, \sigma)$ which is called $\{x_1, .., x_{46}\}$ and find the minimum of the sample, it is distributed according to the first order statistic $x_{(1)} = \min\{x_1, .., x_{46}\}$. Given the basic probability density function

$$f(x) = \frac{1}{\sigma\sqrt{2\pi}} \exp\left[-\frac{(x-\mu)^2}{2\sigma^2}\right], \tag{4.8.16}$$

the distribution function F(x) is

$$F(x) = \frac{1}{2}\left[1 + \mathrm{erf}\left(\frac{x-\mu}{\sigma\sqrt{2}}\right)\right], \tag{4.8.17}$$

and hence that the probability function of the first order statistic is

$$f_1(x_1) = 46[1 - F(x_1)]^{45} f(x_1). \tag{4.8.18}$$

For the simplest case we have $\mu = 0$ and $\sigma = 1$. The maximum of $f_{(1)}(x_1)$, occurs when $f'_{(1)}(x_1) = 0$, which is where

$$f'_{(1)}(x_1) = -\frac{1035\left[\frac{1}{2} - \frac{1}{2}\mathrm{erf}\left(\frac{\sqrt{2}}{2}x_1\right)\right]^{44}(e^{-\frac{1}{2}x_1^2})^2}{\pi} - \frac{23\sqrt{2}\left[\frac{1}{2} - \frac{1}{2}\mathrm{erf}\left(\frac{\sqrt{2}}{2}x\right)\right]^{45} x_1 e^{-\frac{1}{2}x_1^2}}{\sqrt{\pi}},$$

$$\frac{1}{2}\left[1 - \mathrm{erf}\left(\frac{\sqrt{2}}{2}x_1\right)\right]x_1 = -\frac{45}{\sqrt{2\pi}}e^{-\frac{1}{2}x_1^2}. \tag{4.8.19}$$

Solving (4.8.19) numerically yields $x = -2.084$. This is similar to the expected value $\mathbf{E}(f_{(1)}(x_1)) = -2.216$, *i.e..* the mode and mean are close. We expect a cell reach senescence when its shortest telomere reaches zero length, *i.e..* when

$\mu - 2.216\sigma = 0$, or when $\mu = 2.216\sigma$.

We use the recurrence relations $\mu_{g+1} = \mu_g - \frac{1}{2}L$ and $s_{g+1} = \sqrt{s_g^2 + \frac{5}{4}L^2}$ with initial conditions $\mu_0 = 5950$, $s_0 = 0$ and $L = 100$, to estimate that when $g = 76$, $\mu \approx 2.2164\sigma$, *i.e.* senescence is starts when $g = 76$. The stochastic simulation results we obtained earlier, showed that senescence first appears when average $g = 78$, so we have good agreement between the stochastic simulation and theoretical estimates.

4.9   Case II: length dependent loss

As before, we denote by C_m^g the number of cells with total telomere length m at generation g. The amount of telomere lost $y = y(m)$ during replication depends on the cell's telomere length via $y(m) = y_0 + y_1 m$ where y_0, y_1 are constants and each chromosome obeys the replication rule $K_n^g \rightarrow K_n^{g+1} + K_{n-y(m)}^{g+1}$. The discrete cell replication reaction can be written as

$$C_m^g \rightarrow C_{m-j\left(y_0+\frac{my_1}{N}\right)}^{g+1} \quad + \quad C_{m-(N-j)\left(y_0+\frac{my_1}{N}\right)}^{g+1}$$

$$j = 0, 1, .., N \qquad \text{with probability } 2^{-N}\binom{N}{j}. \qquad (4.9.1)$$
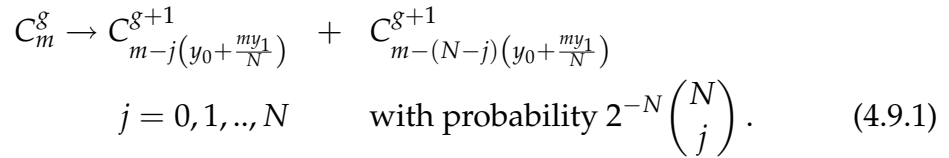
Hence, averaging over all the possible kinetic arrangements of telomere lengths

$$C_m^g \rightarrow \sum_{j=0}^{N} 2^{-N}\binom{N}{j}\left[C_{m-j\left(y_0+\frac{my_1}{N}\right)}^{g+1} + C_{m-(N-j)\left(y_0+\frac{my_1}{N}\right)}^{g+1}\right], \qquad (4.9.2)$$

which implies

$$C_m^{g+1} = 2^{-N}\sum_{j=0}^{N}\binom{N}{j}\left(\frac{C_{m+jy_0}^g}{1-\frac{y_1 j}{N}} + \frac{C_{m+(N-j)y_0}^g}{1-y_1+\frac{y_1 j}{N}}\right). \qquad (4.9.3)$$

In place of the "dispersion relation" $C_m^g \sim \exp(\gamma g + \chi m)$, we seek trial solutions of the form $C_m^g = e^{\gamma g}(\alpha + \beta m)^p$ where γ is the growth rate which depends on the constants (α, β and the parameter p); α and β will be determined later to simplify the algebra. When we put the assumed solution into (4.9.3), we obtain

$$e^{\gamma}(\alpha + \beta m)^p = 2^{-N}\sum_{j=0}^{N}\binom{N}{j}\left\{\left[\alpha + \frac{\beta(m+jy_0)}{1-\frac{y_1 j}{N}}\right]^p + \left[\alpha + \frac{\beta(m+(N-j)y_0)}{1-y_1+\frac{y_1 j}{N}}\right]^p\right\}$$

which implies

$$
\begin{aligned}
e^{\gamma} &= 2^{-N} \sum_{j=0}^{N} \binom{N}{j} \left\{ \left[\frac{\alpha N - \alpha y_1 j + \beta N(m + j y_0)}{(N - y_1 j)(\alpha + \beta m)} \right]^p \right. \\
&\quad + \left. \left[\frac{\alpha(N - N y_1 + j y_1) + \beta N(m + (N - j) y_0)}{(N - N y_1 + j y_1)(\alpha + \beta m)} \right]^p \right\} ,
\end{aligned}
$$

$$
\begin{aligned}
e^{\gamma} &= 2^{-N} \sum_{j=0}^{N} \binom{N}{j} \left\{ \left[\frac{N}{N - y_1 j} + \frac{j(\beta N y_0 - \alpha y_1)}{(N - y_1 j)(\alpha + \beta m)} \right]^p \right. \\
&\quad + \left. \left[\frac{N}{N - N y_1 + j y_1} + \frac{\alpha y_1(j - N) + \beta N y_0(N - j)}{(N - N y_1 + j y_1)(\alpha + \beta m)} \right]^p \right\} . \quad (4.9.4)
\end{aligned}
$$

In order to find the growth rate γ to be independent of the telomere length m,
since α and β are the free parameters, we need fix $\beta N y_0 = \alpha y_1$, which implies
$\alpha = N y_0 \beta / y_1$ and hence

$$
e^{\gamma} = 2^{-N} \sum_{j=0}^{N} \binom{N}{j} \left[\left(\frac{N}{N - y_1 j} \right)^p + \left(\frac{N}{N - N y_1 + j y_1} \right)^p \right] . \quad (4.9.5)
$$

In order to transform (4.9.3) into one that is similar to Case I, we transform
variables from m to x via $e^x = N y_0 + y_1 m$ so that

$$
x = \ln(N y_0 + y_1 m) . \quad (4.9.6)
$$

Letting $\tilde{C}_x^g = C_m^g$, (4.9.3) can be written as

$$
\tilde{C}_x^{g+1} = 2^{-N} \sum_{j=0}^{N} \binom{N}{j} \left[\tilde{C}_{x + \tilde{L}_1}^g + \tilde{C}_{x + \tilde{L}_2}^g \right] , \quad (4.9.7)
$$

where $\tilde{L}_1 = -\ln(1 - y_1 j / N)$ and $\tilde{L}_2 = -\ln(1 - y_1 + y_1 j / N)$. This is because
when $m \to (m + y_0 j)/(1 - y_1 j / N)$,

$$
\begin{aligned}
x &= \ln(N y_0 + y_1 m) \to \ln \left[N y_0 + y_1 \left(\frac{m + y_0 j}{1 - \frac{y_1 j}{N}} \right) \right] \\
&= \ln(N y_0 + y_1 m) - \ln \left(1 - \frac{y_1 j}{N} \right) = x - \ln \left(1 - \frac{y_1 j}{N} \right) , \quad (4.9.8)
\end{aligned}
$$

and when $m \to [m + (N - j) y_0]/(1 - y1 + y_1 j / N)$,

$$
\begin{aligned}
x &= \ln(N y_0 + y_1 m) \to \ln \left\{ N y_0 + y_1 \left[\frac{m + (N - j) y_0}{1 - y_1 + \frac{y_1 j}{N}} \right] \right\} \\
&= \ln(N y_0 + y_1 m) - \ln \left(1 - y_1 + \frac{y_1 j}{N} \right) = x - \ln \left(1 - y_1 + \frac{y_1 j}{N} \right) .
\end{aligned}
$$

$$(4.9.9)$$

We assume (4.9.7) has a separable solution of the form $\tilde{C}_x^g = e^{\gamma g + \chi x}$, the dispersion relation for (4.9.7) is

$$
\begin{aligned}
e^\gamma &= 2^{-N} \sum_{j=0}^N \binom{N}{j} \left[e^{-\chi \ln\left(1 - \frac{y_1 j}{N}\right)} + e^{-\chi \ln\left(1 - y_1 + \frac{y_1 j}{N}\right)} \right] \\
&\approx 2 + 2^{-N} \sum_{j=0}^N \binom{N}{j} \left\{ -\chi \left[\ln\left(1 - \frac{y_1 j}{N}\right) + \ln\left(1 - y_1 + \frac{y_1 j}{N}\right) \right] \right. \\
&\qquad \left. + \frac{1}{2}\chi^2 \left[\ln^2\left(1 - \frac{y_1 j}{N}\right) + \ln^2\left(1 - y_1 + \frac{y_1 j}{N}\right) \right] \right\}.
\end{aligned}
$$

Since y_1 is a small constant satisfying $\mid y_1 j/N \mid \le 1/N$ and $\mid -y_1 + y_1 j/N \mid < 1/N, \forall j = 0, 1, ..., N$ we use the following approximation

$$
\ln\left(1 - \frac{y_1 j}{N}\right) \approx -\frac{y_1 j}{N} - \frac{y_1^2 j^2}{2N^2}, \tag{4.9.10}
$$

$$
\ln\left(1 - y_1 + \frac{y_1 j}{N}\right) \approx -y_1 - \frac{y_1^2}{2} + \frac{y_1 j(1 + y_1)}{N} - \frac{y_1^2 j^2}{2N^2}, \tag{4.9.11}
$$

which implies

$$
\ln\left(1 - \frac{y_1 j}{N}\right) + \ln\left(1 - y_1 + \frac{y_1 j}{N}\right) \approx \frac{y_1^2 j(N - j)}{N^2} - y_1 - \frac{y_1^2}{2}, \tag{4.9.12}
$$

$$
\begin{aligned}
\ln^2\left(1 - \frac{y_1 j}{N}\right) + \ln^2\left(1 - y_1 + \frac{y_1 j}{N}\right) &\approx y_1^2 + y_1^3 + \frac{y_1^4}{4} - \frac{y_1^2 j(y_1^2 + 3y_1 + 2)}{N} \\
&\quad + \frac{y_1^2 j^2(4 + 6y_1 + 3y_1^2)}{2N^2} - \frac{y_1^4 j^3}{N^3} + \frac{y_1^4 j^4}{2N^4}.
\end{aligned} \tag{4.9.13}
$$

so

$$
\begin{aligned}
&2^{-N} \sum_{j=0}^N \binom{N}{j} \left\{ -\chi \left[\ln\left(N - \frac{y_1 j}{N^2}\right) + \ln\left(1 - y_1 + \frac{y_1 j}{N}\right) \right] \right\} \\
&\approx -\chi 2^{-N} \sum_{j=0}^N \binom{N}{j} \left[\frac{y_1^2 j(N - j)}{N^2} - y_1 - \frac{y_1^2}{2} \right] = \chi \left(y_1 + \frac{y_1^2}{4} + \frac{y_1^2}{4N} \right).
\end{aligned} \tag{4.9.14}
$$

Similarly

$$
\begin{aligned}
&2^{-N} \sum_{j=0}^N \binom{N}{j} \left\{ \frac{\chi^2}{2} \left[\ln^2\left(1 - \frac{y_1 j}{N}\right) + \ln^2\left(1 - y_1 + \frac{y_1 j}{N}\right) \right] \right\} \\
&\approx \chi^2 \left(\frac{y_1^2}{4} + \frac{y_1^3}{8} + \frac{y_1^4}{64} + \frac{y_1^2}{4N} + \frac{3y_1^3}{8N} + \frac{3y_1^4}{32N} + \frac{3y_1^4}{64N^2} - \frac{y_1^4}{32N^3} \right). \tag{4.9.15}
\end{aligned}
$$

We substitute (4.9.14), (4.9.15) into (4.9.10), hence the dispersion relation is

$$e^\gamma = 2 + B\chi + F\chi^2 \,, \tag{4.9.16}$$

where

$$B = y_1 + \frac{y_1^2}{4} + \frac{y_1^2}{4N} \,, \tag{4.9.17}$$

$$F = \frac{y_1^2}{4} + \frac{y_1^3}{8} + \frac{y_1^4}{64} + \frac{y_1^2}{4N} + \frac{3y_1^3}{8N} + \frac{3y_1^4}{32N} + \frac{3y_1^4}{64N^2} - \frac{y_1^4}{32N^3} \,, \tag{4.9.18}$$

which implies

$$\gamma = \ln(2) + \ln\left(1 + \frac{B\chi}{2} + \frac{F\chi^2}{2}\right) \approx \ln(2) + \frac{B\chi}{2} + \frac{(4F - B^2)\chi^2}{8} \,, \tag{4.9.19}$$

where we let

$$D = \frac{4F - B^2}{8} = \frac{y_1^2(8y_1 + 2y_1^2 + 8)}{64N} + \frac{y_1^4}{64N^2} - \frac{y_1^4}{64N^3} \,, \tag{4.9.20}$$

hence

$$\gamma = \ln(2) + \frac{B\chi}{2} + D\chi^2 \,. \tag{4.9.21}$$

For the continuous model we replace the generation number by a continuous time variable t and C_m^g and $\tilde{C}_x^g$ by $C(m, t)$ and $\tilde{C}(x, t)$ respectively. Equation (4.9.7) is replaced by a partial differential equation with the dispersion relation (4.9.21), which is

$$\frac{\partial \tilde{C}(x, t)}{\partial t} = \ln(2)\tilde{C}(x, t) + \frac{B}{2}\frac{\partial \tilde{C}(x, t)}{\partial x} + D\frac{\partial^2 \tilde{C}(x, t)}{\partial x^2} \,. \tag{4.9.22}$$

We assume (4.9.22) has a solution of the form

$$\tilde{C}(x, t) = \frac{A(t)}{\sigma(t)\sqrt{2\pi}} \exp\left[-\frac{(x - \mu(t))^2}{2\sigma^2(t)}\right] \,, \tag{4.9.23}$$

where the amplitude $A(t)$ is a function of t, $\sigma^2(t)$ is the variance and $\mu(t)$ is the mean, both evaluated using the logarithmic x-scale (4.9.6). Inserting (4.9.23) into (4.9.22) and equating terms with similar coefficients of $(x - \mu)$ we obtain

$$O(1): \qquad \frac{d}{dt}A(t) - \frac{A(t)}{\sigma(t)}\frac{d}{dt}\sigma(t) = \ln(2)A(t) - \frac{A(t)D}{\sigma(t)^2} \,, \tag{4.9.24}$$

$$O(x - \mu(t)): \qquad \frac{d}{dt}\mu(t) = -\frac{B}{2} \,, \tag{4.9.25}$$

$$O(x - \mu(t))^2: \qquad \frac{d}{dt}\sigma(t) = \frac{D}{\sigma(t)} \,, \tag{4.9.26}$$

We solve (4.9.25) with initial condition $\mu(0) = \ln(Ny_0 + y_1Q)$ where Q is the
initial cell's telomere length, to find

$$\mu(t) = -\frac{Bt}{2} + \ln(Ny_0 + y_1Q), \tag{4.9.27}$$

then (4.9.26) with initial condition $\sigma(0) = \sigma_0$ implies

$$\sigma(t) = \sqrt{\sigma_0^2 + 2Dt}, \tag{4.9.28}$$

and finally (4.9.24) implies

$$A(t) = 2^tG, \tag{4.9.29}$$

for some constant G. Thus

$$\tilde{C}(x,t) = \frac{\sqrt{2}2^tG}{2\sqrt{\pi(\sigma_0^2 + 2Dt)}} \exp\left\{-\frac{[x + \frac{Bt}{2} - \ln(Ny_0 + y_1Q)]^2}{2\sigma_0^2 + 4Dt}\right\}. \tag{4.9.30}$$

From (4.9.30) and (4.9.6), $C(m,t)$ can be written as:

$$C(m,t) = \frac{\sqrt{2}2^tG}{2\sqrt{\pi(\sigma_0^2 + 2Dt)}} \exp\left\{-\frac{[\ln(Ny_0 + y_1m) + \frac{Bt}{2} - \ln(Ny_0 + y_1Q)]^2}{2\sigma_0^2 + 4Dt}\right\}.$$
$$\tag{4.9.31}$$

we determine G by noting that at $t = 0$, there is one cell so that

$$\int_{-\infty}^{+\infty} C(m,0)dm = 1, \tag{4.9.32}$$

If we assume that the integrand is small everywhere except at $n = Q$. Then we
deduce from (4.9.32), get $G = y_1/(Ny_0 + y_1Q)$ and

$$C(m,t) = \frac{\sqrt{2}2^ty_1}{2(Ny_0 + y_1Q)\sqrt{\pi(\sigma_0^2 + 2Dt)}} \times$$
$$\exp\left\{-\frac{[\ln(Ny_0 + y_1m) + \frac{Bt}{2} - \ln(Ny_0 + y_1Q)]^2}{2\sigma_0^2 + 4Dt}\right\}. \tag{4.9.33}$$

This solution (4.9.33) looks like log-normal distribution where μ is the mode.

Now we go back to determine the PDE in the terms of $C(m,t)$, which has the
solution (4.9.33). Since $x = \ln(Ny_0 + y_1m)$

$$\frac{\partial}{\partial m} = \frac{\partial x}{\partial m}\frac{\partial}{\partial x} = \frac{y_1}{Ny_0 + y_1m}\frac{\partial}{\partial x}, \quad \frac{\partial}{\partial x} = \frac{(Ny_0 + y_1m)}{y_1}\frac{\partial}{\partial m}, \tag{4.9.34}$$

$$\frac{\partial^2}{\partial x^2} = \frac{(Ny_0 + y_1m)^2}{y_1^2}\frac{\partial^2}{\partial m^2} + \frac{(Ny_0 + y_1m)}{y_1}\frac{\partial}{\partial m}. \tag{4.9.35}$$

We put (4.9.34), (4.9.35) into the PDE (4.9.22), producing

$$\frac{\partial C(m,t)}{\partial t} = \ln(2)C(m,t) + \frac{(B+2D)(Ny_0+y_1m)}{2y_1}\frac{\partial C(m,t)}{\partial m}$$
$$+D\frac{(Ny_0+y_1m)^2}{y_1^2}\frac{\partial^2 C(m,t)}{\partial m^2}, \tag{4.9.36}$$

where B and D are defined in (4.9.17), (4.9.17) respectively. Thus this PDE
(4.9.36) has the solution (4.9.33).

In order to compare the result (4.9.33) with our stochastic simulation in Chapter
2, Section 2.3.3 Case II, we need obtain the mean and variances from $C(m,t)$. In
the above calculations we view m as a real number. However in reality, it is re-
stricted to the range $0 \ll m \ll Q$. We use $\mu_m(t)$ to denote the average telomere
length of the cell at time t which can be written as

$$\mu_m(t) = \frac{\int_0^Q mC(m,t)dm}{\int_0^Q C(m,t)dm}, \tag{4.9.37}$$

where Q is the cell's initial telomere length. Since $x = \ln(Ny_0 + y_1m)$, we
rewrite the integrals in terms of $\tilde{C}(x,t)$ as

$$\mu_m(t) = \frac{\int_{\ln(Ny_0)}^{\ln(Ny_0+y_1Q)} \left(\frac{e^x - Ny_0}{y_1}\right)\tilde{C}(x,t)\frac{e^x}{y_1}dx}{\int_{\ln(Ny_0)}^{\ln(Ny_0+y_1Q)} \tilde{C}(x,t)\frac{e^x}{y_1}dx}. \tag{4.9.38}$$

Using $\sigma_m(t)$ to denote the variance of the telomere length at time t, we find

$$\sigma_m^2(t) = \frac{\int_0^{M_{max}}[n - \mu_m(t)]^2 C(m,t)dm}{\int_0^{M_{max}} C(m,t)dm}$$
$$= \frac{\int_{\ln(Ny_0)}^{\ln(Ny_0+y_1Q)}\left[\frac{e^x - Ny_0}{y_1} - \mu_m(t)\right]^2\tilde{C}(x,t)\frac{e^x}{y_1}dx}{\int_{\ln(Ny_0)}^{\ln(Ny_0+y_1Q)} \tilde{C}(x,t)\frac{e^x}{y_1}dx}. \tag{4.9.39}$$

For comparison with stochastic simulations obtained earlier (Chapter 2, Sec-
tion 2.3.3, Case II), we choose $Q = 5950 \times 46$, $y_0 = 50$ and $y_1 = 1/60$, this
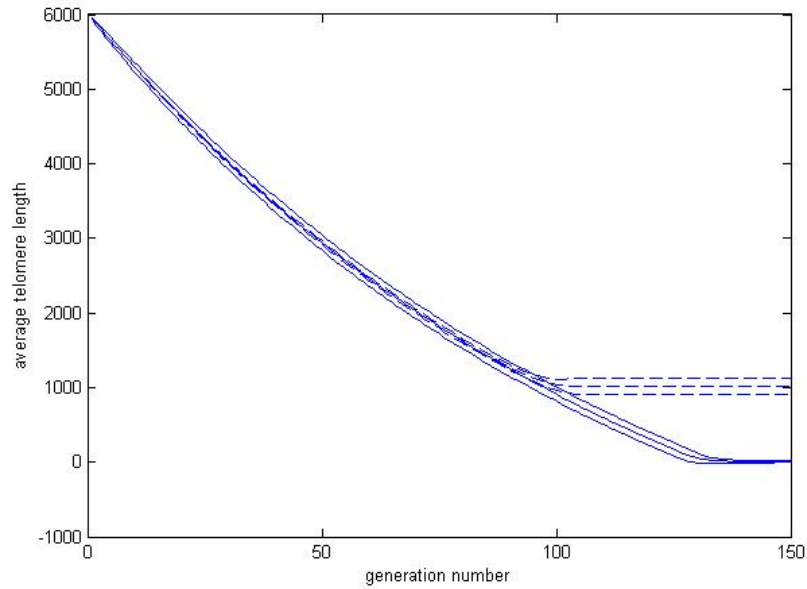
Figure 4.25: *The middle solid line is the average telomere length $\mu_m(t)/N$ and the solid lines above and below is the average telomere length $\mu_m(t)/N$ plus or minus two standard deviations. The middle dashed line is the average telomere length against generation number in stochastic simulation which we got early and the dashed lines above and below is the average telomere length of computer simulations plus or minus two standard deviations.*

ensures that the amount of telomere lost at each replication is the same as for the stochastic simulations. A comparison of results is shown in Figure 4.25. We use average telomere length of the chromosome in the cell $\mu_{chro}(t) = \mu_m(t)/N$. Before $t = 90$, the plots of the mean chromosome telomere length $\mu_{chro}(t)$ for the theoretical model and stochastic simulation are identical. Thereafter the curves separate, the mean telomere length of the stochastic simulation remains at about 1000 and the average telomere length of the chromosome in the cell $\mu_{chro}(t)$ continues to decrease until it reaches zero. The reason why this occurs is that in the stochastic simulation we require all of the cells telomere lengths to be above the threshold, (otherwise the cell stops replicating and becomes the senescent), whereas in the theoretical model, the cell only becomes senescent when its average telomere length is zero.

147

4.10 Case III: length dependent cell division

We return to the length-independent loss rate, but include a telomere length dependent probability of dividing. The probability of a chromosome replicating, is $P_{div} = am + b$ where a, b are constants chosen to ensure that $0 \leq p_{diving} \leq 1$. The discrete cell replication reaction can be written as

$$C_m^g \rightarrow (1 - am - b)C_m^{g+1} + (am + b) \sum_{j=0}^{N} 2^{-N} \binom{N}{j} \left[C_{m-jL}^{g+1} + C_{m-(N-j)L}^{g+1} \right],$$

which implies

$$C_m^{g+1} = (1 - am - b)C_m^g + (am + b)2^{-N} \sum_{j=0}^{N} \binom{N}{j} \left[C_{m+jL}^g + C_{m+(N-j)L}^g \right].$$

$$(4.10.1)$$

One method of generating an approximation solution of this is to assume that (4.10.1) has a solution of the form

$$C(m, g) = \frac{A(g)}{\sigma(g)\sqrt{2\pi}} \exp \left[-\frac{(m - \mu(g))^2}{2\sigma^2(g)} \right], \qquad (4.10.2)$$

where the amplitude $A(g)$, the standard deviation $\sigma(g)$ and the mean $\mu(g)$ of $C(m, g)$ at time g are all functions of g. Define the qth moment ($q = 0, 1, 2, 3$) of the $C(m, g)$ by

$$M_q(g) = \int_{-\infty}^{+\infty} m^q C(m, g) dm, \qquad (4.10.3)$$

then it is possible to show that

$$A(g) = M_0(g), \qquad (4.10.4)$$

$$\mu(g) = \frac{M_1(g)}{M_0(g)}, \qquad (4.10.5)$$

$$\mu^2(g) + \sigma^2(g) = \frac{M_2(g)}{M_0(g)}, \qquad (4.10.6)$$

$$\mu^3(g) + 3\mu(g)\sigma^2(g) = \frac{M_3(g)}{M_0(g)}. \qquad (4.10.7)$$

Integrating (4.10.1) over m, leads to

$$\int_{-\infty}^{+\infty} C_m^{g+1} dm = 2^{-N} \sum_{j=0}^{N} \binom{N}{j} \int_{-\infty}^{+\infty} (am + b) \left[C_{m+jL}^g + C_{m+(N-j)L}^g \right] dm$$

$$+ (1 - am - b) \int_{-\infty}^{+\infty} C_m^g dm. \qquad (4.10.8)$$

We let $\hat{m} = m + jL$, $\tilde{m} = m + (N - j)L$ and substitute from (4.10.8), to find

$$
\begin{aligned}
M_0(g+1) &= (1-b)M_0(g) - M_1(g) + 2^{-N} \sum_{j=0}^{N} \binom{N}{j} \times \\
&\quad \left\{ \int_{-\infty}^{+\infty} (a\hat{m} - ajL + b)C_{\hat{m}}^g d\hat{m} + \int_{-\infty}^{+\infty} [a\tilde{m} - a(N-j)L + b]C_{\tilde{m}}^g d\tilde{m} \right\} \\
&= aM_1(g) + (1 + b - aLN)M_0(g).
\end{aligned}
\tag{4.10.9}
$$

Using similar methods, we multiply (4.10.1) by m and m^2 and integrate to obtain
the identities

$$
\begin{aligned}
M_1(g+1) &= aM_2(g) + (1 + b - 2aLN)M_1(g) \\
&\quad + \left[\frac{aL^2 N(N+1)}{2} - bLN \right] M_0(g),
\end{aligned}
\tag{4.10.10}
$$

$$
\begin{aligned}
M_2(g+1) &= (1 + b - 3aLN)M_2(g) + \left[\frac{3}{2}aL^2 N(N+1) - 2bLN \right] M_1(g) \\
&\quad + \left[\frac{1}{2}bL^2 N(N+1) - \frac{1}{4}aL^3 N(N+3) \right] M_0(g) + aM_3(g).
\end{aligned}
\tag{4.10.11}
$$

We then solve for $A(g)$, $\mu(g)$, $\sigma(g)$, for each generation g, starting for $g = 0$
following the algorithm:

(1) Given $\mu(g)$, $\sigma(g)$, can calculate $M_q(g)$ where $q = 0, 1, 2, 3$ using (4.10.4)-
(4.10.7).

(2) Use $M_q(g)$ obtained from (1) to update $M_0(g+1)$, $M_1(g+1)$ and $M_2(g+1)$
by using (4.10.9)-(4.10.11).

(3) Use $M_0(g+1)$, $M_1(g+1)$ and $M_2(g+1)$ obtained from (2) to update
$\mu(g+1)$ and $\sigma(g+1)$ by (4.10.5)and (4.10.6).

(4) Use (4.10.7) to update $M_3(g+1)$, then return back to (1). At each genera-
tion we can use Use (4.10.9)-(4.10.11) to find $M_0(g)$, $M_1(g)$, $M_2(g)$ and also use
(4.10.5) and (4.10.6) to obtain $\mu(g)$, $\sigma(g)$.

Figure 4.26(a) shows that before generation 50, the approximation solution is
consistent with the stochastic results obtained earlier (see Section 2.3.3 Case III-
IVof Chapter 2). However later on, the theoretical mean decreases faster than
the stochastic simulation. In the stochastic simulations, there is a restriction on
telomere length, when the shortest telomere in the cell reaches a critical value,

(a)   (b)
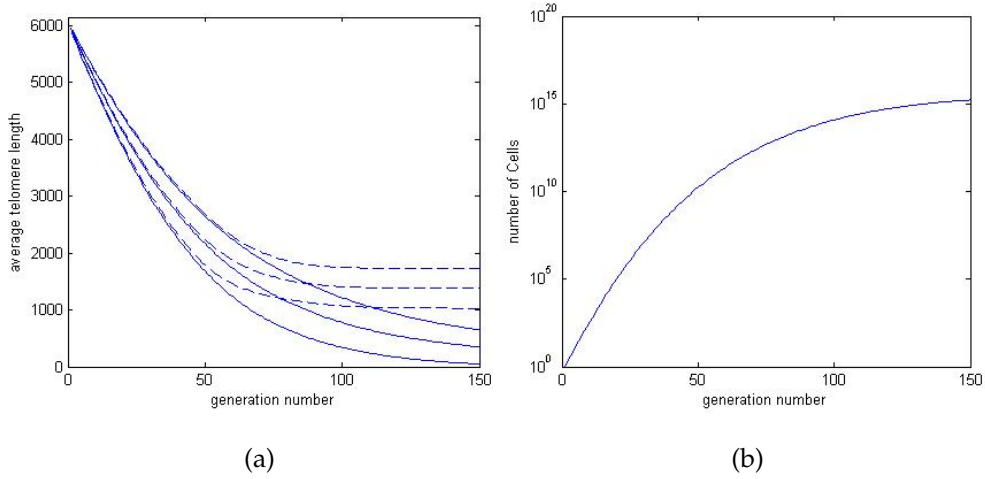
Figure 4.26: *In Figure 4.26(a), the middle solid line is the average telomere length*
$\mu(g)/N$ *from theory and the solid lines above and below show* $\mu(g)/N$ *plus or minus*
two standard deviations. The middle dashed line is the average telomere length against
generation number from stochastic simulations shown earlier (see Section 2.3.3, Case
III-IVof Chapter 2) and the dashed lines above and below are the average telomere
lengths plus or minus two standard deviations. In Figure 4.26(b), show the $A(g)$
plotted against generation number.

it indicates that the cell has become senescent. But in our discrete model reach
senescence when the total telomere length in each cell falls to the critical value
times 46, this results in the difference in Figures 4.26(a) in later generations. Fig-
ure 4.26(b) shows t how the numbers of cells increases with generation number,
we notice that the growth rate no longer increases exponentially.

4.11   Case IV: length-dependent loss and length de-pendent dividing

Case IV combines the previous cases II (length-dependent loss) and III (length-
dependent division probability). The discrete reaction equation can be written

$$
\begin{aligned}
C_m^g \quad \rightarrow \quad & (1 - am - b)C_m^{g+1} \\
& + (am + b)\sum_{j=0}^{N} 2^{-N}\binom{N}{j}\left(C_{m-j(y_0+\frac{my_1}{N})}^{g+1} + C_{m-(N-j)(y_0+\frac{my_1}{N})}^{g+1}\right),
\end{aligned}
$$

$$(4.11.1)$$

which implies

$$C_m^{g+1} = (1 - am - b)C_m^g + (am + b)2^{-N} \sum_{j=0}^{N} \binom{N}{j} \left[C_{\frac{m+jy_0}{1-y_1j/N}}^g + C_{\frac{m+(N-j)y_0}{1-y_1+y_1j/N}}^g \right].$$

(4.11.2)

One method of generating an approximate solution of this is to assume that (4.10.1) has a solution of the form

$$C(m, g) = \frac{A(g)}{\sigma(g)\sqrt{2\pi}} \exp\left(-\frac{(m - \mu(g))^2}{2\sigma^2(g)} \right),$$

(4.11.3)

using the same method as Section 4.10, the recurrence relations can be found as

$$M_0(g+1) = (1 - y_1)aM_1(g) + (1 + b - ay_0N)M_0(g),$$

(4.11.4)

$$
\begin{aligned}
M_1(g+1) = {}& \left[\frac{a(y_1^2N + 2N - 4y_1N + y_1^2)}{2N} \right] M_2(g) \\
& + (1 - by_1 - 2aNy_0 + aNy_0y_1 + b + ay_0y_1)M_1(g) \\
& + \frac{1}{2}Ny_0(ay_0 - 2b + aNy_0)M_0(g),
\end{aligned}
$$

(4.11.5)

$$
\begin{aligned}
M_2(g+1) = {}& \left[1 - 3y_1 + \frac{3y_1^2(1+N)}{2N} - \frac{y_1^3(3+N)}{4N} \right] aM_3(g) \\
& + \left\{ 1 + b(1 - 2y_1) + ay_0y_1 \left[3 - \frac{(9+3N)y_1}{4} + 3N \right] \right. \\
& \left. + \frac{(1+N)by_1^2}{2N} - 3aNy_0 \right\} M_2(g) + \left\{ \frac{3Ny_0^2a(N+1)}{2} - 2Ny_0b \right. \\
& \left. + y_0y_1 \left[(N+1)b - \frac{3aNy_0(3+N)}{4} \right] \right\} M_1(g) \\
& + \left[\frac{Ny_0^2b(N+1)}{2} - \frac{N^2y_0^3a(N+3)}{4} \right] M_0(g).
\end{aligned}
$$

(4.11.6)

Given initial conditions for $\mu(0), \sigma(0), A(0)$, we find initial conditions for $M_0(0), M_1(0), M_2(0), M_3(0)$. Using the same algorithm as in section 4.10 we successively work out $A(g), \mu(g), \sigma(g)$ for each g.

Figure 4.27(a) shows that before generation 50, the approximate solution is consistent with the stochastic results obtained earlier (see section 2.3.3 Case IV-IV of Chapter 2). However, later on, the theoretical mean decreases faster than the stochastic simulation. In the simulations, there is a restriction on telomere

(a) (b)
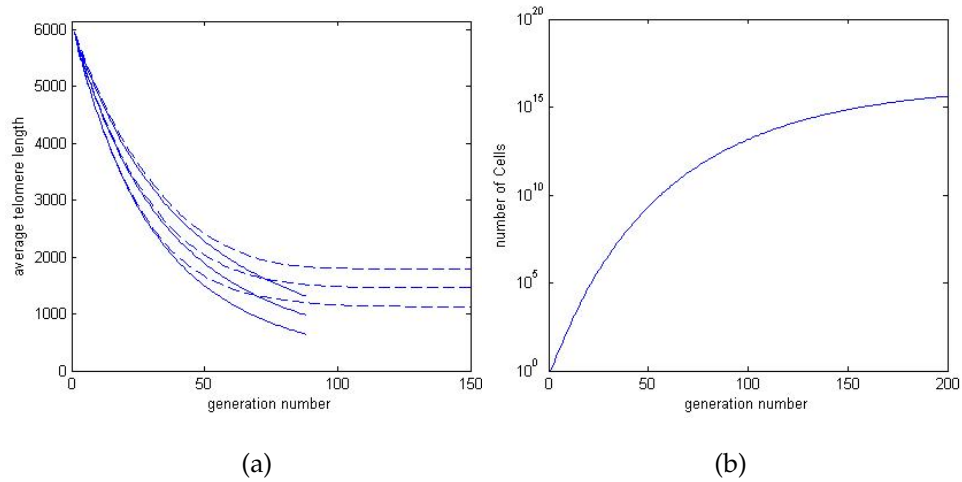
Figure 4.27: *In Figure 4.27(a), the middle solid line is the average telomere length*
$\mu(g)/N$ *from theory and the solid lines above and below are show* $\mu(g)/N$ *plus*
or minus two standard deviations. The middle dashed line is the average telomere
length against generation number from stochastic simulations shown earlier (see sec-
tion 2.3.3, Case IV-IVof Chapter 2) and the dashed lines above and below are the aver-
age telomere lengths plus or minus two standard deviations. In Figure 4.27(b), show
the $A(g)$ plotted against generation number.

length, when the shortest telomere in the cell reaches a critical value indicat-
ing that the cells become senescent. But in our discrete model senescent occurs
when the total telomere length in each cell reaches a critical value times 46, this
results the difference in the later generation. Figure 4.27(b) shows that how the
numbers of cells $A(g)$ increases with generation numbers, we notice that the
growth rate is no longer exponential, due to the dividing rate being dependent
on telomere length.

4.12 Conclusion

In this Chapter, we have developed continuum chromosome-level models and
cell-level models of telomere loss during replication. In order to compare the
continuum solution with Monte Carlo simulations of normal ageing (as pre-
sented in Chapter 2), we now compare the four different choices for chromo-
somes replication and telomere shortening.

Case I represents the constant telomere loss model in which a fixed amount
of telomere is lost during chromosome replication. When studying telomere
shortening in a single chromosomes, firstly, we constructed a discrete model
for the chromosome replication and then the continuum model was assumed
to be the simplest PDE whose dispersion relation matched that of the analogous
discrete model. Analysis of the resulting continuum model reveals that the dis-
tribution of the telomere length is a Gaussian distribution with mean which
decreases linearly in time following $Q - \frac{1}{2}Lt$ and a variance which increases
linearly in time $L^2 t/4$. Comparing this mean with the Monte Carlo simulations
for Case I (in Chapter 2 Section 2.2.4), shows good agreement before the chro-
momere becomes senescent.

Case II corresponds to a situation in which the telomere loss during chromo-
some replication is dependent on the length of the telomere. Constructing the
continuum model by using the same methods as Case I, yields a distribution of
telomere lengths which is log-normal and whose mean is consistence with the
corresponding Monte Carlo simulations (see Section 2.2.5 of Chapter 2).

In Case III the probability of cell division is treated as a random process which
depends on telomere length and telomere loss occurs a constant rate. We obtain
a PDE description by matching with the discrete model, but the PDE does not
admit explicit analytical solutions, therefore we considered the asymptotic limit
for which $l \ll 1$ and the governing PDE simplifies. Here $l =$ amount of telom-
ere lost per generation divided by initial telomere length. We started with the
first order PDE, which yields the mean, and does not give a good approxima-
tion to the mean of the Monte Carlo simulations (see Section 2.2.6 of Chapter 2)
at long time. Thus we analyze the second order PDE with asymptotically over
various time scales.

In Case IV, we combined telomere length-dependent loss and probabilistic cell
division model where the probability is dependent on telomere length. This
continuum model is even more complex than for Cases III, so we only con-

struct solutions for mean for the first order PDE (the O(l) solution). However the mean of first order PDE is consistent with the Monte Carlo simulations for Case IV (present in Section 2.2.7 of Chapter 2). We also considered as a special case, the function of telomere loss is proportional to the function of probability division ($Y(n)/P_{div}$ = constant). For this situation we obtained a mean consistent with Monte Carlo simulations with the same parameters values.

For the cell level model, the construction of continuum model of Cases I and II are similar to that used for model single chromosomes. The mean of the distribution in Continuum model for Case I and Case II give good agreement with Monte Carlo simulations (present in Chapter 2 Sections 2.3.2 and 2.3.3). But Case III and Case IV, we developed a discrete model to compare the mean with Monte Carlo simulations which shown a good consistent before the cell reach senescent.

CHAPTER 5

Telomerase

5.1 Introduction

Telomerase is an enzyme. It has two major components: the telomerase reverse transcriptase TERT and the template RNA component (hTR or hTERC) [8]. These can be encoded to provide a template to add telomeric repeats (human TTAGGG) onto the 3' ends of chromosomes and to elongate the telomere.

In the previous chapter, when we modelled chromosome replication, we did not consider telomerase activity, because the amount of telomerase in normal human cells is usually limited. However, for immortal cell lines such as germline cells, most tumor cells, and early fetal cells, telomerase activity is high. Therefore in this chapter, we focus on telomerase activity, in order to investigate how it maintains telomere length and controls cell proliferation.

In this chapter, we use the same chromosome replication rule as in Chapter 2, and denote by y the average number of basepairs in a pair of telomeres at each end of the chromosome; L represents the average number of basepairs lost per replication. The parent chromosomes has one strand of DNA longer than the other. The normal chromosome replication process can be summarised by

$$\underset{parent}{y} \quad \overset{\longrightarrow}{\underset{replication}{}} \quad \underset{daughter}{(y-L)} \quad + \quad \underset{daughter}{y}, \tag{5.1.1}$$

155

where one daughter chromosome of average length (y) is identical to its parent and the other is shorter, of average length $(y - L)$. In each daughter chromosomes, a shorter strand of DNA is manufactured from the longer parent strand, which results in an inherited deletion of L basepairs at the 5' end, due to the end replication problem.

We denote by T the average number of basepairs gained due to telomerase activity. Since the mechanisms by which telomerase acts have yet to be identified, we assume that telomerase lengthens the telomere at the same time as telomere replication takes place. While some experiments show that telomerase acts on the shortest telomeres [47], [48], [49], other experiments, involving human cancer cells, suggest that telomerase acts randomly on the two daughter chromosomes, regardless of their length [50]. Based on those observations, we consider two alternative mechanisms of action. First, it can be added to the parent chromosomes. Second it can be added to either of the daughter chromosomes.

If telomerase is added before replication, then the process can be represented as

$$
\underset{parent}{y} \quad \underset{telomerase}{\longrightarrow} \quad \underset{}{(y+T)} \quad \underset{replication}{\longrightarrow} \quad \underset{daughter}{(y+T-L)} \quad + \quad \underset{daughter}{(y+T)} . \text{(5.1.2)}
$$

This situation may describe what happens in cancer cells, where both leading and lagging daughter chromosomes are elongated.

If the chromosome replicates before telomerase acts, then the replication rule is more complicated and depends on which daughter chromosomes telomerase acts upon. We assume that telomerase acts on the longer daughter chromosome with probability q and on the shorter daughter chromosome with probability p where $0 \leq p, q \leq 1$ and p, q are independent. This results in four possible

replication rules:

$$y \longrightarrow (y - L) + (y) \quad \longrightarrow (y + T - L) + (y + T) \text{ with probability } pq \text{ ,}$$

(5.1.3)

$$y \longrightarrow (y - L) + (y) \quad \longrightarrow (y - L) + (y + T) \text{ with probability } q(1 - p) \text{ ,}$$

(5.1.4)

$$y \longrightarrow (y - L) + (y) \quad \longrightarrow (y + T - L) + (y) \text{ with probability } p(1 - q) \text{ ,}$$

(5.1.5)

$$y \longrightarrow \underbrace{(y - L) + (y)}_{replication} \quad \underset{telomerase}{\longrightarrow} (y - L) + (y) \text{ with probability } (1 - q)(1 - p) \text{ .}$$

(5.1.6)

We remark that the replication rule for the case for which telomerase acts on neither daughter chromosomes is identical to the rule used for normal ageing in Chapter 2. We note also that the replication process (5.1.2) is a special case of (5.1.3), obtained when $p = q = 1$. Therefore, we henceforth restrict attention to case (5.1.3)-(5.1.6). We remark that if we $p > q$, then telomerase acts preferentially on the shorter chromosomes.

In this chapter we perform stochastic simulations of the chromosome model with telomerase active, and extend our earlier mathematical analysis for the chromosome model to account for telomerase activity. For the stochastic and deterministic models, we focus on two cases: in Case I the amounts of telomere loss and gain are assumed to be constant, whereas in Case II these amounts depend on the telomere length itself, so that shorter telomeres can lose fewer telomeres due to ageing and gain more telomere due to telomerase activity [49], whilst longer telomeres lose more and gain less telomere per replication. We still use MATLAB to run the stochastic simulations, the pseudocode for simulation are similar as in Chapter 2 Section 2.2.3, the differences are when the cell replicate it follows replication rule 5.1.3 to 5.1.6.

5.2 Stochastic simulation of the chromosome model

5.2.1 *Constant loss and constant telomerase activity*

We start by considering a single chromosome of Q basepairs. We assume that the amounts of telomere lost and gained during replication are constant, being equal to L and T basepairs respectively. We assume telomerase acts on offspring with longer chromosomes with probability q and on offspring with shorter chromosomes with probability p where $0 \leq (p,q) \leq 1$ and p, q are independent.

In our simulations, before each chromosome replicates, we check the average telomere length of the chromosome. If the telomere length exceeds the critical telomere length, then the chromosome replicates according to the rules (5.1.3)-(5.1.6); we choose two random numbers q_r and p_r from a uniform distribution on $[0,1]$. If $q_r \leq q$ and $p_r \leq p$, then replication follows rule (5.1.3) where the telomerase active on both longer and shorter offspring chromosomes. If $q_r \leq q$ and $p_r > p$, then replication follows rule (5.1.4) where the telomerase is only active on the longer offspring chromosome. If $q_r > q$ and $p_r \leq p$, then replication follows rule (5.1.5) where the telomerase is only active on the shorter offspring. Otherwise, the chromosome replication follows (5.1.6) where there is no telomerase activity and only normal ageing occurs.

Since L and T are assumed to be much smaller than the initial telomere length Q, initially, the population undergoes exponential growth. Due to restrictions on computer memory, we cannot track the entire progeny as the number of chromosomes rapidly becomes large. Therefore we passage using a passaging model which is similar to the one introduced in Chapter 2.

Our simulations start with a single chromosome and we track its progeny over each generation until the total number of chromosomes exceeds 200. We passage by randomly selecting 200 of these chromosomes. In the next generation, all chromosomes divide (if their telomeres are sufficiently long to allow replica-

tion), and when the population next exceeds 200, we passage again by selecting 200 chromosomes from the population. This process is repeated until all telomere lengths are too short to allow further replication. During the simulation we record not only the average telomere length over each generation but also the fraction of chromosomes which are senescent. We use telomere length to indicate whether a chromosome can proliferate; if the telomere length is less than the critical telomere length, the chromosome is senescent and otherwise it can replicate.
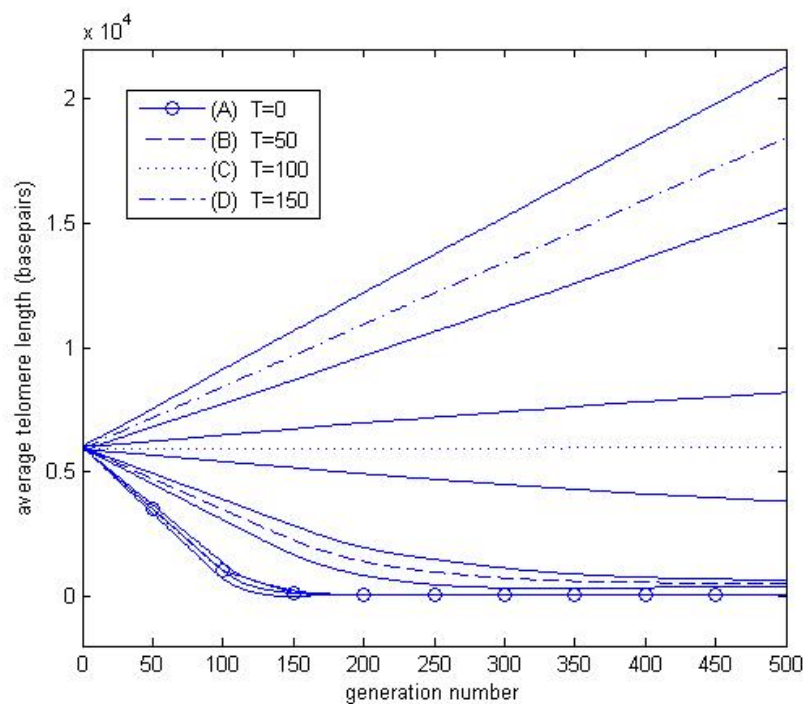
Figure 5.1: *Averaged results from 5000 simulations shows how the average telomere length of the chromosomes changes with generation number for four choices of T. Parameter values: $q = 0.6$, $p = 0.4$, $L = 100$, $Q = 5950$ and $T = 0, 50, 100, 150$ basepairs. The solid lines indicate two standard deviations above and below the mean of each passaging model.*

If there is no telomerase activity ($T = 0$, in Figure 5.1), then the average telomere length always decays (as described in Chapter 2 where we considered normal ageing). When telomerase is active, ($T > 0$), then there are three possible outcomes: the average telomere length decays, stays the same or increases with

generation number (see Figure 5.1). Each case/simulation starts with the same initial telomere length ($Q = 5950$ basepairs) and suffers the same amount of telomere loss, ($L = 100$ basepairs per division), the amount of telomere gain, T, differs. With $T = 50$ basepairs, the average telomere length decays linearly until generation 150 and then decays more slowly, approaching a constant value of 500 basepairs. Before generation 150, the net amount of telomere loss per generation is constant $L - (p + q)T = 50$ basepairs. After generation 150, some chromosomes become senescent. When some cells are senescent, the average telomere length decays more slowly. When the whole population becomes senescent, the average telomere length remains at a constant value.

With $T = 100$ basepairs, the average telomere length remains unchanged, since the net amount of telomere loss per generation is $L - (p + q)T = 0$ basepairs, the average telomere gain T being exactly compensated for by the telomere loss L. In this case, the average telomere length remains basically constant, due to the increasing variance in telomere lengths a few senescent chromosomes are formed, at large times, but for the short and intermediate timescales we have simulated this effect is negligible. With $T = 150$ basepairs, the average telomere length increases linearly with generation number. Since the amount of telomere gain, $(p + q)T$, per division exceeds the telomere loss of L per division, the net telomere gain per generation is constant at $(p + q)T - L = 50$ basepairs.

If there is no telomerase activity ($T = 0$, as in Figure 5.2 (A)), then the fraction of dividing chromosomes starts from one and only starts to decrease to zero after after 100 generations (as in Chapter 2, for normal ageing). When telomerase is activate ($T > 0$), the behaviour depends on the size of T. In more detail, if $(p + q)T > L$, then the average increase in telomere length per division, $(p + q)T$, is more than the average telomere loss, L, and so the average telomere length increases with generation number. Under such conditions all chromosomes remain proliferative, and the fraction of dividing chromosomes remains at 1 as shown in 5.2 (D). If $(p + q)T = L$, then the average amount of telomere gain is the same as the average telomere loss and the average telomere length remains unchanged; the fraction of dividing chromosomes
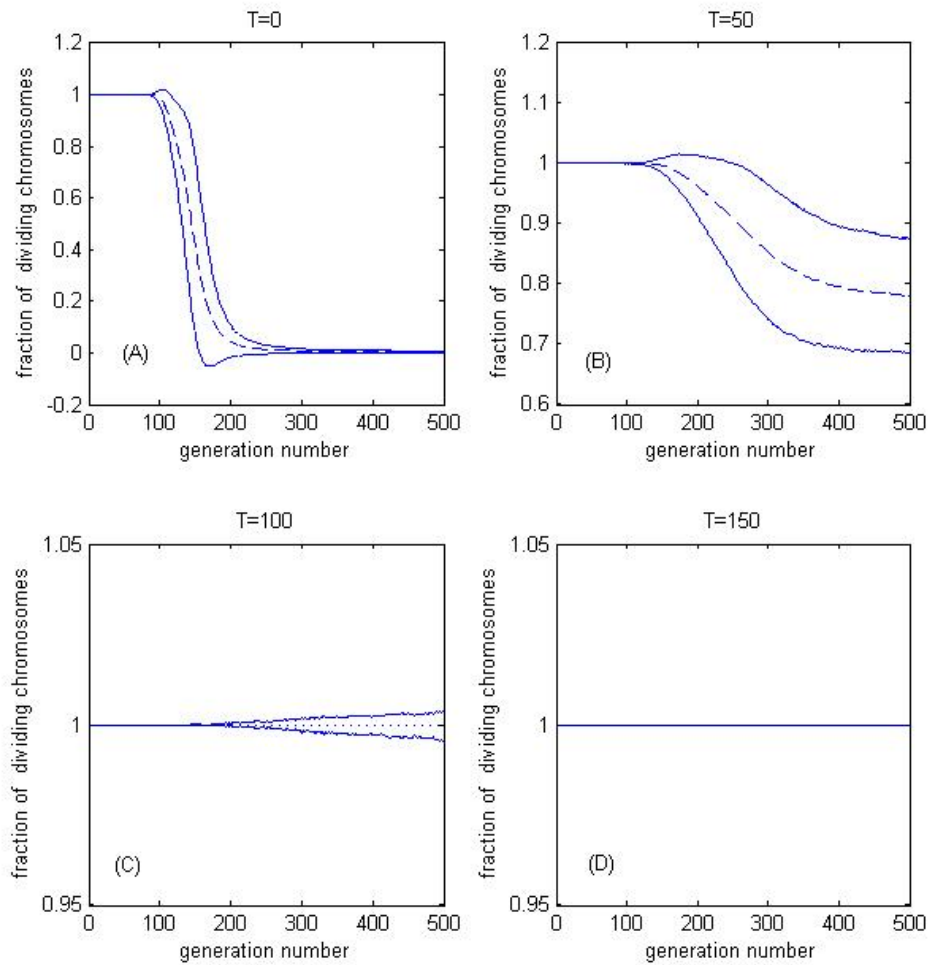
Figure 5.2: *Averaged results of 5000 simulations shows how the fraction of dividing chromosomes varies with generation number and the level of telomerase activity for $T = 50, 100$ basepairs, indicate with dashed line and dotted line respectively. The solid lines indicated two standard deviations above and below the fraction of dividing chromosomes. Parameter values: $q = 0.6$, $p = 0.4$, $L = 100$ basepairs, $Q = 5950$ basepairs and $L_c=200$ basepairs.*

remains unity, with only a small but increasing standard deviation as the generation number increases, as indicated in Figure 5.2 (C). If $(p + q)T < L$, then the average telomere gain is less than the telomere lost so the average telomere length decreases (see the dashed lines in Figure 5.2 (B)). Until generation 150, all the chromosomes replicate. After generation 150, some chromosomes reach the critical value and become senescent hence the fraction of dividing

chromosomes decreases from unity. We note that, even as the average telomere length approaches 500 basepairs, the fraction of dividing chromosomes decreases slowly.

5.2.2 *Case II: telomere loss and gain depends on telomere length*

As before, we start with a single chromosome of telomere length Q basepairs. Telomere loss due to normal ageing, $L = L(n)$ is now assumed to depend linearly on telomere length n so that

$$L(n) = L_0 + L_1 n, \tag{5.2.1}$$

where L_0, L_1 are positive constants and $L_1 \ll 1$. When telomerase is active, we assume that the offspring with the longer chromosome is extended with probability q and the offspring with the shorter chromosome is extended with probability p. The increase in telomere length due to the action of telomerase, $T = T(n)$, also depends on the telomere length itself, with shorter telomeres having more potential to gain than longer ones. Accordingly we set

$$T(n) = T_0 - T_1 n, \tag{5.2.2}$$

where T_0, T_1 are positive constants and $T_1 \ll 1$. The replication rule for each chromosome follows equations (5.1.3)-(5.1.6), where now $L = L(n)$ and $T = T(n)$. We remark that. Case I is a special case of Case II in which $L_1 = T_1 = 0$.

The stochastic simulations are similar to those presented for the passaging model in Section 5.2.1 (Case I). We start by considering a single chromosome, with telomere length 5950 basepairs, which we passage its progeny to senescence. The difference between this simulation and that of Section 5.2.1 is that the amounts of telomere lost and gained are non-constant.

However, in this case, there are four possible long-time outcomes for the average telomere length and these depend on the values of L_0, L_1, T_0, T_1, p and q. With $L(n) = L_0 + L_1 n$ and $T(n) = T_0 - T_1 n$ it is possible to show that $L(n)$ is the decay function with telomere length and $T(n)$ is an increase function of telomere length. If $L_0 > T_0(p + q)$, then the curves $L = L(n)$ and $T = T(n)$ never
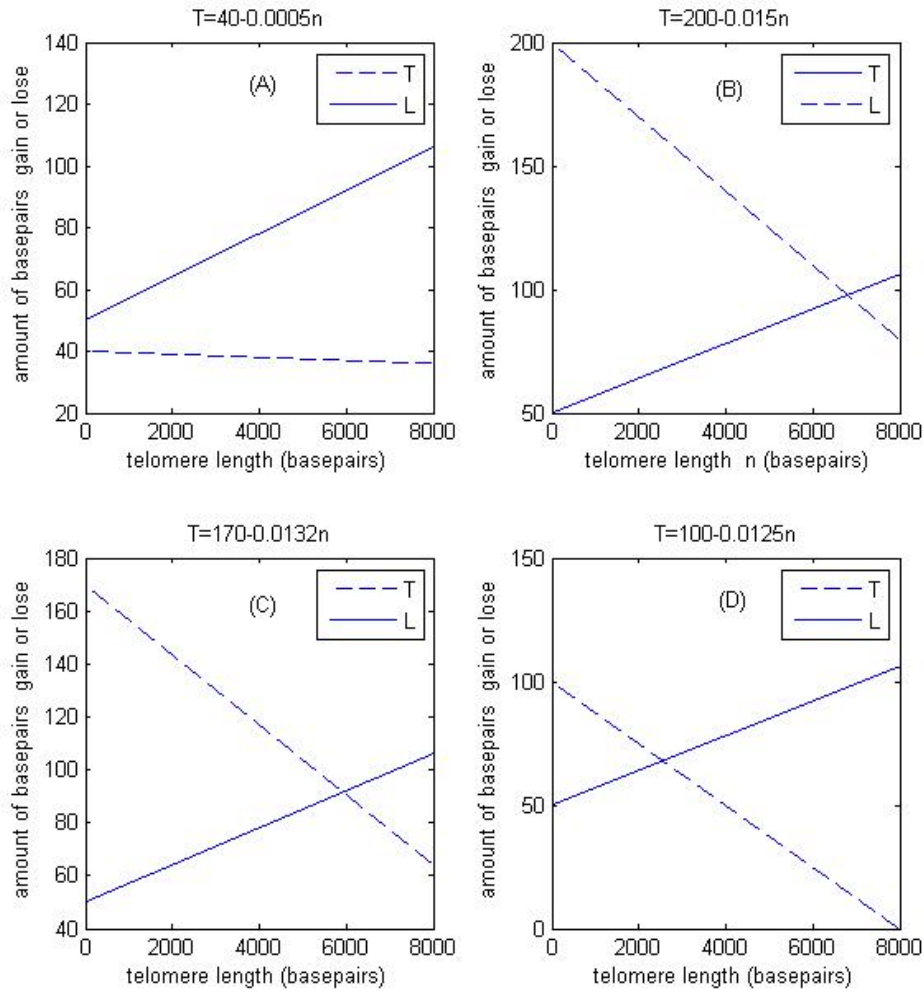
Figure 5.3: *The solid lines indicate the telomere loss $L(n) = 50 + 0.007n$ basepairs and the dashed lines indicate the average amount of telomere gain $(p + q)T(n) = (p + q)(T_0 - T_1 n)$ basepairs, with parameters $q = 0.6$, $p = 0.4$. Here we pick four sets of values of T_0, T_1, which are (A) $T_0 = 40$, $T_1 = 0.0005$; (B) $T_0 = 200$, $T_1 = 0.015$; (C) $T_0 = 170$, $T_1 = 0.0132$; (D) $T_0 = 100$, $T_1 = 0.0125$.*

intersect. If the average telomere loss per replication always exceeds the average telomere gain, the average telomere length decays (see Figure 5.3(A)) until the average telomere length reaches the critical telomere length $n_{critical} = 0$. If $L_0 < T_0(p + q)$, then the lines $L(n) = L_0 + L_1 n$ and $T(n) = T_0 - T_1 n$ intersect, where

$$n_{inter} = \frac{(p + q)T_0 - L_0}{(p + q)T_1 + L_1}.$$ (5.2.3)

Depending on the relative values of the point of intersection n_{inter} and the initial telomere length Q, four different types of behaviors can arise (illustrated in Figure 5.3). In Figure 5.3, in order to understand how telomerase activity effects average telomere length, we fix

$$L(n) = 50 + 0.007n\,, \tag{5.2.4}$$

and consider four choices of the parameters T_0 and T_1, which generate all possible behaviors.

Figure 5.3(A) shows that when $n_{inter} < 0$, the average telomere gain is always less than that lost so that the average telomere length decreases from Q, until the average telomere length reaches $n_{critical}$ (the critical telomere length) and the chromosomes stop replicating. Figure 5.3(B), shows that when $n_{inter} > Q$ the average telomere length increases from Q, since the amount of telomere gain exceeds the amount lost. When the average telomere length reaches n_{inter}, the average telomere length remains at that value, since the amount of telomere gained and lost balance. In Figure 5.3(C) $n_{inter} = Q$ the average telomere length remains at Q because the average telomere gain and loss are the same. Lastly, in Figure 5.3(D), $n_{inter} < Q$ so the average telomere length decreases from Q to $n_{inter} > 0$ since the average telomere gain is less than that lost. When the average telomere length reaches n_{inter} (assuming $n_{inter} > n_{critical}$), the average telomere length remains at that value. If $n_{inter} < n_{critical}$, than the average telomere length decreases from Q to $n_{critical}$ at which stage, the chromosomes stop replicating.

The simulation results are presented in Figure 5.4. The dashed line shows the average telomere length varying with generation number when $T(n) = 40 - 0.005n$ basepairs. As the generation number increases, the average telomere length decreases until it reaches the critical length. This behaviour can be explained by referring to Figure 5.3(A) where we plot $T(n)$ and $L(n)$. As $T(n) > L(n)$, there is no intersection between the two curves and telomere loss always exceeds the gain. The circled solid line in Figure 5.4 correspond to the case for which $T(n) = 100 - 0.0125n$ basepairs. As the generation num-
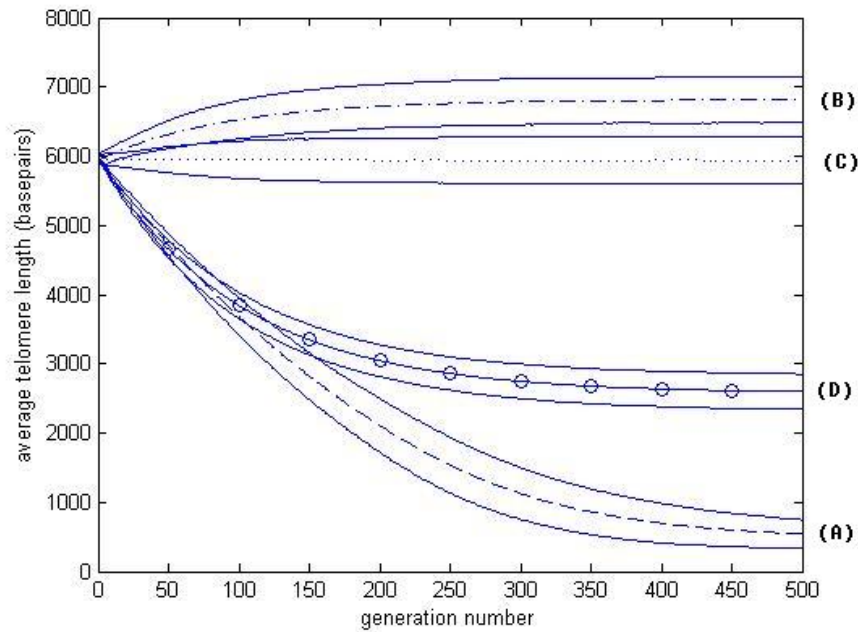
Figure 5.4: *Averaged results from 5000 simulations showing how the average telomere length of the chromosomes changes with generation number for four choices of T, the gain in telomere length where telomerase is achieve. Parameter values: $q = 0.6$, $p = 0.4$, $L = 100$, $Q = 5950$ and (A) $T(n) = 40 - 0.0005n$, (B) $T(n) = 200 - 0.015n$, (C) $T(n) = 170 - 0.0132n$ and (D) $T(n) = 100 - 0.0125n$ basepairs, indicate with dash-dot line, dotted line, solid circle line and dashed line, respectively. The solid lines indicate two standard deviations above and below the mean of each passaging model.*

ber increases, the average telomere length decreases until it reaches about 2600 basepairs and remains at that length there after. In this case, our calculating suggests $n_{inter} = 2564$ basepairs. This behaviour can be explained by referring to Figure 5.3(D), since $0 < n_{inter} < Q$, at earlier generations, those chromosomes for which $n > n_{inter}$, lose more basepairs than they gain, so the average telomere length decreases until it reaches n_{inter} and thereafter it remains unchanged, due the the balance between the loss and gain. The dotted lines in Figure 5.4 corresponds to the case for which $T(n) = 170 - 0.0132n$ basepairs. In this case, the average telomere length remains fixed at its initial value, $n_{inter} = Q = 5950$ basepairs. Telomere loss balances telomere gain as shown in Figure 5.3(C) and there is no change in the average telomere length.

The dashed lines in Figure 5.4 shows average telomere length against generation number when $T(n) = 200 - 0.015n$ basepairs as illustrated in Figure 5.3(B). As the generation number increases, the average telomere length increases until it reaches 6800 basepairs and then remains at that length. In this case, (5.2.3) suggests $n_{inter} = 6818$ basepairs. At earlier generations, telomere gain exceeds loss, so the average telomere length increases, until it reaches n_{inter}. In all the four cases above, we note that there is an equilibrium stage when telomere length reach n_{inter} or zero.

Now we consider the proportions of proliferating and senescent cells illustrated in Figure 5.5. If there is no telomerase activity or insufficient telomerase to maintain telomere length, then the fraction of dividing chromosomes remains at unity for many generations and then decrease until it reaches zero (as shown in Chapter 1, Case II normal ageing, Figure 2.6). When telomerase is active, the dynamics of the fraction of dividing chromosomes is different and depends on the functional forms $T(n)$ and $L(n)$. Figure 5.5 shows the four cases considered in Figure 5.3 and 5.4, the fraction of dividing chromomeres changes with generation numbers. In Figure 5.5(B), (C), (D), telomerase is sufficiently active to maintain a positive average telomere length. However, the spread of the distribution means that some chromosomes' telomeres reach zero length and so becomes senescent. This causes the line to deviate from unity in the Figure. This is more noticeable in 5.5(D) since this has a significantly smaller value of n_{inter}. Although the standard deviation curves exceed unity, this is due to the non-symmetry form of the fluctuates away from the mean.

5.3 Deterministic model Case I

5.3.1 *Discrete model*

We assume that during chromosome replication, the average telomere loss is constant and all cells/chromosomes replicate on each generation. When telomerase is active, we assume that a constant amount of telomere is gained at the

Figure 5.5: *Averaged results from 5000 simulations showing how the the fraction of dividing chromosomes changes with generation number for four choices of T, the gain in telomere length where telomerase is achieve. Parameter values: $q = 0.6$, $p = 0.4$, $L = 100$, $Q = 5950$ and (A) $T(n) = 40 - 0.0005n$, (B) $T(n) = 200 - 0.015n$, (C) $T(n) = 170 - 0.0132n$, (D) $T(n) = 100 - 0.0125n$ basepairs, indicate with dashed line, dash-dot line, dotted line and solid circle line,respectively. The solid lines indicate two standard deviations above and below the fraction of dividing chrommeres of each passaging model.*

end of the offspring with the longer chromosome with probability q and that there is a gain at the end of the offspring with the shorter chromosome with probability p. We denote by K_n^g the number of chromosomes with telomere

length n at generation g; by L, the constant amount of basepairs that are lost; and by T, the constant amount of basepairs gained by telomerase activity. Following the replication rules (5.1.3)-(5.1.6), it is straightforward to show that the discrete chromosome replication process can be written as

$$K_n^g \to (1-q)K_n^{g+1} + qK_{n+T}^{g+1} + (1-p)K_{n-L}^{g+1} + pK_{n-L+T}^{g+1}, \tag{5.3.1}$$

where the probability of the chromosome dividing is 1. In (5.3.1), g, n, T, $L \in \mathbb{N}$, $0 \le p, q \le 1$. We assume that there is initially one chromosome of telomere length $n_{initial} = Q$ basepairs, so that $K_n^0 = \delta_{n,Q}$, where δ_{ij} is the Kronecker delta function.

The process (5.3.1) is modelled mathematically by the kinetic equation

$$K_n^{g+1} = (1-q)K_n^g + qK_{n-T}^g + (1-p)K_{n+L}^g + pK_{n+L-T}^g. \tag{5.3.2}$$

In order to solve (5.3.2), we use the method outlined in Section 4.3.1 of Chapter 4 . Firstly we note that (5.3.2) admits separable solutions of the form $K_n^g = e^{\gamma g + \chi n}$ where the growth rate γ depends on χ, the rate of change of the distribution with n. We substitute this trial solution into (5.3.2) to deduce

$$e^\gamma = 1 - q + qe^{-\chi T} + (1-p)e^{\chi L} + pe^{\chi(L-T)}. \tag{5.3.3}$$

This has the form of a dispersion relation. In order to construct continuum models which accurately for a wave equation described the evolution of distributions which are slowly varying in n. Hence we assume that χ is small, and expand this expression obtain to

$$e^\gamma = 2 + \chi(L - qT - pT) + \frac{\chi^2}{2}(qT^2 + L^2 + pT^2 - 2pLT), \tag{5.3.4}$$

or

$$\gamma \approx \ln 2 + \frac{A}{2}\chi + \frac{1}{8}\chi^2(2B - A^2), \tag{5.3.5}$$

where $A = L - (q+p)T$ and $B = (L - pT)^2 + (p + q - p^2)T^2$.

Let

$$C = 2B - A^2 = [L + T(q-p)]^2 + 2T^2[q(1-q) + p(1-p)]. \tag{5.3.6}$$

Since $0 \leq p, q \leq 1$, $2T^2[q(1-q) + p(1-p)] \geq 0$, so $C \geq 0$. The only way $C = 0$ can occur if $p = 1$, $q = 0$ and $L = T$, in this case $A = C = 0$ which means the telomerase always acts on the shorter chromosome and the gain in telomere length is the same as the loss, so that $K_n^g \to 2K_n^{g+1}$. The Case $C = 0$ is thus trivial since the average we require $C > 0$, in which case the dispersion relation simplifies to

$$\gamma \approx \ln 2 + \frac{A}{2}\chi + \frac{C}{8}\chi^2, \tag{5.3.7}$$

where A and C are known constants.

5.3.2 *Continuum model*

We have obtained an expression relating the growth rate $\gamma = \gamma(\chi)$ (5.3.7) of the discrete reaction (5.3.2) to system parameters. Now our aim is to focus on the continuum analogue of the discrete model, this being obtained by matching their "dispersion relations". In general, the number of chromosomes $\sum K_n^g$ becomes large after a few generations (g) and can be treated as a continuous real number. Since we are interested in the evolution over many generation we replace the discrete generation number, g, by a continuous time variable t. Experimented data shows that telomere length in normal human cells is approximately 3k to 15k basepairs with the telomere shorting rate is $50 - 200$ basepairs per replication [14], which is much less than the initial telomere length, hence the telomere length n can be treated as a continuous variable as well. To construct a model in which the telomere length n, generation number g and chromosome number K are all continuous, we replace K_n^g by $K(n, t)$ where $t = g$, so $t, n, K \in \mathbb{R}$. The continuous analogue of (5.3.2) is then the simplest partial differential equation which has the same "dispersion relation" as (5.3.7), namely

$$\frac{\partial K}{\partial t} = K \ln 2 + \frac{A}{2}\frac{\partial K}{\partial n} + \frac{C}{8}\frac{\partial^2 K}{\partial n^2}. \tag{5.3.8}$$

For the discrete model, we start with a single chromosome with telomere length $n_{initial} = Q$. For the continuum model, we replace the initial telomere length $n_{initial} = Q$ by the generalized function $K(n, 0) = \delta(n - Q)$, where δ is the Dirac delta function. Hence we solve (5.3.8) subject to the following initial and

boundary conditions:

$$K(n,0) = \delta(n - Q) \quad \text{and} \quad K(n,t) \to 0 \quad \text{as} \quad n \to \pm\infty. \qquad (5.3.9)$$

Following the approach outlined in Chapter 4, it is straightforward to show that the general solutio to (5.3.8)-(5.3.9) is

$$K(n,t) = \frac{2^{t+1}}{\sqrt{2C\pi t}} \exp\left[-\frac{2(n + \frac{1}{2}At - Q)^2}{Ct}\right]. \qquad (5.3.10)$$

This solution is a Gaussian distribution with

$$\text{number of chromosomes} = 2^t, \qquad (5.3.11)$$

$$\text{mean} = Q - \tfrac{1}{2}At = Q - \tfrac{1}{2}[L - (q+p)T]t, \qquad (5.3.12)$$

$$\text{variance} = \tfrac{1}{4}Ct = \tfrac{1}{4}[L + T(q-p)]^2 t + \tfrac{1}{2}T^2[q(1-q) + p(1-p)]t. \qquad (5.3.13)$$

If there is no telomerase activity ($T = 0$), then (5.3.10) can be written as

$$K(n,t) = \frac{2^{t+1}}{L\sqrt{2\pi t}} \exp\left[-\frac{2(n + \frac{1}{2}Lt - Q)^2}{L^2 t}\right]. \qquad (5.3.14)$$

We remark that solution (5.3.14) is identical to the continuum solution of Case I in Chapter 4, Section 4.3 where telomere loss was assumed constant and there was no telomerase. When there is no telomerase activity ($T = 0$), the average telomere length decays over time at rate $Lt/2$ which is faster than when the telomerase is active and the decay rate is $[L - (q+p)T]/2$. These results confirm that telomerase slows down the rate of telomere loss.

When telomerase is active, there are three possible cases to consider (all illustrates in Figure 5.6(a)). First, if $L > T(p+q)$ then the average telomere length decays over time at decay rate $(L - qT - pT)/2$, as indicated by the straight solid line. If, however, $L = T(p+q)$ then the average telomere length remains fixed as indicated by the dashed line. Finally if $L < T(p+q)$ then the average telomere length increases linearly with time at rate $(qT + pT - L)/2$, as indicated by the dash-dot line. Figure 5.6(b) shows how the variance of the distribution of $K(n,t)$ increases as T increases.

(a)   (b)
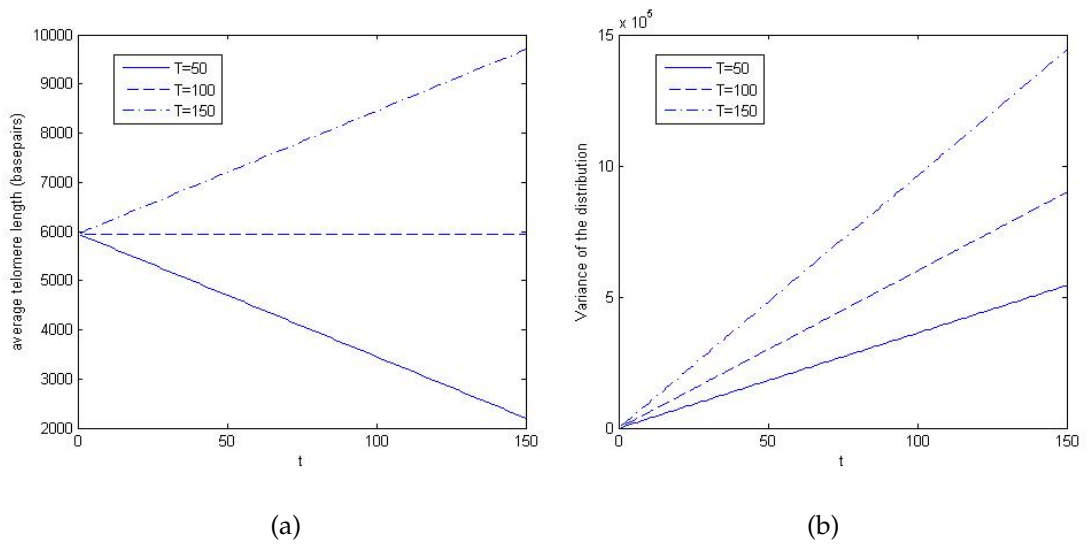
Figure 5.6: *Figure 5.6(a) shows the average telomere length (5.3.12) of the chromo-
somes changes with time for three choices of T, the gain in telomere length where telom-
erase is active. Figure 5.6(b) shows the variance (5.3.13) of the distribution for three
choices of T respectively. Parameter values: $q = 0.6$, $p = 0.4$, $L = 100$, $Q = 5950$
and $T = 50, 100, 150$ basepairs indicated by solid line, dashed line and dash-dot lines
respectively.*

Figure 5.7 shows how the average telomere length varies with generation num-
ber (where time = generation number), for three choices of T, the telomere gain
($T = 50, 100, 150$ basepairs). The solid lines correspond to the deterministic so-
lution (5.3.10) and the dashed lines to stochastic simulations (see Section 5.2.1
). We notice that for $T = 100$ and $T = 150$, both lines are identical, which indi-
cates that the solutions are in good agreement. When $T = 50$, these two curves
are identical provided that the generation number is below 150. If the genera-
tion number is above 150, then the deterministic solution decreases faster than
the stochastic solution and eventually approaches zero, whereas the stochas-
tic solutions approach a positive constant as the generation number increase.
This is because in the deterministic solution there is no lower restriction on the
telomere length of chromosomes, whereas in the stochastic simulation chromo-
somes became senescent. The only requirement on the deterministic solution is
that the telomere length, n, is positive. Those with zero or negative length are
assumed to be senescent. In contrast, in the stochastic model, we specify the
critical telomere length and when the chromosome's telomere reaches this crit-
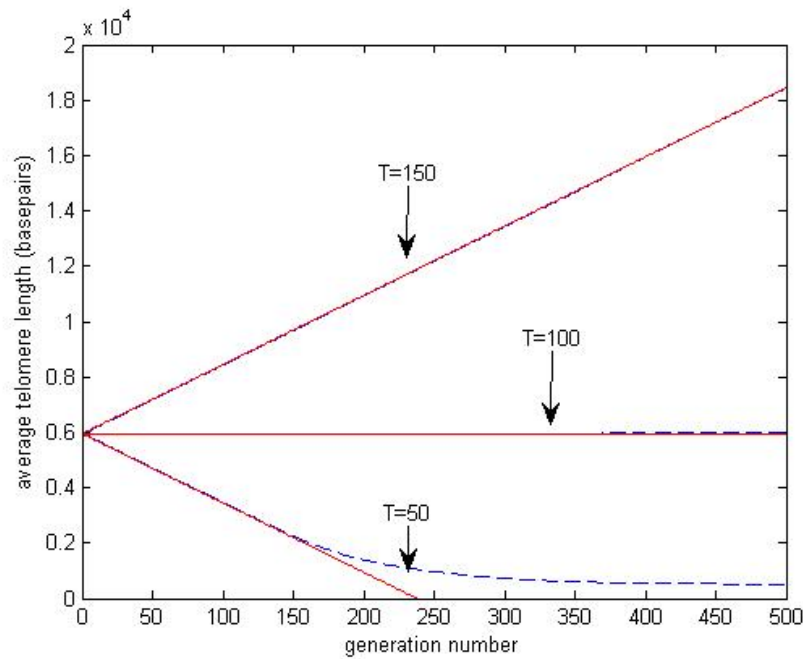
Figure 5.7: *With parameters: $q = 0.6$, $p = 0.4$, $L = 100$ basepairs and $Q = 5950$ basepairs, the average telomere length of the chromosome against generation numbers with three different amounts of telomere gain: $T = 50, 100, 150$ basepairs. The solid lines are the deterministic solution (5.3.10) and the dashed lines are the stochastic simulations from Section (5.2.1). For the x-axis we use time = generation number.*

ical length, the chromosome becomes senescent. Therefore the chromosomes in the stochastic model reach senescence later than those for the deterministic model.

From (5.3.10), we observe the number of chromosomes grows like 2^t. In order to see clearly how the telomere length $K(n, t)$ is distributed, we plot in Figure 5.8 $2^{-t}K(n, t)$ against of n for varies times, this shows how the distribution changes as the telomere gain T is varied. The top graph shows the distribution of telomere lengths moves to the left and becoming more diffuse for $L > (p + q)T$. The graph in the middle shows that when $L = (p + q)T$, the distribution of telomere lengths remains centered at the initial telomere length but the spread increases. The bottom graph shows that when $L < (p + q)T$, the distribution of telomere lengths moves towards the right with increasing variance.
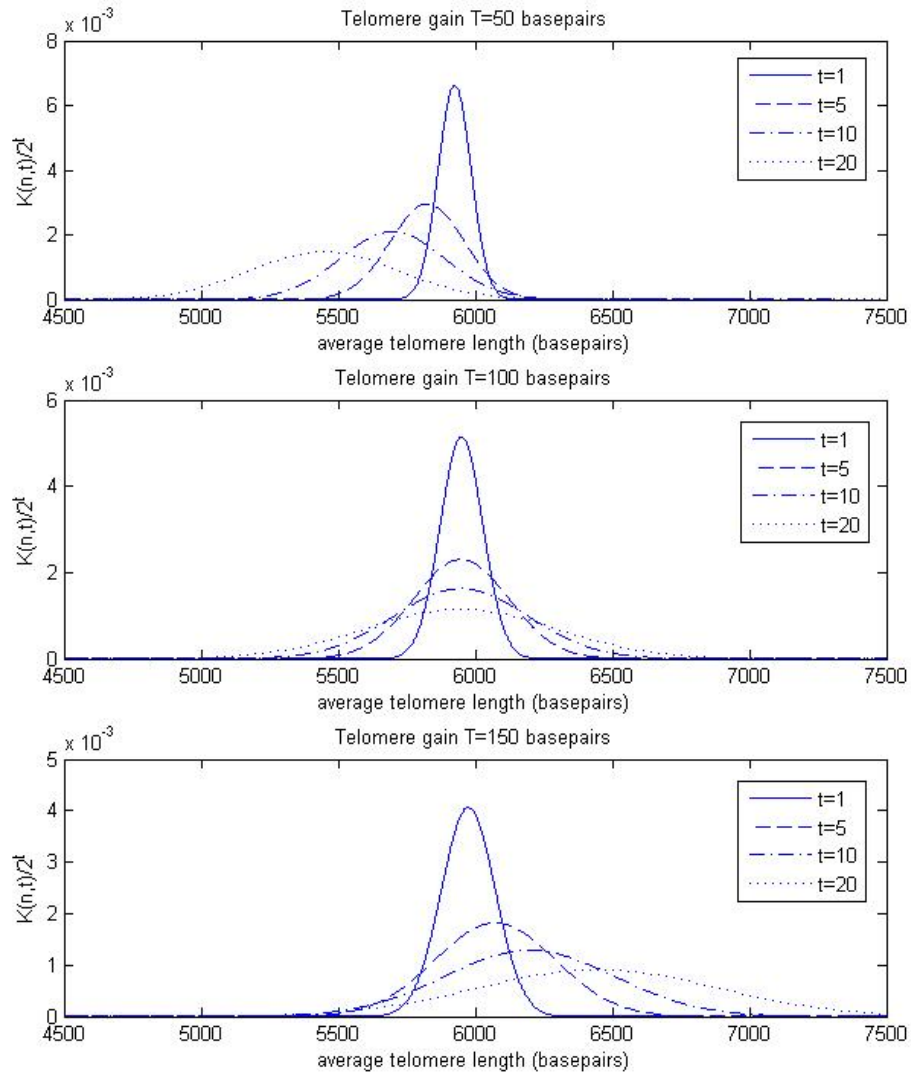
Figure 5.8: *Distribution of $2^{-t}K(n,t)$ at times $t = 1, 5, 10, 20$, for 3 different values of T, the telomere gain ($T = 50, 100, 150$) indicate in top, middle and bottom graphes respectively, with parameters $q = 0.6$, $p = 0.4$, $L = 100$ basepairs and $Q = 5950$ basepairs.*

The values of p, q, T and L control the evolution of the average telomere length. When the average telomere gain is less than that lost, the average telomere length decays and the distribution moves towards senescence. When the average telomere gain is equal to the average amount of telomere loss, the average telomere length remains the same and the distribution remains centered at the

initial state. When the average telomere gain exceeds that lost, the average telomere length increases without limit, and the distribution moves away from senescence. This case is not really physically realistic because in practice telomere length cannot increase indefinitely, even in immortal cells (whose telomere length is approximately constant).

5.4 Deterministic model Case II

5.4.1 *Discrete model*

As before, we denote by K_n^g the number of chromosomes with telomere length n at generation g. The amount of telomere lost and gained is given by $L(n) = L_0 + L_1 n$ (5.2.1), $T(n) = T_0 - T_1 n$ (5.2.2). Let $l = 1/Q \ll 1$, where Q is the initial telomere length, so $T_0, L_0 = O(1)$ and $T_1, L_1 = O(l)$. The chromosome replication process can be written as

$$K_n^g \rightarrow (1-q)K_n^{g+1} + qK_{n+T_0-T_1 n}^{g+1} + (1-p)K_{n-L_0-L_1 n}^{g+1} + pK_{n-L_0-L_1 n+T_0-T_1 n}^{g+1},$$

(5.4.1)

with $0 \leq p, q \leq 1$ and we start with one chromosome with initial telomere length $n_{initial} = Q$ basepairs, that is, $K_n^0 = \delta_{n,Q}$, where δ_{ij} is the Kronecker delta function.

Using (5.4.1), we know K_n^{g+1} can come from K_n^g or K_i^g where $i + T_0 + T_1 i = n$, K_j^g where $j - L_0 - L_1 j = n$, or K_k^g where $k - L_0 - L_1 k + T_0 - T_1 k = n$, these imply $i = (n - T_0)/(1 - T_1)$, $j = (n + L_0)/(1 - L_1)$, $k = (n + L_0 - T_0)/(1 - L_1 - T_1)$. We deduce that the process (5.4.1) may be modelled mathematically by

$$K_n^{g+1} = (1-q)K_n^g + qK_{\frac{n-T_0}{1-T_1}}^g + (1-p)K_{\frac{n+L_0}{1-L_1}}^g + pK_{\frac{n+L_0-T_0}{1-L_1-T_1}}^g.$$

(5.4.2)

In (5.4.2), if L and T are $O(1)$, than T_1, L_1 are $O(l)$ and $L_0 T_1, T_0 L_1, L_0 L_1$ and $T_0 T_1$ can be neglected since they are $O(l)$. Then (5.4.2) reduces to

$$K_n^{g+1} = (1-q)K_n^g + qK_{n+T_1 n-T_0}^g + (1-p)K_{n+L_1 n+L_0}^g + pK_{n+L_1 n+T_1 n+L_0-T_0}^g.$$

(5.4.3)

We perform Taylor series expansions of the terms, on the right hand side of (5.4.3) and use K^{g+1} instead of K_n^{g+1}, to obtain

$$
\begin{aligned}
K^{g+1} \approx \quad & (1-q)K^g + qK^g + q(T_1 n - T_0)\frac{\partial K^g}{\partial n} + \frac{1}{2}q(T_1 n - T_0)^2\frac{\partial^2 K^g}{\partial n^2} \\
& + (1-p)K^g + (1-p)(L_1 n + L_0)\frac{\partial K^g}{\partial n} + \frac{1}{2}(1-p)(L_1 n + L_0)^2\frac{\partial^2 K^g}{\partial n^2} \\
& + pK^g + p(L_1 n + T_1 n + L_0 - T_0)\frac{\partial K^g}{\partial n} \\
& + \frac{1}{2}p(L_1 n + T_1 n + L_0 - T_0)^2\frac{\partial^2 K^g}{\partial n^2} \; .
\end{aligned}
$$

$$\text{(5.4.4)}$$

or equivalently

$$
K^{g+1} = 2K^g + A(n)\frac{\partial K^g}{\partial n} + \frac{1}{2}B(n)\frac{\partial^2 K^g}{\partial n^2}, \tag{5.4.5}
$$

where $A(n) = A_0 + A_1 n$ and $B(n) = B_0 + B_1 n + B_2 n^2$ are given by

$$
\begin{aligned}
A_0 &= L_0 - (q+p)T_0 & \sim \quad & O(l^2), & \text{(5.4.6)} \\
A_1 &= L_1 + (q+p)T_1 & \sim \quad & O(l), & \text{(5.4.7)} \\
B_0 &= (p+q)T_0^2 + L_0^2 - 2pL_0T_0 & \sim \quad & O(1), & \text{(5.4.8)} \\
B_1 &= 2(L_1L_0 - pL_1T_0 - pT_1T_0 + pL_0T_1 - qT_1T_0) & \sim \quad & O(l), & \text{(5.4.9)} \\
B_2 &= 2pL_1T_1 + (p+q)T_1^2 + L_1^2 & \sim \quad & O(l^2). & \text{(5.4.10)}
\end{aligned}
$$

Since L_0, L_1, T_0, T_1, p and q are known constants, A_0, A_1, B_0, B_1, B_2 are known as well.

We denote by H_g the total number of chromosomes at generation g, which implies

$$
H_g = \sum_n K_n^g = \int_0^\infty K_n^g dn. \tag{5.4.11}
$$

Integrating both sides of (5.4.5) over n, yields

$$
\int_0^\infty K^{g+1} dn = 2\int_0^\infty K^g dn + \int_0^\infty A(n)\frac{\partial K^g}{\partial n} dn + \frac{1}{2}\int_0^\infty B(n)\frac{\partial^2 K^g}{\partial n^2} dn, \tag{5.4.12}
$$

or

$$
H_{g+1} = (2 - A_1 + 2B_2)H_g, \tag{5.4.13}
$$

since

$$\int_0^\infty (A_0 + A_1 n) \frac{\partial K^g}{\partial n} dn = -A_1 H_g, \tag{5.4.14}$$

$$\int_0^\infty (B_0 + B_1 n + B_2 n^2) \frac{\partial^2 K^g}{\partial n^2} dn = -\left[K^g (B_1 + 2B_2 n) \right]_0^\infty + \int_0^\infty 2B_2 K^g dn$$

$$= 2B_2 H_g. \tag{5.4.15}$$

Since $l \ll 1$ and due to the scalings noted in (5.4.6)-(5.4.10), we have

$$H_{g+1} \approx 2H_g, \tag{5.4.16}$$

which implies

$$H_g = C_0 2^g, \tag{5.4.17}$$

where C_0 is a constant. Initially we start with one chromosome which implies $C_0 = 1$, so $H_g = 2^g$.

To investigate the shape of the distribution, we write $K^g = 2^g \overline{K}^g$ where $\overline{K}^g$ is the distribution of the telomere length at generation g and 2^g the total number of chromosomes at generation g. With $K^g = 2^g \overline{K}^g$, (5.4.5) transforms to

$$2\overline{K}^{g+1} = 2\overline{K}^g + A(n) \frac{\partial \overline{K}^g}{\partial n} + \frac{1}{2} B(n) \frac{\partial^2 \overline{K}^g}{\partial n^2}. \tag{5.4.18}$$

Using Taylor's series in g, implies

$$\frac{\partial \overline{K}^g}{\partial g} = \frac{1}{2} A(n) \frac{\partial \overline{K}^g}{\partial n} + \frac{1}{4} B(n) \frac{\partial^2 \overline{K}^g}{\partial n^2}, \tag{5.4.19}$$

and our initial conditions are $\overline{K}_n^0 = \delta(n - Q)$, that is, one chromosome with initial telomere length $n_{initial} = Q$ basepairs.

5.4.2   *Continuum model*

Our aim now is to investigate on the continuum analogue of the discrete model, this being obtained by matching the same PDE (5.4.19). For the continuous model we replace the generation number by a continuous time variable t, K_n^g by $K(n,t)$, H^g by $H(t)$ and $\overline{K}_n^g$ by $\overline{K}(n,t)$ respectively, so $K(n,t) = H(t)\overline{K}(n,t)$.

From the discrete model we have calculated that the total number of chromosomes at generation g is $H_g = 2^g$, so $H(t) = 2^t$. In the continuum model we focus on the shape of the distribution, $\overline{K}(n,t)$. The continuous analogue of (5.4.2) is assumed to be the simplest partial differential equation which has the same dispersion relation as (5.4.19), namely

$$\frac{\partial \overline{K}}{\partial t} = \frac{1}{2}A(n)\frac{\partial \overline{K}}{\partial n} + \frac{1}{4}B(n)\frac{\partial^2 \overline{K}}{\partial n^2}, \tag{5.4.20}$$

where $A(n)$ and $B(n)$ are as defined for the discrete model. We fix $\overline{K}(n,0) = \delta(n-Q)$ where Q is the initial telomere length and $\int_0^\infty \overline{K}(n,0)dn = 1$ so that we start with only one chromosome.

Introducing $x = ln$ where $l = 1/Q \ll 1$, $\overline{K}(n,t) = \widetilde{K}(x,t)$, $A_0 = \hat{A}_0$, $A_1 = l\hat{A}_1$, $B_0 = \hat{B}_0$, $B_1 = l\hat{B}_1$ and $B_2 = l^2\hat{B}_2$, implies $A(n) = \hat{A}(x) = \hat{A}_0 + \hat{A}_1 x$, $B(n) = \hat{B}(x) = \hat{B}_0 + \hat{B}_1 x + \hat{B}_2 x^2$ where $\hat{A}_0$, $\hat{A}_1$, $\hat{B}_0$, $\hat{B}_1$, $\hat{B}_2$, x, $\hat{A}(x)$, $\hat{B}(x)$ are $O(1)$. Then (5.4.20) can be written as

$$\frac{\partial \widetilde{K}}{\partial t} = \frac{1}{2}\hat{A}(x)l\frac{\partial \widetilde{K}}{\partial x} + \frac{1}{4}\hat{B}(x)l^2\frac{\partial^2 \widetilde{K}}{\partial x^2}, \tag{5.4.21}$$

with the initial condition $\widetilde{K}(x,0) = H_1\delta(x-1)$ where H_1 is a constant. Since $\int_0^\infty \overline{K}(n,0)dn = 1$ and $x = n/Q$, we have $Q\int_0^\infty H_1\overline{K}(x,0)dx = 1$, so $H_1 = 1/Q$. The initial condition is $\widetilde{K}(x,0) = \delta(x-1)/Q$.

Before analyzing (5.4.21), we consider by solving the first order PDE that is obtained in the limit $l \to 0$ when terms linear in l are retained and quadratic terms are neglected.

5.4.3 *First order PDE*

An approximate solution to (5.4.21) can be determined by neglecting the diffusion term which is $O(l^2)$, where $l = 1/Q \ll 1$. Retaining only $O(l)$ terms, (5.4.21) simplifies to

$$\frac{\partial \widetilde{K}}{\partial t} = \frac{1}{2}\hat{A}(x)l\frac{\partial \widetilde{K}}{\partial x}. \tag{5.4.22}$$

We use the method of characteristics to solve this first order PDE. We introduce the characteristic variables where $ds = dt = -2dx/(l\hat{A})$ and parameterized

the initial conditions on $s = 0$ by α so that when $s = 0$, $t = 0$, $x = \alpha$, $\tilde{K} = \delta(\alpha - 1)/Q$.

$$\frac{dt}{ds} = 1 \quad \text{implies} \quad t = s, \tag{5.4.23}$$

since $t = 0$ when $s = 0$. Next

$$\frac{dx}{ds} = -\frac{l}{2}\hat{A}_1 x - \frac{l}{2}\hat{A}_0, \tag{5.4.24}$$

$$x = e^{-sl\hat{A}_1/2}\left(\alpha + \frac{\hat{A}_0}{\hat{A}_1}\right) - \frac{\hat{A}_0}{\hat{A}_1}, \tag{5.4.25}$$

since $x = \alpha$ when $s = 0$. Which implies

$$\alpha = \frac{\hat{A}_0}{\hat{A}_1}(e^{sl\hat{A}_1/2} - 1) + xe^{sl\hat{A}_1/2}. \tag{5.4.26}$$

Finally, solving

$$\frac{d\tilde{K}}{ds} = 0 \quad \text{we find} \quad \tilde{K}(s, \alpha) = \frac{1}{Q}\delta(\alpha - 1), \tag{5.4.27}$$

since $s = 0$ where $\tilde{K} = \delta(\alpha - 1)/Q$.

We have derived expressions for t, n and $\tilde{K}$ in the terms of s and α, from (5.4.23)-(5.4.27) the explicit solution is

$$\tilde{K}(x, t) = \frac{1}{Q}\delta\left(\frac{\hat{A}_0}{\hat{A}_1}(e^{tl\hat{A}_1/2} - 1) + xe^{tl\hat{A}_1/2} - 1\right), \tag{5.4.28}$$

so $\tilde{K} = 0$ except on the curve

$$x(t) = e^{-\frac{t}{l}\hat{A}_1/2} + \frac{\hat{A}_0}{\hat{A}_1}(e^{-tl\hat{A}_1/2} - 1). \tag{5.4.29}$$

Since $x = nl$, the solution for $\bar{K}(n, t)$ is

$$\bar{K}(n, t) = \frac{1}{Q}\delta\left(\frac{\hat{A}_0}{\hat{A}_1}(e^{tl\hat{A}_1/2} - 1) + nle^{tl\hat{A}_1/2} - 1\right), \tag{5.4.30}$$

so $\bar{K} = 0$ except on the curve

$$n(t) = \frac{1}{l}e^{-tl\hat{A}_1/2} + \frac{\hat{A}_0}{l\hat{A}_1}(e^{-tl\hat{A}_1/2} - 1). \tag{5.4.31}$$
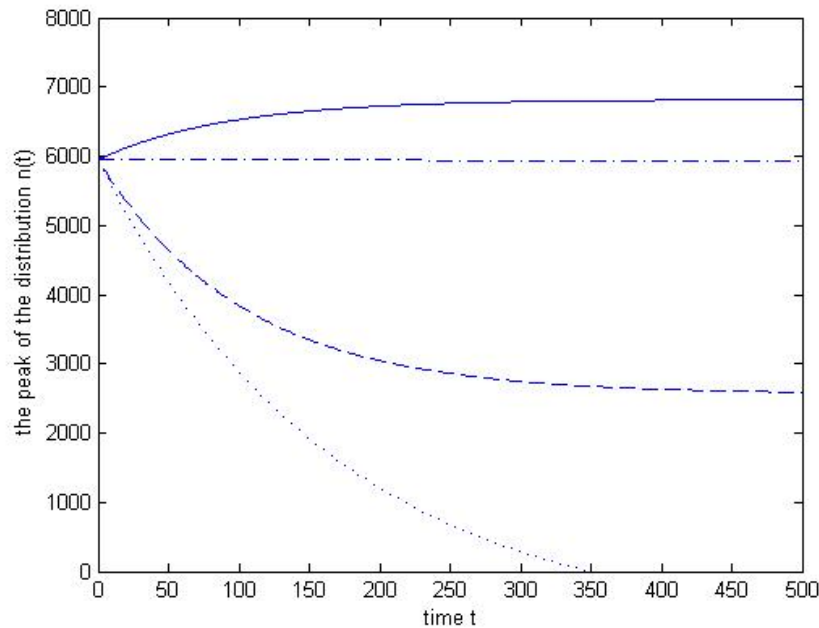
Figure 5.9: *The peak $n(t)$ from (5.4.31) of the distribution of $\bar{K}(n,t)$ plotted against time t, with the amount of telomere loss $L(n) = 50 + 0.007n$ basepairs and four different sets of T_0, T_1. The solid line corresponds to $T(n) = 200 - 0.015n$; the dash-dotted line corresponds to $T(n) = 170 - 0.0132n$; the dashed line corresponds to $T(n) = 100 - 0.0125n$; the dotted line corresponds to $T(n) = 40 - 0.005n$. In all cases $q = 0.6$, $p = 0.4$.*

Figure 5.9 shows the location of the peak $n(t)$ given by (5.4.31) plotted against time for four different telomere gain functions. The dotted line indicates the peak of $n(t)$ where the amount of telomere gain is $T(n) = 40 - 0.0005n$ base-pairs, as t increases the peak of the distribution moves to the left (shorter telomeres) until it hits the critical telomere length of zero. This behaviour can be explained by Figure 5.3(A); the amount of telomere loss is always bigger than the telomere gain. The dashed line in Figure 5.9 indicates the peak of $n(t)$ where the amount of telomere gain is $T(n) = 100 - 0.0125n$ basepairs, corresponded to Figure 5.3(D). The peak of the distribution moves to lower n, until the peak reaches $n_{inter} = 2564$ basepairs, after which the peak remains stationary. The dash-dot line indicates the case of Figure 5.3(C) where the amount of telomere gain is $T(n) = 170 - 0.0132n$ basepairs. Here the peak of the distribution remains the same as the initial telomere length. The solid line in Figure 5.9 cor-

responds to $T(n) = 200 - 0.015n$ basepairs. The peak moves to larger n, until it reaches $n_{inter} = 6818$ basepairs, after which it remains stationary. This behaviour is explained by Figure 5.3(B) where $n_{inter} > Q$.

By comparing Figure 5.9 with Figure 5.4, we notice that when $n_{inter} > 0$, the average telomere obtained from the stochastic simulation (dash-dot line, dotted lines and solid circle line in Figure 5.4 is identical to the peak of the distribution obtained from the first order-PDE (see Figure 5.9. When $n_{inter} < 0$, the curves are identical at earlier generations, but as the generations increases, the average telomere length of deterministic model decreases faster than the stochastic model because in the stochastic model, the restriction of the telomere length (critical telomere length), results the chromosomes reaching senescence, but in the deterministic model the only restriction is that the average telomere length is positive.

The first-order solution only describes how the peak of the distribution moves. In order to investigate the spread of the distribution, we consider the second-order PDE.

5.4.4 *Second order PDE*

Now we return to (5.4.21) retaining terms which are quadratic in l^2, so that

$$\frac{\partial \widetilde{K}}{\partial t} = \frac{1}{2}\hat{A}(x)l\frac{\partial \widetilde{K}}{\partial x} + \frac{1}{4}\hat{B}(x)l^2\frac{\partial^2 \widetilde{K}}{\partial x^2}, \tag{5.4.32}$$

with the initial condition $\widetilde{K}(x,0) = \delta(x-1)/Q$.

The problem for $\check{K}(y,t)$

For Case II from the Chapter 4, telomere loss depends on telomere length in normal ageing and the assumed partial differential equation is

$$\frac{\partial K(n,t)}{\partial t} = \ln(2)K(n,t) + \frac{(y_0 + y_1 n)[\ln^2(1-y_1) - 4\ln(1-y_1)]}{8y_1}\frac{\partial K(n,t)}{\partial n}$$

$$+ \frac{(y_0 + y_1 n)^2 \ln^2(1-y_1)}{8y_1^2}\frac{\partial^2 K(n,t)}{\partial n^2}. \tag{5.4.33}$$

Since $0 \leq y_1 \leq 1$, (5.4.33) can be approximated by

$$\frac{\partial K(n,t)}{\partial t} = \ln(2)K(n,t) + U(n)\frac{\partial K(n,t)}{\partial n} + \frac{1}{2}V(n)\frac{\partial^2 K(n,t)}{\partial n^2}, \quad (5.4.34)$$

where

$$U(n) = -\frac{(y_0 + y_1 n)\ln(1 - y_1)}{2y_1}, \quad (5.4.35)$$

$$V(n) = \frac{(y_0 + y_1 n)^2 \ln^2(1 - y_1)}{4y_1^2} = U^2(n). \quad (5.4.36)$$

Section 5.4 in Chapter 4 shows that the solution of (5.4.33) has a log-normal distribution. We notice that the PDE (5.4.32) is similar in form to (5.4.34), hence we shall here look for a solution using similar techniques and exploiting the fact that $l \ll 1$. However no exact solution is possible since in general there is no special relationship between $\hat{A}$ and $\hat{B}$, from (5.4.34) (where $V(n) = U^2(n)$). We proceed by transforming from x to y via $e^y = \alpha x + \beta$, or equivalently

$$y = \ln(\alpha x + \beta), \quad (5.4.37)$$

where α, β are constants, so that

$$x = \alpha^{-1}(e^y - \beta), \quad (5.4.38)$$

$$\frac{\partial}{\partial x} = \frac{\alpha}{\alpha x + \beta}\frac{\partial}{\partial y} = \alpha e^{-y}\frac{\partial}{\partial y}, \quad (5.4.39)$$

$$\frac{\partial^2}{\partial x^2} = \alpha e^{-y}\frac{\partial}{\partial y}\left(\alpha e^{-y}\frac{\partial}{\partial y}\right) = \alpha^2 e^{-2y}\frac{\partial^2}{\partial y^2} - \alpha^2 e^{-2y}\frac{\partial}{\partial y}. \quad (5.4.40)$$

Letting $\check{K}(y,t) = \widetilde{K}(x,t)$, (5.4.32) can be written as

$$\frac{\partial \check{K}}{\partial t} = \frac{1}{2}F(y)l\frac{\partial \check{K}}{\partial y} + \frac{1}{4}D(y)l^2\frac{\partial^2 \check{K}}{\partial y^2}, \quad (5.4.41)$$

where

$$\begin{aligned}
F(y) &= \alpha e^{-y}\hat{A} - \frac{1}{2}\alpha^2 e^{-2y}l\hat{B} \\
&= \hat{A}_1 - \frac{1}{2}l\hat{B}_2 + e^{-y}(\hat{A}_0\alpha - \hat{A}_1\beta - \frac{1}{2}l\hat{B}_1\alpha + l\hat{B}_2\beta) \\
&\quad + \frac{1}{2}e^{-2y}l(\hat{B}_1\alpha\beta - \hat{B}_0\alpha^2 - \hat{B}_2\beta^2), \\
D(y) &= \hat{B}_2 + e^{-y}(\hat{B}_1\alpha - 2\hat{B}_2\beta) + e^{-2y}(\hat{B}_0\alpha^2 - \hat{B}_1\alpha\beta + \hat{B}_2\beta^2),
\end{aligned}$$

$$(5.4.42)$$

We let

$$F_0 = \hat{A}_1 - \frac{1}{2}l\hat{B}_2,$$ (5.4.43)

$$F_1 = \hat{A}_0\alpha - \hat{A}_1\beta - \frac{1}{2}l\hat{B}_1\alpha + l\hat{B}_2\beta,$$ (5.4.44)

$$F_2 = \frac{1}{2}(\hat{B}_1\alpha\beta - \hat{B}_0\alpha^2 - \hat{B}_2\beta^2),$$ (5.4.45)

$$D_0 = \hat{B}_2,$$ (5.4.46)

$$D_1 = \hat{B}_1\alpha - 2\hat{B}_2\beta,$$ (5.4.47)

$$D_2 = \hat{B}_0\alpha^2 - \hat{B}_1\alpha\beta + \hat{B}_2\beta^2,$$ (5.4.48)

all of which are $O(1)$, and note that F and D can be written as $F(y) = F_0 + F_1 e^{-y} + F_2 l e^{-2y}$ and $D(y) = D_0 + D_1 e^{-y} + D_2 e^{-2y}$.

The initial condition for (5.4.41) is $\hat{K}(y,0) = H_2\delta(y - \ln(\alpha + \beta))$ where H_2 is a constant. Since $Q \int_0^\infty \bar{K}(x,0)dx = 1$, the constant H_2 can be deduced from

$$1 = Q \int_0^\infty \check{K}(y,0)\frac{e^y}{\alpha}dy = \frac{Q}{\alpha}\int_0^\infty H_2\delta(y - \ln(\alpha + \beta))e^y dy = \frac{Q}{\alpha}H_2(\alpha + \beta),$$ (5.4.49)

hence

$$H_2 = \frac{\alpha}{(\alpha + \beta)Q}.$$ (5.4.50)

So the initial condition is

$$\check{K}(y,0) = \frac{\alpha\delta(y - \ln(\alpha + \beta))}{(\alpha + \beta)Q}.$$ (5.4.51)

The problem for $\hat{K}(z, \widehat{T})$

We now transform to a moving frame of reference by via $y = S(\widehat{T}) + l^\theta z$, where $\widehat{T} = l^\sigma t$ and $S(\widehat{T})$ is the function which determines the position of the center of the distribution, and θ is a positive constant which describes the width scale of the distribution. We write $\hat{K}(z, \widehat{T}) = \hat{K}(y,t)$; and θ, σ will be determined by balancing terms in the ensuring asymptotic calculation.

By (5.4.37) we obtain $S(0) = \ln(\alpha + \beta)$. Letting $dS/d\widehat{T} = S'$ so

$$\frac{\partial}{\partial y} = \frac{\partial z}{\partial y}\frac{\partial}{\partial z} + \frac{\partial \widehat{T}}{\partial y}\frac{\partial}{\partial \widehat{T}} = l^{-\theta}\frac{\partial}{\partial z}, \tag{5.4.52}$$

$$\frac{\partial}{\partial t} = \frac{\partial z}{\partial t}\frac{\partial}{\partial z} + \frac{\partial \widehat{T}}{\partial t}\frac{\partial}{\partial \widehat{T}} = -l^{\sigma-\theta}S'\frac{\partial}{\partial z} + l^{\sigma}\frac{\partial}{\partial \widehat{T}}, \tag{5.4.53}$$

and (5.4.41) can be rewritten as

$$l^{\sigma}\frac{\partial \widehat{K}}{\partial \widehat{T}} = \frac{1}{2}\tilde{F}\frac{\partial \widehat{K}}{\partial z} + \frac{1}{4}\tilde{D}\frac{\partial^2 \widehat{K}}{\partial z^2}, \tag{5.4.54}$$

with the initial condition $\widehat{K}(z,0) = \delta(l^{\theta}z)$ and where

$$\tilde{F} = Fl^{1-\theta} + 2l^{\sigma-\theta}S' = l^{1-\theta}(F_0 + F_1 e^{-S-l^{\theta}z} + F_2 l e^{-2S-2l^{\theta}z}) + 2l^{\sigma-\theta}S', \tag{5.4.55}$$

$$\tilde{D} = l^{2-2\theta}D = l^{2-2\theta}(D_0 + D_1 e^{-S-l^{\theta}z} + D_2 e^{-2S-2l^{\theta}z}). \tag{5.4.56}$$

Since $e^{-l^{\theta}z} \approx 1 - l^{\theta}z$

$$\begin{aligned}
\tilde{F} &\approx l^{1-\theta}(F_0 + F_1 e^{-S} + F_2 l e^{-2S} - l^{\theta}z F_1 e^{-S} - 2l^{1+\theta}z F_2 e^{-2S}) + 2l^{\sigma-\theta}S' \\
&= l^{1-\theta}(F_0 + F_1 e^{-S} + F_2 l e^{-2S}) + 2l^{\sigma-\theta}S' - lz F_1 e^{-S} - 2l^2 z F_2 e^{-2S},
\end{aligned} \tag{5.4.57}$$

$$\begin{aligned}
\tilde{D} &\approx l^{2-2\theta}(D_0 + D_1 e^{-S} + D_2 e^{-2S} - l^{\theta}z D_1 e^{-S} - 2l^{\theta}z D_2 e^{-2S}) \\
&= l^{2-2\theta}(D_0 + D_1 e^{-S} + D_2 e^{-2S}) - l^{2-\theta}(z D_1 e^{-S} + 2z D_2 e^{-2S}).
\end{aligned} \tag{5.4.58}$$

If we choose $\sigma = 1$ and $\theta > 0$, then the leading order terms in (5.4.54) all arise in $\tilde{F}$ and are $O(l^{1-\theta})$ and $S(\widehat{T})$ can be chosen to make these sum to zero. Since F_2 are $O(1)$ and F_1 contains $O(1)$ and $O(l)$ terms, we obtain the equation

$$2S' = -F_0 - F_1 e^{-S} - F_2 l e^{-2S}, \tag{5.4.59}$$

$$\begin{aligned}
S' &= -\frac{1}{2}\hat{A}_1 + \frac{1}{4}l\hat{B}_2 - \frac{1}{2}(\hat{A}_0\alpha - \hat{A}_1\beta - \frac{1}{2}l\hat{B}_1\alpha + l\hat{B}_2\beta)e^{-S} \\
&\quad - \frac{1}{4}(\hat{B}_1\alpha\beta - \hat{B}_0\alpha^2 - \hat{B}_2\beta^2)l e^{-2S},
\end{aligned} \tag{5.4.60}$$

The evolution of the mean of the distribution

Since $l \ll 1$ and we pick $\hat{A}_0\alpha = \hat{A}_1\beta$, the leading order solution to (5.4.60) is given by $S'_0 = -\hat{A}_1/2$, hence

$$S_0 = -\frac{1}{2}\hat{A}_1\widehat{T} + C_4, \tag{5.4.61}$$

where C_4 is an integration constant. The initial condition, $S_0(0) = \ln(\alpha + \beta)$, which implies

$$S_0(\widehat{T}) = \ln(\alpha + \beta) - \frac{1}{2}\hat{A}_1\widehat{T}. \tag{5.4.62}$$

This leading order solution for $S(T)$ exhibits linear decay/growth of S. Converting back to earlier variables, we find $y = S(\widehat{T})$ corresponds to $x = \alpha^{-1}(e^y - \beta)$, $n = Q(e^y - \beta)/\alpha$, hence the mean of the distribution is given by $\mu = Q(e^{S(\widehat{T})} - \beta)/\alpha$. Since $l \ll 1$, the mean of the distribution can be approximated by

$$\begin{aligned}
\mu(\widehat{T}) &\sim \frac{Q}{\alpha}\left[(\alpha + \beta)e^{-\frac{1}{2}\hat{A}_1\widehat{T}} - \beta\right] \\
&= \frac{Q\hat{A}_0}{\hat{A}_1}\left[\left(\frac{\hat{A}_1}{\hat{A}_0} + 1\right)e^{-\frac{1}{2}\hat{A}_1\widehat{T}} - 1\right].
\end{aligned} \tag{5.4.63}$$

Thus we observe convergence to the equilibrium

$$\mu(\widehat{T})_{eq} \sim -\frac{Q\beta}{\alpha} = -\frac{Q\hat{A}_0}{\hat{A}_1}. \tag{5.4.64}$$

Figure 5.10 shows how the average telomere length varies with time (where time $=$ generation number), for four choices of T, the telomere gain: (A), $T(n) = 40 - 0.0005n$, (B), $T(n) = 200 - 0.015n$, (C), $T(n) = 170 - 0.0132n$, (D), $T(n) = 100 - 0.0125n$ basepairs. The solid lines correspond to the deterministic solution (5.4.63) and the dashed lines to stochastic simulations (see Section 5.2.2). When (B) $T(n) = 200 - 0.015n$, (C) $T(n) = 170 - 0.0132n$ and (D) $T(n) = 100 - 0.0125n$, lines from simulations and (5.4.63) are identical, indicating good agreement. When $T(n) = 40 - 0.0005n$, these two lines are identical in early generations. However, for generation numbers > 250, the deterministic solution decreases faster than the stochastic solution, because the deterministic solution has no longer restriction on telomere length. In contrast, in the stochastic model, the chromosomes becomes senescent.

The shape of the distribution

Having solved the leading order terms in (5.4.54) to determine the evolution of average telomere over time, we return to consider the next order terms. Using
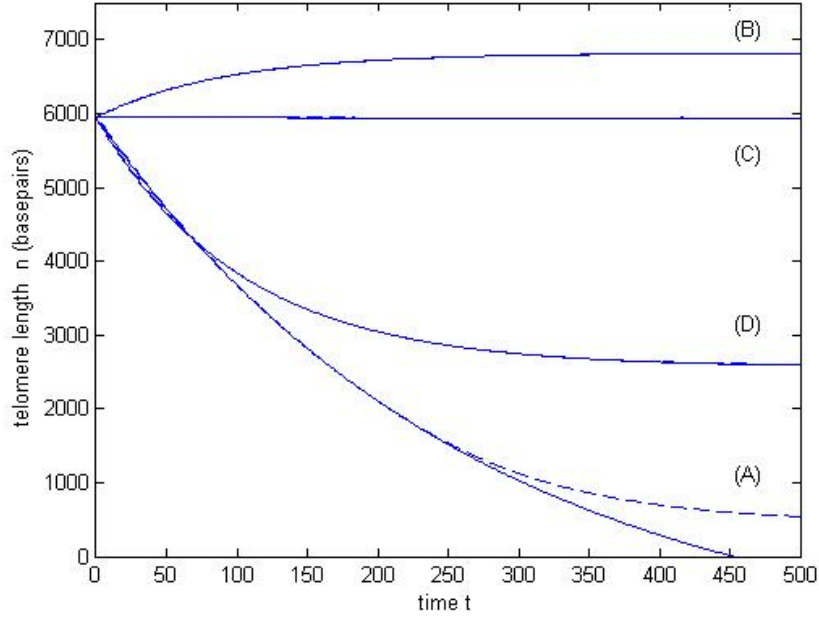
Figure 5.10: *Plots showing the average telomere length of the chromosomes against time for four choices of $T(n)$ with $L(n) = 50 + 0.007n$. The solid lines show the means obtained from (5.4.63) and the dashed lines are the means obtained from the stochastic stimulations in Section (5.2.2). Parameter values: $q = 0.6$, $p = 0.4$, $L = 100$, $Q = 5950$, (A) $T(n) = 40 - 0.0005n$, (B) $T(n) = 200 - 0.015n$, (C) $T(n) = 170 - 0.0132n$, (D) $T(n) = 100 - 0.0125n$ basepairs.*

$\sigma = 1$, $S(\widehat{T}) = S_0(\widehat{T})$, (5.4.54) can be written as

$$\frac{\partial \hat{K}}{\partial \widehat{T}} = \frac{1}{4}\left[l^{1-2\theta}(D_0 + D_1 e^{-S} + D_2 e^{-2S}) - l^{1-\theta}(zD_1 e^{-S} + 2zD_2 e^{-2S})\right]\frac{\partial^2 \hat{K}}{\partial z^2}$$
$$- \frac{1}{2}(zF_1 e^{-S} + 2lzF_2 e^{-2S})\frac{\partial \hat{K}}{\partial z}, \tag{5.4.65}$$

with the initial condition $\hat{K}(z, \widehat{T} = 0) = H_3\delta(S(0) + l^\theta z - \ln(\alpha + \beta)) = H_3\delta(l^\theta z)$ where H_3 is a constant. Since $Q \int_0^\infty \bar{K}(x,0)dx = 1$, so

$$\begin{aligned}
1 &= \int_0^\infty K(n,0)dn = Q\int_0^\infty \bar{K}(x,0)dx = \frac{Q}{\alpha}\int_0^\infty \check{K}(y,0)e^y dy \\
&= l^\theta \frac{Q}{\alpha}\int_0^\infty \hat{K}(z,0)e^{S(0)+l^\theta z}dz = l^\theta \frac{Q}{\alpha}\int_0^\infty H_3\delta(l^\theta z))e^{S(0)+l^\theta z}dz \\
&= \frac{Q}{\alpha}H_3(\alpha + \beta)dz, \\
H_3 &= \frac{\alpha}{(\alpha + \beta)Q}, \tag{5.4.66}
\end{aligned}$$

So the initial condition for $\hat{K}(z,0)$ is $\hat{K}(z,0) = \delta(l^\theta z) \times \alpha / [(\alpha + \beta)Q]$.

Since D_0, D_1 D_2 and F_2 are $O(1)$ and F_1 contains $O(1)$ and $O(l)$ terms, (5.4.65) contains $O(l^{1-2\theta})$, $O(l^{1-\theta})$, $O(1)$ and $O(l)$ terms. Due to a θ being positive constant, we can neglected $O(l^{1-\theta})$, $O(l)$ terms, so F_1 can be rewritten as $\tilde{F}_1 = \hat{A}_0 \alpha - \hat{A}_1 \beta$. Since we have already chosen $\beta = 1$ and $\alpha = \hat{A}_1 / \hat{A}_0$, $\tilde{F}_1 = 0$. Hence (5.4.65) can be simplified to

$$\frac{\partial \hat{K}}{\partial \widehat{T}} = \frac{1}{4} l^{1-2\theta} (D_0 + D_1 e^{-S} + D_2 e^{-2S}) \frac{\partial^2 \hat{K}}{\partial z^2}, \qquad (5.4.67)$$

where $S = S_0(\widehat{T})$ is give by (5.4.72).

We solve this (5.4.67) by choose $\theta = 1/2$ and using $S(\widehat{T}) = S_0$, the leading order expression for $S(\widehat{T})$, so (5.4.67) can be rewritten as

$$\frac{\partial \hat{K}}{\partial \widehat{T}} = \frac{1}{4} \left[D_0 + \frac{D_1}{\alpha + \beta} e^{\hat{A}_1 T/2} + \frac{D_2}{(\alpha + \beta)^2} e^{\hat{A}_1 T} \right] \frac{\partial^2 \hat{K}}{\partial z^2}, \qquad (5.4.68)$$

with the initial condition $\hat{K}(z, \widehat{T} = 0) = \delta(l^\theta z) \times \alpha / [(\alpha + \beta)Q]$. This is simply a diffusion equation where the time variable has been subjected to a transformation.

We rescale time $\widehat{T}$ to τ, via

$$\begin{aligned} \tau(\widehat{T}) &= \frac{1}{4} \int_0^{\widehat{T}} \left[D_0 + \frac{D_1}{\alpha + \beta} e^{\hat{A}_1 \widetilde{T}/2} + \frac{D_2}{(\alpha + \beta)^2} e^{\hat{A}_1 \widetilde{T}} \right] d\widetilde{T} \\ &= \frac{1}{4} \left[D_0 \widehat{T} + \frac{2D_1}{\hat{A}_1 (\alpha + \beta)} e^{\hat{A}_1 \widehat{T}/2} + \frac{D_2}{\hat{A}_1 (\alpha + \beta)^2} e^{\hat{A}_1 \widehat{T}} \right] + C_6, \end{aligned}$$

$$(5.4.69)$$

and C_6 is an integration constant. The initial condition for $\tau(0) = 0$, which implies

$$C_6 = -\frac{1}{4\hat{A}_1 (\alpha + \beta)} \left[2D_1 + \frac{D_2}{(\alpha + \beta)} \right]. \qquad (5.4.70)$$

So (5.4.69) can be written as

$$\tau(\widehat{T}) = \frac{1}{4} \left[D_0 \widehat{T} + \frac{2D_1}{\hat{A}_1 (\alpha + \beta)} \left(e^{\hat{A}_1 \widehat{T}/2} - 1 \right) + \frac{D_2}{\hat{A}_1 (\alpha + \beta)^2} \left(e^{\hat{A}_1 \widehat{T}} - 1 \right) \right]. \qquad (5.4.71)$$

Equation (5.4.68) can be written as

$$\frac{\partial \hat{K}}{\partial \tau} = \frac{\partial^2 \hat{K}}{\partial z^2}, \tag{5.4.72}$$

with the initial condition $\hat{K}(z, \tau(0)) = \alpha \delta(l^{1/2}z)/[(\alpha + \beta)Q]$. This system has the solution

$$\hat{K}(z, \tau) = \frac{\alpha}{2(\alpha + \beta)Q\sqrt{l\pi\tau}} \exp\left(-\frac{z^2}{4\tau}\right), \tag{5.4.73}$$

which is a Gaussian distribution with mean zero, variance$= 2\tau$. This determines the shape of the distribution, solving our problems. All that remains is to back to substitute all the transformations so as to express the solution in terms of our original variables $K(n, t)$.

Since $t = l^{-1}\widehat{T}$, (5.4.71) implies

$$\tau(t) = \frac{1}{4}\left[D_0 lt + \frac{2D_1}{\hat{A}_1(\alpha + \beta)}\left(e^{\hat{A}_1 lt/2} - 1\right) + \frac{D_2}{\hat{A}_1(\alpha + \beta)^2}\left(e^{\hat{A}_1 lt} - 1\right)\right], \tag{5.4.74}$$

we also have $y = S(\widehat{T}) + l^\theta z = \ln(\alpha + \beta) - \frac{1}{2}\hat{A}_1 lt + l^{1/2}z$ and $y = \ln(\alpha x + \beta)$, hence

$$z = l^{-1/2}\left[\ln\left(\frac{\alpha x + \beta}{\alpha + \beta}\right) + \frac{1}{2}\hat{A}_1 lt\right]. \tag{5.4.75}$$

Inserting (5.4.74) and (5.4.75) back into (5.4.73), we obtain

$$\bar{K}(x, t) = \frac{|\alpha|\sqrt{\hat{A}_1}}{Q\sqrt{\pi l M(t)}} \exp\left\{-\frac{\hat{A}_1(\alpha + \beta)^2}{l M(t)}\left[\ln\left(\frac{\alpha x + \beta}{\alpha + \beta}\right) + \frac{1}{2}\hat{A}_1 lt\right]^2\right\}, \tag{5.4.76}$$

where

$$M(t) = \left[D_0 lt \hat{A}_1(\alpha + \beta)^2 + 2D_1(\alpha + \beta)(e^{\hat{A}_1 lt/2} - 1) + D_2(e^{\hat{A}_1 lt} - 1)\right]. \tag{5.4.77}$$

Since $x = nl$ where $l = 1/Q$

$$\bar{K}(n, t) = \frac{|\alpha|\sqrt{\hat{A}_1}}{Q\sqrt{\pi l M(t)}} \exp\left\{-\frac{\hat{A}_1(\alpha + \beta)^2}{l M(t)}\left[\ln\left(\frac{\alpha nl + \beta}{\alpha + \beta}\right) + \frac{1}{2}\hat{A}_1 lt\right]^2\right\}. \tag{5.4.78}$$

Since $K(x,t) = H(t)\bar{K}(n,t)$, we have

$$K(n,t) = \frac{2^t \mid \alpha \mid \sqrt{\hat{A}_1}}{\sqrt{Q\pi M(t)}} \exp\left\{ -\frac{\hat{A}_1(\alpha+\beta)^2}{lM(t)} \left[\ln\left(\frac{\alpha nl+\beta}{\alpha+\beta}\right) + \frac{1}{2}\hat{A}_1 lt \right]^2 \right\},$$

(5.4.79)

where $\hat{A}_1 = A_1 l^{-1}$ and $M(t)$, A_1, D_0, D_1 and D_2, are given by equations (5.4.77), (5.4.7), (5.4.46), (5.4.47), (5.4.48).

Note that in (5.4.79) we need $(\alpha ln + \beta)/(\alpha + \beta) > 0$ due to the singularity of the logarithm, so there is a singularity at $(\alpha ln + \beta)(\alpha + \beta) = 0$. From the expressions $\hat{A}_0 = L_0 - (q+p)T_0$ and $\hat{A}_1 = [L_1 + (q+p)T_1]l^{-1}$, we see that $\hat{A}_1 > 0$ and $\hat{A}_0$ can be either positive or negative, so α can be either positive or negative. If $\alpha \geq 0$, there is no singularity. If $\alpha < 0$, there is a singularity at $n_{sing} = -1/(l\alpha)$.

From the earlier stochastic simulation of Case II, we obtain the equilibrium state is (5.2.3) and note that

$$n_{inter} = \frac{(p+q)T_0 - L_0}{(p+q)T_1 + L_1} = \frac{-\hat{A}_0}{l\hat{A}_1} = -\frac{1}{l\alpha} = n_{sing}.$$

(5.4.80)

So the solution (5.4.79) cannot reach the equilibrium state, due to there being a singularity at n_{inter}. The distribution of telomere lengths of the telomere approaches the singular point $1/(l\alpha)$ as $t \to \infty$.

Now we comment on the shape of the distribution for the different choices of parameters. If $n_{inter} < 0$ (see Figure 5.11), the distribution of $\bar{K}(n,t)$ (5.4.78) starts like a Dirac delta function and as time increases, the distribution moves toward lower values of telomere length with increases diffusion. The distribution spreads by diffusion appearing symmetric at early times, at $t = 300$, we observe the peak of the distribution moving to the left (toward the value of n_{inter}). This distribution can move all the way to zero, due to the equilibrium length formally being negative value as a result of the telomere loss being larger than the gain.
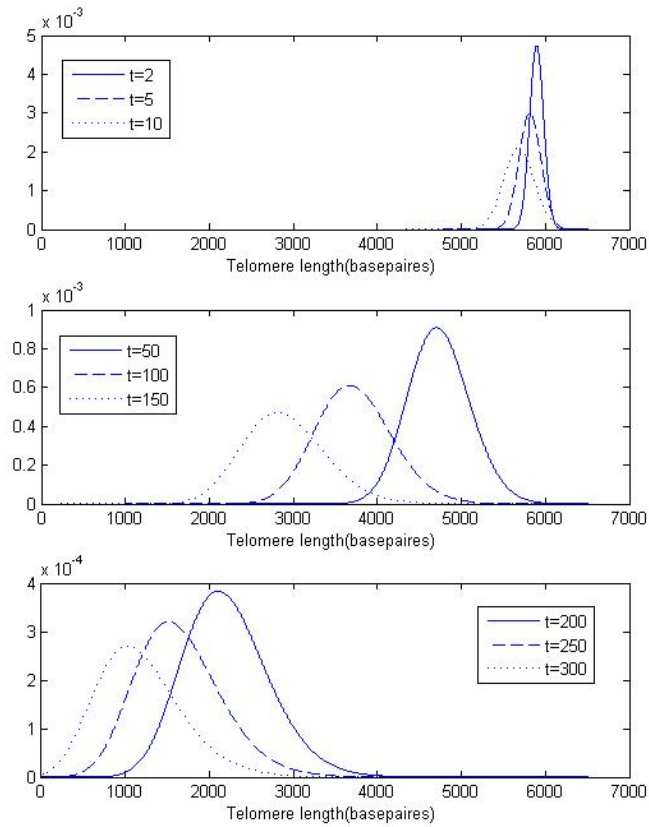
Figure 5.11: *Series of plots showing how the distribution of $\bar{K}(n,t)$ (see equation 5.4.78) changes over time t, when the amount of telomere loss $Y(n) = 50 + 0.007n$ basepairs and the amount of telomere gain $T(n) = 40 - 0.0005n$ basepairs. Parameter values: $q = 0.6$, $p = 0.4$, $Q = 5950$ basepairs.*

If $Q_{initial} > n_{inter} > 0$ (see Figure 5.12), the distribution of $\bar{K}(n,t)$ (5.4.78) starts like delta function, as time increase, the distribution moves toward the value of n_{inter}. The shape of the distribution looks symmetric at early times. The distribution cannot move cross the equilibrium state, this results in the distribution accumulating near the length of n_{inter}, due the amount of the telomere loss being compensated for the telomere gain at this point.

If $Q_{initial} < n_{inter}$ (see Figure 5.13), with start with telomere length 2000 basepairs, the distribution of $\bar{K}(n,t)$ (5.4.78) again starts like Dirac delta function. As time increases, the distribution moves toward the value of $n_{inter} = 6818$ basepairs. The shape of the distribution looks symmetric at earlier time, as time
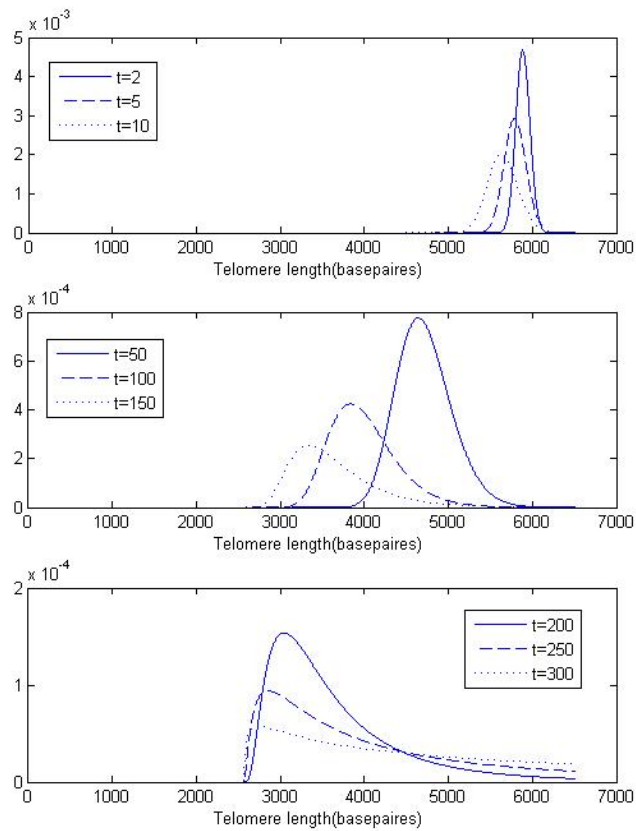
Figure 5.12: *Series of plots showing how the distribution of $\bar{K}(n,t)$ (see equation 5.4.78) changes over time t, when the amount of telomere loss $Y(n) = 50 + 0.007n$ basepairs and the amount of telomere gain $T(n) = 100 - 0.0125n$ basepairs. Parameter values: $q = 0.6$, $p = 0.4$, $Q = 5950$ basepairs.*

increases the peak of the distribution moves to the right (toward the value of n_{inter}). The distribution can not move cross the equilibrium state, result is an accumulating of the distribution near the length of n_{inter}, since here the amount of the telomere loss and gain almost compensate each other. This results also shows that, under the telomerase active, the shorter chromosome can lengthen their telomeres.
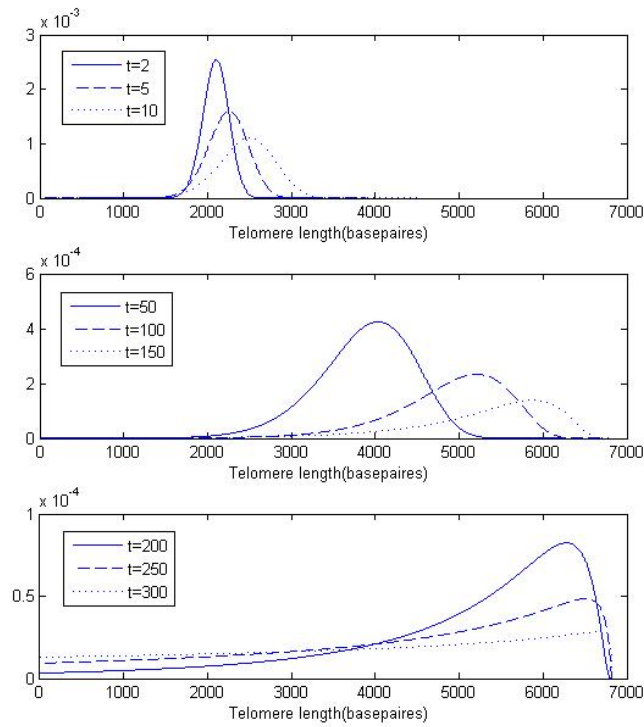
Figure 5.13: *Series of plots showing how the distribution of $\bar{K}(n,t)$ (see equation 5.4.78) changes over time t, when the amount of telomere loss $Y(n) = 50 + 0.007n$ basepairs and the amount of telomere gain $T(n) = 200 - 0.015n$ basepairs. Parameter values: $q = 0.6$, $p = 0.4$, $Q = 5950$ basepairs.*

5.5 Conclusion

In this chapter we have extended our earlier discrete and continuum models of chromosomes replication to investigate the effect of telomerase on telomere shorting. We produced Monte Carlo simulations for two different cases: Case I, is characterized by a constant loss of telomeres L and constant telomerase gain T. The stochastic simulations reveal that the average telomere length depends on the value of $T - (p+q)L$. If $(p+q)T > L$, then the amount of telomere gain $(p+q)T$ per division is longer than the telomere loss L per division, the average telomere length increase with generation number, this results in almost all the chromosomes dividing. This case is not really physically realistic because in practice telomere length can not increase indefinitely, even in immortal cells (whose telomere length is approximately constant). If $(p+q)T = L$, then the

amount of telomere gain $(p + q)T$ per division is same as the telomere loss L per division, the average telomere length stays the same. If $(p + q)T < L$, the amount of telomere gain $(p + q)T$ per division is less than the telomere loss L per division, the average telomere length decreases until the telomere length reaches the critical value.

Case II is more complicated than Case I. In Case II, both the rate of telomere loss $L(n)$ and the rate of gain $T(n)$ depend on telomere length. There is an equilibrium state of the average telomere, length n_{inter}, where $n_{inter} = [(p + q)T_0 - L_0]/[(p + q)T_1 + L_1]$, obtained in (5.2.3). If $n_{inter} < n_{critical}$, the average telomere length decreases from Q to $n_{critical}$ and remains at $n_{critical}$, due to chromosomes ceasing to replicate. If $Q > n_{inter} > n_{critical}$ the average telomere length decreases from Q until it reaches the equilibrium value n_{inter} and then remains at that value. If $n_{inter} = Q$ the average telomere length remain at Q basepairs. If $n_{inter} > Q$ the average telomere length increases from Q to the equilibrium value n_{inter}. Blagoev's model showed regardless of whether they start with longer telomere or shorter telomere, the average telomere will approach the same value as time increase. Thus the equilibria telomere length n_{inter} is consistent with telomere steady state length in Blagoev's model [66].

After the Monte Carlo simulations we modelled both cases mathematically. For Case I, we constructed a discrete model for the chromosome replication. By matching the dispersion relation to the discrete model, we obtain a continuum model, which shows that the distribution of the telomere length is a Gaussian distribution with mean $Q - \frac{1}{2}(L - qT - pT)t$. Comparing this mean with the Monte Carlo simulations, shows good agreement. For Case II, we again transform from a discrete model to continuum model. The mean obtained form the PDE gives good agreement with our Monte Carlo simulation. The shape of the distribution is no longer symmetric, they start symmetric initially, but as time increases the distribution moves toward the value of n_{inter}, and the peak of the distribution move to n_{inter} side. The solution form of the deterministic model (5.4.79) cannot reach n_{inter}, the equilibrium state length, as there is a singularity at that point. For Case II, we have only considered the case where we

start with one chromosome. If we start N chromosomes of different telomere lengths, then as time increases, the chromosomes with initial telomere length bigger than n_{inter} will lose more telomere than they gain and will approach to the value near n_{inter} from above, and chromosomes with initial telomere length lower than n_{inter} will gain more telomere than they lose and will approach the value near n_{inter} from below. So n_{inter} is a stable equilibrium value.

As we can see, telomerase can maintain or lengthen telomere. However, the amount of telomerase in normal human cells is limited, except during early fetal development and in tumor cells where the telomerase activity is high. By verify the telomerase activity, our models showing different proliferative potential. Therefore it is important to understand how telomerase acts and its role in ageing and tumor progression (cancer). Telomerase inhibitors are designed to counter theses effects by neutralizing or deactivating telomerase, in this way halting tumor progression [72].

CHAPTER 6

Concluding discussion

Each time a cell divides, incomplete replication leads to a shortening of its DNA. This occurs predominantly at the ends of chromosomes in regions called telomeres. Telomere length is a key factor in determining a cell's potential for proliferation. In this thesis, we have considered the dynamics of telomere length in a cell in order to understand the normal ageing process (telomere shortening), Werner's syndrome (an accelerated ageing disease) and the immortality of cells with telomerase (telomere lengthening).

Experiments show that telomere length plays an important role in cell division, we assume that both changes in telomere length and cell division depend on telomere length. Using various types of length-dependent loss and replication probabilities, we started with Monte Carlo simulations of normal ageing (Chapter 2) which gave us a guide on how telomere loss affects the ageing process. Then we generalized the Monte Carlo simulations to Werner's syndrome (Chapter 3), an accelerating ageing process, in which extra telomere is lost during cell division. We replaced the discrete models by continuum models of normal ageing by taking the simplest PDE whose dispersion relation matches that of the analogous discrete model from Chapter 2. The solutions obtained from the continuum models are consistent with Monte Carlo simulations. In Chapter 5, we developed Monte Carlo simulations and continuum models of cases in which telomerase is active, so modelling the lengthening as well as shortening of telomeres. By verifying the telomerase activity, our models show different

proliferative potential and also the solution obtained from the continuum models are consistent with Monte Carlo simulations. Monte Carlo simulations and continuum models in this thesis have both led to be discovery of many interesting results, as discussed below.

In Chapter 1, we gave a brief literature review covering both the biological background and modelling of telomeres, senescence, Werner's syndrome and telomerase. In Chapter 2, we developed a chromosome-level model and a cell-level model of telomere loss during replication and compared four different models which describe chromosome replication and telomere shortening. Case I represents the constant telomere loss model, in which a fixed amount of telomere is lost during each chromsome/cell replication. Case II corresponds to a situation in which the telomere loss during each replication is dependent on the length of the telomere. In Case III, the probability of cell division is a random process which depends on telomere length, whereas telomere loss occurs a constant rate. Case IV, combines telomere length-dependent loss and a probabilistic cell division term with probability dependent on telomere length. If the parameters are chosen appropriately, Cases I, II and III can be considered as special cases of Case IV.

Cases I, II and III have been considered by previous researchers. Levy *et al.* [1] studied Case I and predicted that average telomere length decreases linearly with generation numbers. They also obtain the fraction of dividing chromosomes. Our simulation results for Case I are consistent with Levy's results. Buijs [64] *et al.* analyzed Case II, with telomere loss linearly depend on the telomere length. They fitted experimental data of distribution of telomere length, by verify the shorting parameters, which predict telomere shortening depended on telomere length. Portugal considered Case III [65] where the probability of cell's replication is linearly dependent on telomere length. However in our analysis of Case III, as well predicting the average telomere length, we have also considered the fraction of senescent cells. We also considered a non-linear probability of cells replicating. Our work on Case IV is entirely novel and can fit well experimental data [2] in terms of both average telomere length and the

fraction of dividing cells. Thus we can use our model to compare with experimental data to estimate the amount of telomere loss and the probability of a cell dividing.

We note that cells with one chromosome become senescent when their telomeres reach about 150 to 250 basepairs, however, the cell model with 46 chromosomes reach senescence at about 1150 to 1500 basepairs per chromosomes, because if the length of any one chromosome is lower than the critical value, then the cell must stop dividing. Thus, as the number of chromosomes in the cell, N, increases, the average telomere length at which they become senescent also increases.

In Chapter 3 we show the effects of Werner's syndrome on chromosome replication and telomere length. Experiments have shown that there is dramatic shortening of telomeres in Werner's syndrome fibroblasts [40] . During replication, not only are a certain number of basepairs lost from one of the daughter chromosome due to normal ageing, but there is an additional loss of basepairs from one or other end of one of the daughter chromosomes caused by Werner's syndrome. Based on this replication rule, we have generated Monte Carlo simulations for a single chromosome model and a cell-level model for Werner's syndrome. Comparing these results with those for normal ageing (Chapter 2) shows that, cells with Werner's syndrome become senescent much earlier than normal cells matching the Werner's syndrome's characteristic clinical feature, the appearance of rapid ageing [34]. Another significant observation from the Werner's syndrome cell level model is that when cells with Werner's syndrome become senescent, they contain much longer telomeres than cells undergoing normal ageing. If we focus on the shortest telomere length of the chromosomes in these cells (Figure 3.7), we found that when the shortest telomere length of the chromosomes in the cells reaches the critical value, the average telomere length is still quite long. These results are consistent with an explanation of Werner's syndrome cells [41], which predicts that populations of cells with Werner's syndrome will contain some very short telomeres but the majority will retain longer telomeres. Thus in Werner's syndrome not only do we ob-

serve an accelerated telomere shortening, but we also find that short telomeres in cells can cause premature senescence. Both of these properties contribute to the accelerated ageing that characterizes Werner's syndrome.

In Chapter 4, we developed continuum models of chromsome/cell replication in normal ageing for several different functional forms for the rate of telomere loss. For comparison with the Monte Carlo simulations from Chapter 2, we considered the same four cases outlined above. When studying telomere shortening in a single chromosomes, the continuum model was assumed to be the simplest PDE whose dispersion relation matched that of the analogous discrete model from Chapter 2. Analysis of the resulting continuum model reveals that for Case I, the telomere lengths is a Gaussian distribution whose mean is in good agreement with that obtained from the Monte Carlo simulations (see Section 2.2.4 of Chapter 2) until the chromomere start to senescent. The continuum model for Case II yields a distribution of telomere lengths which is a log-normal and whose mean is consistent with the corresponding Monte Carlo simulations (see Section 2.2.5 of Chapter 2). In Case III, the continuum model does not admit explicit analytical solutions. Therefore we considered the asymptotic limit $l \ll 1$ for which the governing PDE simplifies. Here $l =$ amount of telomere lost per generation divided by initial telomere length. We started with the first order PDE, which yields the mean, and does not give a good approximation to the mean of the Monte Carlo simulations (see Section 2.2.6 of Chapter 2) at long time. Thus we need to go to the second order PDE which we cannot solve for explicitly. For Case IV, the continuum model is even more complex than for Case III, so we only construct solutions for mean for the first order PDE (the O(l) solution). Here the mean is consistent with the Monte Carlo simulations of Case IV (see Section 2.2.7 of Chapter 2). We also considered a special case, for which telomere loss is assumed to be proportional to the probability division ($y(n)/p_{div} =$ constant). In this case we obtain a mean which is consistent with Monte Carlo simulations with the same parameters values.

For the cell level model, the construction of a continuum model is similar to that used for model single chromosomes. The mean of the distribution of the

telomere length in the cells in continuum model for Cases I and II are in good agreement with the Monte Carlo simulations (see sections 2.3.2 and 2.3.3 of Chapter 2 respectively). However, for Case III and IV we use a discrete mode to obtain the average telomere length, which are also good agreement with Monte Carlo simulations (see sections 2.3.2 Case III-IV and IV-IV of Chapter 2 respectively).

In Chapter 5, we extended our discrete and continuum models of chromosome replication from Chapter 4 to investigate the effect of telomerase on telomere shortening. Here we only considered two cases: Case I is characterized by a constant loss of telomeres, L, and constant gain, T due to telomerase; Case II is characterized by telomere losses $L(n)$ and gains $T(n)$ which depend on telomere length, n.

The Monte Carlo simulations of Case I reveal that the average telomere length depends on the value of $T - (p + q)L$ where p and q are the probability that telomere are added to the longer or shorter offspring. If $(p + q)T = L$, then $(p + q)T$, the amount of telomere gain is same as L, the telomere loss, and the average telomere length remains constant. If $(p + q)T < L$, then the amount of telomere gain per division is less than the telomere loss per division and the average telomere length decreases until it reaches the critical value and senescence is triggered. If $(p + q)T > L$, the the amount of telomere gain per division is grater than the amount of telomere loss per division and the average telomere length increases with generation number. In this case almost all the chromosomes are always dividing. The case of $(p + q)T > L$ is not physically realistic because in practice telomere length can not increase indefinitely, even in immortal cells (whose telomere length is approximately constant).

In addition to the Monte Carlo simulations we also derived continuum models for both cases. For Case I, we found that distribution of the telomere lengths is a Gaussian distribution with mean which reduces/increases linearly with time and the variance increases linearly with time. This mean (average telomere length) is in good agreement with the mean of Monte Carlo simulations.

For Case II, the mean obtained form the continuum model is also in good agreement that for the Monte Carlo simulation. However, the shape of the distribution is no longer always symmetric. Over time the distribution moves toward the equilibrium value n_{inter}, and the peak of the distribution approaches to n_{inter}. However the deterministic model cannot reach the equilibrium state value n_{inter}, because there is a singularity at that point in equation (5.4.79). If we start with N chromosomes of different telomere lengths then, over time all the chromosomes approach n_{inter} either from below or above. In this respect we can view n_{inter} as a stable equilibrium value. Thus simulations suggests Case II is more physical realistic than Case I. As we can see, by verifying the telomerase activity, our models show different proliferative potential. However, the amount of telomerase in normal human cells is limited, excepts during early fetal development and in tumor cells where the telomerase activity is high. Telomerase inhibitors are designed to counter theses effects by neutralizing or inactivation telomerase, and in this way, halt tumor progression [72].

In this thesis, as well as performing Monte Carlo simulations of three models: normal ageing, Werner's syndrome and the cells with active telomerase, we have formulated continuum analogues and found good agreement between asymptotic solutions of the partial differential equations and Monte Carlo simulations.

We have proposed several extensions for future work, particularly to develop continuum analogues of Werner's syndrome, to compare with our Monte Carlo simulations. Also in our telomerase models, we consider different types of telomere loss and gain, if we can extend these models to include a probability of cell division, we might obtain a better understanding of telomerase action. Also this thesis has examined only Monte Carlo simulations model systems of telomerase, not involving physical data. If we could compare our continuum analogues with experimental data to verify the parameters, we might gain a better understanding the problem in vivo, where differing cell types have varying initial telomere lengths and a variety of amounts lost/gain each replication.

Matlab code

A.1   Matlab code for normal ageing

Matlab code file numtelcell.m

```
function  [Cell Data] = numtelcell(emax, lmin, NumGen)
% [emax] is the maximum number of cells in each generation.
% [lmin] is the minimum length of telomere where cell could divide.
% [NumGen] is the generation number
% returns matrix Cell of size 7*NumGen defined as:
% Cell(1,:) is the average mean telomere length in each generation.
% Cell(2,:) is variance of telomere length of cells.
% Cell(3,:) is fraction of cells which actually divided in the
            previous generation.
% Cell(4,i) is fraction of senescent cells.
% Cell(5,i) is fraction of  cells which had potential  divided,
            but did not due to the probability of dividing.
% Cell(6,i) is number of cells before passaging.
% Cell(7,i) is number of cells after passaging.
%%%%%%%%%%%%Constant and initial data for simulations%%%%%%%%%%%%%%
N=46;% number of telomere in the cell.
Cell = zeros(7, NumGen);
Data(1).NumCell = 1; %start with one cell.
% Initial 4 telomere length of a pair of chromosomes.
Tlength=6000; %Telomere length.
% Initial telomere length in the cell. Assume all the chromosome
% in the cells contains the same length.
for i=1:N
    Data(1).Chrom(i,:,1)  = [Tlength; Tlength; Tlength; Tlength-200];
end;
% Telomere loss [y = yo+y1*telomere length]. Probability of cell
% dividing [P = ((n-lmin) / 5800)^(alpha)].
```

```
yo = 207; y1  = 1/14; alpha = 1;
Cell(1,1) = mean(Data(1).Chrom(:,1));
Cell(2,1) = 0; Cell(3,1) = 1; Cell(4,1) = 0;
Cell(5,1) = 0; Cell(6,1) = 1; Cell(7,1) = 1;
%%%%%%%%%%%%%%% Simulation loop%%%%%%%%%%%%%%%%%%%%%%%
for i = 2:NumGen
    Temp = zeros(N,4, 2*emax); % Temp data
    nc = 0; %Number of cells actually after one generation.
    ns = 0; %Number of senescent cells.
    %Number of cells have potential to divide but did not divide in
    %the previous generation due to the probability of dividing.
    np = 0;
    for j  = 1 : Data(i-1).NumCell;
        for i1 = 1 : N
            Ave(i1) = (mean(Data(i-1).Chrom(i1,:,j)));
        end
        n = mean(Ave); % n is average telomere length in the cell.
        y = y0 + y1*n;
        for i2 = 1:N % Check each telomere length over critical vale.
            if Data(i-1).Chrom(i2,1, j) > lmin ...
            && Data(i-1).Chrom(i2,4, j) > lmin ...
            && Data(i-1).Chrom(i2,2, j) > lmin ...
            && Data(i-1).Chrom(i2,3, j) > lmin ...
                    flag(i2) = 1;
            else
                flag(i2) = 0;
            end
        end;
        Flag=min(flag);
        if Flag > 0 %Telomere length allow a  cell replicate.
            nn = nn + 2;
            p  = rand(1); %Randomly select from 0 to 1.
            p1  = ((n-lmin) / 5800)^(alpha);
            if p < p1 % Split into two cells.
                for i3 = 1 : N
                    pp1 = rand(1); %Randomly select from 0 to 1.
                    %Randomly relocated in one of two daughter cells.
                    if pp1 > 0.5
                        %First daughter cells
                        Temp(i3,:, nc+1) = Data(i-1).Chrom(i3,:, j);
                        %Second  daughter cells
                        Temp(i3,1, nc+2) = Data(i-1).Chrom(i3,4, j);
                        Temp(i3,2, nc+2) = Data(i-1).Chrom(i3,3, j);
                        Temp(i3,3, nc+2) = Data(i-1).Chrom(i3,2, j)-y;
                        Temp(i3,4, nc+2) = Data(i-1).Chrom(i3,1, j)-y;
                    else
```

201

```
                        %First daughter cells
                        Temp(i3,1, nc+1) = Data(i-1).Chrom(i3,4, j);
                        Temp(i3,2, nc+1) = Data(i-1).Chrom(i3,3, j);
                        Temp(i3,3, nc+1) = Data(i-1).Chrom(i3,2, j)-y;
                        Temp(i3,4, nc+1) = Data(i-1).Chrom(i3,1, j)-y;
                        %Second  daughter cells
                        Temp(i3,:, nc+2) = Data(i-1).Chrom(i3,:, j);
                    end
                end
                nc = nc + 2;
            else
                np=np+1;
                nc = nc + 1;
                Temp(1:N,1:4, nc) = Data(i-1).Chrom(1:N,1:4, j);
            end
        else
            ns = ns + 1;  nn = nn + 1;  nc = nc + 1;
            Temp(1:N,1:4, nc) = Data(i-1).Chrom(1:N,1:4, j);
        end
    end
    if nc <= emax
        Data(i).Chrom  = Temp(:,:, 1:nc);
        Data(i).NumCell = nc;
    else %Passaging, randomly select emax cells from nc cells.
        m1 = randperm(nc);    m2=sort(m1(1:emax))';
        for in = 1 : emax
            Data(i).Chrom(:,:, in) = Temp(:,:, m2(in));
        end
        Data(i).NumCell = emax;
    end
    %Store the data we need.
    %Average telomere length of one chromosomes in cell.
    a=mean(Data(i).Chrom(:,:,:));
    b=mean(a); %Average telomere length of the cell.
    %Average telomere length of all the cells.
    Cell(1,i) = sum(b)/Data(i).NumCell;
    %Variance of telomere length of cells.
    Cell(2,i)=var(b);
    %Fraction of cells which actually divided.
    Cell(3, i) = (nc - Data(i-1).NumCell )/ Data(i-1).NumCell;
    %Fraction of senescent cells.
    Cell(4,i) = ss/Data(i-1).NumCell;
    %Fraction of  cells which had potential  divided, but did not.
    Cell(5, i) = np/Data(i-1).NumCell;
    Cell(6,i) = nc;% Number of cells before passaging.
    Cell(7,i) = Data(i).NumCell; %Number of cells after passaging.
```

```
end
```

This is one simulation, we can repeat this to obtain average Data.

References

[1] M Z Levy, R C Allsopp, A B Futcher, C W Greider, and C B Hareley. Telomere end-replication problem and cell aging. *J. Mol. Biol.*, 225:951–960, 1992.

[2] L Zhang, H Aviv, J P Gardner, K Okuda, S Patel, M Kimura, A Bardeguez, and A Aviv. Loss of chromosome 13 in cultured human vascular endothelial cells. *Experimental Cell Research*, 260:357–364, 2000.

[3] T B L Kirkwood. Time of our lives. *European Molecular Biology Organization*, 6:4–8, 2005.

[4] T B L Kirkwood and S N Austad. Why do we age? *Nature*, 408:233–237, 2000.

[5] L Hayflick and P S Moorehead. The serial cultivation of human diploid cell strains. *Exp. Cell Res*, 25:585–621, 1961.

[6] V J Cristofalo, A Lorenzini, R G Allen, C Torres, and M Tresini. Replicative senescence: a critical review. *Mechanisms of Ageing and Development*, 125:827–848, 2004.

[7] J W Shay and W E Wright. Hayflick, his limit and cellular ageing. *Nature*, 1:72–76, 2000.

[8] G M Cooper and R E Hausman. *The cell: a molecular approach*. ASM Press and Sinauer Associates, Inc., 2009.

[9] C W Greider and E H Blackburn. Identification of a specific telomere terminal transferase activity in tetrahymena extracts. *Cell*, 43:405–413, 1985.

[10] E H Blackburn. Telomeres and their synthesis. *Science*, 249:489–490, 1990.

REFERENCES

[11] G B Morin. The human telomere terminal transferase enzyme is a ribonu-cleoprotein that synthesizes TTAGGG repeats. *Cell*, 59:521–529, 1989.

[12] A M Olovnikov. Principle of marginotomy in template synthesis of polynucleotides. *Dokl Akad Nauk SSSR*, 201:1496–1499, 1971.

[13] A M Olovnikov. A theory of marginotomy. *Journal of Theoretical Biology*, 41:181–190, 1973.

[14] C B Harley, A B Futcher, and C W Greider. Telomeres shorten during ageing of human fibroblasts. *Nature*, 345:458–460, 1990.

[15] T Ogawa and T Okazaki. Discontinuous DNA replication. *Annual Review of Biochemistry*, 49:421–457, 1980.

[16] E S Epel, E H Blackburn, J Lin, F S Dhabhar, N E Adler, J D Morrow, and R M Cawthon. Accelerated telomere shortening in response to life stress. *Proc. Nat. Acad. Sci.*, 101:17312–17315, 2004.

[17] T von Zglinicki, R Pilgera, and N Sittea. Accumulation of single-strand breaks is the major cause of telomere shortening in human fibroblasts. *Free Radical Biology & Medicine*, 28:64–74, 2000.

[18] J F Passos and T von Zglinicki. Mitochondria, telomeres and cell senes-cence. *Experimental Gerontology*, 40:466–472, 2005.

[19] C Michaloglou, L C W Vredeveld, M S Soengas, C Denoyelle, T Kuilman, C M A M van der Horst, D M Majoor, J W Shay, W J Mooi, and D S Peeper. BRAFE600-associated senescence-like cell cycle arrest of human naevi. *Nature*, 436:720–724, 2005.

[20] R C Allsopp and C B Harley. Evidence for a critical telomere length in senescent human fibroblasts. *Experimental cell research*, 219:130–136, 1995.

[21] M Collado, M A Blasco, and M Serrano. Cellular senescence in cancer and aging. *Cell*, 130:223–233, 2007.

[22] J Campisi. Senescent cells, tumor suppression, and organismal aging: good citizens, bad neighbors. *Cell*, 120:513–522, 2005.

[23] F L Mullera, M S Lustgartenb, Y Janga, A Richardsona, and H Van Remmen. Trends in oxidative aging theories. *Free Radical Biology & Medicine*, 43:477–503, 2007.

[24] Y H Wei and H C Lee. Oxidative stress, mitochondrial DNA mutation, and apoptosis in aging. *Experimental Biology and Medicine*, 227:671–682, 2002.

[25] T B L Kirkwood and C J Proctor. Somatic mutations and ageing in silico. *Mechanisms of Ageing and Development*, 124:85–92, 2003.

[26] S Kawanishi and S Oikawa. Mechanism of telomere shortening by oxidative stress. *Annals of the New York Academy of Sciences*, 1019:278–284, 2004.

[27] T Richtera and T Von Zglinicki. A continuous correlation between oxidative stress and telomere shortening in fibroblasts. *Experimental Gerontology*, 42:1039–1042, 2007.

[28] J F Passos, T Von Zglinicki, and T B L Kirkwood. Mitochondria and ageing: winning and losing in the numbers game. *BioEssays*, 29:908–917, 2007.

[29] D Xu and T Finkel. A role for mitochondria as potential regulators of cellular life span. *Biochemical and Biophysical Research Communications*, 294:245–248, 2002.

[30] R Holliday. Somatic mutations and ageing. *Mutation Research*, 463:173–178, 2000.

[31] A A Morley. The somatic mutation theory of ageing. *Mutation Research*, 338:19–23, 1995.

[32] E H Blackburn. Telomere states and cell fates. *Nature*, 408:53–56, 2000.

[33] E H Blackburn. Switching and signaling at the telomere. *Cell*, 106:661–673, 2001.

[34] K Yamamoto, A Imakiire, N Miyagawa, and T Kasahara. A report of two cases of Werner's syndrome and review of the literature. *Journal of Orthopaedic Surgery*, 11:224–233, 2003.

REFERENCES

[35] R G Faragher, I R Kill, J A A Hunte, F M Pope, C Tannock, and S Shall. The gene responsible for Werner syndrome may be a cell division "counting" gene. *Proceedings of the National Academy of Sciences of the United States of America*, 90:12030–12034, 1993.

[36] M Goto, R W Miller, Y Ishikawa, and H Sugano. Excess of rare cancers in Werner syndrome (adult progeria). *Cancer Epidemiol Biomarkers Prevention*, 5:239–246, 1996.

[37] S M Bailey and J P Murnane. Telomeres, chromosome instability and cancer. *Nucleic Acids Research*, 34:2408–2417, 2006.

[38] Yasuhiro Furuichi. Premature aging and predisposition to cancers caused by mutations in recq family helicases. *Annals of the New York Academy of Sciences*, 928:121–31., 2001.

[39] K Fukuchi, GM Martin, and R J Monnat. Mutator phenotype of Werner syndrome is characterized by extensive deletions. *Proc Natl Acad Sci USA*, 86:5893–5897, 1989.

[40] H Tahara, Y Tokutake, S Maeda, H Kataoka, T Watanabe, M Satoh, T Matsumoto, M Sugawara M, T Ide, M Goto, Y Furuichi, and M Sugimoto. Abnormal telomere dynamics of B-lymphoblastoid cell strains from Werner's syndrome patients transformed by Epstein-Barr virus. *Oncogene*, 15:1911–1920, 1997.

[41] S Chang. A mouse model of Werner syndrome: what can it tell us about aging and cancer? *The International Journal of Biochemistry & Cell Biology*, 37:991–999, 2005.

[42] C Z Bachrati and I D Hickson. RecQ helicases: suppressors of tumorigenesis and premature aging. *Biochem J.*, 15:577–606, 2003.

[43] E Hiyama and K Hiyama. Telomere and telomerase in stem cells. *British Journal of Cancer*, 96:1020–1024, 2007.

[44] L L Mantell and C W Greider. Telomerase activity in germline and embryonic cells of Xenopus. *The EMBO Journal*, 13:3211 – 3217, 1994.

REFERENCES

[45] N W Kim, M A Piatyszek, K R Prowse, C B Harley, M D West, P L C Ho, G M. Coviello, W E Wright, S L Weinrich, and J W Shay. Specific association of human telomerase activity with immortal cells and cancer. *Science*, 266:2011–2014, 1994.

[46] A G Bodnar, M Ouellette, M Frolkis, SE Holt, C P Chiu, G B Morin, C B Harley, J W Shay, S Lichtsteiner, and W E Wright. Extension of life-span by introduction of telomerase into normal human cells. *Science*, 279:349–352., 1998.

[47] M T Hemann, M A Strong, L Y Hao, and C W Greider. The shortest telomere, not average telomere length, is critical for cell viability and chromosome stability. *Cell*, 107:67–77, 2001.

[48] M T Teixeira, M Arneric, P Sperisen, and J Lingner. Telomere length homeostasis is achieved via a switch between telomerase- extendible and nonextendible states. *Cell*, 17:323–335, 2004.

[49] M Chang, M Arneric, and J Lingner. Telomerase repeat addition processivity is increased at critically short telomeres in a tel1-dependent manner in Saccharomyces cerevisiae. *Gene and Development*, 21:2485–2494, 2007.

[50] Y Zhao, A J Sfeir, Y Zou, C M Buseman, T T Chow, J W Shay, and W E Wright. Telomere extension occurs at most chromosome ends and is uncoupled from fill-in in human cancer cells. *Cell*, 138:463–475, 2009.

[51] D Loayzaa and T De Lange. Telomerase regulation at the telomere: a binary switch. *Cell*, 117:279–280, 2004.

[52] T M Bryan, A Englezou, J Gupta, S Bacchetti, and R R Reddel. Telomere elongation in immortal human cells without detectable telomerase activity. *The EMBO Journal*, 14:4240–4248, 1995.

[53] T M Bryan, A Englezou, L Dalla-Pozza, M A Dunham, and R R Reddel. Evidence for an alternative mechanism for maintaining telomere length in human tumors and tumor-derived cell lines. *Nature Med*, 3:1271–1274, 1997.

[54] M A Dunham, A A Neumann, C L Fasching, and R R Reddel. Telomere maintenance by recombination in human cells. *Nature Genetics*, 26:447–450, 2000.

[55] S M Bailey, M A Brenneman, and E H Goodwin. Frequent recombination in telomeric DNA may extend the proliferative life of telomerase-negative cells. *Nucleic Acids Research*, 32:3743–3751, 2004.

[56] J D Henson, A A Neumann, T R Yeager, and R R Reddel. Alternative lengthening of telomeres in mammalian cells. *Oncogene*, 21:598–610, 2002.

[57] O Arino, M Kimmel, and G F Webb. Mathermatical modeling of the loss of telomere sequences. *J. Ther. Biol.*, 177:45–57, 1995.

[58] P Olofsson and M Kimmel. Stochastic models of telomere shortening. *Mathematical Biosciences*, 158:750–92, 1999.

[59] I Rubelj and Z Vondracek. Stochastic mechanism of cellular aging-abrupt telomere shortening as a model for stochastic nature of cellular aging. *J. Theor. Biol.*, 197:425–438, 1999.

[60] P D Sozou and T B L Kirkwood. A stochastic model of cell replicative senescence based on telomere shortening, oxidative stress, and somatic mutations in nuclear and mitochondrial DNA. *J. Theor. Biol.*, 213:573–586, 2001.

[61] C J Proctor and T B L Kirkwood. Modeling telomere shorenting and the role of oxidative stress. *Mechanisms of Ageing and Development*, 123:351–363, 2002.

[62] C J Proctor and T B L Kirkwood. Modelling cellular senescence as a result of telomere state. *Aging cell*, 2:151–157, 2003.

[63] T Richter and C Proctor. The role of intracellular peroxide levels on the development and maintenance of telomere-dependent senescence. *Experimental Gerontology*, 42:1043–1052, 2007.

[64] J Buijs, P P J Bosch, M W J M Muster, and N A W Riel. Mathematical modeling confirms the length-dependency of telomere shortening. *Mechanisms of Ageing and Development*, 125:437–444, 2004.

[65] R D Portugal, M G P Land, and B F Svaiter. A computational model for telomere-dependent cell-replicative aging. *BioSystems*, 91:262–267, 2008.

[66] K B Blagoev. Cell proliferation in the presence of telomerase. *Plosone*, 4:e4622, 2009.

[67] CB Harley and S Goldstein. Retesting the commitment theory of cellular aging. *Science*, 207:191–193, 1980.

[68] B Alberts, A Johnson, J Lewis, M Raff, K Roberts, and P Walter. *Molecular biology of the cell*. Garland Science, Taylor & Francis Goup, LLC, 2008.

[69] A Asghari, F Izadi, and F Memari. Werner's syndrome: a rare cause of hoarseness. *Journal of Voice*, 22:509–511, 2008.

[70] F S Wyllie, C J Jones, J W Skinner, M F Haughton, C Wallis, D W Thomas, R G A Faragher, and D Kipling. Telomerase prevents the accelerated cell ageing of werner syndrome fibroblasts. *Nature Genetics*, 24:16–17, 2000.

[71] P L Opresko, W Cheng, C von Kobbe, J A Harrigan, and V A Bohr. Werner syndrome and the function of the werner protein; why they can teach us about the molecular aging process. *Carcinogenesis*, 24:791–802, 2003.

[72] J W Shay, Y Zou, E Hiyama, and W E Wright. Telomerase and cancer. *Human Molecular Genetics*, 10:667–685, 2001.